DEPARTMENT OF PHYSICS
UNIVERSITY OF JYVÄSKYLÄ
RESEARCH REPORT No. 3/2010

PROCEEDINGS OF THE 44. ANNUAL CONFERENCE OF THE FINNISH PHYSICAL SOCIETY

March 11-13, 2010, Jyväskylä

Editors: Timo Sajavaara
with
Ilari Maasilta
Laura Mättö
Juhani Julin
Panu Rahkila

Jyväskylä, Finland
March 2010

PROGRAM COMMITTEE:
I. Maasilta, chairman
T. Sajavaara, secretary
R. Julin
J. Maalampi

ORGANIZING COMMITTEE:
K. J. Eskola, chairman
H. Häkkinen, vice-chairman
E. Hänninen, SFS, secretary
A. Virtanen, exhibitions
M. Manninen
J. Uusitalo, security

ORGANIZERS:
The Finnish Physical Society
Department of Physics, University of Jyväskylä

ISBN: 978-951-39-3834-5
ISSN: 0075-465X

Kopi-Jyvä Oy, Jyväskylä, 2010.

PREFACE

The physics community of Finland convenes this year in Jyväskylä to the 44th annual conference of the Finnish Physical Society. Our local host organization, the Department of Physics at the University of Jyväskylä, is kind of a role model of a well working unit, with high level research in an encouraging environment without borders. I felt this personally during my 10 years at JYFL, and the same atmosphere greets me each time I visit here for whatever reason. We outsiders can now enjoy for a few days and learn from the positive tradition and atmosphere that has been developed by many of the early professors and mentors, and maintained successfully by the present ones and by the whole staff.

I want to thank the organizing and program committees, lead by professors Kari J. Eskola and Ilari Maasilta respectively, and the secretary general of the Finnish Physical Society, Ella Hänninen, already at this stage for their efforts in putting together this conference in a professional way. It is significant that our society of 1000 members gathers in Physics Days again almost 400 participants; they present 90 talks in 15 parallel sessions and about 175 posters. Again, it is a pleasure to notice that a large fraction of the participants are students and young researchers. This year we will follow the ceremony for the Magnus Ehrnrooth Foundation award as well.

I remind you that the general meeting of the Finnish Physical Society takes place during the Physics Days. I encourage you to attend this meeting that gives an opportunity for the members to participate in decision making and discussions about the activities of the Society.

On behalf of the Finnish Physical Society I welcome you all to the Jyväskylä Physics Days to enjoy the scientific program and the exhibition, and to meet colleagues from all over the country and beyond.

Jukka Pekola
President of the Finnish Physical Society

Contents

0 Plenary sessions **1**

0.1 Plenary session I, Thursday 11 March 13:00-14:30 2

0.1.1 Philip Withers: X-RAY TOMOGRAPHY OF MATERIALS 2

0.1.2 Jorma Tuominiemi: LHC NEW ERA IN HIGH ENERGY PHYSICS 3

0.2 Plenary session II, Friday 12 March 9:00-10:30 4

0.2.1 Günter Steinmeyer: TAMING OPTICAL NONLINEARITIES: FROM FEW-FEMTOSECOND BEAM DELIVERY TO FILAMENT SELF-COMPRESSION 4

0.2.2 Eberhard Gross: ANALYSIS AND CONTROL OF ELECTRONIC MOTION ON THE FEMTOSECOND TIME SCALE 5

0.3 Plenary session III, Friday 12 March 11:00-13:15 6

0.3.1 Stephan Friedrich: SUPERCONDUCTING X-RAY AND GAMMA-RAY SPECTROMETERS: FROM MATERIAL SCIENCE TO NUCLEAR SECURITY 6

0.3.2 Chad Finley: THE ICECUBE NEUTRINO OBSERVATORY: OPENING A NEW WINDOW ON THE UNIVERSE 7

0.3.3 Peter Butler: PROBING NUCLEI AT THE EDGE OF STABILITY 8

0.4 Plenary session IV, Saturday 13 March 11:00-12:30 9

0.4.1 Jouni Viiri: EVIDENCE BASED PHYSICS EDUCATION 9

0.4.2 Matti Weckström: PHYSICS OF INSECT VISION 10

1 Applied physics, instrumentation and optics **11**

1.1 Oral session I, Thursday 11 March 15:00-16:30 12

1.1.1 T.J. Isotalo and I.J. Maasilta: BOUNDARY ENGINEERING FOR SINIS BOLOMETERSWITH INTEGRATED TUNNEL JUNCTION COOLERS . 12

1.1.2 M. Grönholm, L. Grönberg, P. Lappalainen, M. Leivo, P. Helistö, A. Rautiainen, H. Seppä, H. Sipola, C. R. Dietlein, E. N. Grossman and A. Luukanen: VIDEO-RATE TERAHERTZ IMAGING USING SUPERCONDUCTING BOLOMETERS 13

1.1.3 O. Kimmelma, S. Suihkonen, I. Tittonen, M. Sopanen, and H. Lipsanen: MEASUREMENTS OF InGaN QUANTUM WELL RELAXATION WITH PULSED UV-LASER EXCITATION 14

1.1.4 J. Luomahaara, J. Hassel, J. Penttilä, M. Kiviranta and L. Grönberg: FIELD-TOLERANT SQUID SENSORS FOR A COMBINED MEG-MRI SYSTEM 15

1.1.5 V. F. Maisi, S. Kafanov, Yu. A. Pashkin, A. Kemppinen, N. Chekurov, O.-P. Saira, M. Möttönen, J. S. Tsai, A. Manninen, J. P. Pekola: PERFORMANCE IMPROVEMENTS OF A SINGLE ELECTRON TURNSTILE 16

1.1.6 M. Möttönen, K. Y. Tan, K. W. Chan, A. Morello, C. Yang, J. van Donkelaar, A. Alves, J.-M. Pirkkalainen, D. N. Jamieson, R. G. Clark, and A. S. Dzurak: SINGLE-ATOM TRANSISTOR 17

1.2 Oral session II, Friday 12 March 14:30-16:00 18
1.2.1 E. Hirvijoki, S. Jämsä, T. Kurki-Suonio: DEVELOPING A MODEL FOR FAST ION DETECTION IN FUSION REACTORS 18
1.2.2 M. Laitinen, M. Rossi, P. Rahkila, H.J. Whitlow and T. Sajavaara: NEW HIGH RESOLUTION SPECTROMETER FOR NANOMETER LEVEL ELEMENTAL DEPTH PROFILING 19
1.2.3 T. Makkonen, T. Kurki-Suonio, K. Krieger, M. Groth, L. Aho-Mantila, and A. Hakola: TRANSPORT OF TRACE IMPURITIES INSIDE A TOKAMAK PLASMA 20
1.2.4 T. Eronen, J. Hakala, A. Jokinen, A. Kankainen, P. Karvonen, V.S. Kolhinen, I.D. Moore, H. Penttilä, J. Rissanen, M. Reponen, A. Saastamoinen, V. Sonnenschein and J. Äystö: APPLICATIONS AT THE IGISOL FACILITY . . . 21
1.2.5 A. Seppänen, K. Karhunen, A. Lehikoinen, J. Blunt, J.P. Kaipio and P.J.M. Monteiro: ELECTRICAL RESISTANCE TOMOGRAPHY IMAGING OF CONCRETE 22
1.2.6 S.-P. Simonaho and T. Lähivaara: AUTOMATED MEASUREMENT SYSTEM FOR VALIDATION OF ACOUSTICAL SIMULATION RESULTS 23
1.3 Oral session III, Saturday 13 March 9:00-10:30 24
1.3.1 M. Erkintalo, G. Genty, and J. M. Dudley: SOLITON COLLISION INDUCED DISPERSIVE WAVE GENERATION 24
1.3.2 V. Heikkinen, I. Kassamakov, J. Aaltonen and E. Hæggström: DETERMINING THE CHRONOLOGICAL ORDER OF CROSSING LINES USING SCANNING WHITE LIGHT INTERFEROMETRY 25
1.3.3 J. Kauppinen, T. Kuusela, P. Malmi and J. Raittila: PHYSICAL MODELLING OF THE INTERFEROMETRIC CANTILEVER MICROPHONE USED IN PHOTOACOUSTIC GAS DETECTORS 26
1.3.4 T. Luostari, T. Huttunen and P. Monk: THE ULTRA WEAK VARIATIONAL FORMULATION WITH BESSEL BASIS FUNCTIONS 27
1.3.5 L.J. Taskinen, R.P. Starrett, T.P. Martin, J. C. H. Chen, A.P. Micolich, A.R. Hamilton, M.Y. Simmons, D.A. Ritchie and M. Pepper: HIGH BANDWIDTH MEASUREMENTS OF LARGE AREA 2-DIMENSIONAL SYSTEMS USING RF REFLECTOMETRY 28
1.3.6 V. Vesterinen, A.O. Niskanen, L. Grönberg, P. Helistö, M. Tikander, P. Maijala and J. Hassel: PERFORMANCE OF A THERMOACOUSTIC METAL WIRE ARRAY LOUDSPEAKER 29
1.4 Poster session I, Thursday 11 March 16:30-18:30 30
1.4.1 T. Fabritius, J. Eskelinen and E. Hæggström: LASER-ULTRASONICS CHARACTERIZES LAYERED POLYMERS 30

1.4.2 T. Setälä, T. Hakkarainen, A. T. Friberg, and B. J. Hoenders: PERFECT CLOAKING IN FIRST BORN APPROXIMATION 31
1.4.3 M. J. Huttunen, M. Virkki, M. Erkintalo, E. Vuorimaa, A. Efimov, H. Lemmetyinen and M. Kauranen: UNAMBIGUOUS PROBE OF SURFACE CHIRALITY BASED ON FOCUSED CIRCULAR POLARIZATIONS 32
1.4.4 S. Jämsä: FRONTIERS IN FUSION ENERGY RESEARCH: A REVIEW . . . 33
1.4.5 P. Junell, J. Alarinta and M. Kärkkäinen: CORROSION OCCURING IN THE FOOD PROCESSING INDUSTRY 34
1.4.6 S. Jussila, M.Valkiainen, K. Solehmainen and S. Kielosto: PRINTABLE POLYANILINEALUMINUM THIN FILM BATTERIES 35
1.4.7 E. Korhonen, F. Reurings and F. Tuomisto: THE HELSINKI POSITRON LIFETIME BEAM - PRESENT STATUS AND DATA ANALYSIS TECHNIQUE 36
1.4.8 O. Korniyenko, T. Enqvist, K. Loo and W.H. Trzaska: APPLICATION OF R-FUNCTIONS FOR GAMMA-RAY DETECTION EFFICIENCY WHEN MEASURING ACTIVITY OF RADIOACTIVE SAMPLES WITH COMPLEX SHAPES 37
1.4.9 J. Lääkkö, A. Salmi, F. Gates, T. Karppinen and E. Hæggström: DYNAMIC MECHANICAL ANALYSIS TESTING OF NORWEGIAN SPRUCE 38
1.4.10 M. Laitinen, V. Nieminen, O. Vaittinen, L. Mättö, A. Arcot, J. Julin, M. Napari, H.J. Whitlow and T. Sajavaara: NEW HEAVY ION SOURCE, MODIFIED INJECTOR AND NEW TOF-ERD BEAMLINE FOR PELLETRON ACCELERATOR 39
1.4.11 A. Lindell, A. Latvala and J. Viiri: SEITSEMÄN IHMETTÄ – SEVEN MIRACLES OF PHYSICS ROAD SHOW 40
1.4.12 A. Lindell, A. Latvala, J. Lauros, T. Nevanpää and J. Viiri: EXPERIMENTAL PHYSICS FOR ADVANCED STUDENTS 41
1.4.13 A. Lipponen, A. Seppänen and J.P. Kaipio: PROCESS TOMOGRAPHY UNDER NONSTATIONARY VELOCITY FIELDS 42
1.4.14 J. Mäkitalo, H. Husu and M. Kauranen: MODELING THE OPTICAL PROPERTIES OF METAL NANOPARTICLES WITH THE FINITE DIFFERENCE TIME DOMAIN METHOD 43
1.4.15 A. Nikitin, A. Semenov, S. Karmanenko and E. Lähderanta: THE ANALYSIS OF HYBRID ELECTROMAGNETIC-SPIN WAVES PROPAGATION IN SLOT TRANSMISSION LINE 44
1.4.16 N. Nikitina, V. Barchenko, E. Lahderanta: MODELING OF PROCESSES IN THE MAGNETRON SPUTTERING SYSTEM WITH HIGH CURRENT DENSITIES 45
1.4.17 R. Norarat, H.J. Whitlow, T. Sajavaara and M. Laitinen: DEVELOPMENT OF RESEARCH WITH AN ACCELERATOR MICROBEAM (DREAM) 46

1.4.18 L. Olanterä, K. Arstila, T. Hantschel, S. Palanne, and T. Sajavaara: NANOPROBER AS A TOOL FOR ELECTRICAL MEASUREMENTS OF NANOSTRUCTURES 47
1.5 Poster session II, Friday 12 March 16:00-18:00 48
1.5.1 L. Orsila, C. Grebing and G. Steinmeyer: TOWARDS A HIGH POWER ULTRASHORT-PULSE CARRIER-ENVELOPE PHASE STABLE HIGH REPETITION LASER SYSTEM 48
1.5.2 A.-I. Partanen, H. Kokkola and H. Korhonen: GEOENGINEERING WITH SEA SPRAY EMISSIONS 49
1.5.3 T. Peltola, J. Aaltonen, S. Czellar, J. Härkönen, I. Kassamakov, and E. Tuominen: TRANSIENT CURRENT TECHNIQUE FOR THE STUDY OF RADIATION HARDNESS OF SEMICONDUCTOR DETECTORS 50
1.5.4 J. Pentikäinen, I. Lassila, E. Hæggström: HIGH INTENSITY AIRBORNE ULTRASOUND SOURCE FOR SENSING AND MACHINING 51
1.5.5 V. Polojärvi, J. Tommila, J. Salmi, A. Aho, A. Tukiainen, A. Schramm, J. Viheriälä, and M. Guina: SUB WAVELENGTH NANOSTRUCTURES FOR BROAD BAND SOLAR CELLS ANTI-REFLECTION COATINGS 52
1.5.6 M.Reponen, V. Sonnenschein, I. Pohjalainen, M. Savonen I.D. Moore and J. Äystö: NOVEL TECHNIQUES FOR HOT CAVITY CATCHERS AND GAS CELLS AT IGISOL 53
1.5.7 V. Rimpiläinen, L.M. Heikkinen, M. Vauhkonen and J. Ketolainen: ELECTRICAL IMAGING MODALITIES IN PHARMACEUTICAL APPLICATIONS 54
1.5.8 A. Snicker, S. Sipilä and T. Kurki-Suonio: REALISTIC CALCULATION OF ITER WALL LOADS INCLUDING FINITE ORBIT EFFECTS 55
1.5.9 J. Takalo and J. Timonen: WAVELET-BASED INVERSE METHOD AS A TOOL IN PAPER QUALITY ASSESSMENT 56
1.5.10 J. Turunen, K. Peräjärvi, T. Eronen, V.-V. Elomaa, J. Hakala, A. Jokinen, H. Kettunen, V. Kolhinen, M. Laitinen, I.D. Moore, H. Penttilä, J. Rissanen, A. Saastamoinen, H. Toivonen and J. Äystö: ULTRA-PURE ^{133m}Xe STANDARD FOR SENSITIVE DETECTION OF NUCLEAR WEAPONS TESTS 57
1.5.11 M. Virkki, A. Priimägi, M. Kauranen: OPTIMIZING STABILITY OF ALL-OPTICALLY POLED MATERIALS 58
1.5.12 T. Voipio, T. Setälä, A. Shevchenko, and A. T. Friberg: CHARACTERIZATION OF POLARIZATION DYNAMICS IN RANDOM THREE-DIMENSIONAL ELECTROMAGNETIC FIELDS 59

2 Astrophysics, cosmology and space physics **61**
2.1 Oral session, Saturday 13 March 9:00-10:30 62

2.1.1 I. Honkonen, M. Palmroth, T.I. Pulkkinen and P. Janhunen: LARGE PLASMOIDS IN GLOBAL MHD SIMULATIONS: SOLAR WIND DEPENDENCE AND IONOSPHERIC MAPPING 62
2.1.2 M. Palmroth, T.I. Pulkkinen, C.R. Anekallu, I. Honkonen, H.E.J. Koskinen, E.A. Lucek, and I. Dandouras: MAGNETOSPHERIC FEEDBACKS IN SOLAR WIND ENERGY TRANSFER: IMPLICATIONS FOR THE SUBSTORM CYCLE 63
2.1.3 P. Janhunen and P. Toivanen: ELECTRIC SOLAR WIND SAIL PROPULSION: TOWARDS TEST MISSIONS 64
2.1.4 E. Keihänen, H. Kurki-Suonio, T. Poutanen, M. Savelainen and A.-S. Sirviö: THE STATUS OF PLANCK 65
2.1.5 K. Kainulainen, K. Tuominen and J. Virkajärvi: ADJOINT DARK MATTER . 66
2.1.6 M.Valtonen, S. Mikkola, H. Lehto and A.Gopakumar: TESTING GENERAL RELATIVITY WITH THE BINARY BLACK HOLE SYSTEM OJ287 . . . 67
2.2 Poster session, Friday 11 March 16:00-18:00 68
2.2.1 R. Järvinen, E. Kallio, S. Dyadechkin, P. Janhunen and I. Sillanpää: VENUS IN THE SOLAR WIND: A HYBRID MODELLING OVERVIEW 68
2.2.2 M. Battarbee, T. Laitinen, R. Vainio and N. Agueda: SHOCK OBLIQUITY AND PRE-HEATED PARTICLE POPULATIONS IN SELFCONSISTENT PARTICLE SHOCK ACCELERATION 69
2.2.3 N. Partamies, M. Syrjäsuo and E. Donovan: TOWARDS MULTI-SCALE AURORAL OBSERVATIONS 70
2.2.4 J. Pasanen, K. Kainulainen and P. M. Rahkila: EXACT 2-POINT WIGHTMAN FUNCTIONS AND CQPA 71
2.2.5 J. Pomoell, R. Vainio, E.K.J. Kilpua and R. Kissmann: ON THE DEFLECTION OF CORONAL MASS EJECTIONS IN THE SOLAR CORONA 72
2.2.6 P. K. Toivanen and P. Janhunen: ELECTRIC SAILING AND SOLAR WIND VARIATIONS 73
2.2.7 P. T. Verronen, A. Seppälä, C. J. Rodger, M. A. Clilverd, C.-F. Enell, A. Kero, S.-M. Salmi, T. Ulich, J. Tamminen, E. Kyrölä, and E. Turunen: SPACE WEATHER AND STRATOSPHERIC OZONE 74
2.2.8 C.R. Anekallu, M. Palmroth, T. Pulkkinen, E. Lucek, I. Dandouras: ENERGY CONVERSION AT THE EARTH'S MAGNETOPAUSE: VALIDATING SINGLE SPACECRAFT METHODS 75

3 Biological and medical physics **77**
3.1 Oral session, Thursday 11 March 15:00-16:30 78
3.1.1 P. Toroi: PATIENT EXPOSURE MONITORING AND RADIATION QUALITIES IN DIGITAL X-RAY IMAGING 78

3.1.2 E. Hippeläinen: PATIENT SPECIFIC MONTE CARLO DOSE SIMULATIONS: INTERNAL EMITTERS 79

3.1.3 T.S. Silvast, A.S. Aula, H.T. Kokkonen, J.S. Jurvelin and J. Töyräs: NOVEL COMPUTED TOMOGRAPHY METHOD FOR DIAGNOSTICS OF ARTICULAR CARTILAGE DEGENERATION 80

3.1.4 O. Lehtikangas, T. Tarvainen, V. Kolehmainen, S.R. Arridge, and J. P. Kaipio: FINITE ELEMENT APPROXIMATION OF THE FOKKER-PLANCK EQUATION FOR DIFFUSE OPTICAL TOMOGRAPHY 81

3.1.5 T. Kühn, T. O. Ihalainen, J. Hyväluoma, J. Timonen and M. Vihinen-Ranta: SIMULATION APPROACH TO QUANTITATIVE FRAP ANALYSIS 82

3.1.6 M. Sovago, E. Vartiainen and M. Bonn: OBSERVATION OF BURIED WATER MOLECULES IN PHOSPHOLIPID MEMBRANES BY SURFACE SFG SPECTROSCOPY 83

3.2 Poster session, Thursday 11 March 16:30-18:30 84

3.2.1 L.M. Heikkinen, J. Aaltonen, S.-P. Simonaho, E. Nippolainen, R. Pellinen, M. Vauhkonen, V.-P. Lehto, K. Järvinen, and J. Ketolainen: PROMIS CENTRE MULTIDISCIPLINARY RESEARCH CONSORTIUM AS A LINK BETWEEN PHYSICS AND PHARMACEUTICS 84

3.2.2 M. Javanainen, L. Monticelli and I. Vattulainen: LATERAL DIFFUSION IN LUNG SURFACTANT 85

3.2.3 H. Koivunoro, T. Siiskonen, P. Kotiluoto, E. Hippeläinen, I. Auterinen and S. Savolainen: COMPARISON OF MCNP5 ELECTRON TRANSPORT WITH EGSnrc AND PENELOPE: ENERGY-LOSS DISTRIBUTION AND DOSE CALCULATION IN A SMALL GAS CAVITY 86

3.2.4 T. Mäkelä and A. Annila: NATURAL PATTERNS OF ENERGY DISPERSAL 87

3.2.5 M.K.H. Malo, O. Riekkinen, J.P. Karjalainen, H. Isaksson, J.S. Jurvelin and J.Töyräs: NON-OPTIMAL FOCUSING OF ULTRASOUND DOES NOT AFFECT DUAL FREQUENCY ULTRASOUND MEASUREMENT OF BONE 88

3.2.6 V. Mannila and O. Sipilä: B-MODE ULTRASOUND QUALITY ASSURANCE: PHANTOM MEASUREMENTS 89

3.2.7 M. Nyrhinen and O. Sipilä: T2* MAPS TO ASSESS TISSUE IRON CONCENTRATION 90

3.2.8 P. Sane, F. Tuomisto, I. Vattulainen and J. Holopainen: REVEALING THE MICROSTRUCTURAL CHANGES IN TISSUES IN-SITU WITH POSITRON ANNIHILATION SPECTROSCOPY 91

3.2.9 S. Savolainen: THE FINNISH BORON NEUTRON CAPTURE THERAPY (BNCT) - 87.00 PROJECT 92

3.2.10 M. Timonen, L. Kankaanranta, N. Lundbom, S. Savolainen and S. Heikkinen: PROTON MAGNETIC RESONANCE SPECTROSCOPY OF BNCT 10BCARRIER, LPBORONOPHENYLALANINEFRUCTOSE COMPLEX . 93
3.2.11 P. Välimäki, A. Kuronen and S. Savolainen: COMPARISON BETWEEN VOXEL BASED AND DOUBLE FOLDED INTEGRAL CALCULATION METHODS FOR CELLULAR DOSIMETRY 94
3.2.12 P. Jääskeläinen, P. Engelhardt, M. Torkkeli, U. Hynönen, H. Vilen, J. Heikkonen, A. Palva and R. Serimaa: LACTOBACILLUS BREVIS S-LAYER STUDIED BY SAXS AND ELECTRON MICROSCOPY 95

4 Condensed matter: Structural properties 97
4.1 Oral session, Friday 12 March 14:30-16:00 98
4.1.1 T. Pylkkänen, V.M. Giordano, A. Sakko, M. Hakala, J. A. Soininen, K. Hämäläinen, G. Monaco and S. Huotari: EXOTIC DENSE ICES 98
4.1.2 T. Tallinen, J.A. Åström and J. Timonen: COMPRESSING A THIN-WALLED ELASTIC BOX 99
4.1.3 J. Andersin and K. Honkala: DENSITY FUNCTIONAL STUDY ON ETHYLENE DECOMPOSITION ON FLAT AND STEPPED PALLADIUM 100
4.1.4 P. Penttilä, A. Várnai, K. Leppänen, M. Peura, A. Kallonen, P. Jääskeläinen, J. Lucenius, A. Nykänen, M. Siika-aho, L. Viikari, and R. Serimaa: THE EFFECT OF ENZYMATIC HYDROLYSIS ON THE SUB-MICROMETER STRUCTURE OF MICROCRYSTALLINE CELLULOSE 101
4.1.5 J. Hosio, V.B. Eltsov, R. de Graaf, and M. Krusius: ANDREEV REFLECTION FROM VORTICES IN SUPERFLUID 3He-B 102
4.1.6 H. Ali-Löytty, P. Jussila, K. Lahtonen, M. Hirsimäki, and M. Valden: EFFECT OF SURFACE HYDROXYL CONCENTRATION ON THE BONDING AND MORPHOLOGY OF AMINOPROPYLSILANE THIN FILMS ON AUSTENITIC STAINLESS STEEL 103
4.2 Poster session I, Thursday 11 March 16:30-18:30 104
4.2.1 M.G. Ganchenkova: HYDROGEN IN FePd:L10 : SOLUBILITY AND MIGRATION 104
4.2.2 I. Gazuz, A. M. Puertas and M. Fuchs: NONLINEAR MICRORHEOLOGY OF DENSE COLLOIDAL SUSPENSIONS 105
4.2.3 P.J. Heikkinen, Yu.M. Bunkov, V.B. Eltsov, R. de Graaf, M. Krusius, and G.E. Volovik: BOSE-EINSTEIN CONDENSATION OF MAGNONS IN SUPERFLUID 3He-B 106
4.2.4 V. Heinonen, T. Hynninen, T. Ala-Nissilä and A. Foster: MD SIMULATIONS ON CUTTING ICE WITH A NANOSCALE WIRE USING 3D MERCEDES-BENZ MODEL 107

4.2.5 E. Hujala, A. Pulkkinen, E. Lähderanta, A.V. Lashkul and R. Laiho: FERROMAGNETISM IN CARBON NANOPOWDER 108

4.2.6 J. Juntunen and J. Merikoski: DIFFUSION BETWEEN EVOLVING INTERFACES 109

4.2.7 A. Kallonen, J.-P. Suuronen, M. Peura, E. Harjunmaa, I. Corfe, O. Manninen, J. Jernvall, K. Fagerstedt, P. Saranpää, A.-E. Lehesjoki, R. Serimaa and K. Hämäläinen: CHARACTERISATION OF BIOLOGICAL STRUCTURES BY X-RAY ABSORPTION MICROTOMOGRAPHY 110

4.2.8 L. Kanninen, K. Lahtonen, N. Jokinen, P. Jussila, O. Tarvainen, M. Kuzmin, M. Hirsimäki, and M. Valden: CHEMICAL AND STRUCTURAL CHARACTERIZATION OF TRIMESIC ACID ON Cu(100) AND O/Cu(100) STUDIED BY XPS AND STM 111

4.2.9 J. Kauttonen and J. Merikoski: RATCHET EFFECT FOR POLYMERS 112

4.2.10 S. Kilpeläinen, K. Kuitunen, F. Tuomisto and J. Slotte: THERMAL EVOLUTION OF VACANCY COMPLEXES IN n-TYPE $Si_{1-x}Ge$:P 113

4.2.11 A. Korolyuk, J. Kinnunen, and P. Törmä: DENSITY RESPONSE OF A STRONGLY INTERACTING TRAPPED FERMI GAS 114

4.2.12 M. Lahti, K. Pussi and M. Alatalo: DFT and LEED study of Sn/Cu(100) p(2×6) structures 115

4.2.13 K. Leppänen, Y. Wang, S. Andersson, R. Serimaa, H. Ren and B.H. Fei: X-RAY STUDY ON THE CELL WALL STRUCTURE OF MOSO BAMBOO 116

4.3 Poster session II, Friday 12 March 16:00-18:00 117

4.3.1 J. Lucenius, K. Leppänen, P. Penttilä, R. Serimaa, M. Peura P. Immerzeel, E. Mellerowicz: STUDY OF WILD POPULUS TREMULA L. X TREMULOIDES MICHX. SEEDLINGS USING WAXS AND X-RAY MICROTOMOGRAPHY 117

4.3.2 J.-M. Mäki, F. Tuomisto, M. von Kurnatowski, B. Bastek, M. Wieneke, T. Hempel, F. Bertram, A. Dadgar, J. Christen, A. Krost: VACANCY DEFECTS IN A- AND C-PLANE ALN THIN FILM LAYERS 118

4.3.3 R. Oja and R.M. Nieminen: MODELING CHARGE-IMBALANCED NaNbO3/SrTiO3 SUPERLATTICES 119

4.3.4 K. Pirkkalainen, J. Lucenius, A. Meriläinen, A. Salmi, A. Kallonen, M. Peura and R. Serimaa: MICROANALYSIS ON TRACHEIDS AND RAY PARENCHYMA CELLS OF FERTILISED NORWAY SPRUCE WOOD . . 120

4.3.5 H. Pitkänen, M. Alatalo, A. Puisto, M. Ropo, K. Kokko and L. Vitos: AB-INITIO STUDY OF MECHANICAL PROPERTIES OF AUSTENITIC STAINLESS STEEL ALLOYS 121

4.3.6 T. Pitkänen, S. Majaniemi and T. Ala-Nissila: A DATA BANK APPROACH TO MULTISCALE MODELLING OF MICROSTRUCTURE FORMATION IN POLYMER CASTING 122
4.3.7 A. Pohjonen, S. Fitzgerald, F. Djurabekova, K. Nordlund: DISLOCATIONS EMITTED FROM VOID UNDER STRESS - GROWTH ON SURFACE . . 123
4.3.8 Y. Senda, J. Blomqvist and R.M Nieminen: MULTISCALE SIMULATION FOR LIQUID POLYMER USING MD/CONTINUUM HYBRID METHOD 124
4.3.9 J.-P. Suuronen, P. Penttilä, S. Kirjoranta, M. Peura, K. Jouppila, M. Tenkanen, and R. Serimaa: X-RAY STUDIES ON THE PORE STRUCTURE OF BARLEY EXTRUDATES 125
4.3.10 T. Turpeinen, V. Koivu, M. Kataja and J. Timonen: PORE SPACE ANALYSIS OF HETEROGENEOUS POROUS MATERIALS USING X-RAY TOMOGRAPHY 126
4.3.11 T. H. Virtanen and E. V. Thuneberg: FERMI LIQUID THEORY APPLIED TO VIBRATING WIRE IN 3He-4He MIXTURES 127
4.3.12 K. Vörtler, C. Björkas, D. Terentyev, L. Malerba, and K. Nordlund: MOLECULAR DYNAMICS SIMULATIONS OF PRIMARY RADIATION DAMAGE IN Fe-Cr 128
4.3.13 M. Zelený, J. Hegedus, A. Foster, and R. M. Nieminen: FIRST PRINCIPLES STUDY OF DIFFUSION OF ATOMIC COPPER IN SILICON DIOXIDE . 129

5 Condensed matter: Electronic properties 131
5.1 Oral session I, Thursday 11 March 15:00-16:30 132
5.1.1 S. Auvinen, M. Alatalo, H. Haario, J-P. Jalava, and R-J. Lamminmäki: MULTISCALE MODELING OF TiO_2 NANOPARTICLES 132
5.1.2 G. Bårdsen, E. Tölö, and A. Harju: TUNABLE MAGNETISM IN QUANTUM RINGS 133
5.1.3 P. Havu, M.J. Hashemi, M. Kaukonen, E.T. Seppälä and R.M. Nieminen: ELECTRON TRANSPORT IN METALLIC AND SEMICONDUCTING NANOTUBE CROSS JUNCTIONS 134
5.1.4 X. Lin, N. Nilius, M. Sterrer, P. Koskinen, H. Häkkinen, and H.-J. Freund: CHARACTERIZING THE PERIPHERY ATOMS OF Au ISLANDS ON MgO THIN FILMS 135
5.1.5 V. Kotimäki and E. Räsänen: MANY-ELECTRON AHARONOV-BOHM EFFECT IN QUANTUM RINGS 136
5.1.6 O. Vänskä, M. Kira, and I. Tittonen: MANIPULATING OPTICAL ACTIVITY OF EXCITONS IN SEMICONDUCTOR QUANTUM RINGS 137
5.2 Oral session II, Saturday 13 March 9:00-10:30 138

5.2.1 J. Akola and R.O. Jones: DENSITY FUNCTIONAL SIMULATIONS OF PHASE-CHANGE MATERIALS: CHARACTERIZATION OF AMORPHOUS PHASES 138
5.2.2 E. Holmström, M. Hakala and K. Nordlund: AMORPHOUS DEFECT CLUSTERS OF PURE SI AND THE TYPE INVERSION IN SI DETECTORS . . 139
5.2.3 O. O. Kit and P. Koskinen: FROM THE REVISION OF BLOCH'S THEOREM TO SPHERICAL DISTORTIONS OF SINGLE- AND MULTILAYER GRAPHENE 140
5.2.4 I. Makkonen, A. Snicker, M. J. Puska, J.-M. Mäki and F. Tuomisto: INTERFACE SENSITIVITY OF POSITRONS IN POLAR SEMICONDUCTOR HETEROSTRUCTURES 141
5.2.5 O.-P. Saira, M. Möttönen, J. P. Pekola: EFFECT OF ENVIRONMENTAL FLUCTUATIONS ON SINGLE-ELECTRON PROCESSES IN HYBRID TUNNEL JUNCTIONS 142
5.2.6 A. Sakko, S. Galambosi, J. Inkinen, J. Röntynen, T. Pylkkänen, M. Hakala, S. Huotari, and K. Hämäläinen: TOWARDS IN SITU SPECTROSCOPY OF CHEMICAL REACTIONS: INELASTIC X-RAY SCATTERING FROM GASEOUS N_2O, CO_2, AND N_2 143
5.3 Poster session I, Thursday 11 March 16:30-18:30 144
5.3.1 J. Blomqvist and P. Salo: MODELING OF POLYMER-METAL HYBRID MATERIALS 144
5.3.2 A. Gulans, O. Pakarinen, M. Mura, T. Thonhauser, M. Puska, L. Kantorovich and A. Foster: ROLE OF THE VAN DER WAALS INTERACTION IN FORMATION OF SELFASSEMBLED STRUCTURES 145
5.3.3 V. Havu, V. Blum, P. Havu and M. Scheffler: EFFICIENT GRID-BASED OPERATIONS FOR ALL-ELECTRON ELECTRONICSTRUCTURE CALCULATION USING NUMERIC BASIS FUNCTIONS 146
5.3.4 M. Kuisma, J. Ojanen, J. Enkovaara and T. T. Rantala: AN EFFICIENT APPROACH TO THE BAND GAP PROBLEM IN DFT 147
5.3.5 O. Kupiainen and A. Harju: LAGRANGE MESH METHOD APPLIED TO QUANTUM DOTS 148
5.3.6 L. Lehtovaara, V. Havu and M. Puska: TIME-DEPENDENT DENSITY FUNCTIONAL THEORY WITH FINITE ELEMENTS 149
5.3.7 V. Mäkinen, H. Häkkinen and P. Koskinen: MODELING THIOLATE-PROTECTED Au SUPERATOMS WITH DENSITYFUNCTIONAL TIGHT-BINDING . . 150
5.3.8 P. Myöhänen, A. Stan, G. Stefanucci, A-M. Uimonen and R. van Leeuwen: TIME-DEPENDENT QUANTUM TRANSPORT WITH THE KADANOFF-BAYM EQUATIONS 151

5.3.9 L.E. Oikkonen, M.G. Ganchenkova, A.P. Seitsonen, and R.M. Nieminen: HYBRID FUNCTIONAL STUDY OF VACANCY PROPERTIES IN $CuInSe_2$ AND $CuGaSe_2$ 152
5.3.10 M. Prunnila and J. Meltaus: ACOUSTIC PHONON TUNNELING AND HEAT TRANSPORT BETWEEN PIEZOELECTRIC BODIES 153
5.3.11 A. Putaja and E. Räsänen: COHERENT CONTROL OF CHARGE IN A DOUBLE QUANTUM DOT 154
5.3.12 E. Räsänen, S. Pittalis, and C. R. Proetto: UNIVERSAL EXTENSION TO THE BECKE-JOHNSON EXCHANGE POTENTIAL 155
5.3.13 S. Sakiroglu and E. Räsänen: LOCAL DENSITY FUNCTIONAL FOR THE ELECTRONIC CORRELATION 156
5.3.14 J. Särkkä and A. Harju: CHARGE DYNAMICS IN TWO-ELECTRON QUANTUM DOTS 157
5.4 Poster session II, Friday 12 March 16:00-18:00 158
5.4.1 P. Belova, M. Safonchik, K.B. Traito, E. Lähderanta: MAGNETIC FIELD DEPENDENCE OF VORTEX CORE SIZE IN PNICTIDE SUPERCONDUCTORS 158
5.4.2 P. Häkkinen, A. Fay, P. Lähteenmäki, and P. Hakonen: WIDE-BAND SUPERCONDUCTING CARBON NANOTUBE FET 159
5.4.3 E. Holm, S. Majumdar, H. S. Majumdar , R. Österbacka: THE ROLE OF INJECTION AND CHARGE-CARRIER CONCENTRATION ON ORGANIC MAGNETORESISTANCE 160
5.4.4 F. Jansson, A. V. Nenashev, S. D. Baranovskii, F. Gebhard, R. Österbacka: EFFECT OF ELECTRIC FIELD ON DIFFUSION IN DISORDERED MATERIALS 161
5.4.5 M. Palosaari, K. Kinnunen and I. Maasilta: THERMAL MODELS OF SUPERCONDUCTING TRANSITION-EDGE SENSORS 162
5.4.6 M. Pesonen, S. Majumdar, H. S. Majumdar and R. Österbacka: FABRICATION AND CHARACTERIZATION OF GRAPHENE-BASED SPIN VALVES . . 163
5.4.7 F. S. Pettersson, N. Björklund and R. Österbacka: LIGHT, WATER AND ELECTRICAL PROPERTIES OF LISICON BASED Al2O3 OFETS 164
5.4.8 C. Rauch, F. Tuomisto, S. Eisermann, S. Lautenschläger, B. K. Meyer, M. R. Wagner, and A. Hoffmann: CHARACTERIZATION OF DEFECTS IN HOMOEPITAXIAL NON-POLAR ZNO:N GROWN BY CVD 165
5.4.9 S. Seppälä, E. Häkkinen, M. J. Alava, V. Ermolov, E. T. Seppälä: PROPERTIES OF RANDOM NETWORKS OF CARBON NANOTUBE BUNDLES 166
5.4.10 A. Stan, A.-M. Uimonen, P. Myöhänen, R. van Leeuwen: NONEQUILIBRIUM GREEN FUNCTION APPROACH TO ELECTRONIC DYNAMICS IN FINITE INHOMOGENEOUS SYSTEMS 167

5.4.11 A.-M. Uimonen, A. Stan, P. Myöhänen, R. van Leeuwen: REAL-TIME SWITCHING BETWEEN MULTIPLE STEADY-STATES IN QUANTUM TRANSPORT 168
5.4.12 A. Fay, J. K. Viljas, R. Danneau, F.Wu, M. Y. Tomi, J.Wengler, M.Wiesner, and P. J. Hakonen: CONDUCTIVITY, SHOT NOISE, AND HOT PHONONS IN BILAYER GRAPHENE 169
5.4.13 A. Fay, M. Tomi, P. Lähteenmäki, J. Viljas and P. Hakonen: SHOT NOISE IN SUPERCONDUCTOR-GRAPHENE SUPERCONDUCTOR JUNCTIONS . 170
5.4.14 V. Virkkala and V. Havu: CORRECTIONS FOR CHARGED-DEFECT SUPERCELL DENSITY FUNCTIONAL CALCULATIONS 171
5.4.15 A. Zubiaga, F. Tuomisto and M. Puska: MODELLIZATION OF POSITRONIUM IN SOFT MATTER 172

6 Particle and nuclear physics **173**
6.1 Oral session I, Thursday 11 March 15:00-16:30 174
6.1.1 F. Garcia, R. Janik, M. Kalliokoski, R. Lauhakangas, A. Numminen, M. Pikna, B. Sitar, P. Strmen, I. Szarka and E. Tuominen: STATUS OF THE GEM-TPC DETECTORS FOR THE BEAM DIAGNOSTICS OF THE SUPER-FRS . . 174
6.1.2 A. Kankainen, V.-V. Elomaa, T. Eronen, J. Hakala, A. Jokinen, V.S. Kolhinen, I.D.Moore, J. Rissanen, A. Saastamoinen and J. Äystö: MASSES FOR NUCLEAR ASTROPHYSICS WITH JYFLTRAP 175
6.1.3 I.D. Moore: LASER SPECTROSCOPY: ACTIVITIES AT ISOLDE AND PROSPECTS AT THE FUTURE FAIR FACILITY 176
6.1.4 M.T. Mustonen and J. Suhonen: NEW CHALLENGES BEYOND LOW BETA-DECAY Q VALUES 177
6.1.5 P. Peura, C. Scholey, T. Bäck, D. O'Donnell, P. T. Greenlees, U. Jakobsson, P. Jones, D. T. Joss, D. S. Judson, R. Julin, S. Juutinen, S. Ketelhut, M. Labiche, M. Leino, M. Nyman, R. D. Page, P. Rahkila, P. Ruotsalainen, M. Sandzelius, P. J. Sapple, J. Sarén, J. Simpson, J. Thomson, J. Uusitalo, and H. V. Watkins: RECOIL DECAY TAGGING STUDIES OF ^{173,175}Pt 178
6.1.6 P. Rahkila, P. Greenlees, U. Jakobsson, P. Jones, R. Julin, S. Juutinen, H. Koivisto, M. Leino, P. Nieminen, M. Nyman, P. Peura, T. Ropponen, P. Ruotsalainen, J. Sarén, C. Scholey, J. Sorri, J. Uusitalo, D.G. Jenkins, O.J. Roberts, A.G. Tuff, R. Wadsworth, J. Pakarinen, C. Gray-Jones, P. Papadakis, S. Paschalis, M. Petri, M. Bender, P.-H. Heenen, K. Heyde: STUDY OF ^{180}Pb 179
6.2 Oral session II, Friday 12 March 14:30-16:00 180
6.2.1 J. Rak: NEWS FROM ALICE COLLABORATION AT CERN LHC 180
6.2.2 M. Antola, M. Heikinheimo, F. Sannino and K. Tuominen: UNNATURAL ORIGIN OF FERMION MASSES FOR TECHNICOLOR 181

6.2.3 J. Sarkamo, T. Enqvist, J. Joutsenvaara, J. Karjalainen, P. Kuusiniemi, K. Loo, L. Olanterä, T. Räihä, P. Jones, T. Kalliokoski, M. Slupecki, W.H. Trzaska, A. Virkajärvi, L. Bezrukov, L. Inzhechik, B. Lubsandorzhiev, V. Petkov, H. Fynbo: PHYSICS TOPICS FOR EMMA 182

6.2.4 L. Wendlandwith A. Attikis, R. Kinnunen, M.J. Kortelainen, S. Lehti, and A. Nikitenko: SEARCH FOR THE LIGHT CHARGED MSSM HIGGS BOSON WITH HADRONIC FINAL STATE IN THE CMS EXPERIMENT AT THE CERN LHC 183

6.2.5 M. Herranen, K. Kainulainen and P.M. Rahkila: QUANTUM BOLTZMANN EQUATIONS FROM cQPA 184

6.2.6 A. Tranberg, A. Hernandez, T. Konstandin, M. G. Schmidt: BARYOGENESIS FROM STANDARD MODEL CP-VIOLATION 185

6.3 Oral session III, Saturday 13 March 9:00-10:30 186

6.3.1 J. Sorri, P. Greenlees, P. Jones, P. Rahkila, P. Peura, R. Julin, S. Juutinen, P. Nieminen, M. Nyman, S. Ketelhut, M. Leino, J. Uusitalo, C. Scholey, J. Sarén, U. Jakobsson, P. Ruotsalainen, A. Herzan, K. Hauschild, A. Lopez-Martens, R.-D. Herzberg, P. Papadakis, J. Pakarinen, P.A. Butler, R.D. Page, E. Parr, J.R. Cresswell, D.A. Seddon, J. Thornhill, D. Wells, D. Cox, J. Simpson, P.J. Coleman-Smith, I.H. Lazarus, S.C. Letts, V.F.E. Pucknell: AN OVERVIEW OF THE SAGE SPECTROMETER 186

6.3.2 M. Norrby: ALPHA CLUSTERS IN ^{32}S, ^{34}S AND ^{40}Ca 187

6.3.3 E. Ydrefors and J. Suhonen: THEORETICAL DESCRIPTION OF NEUTRINO-NUCLEUS SCATTERING ON THE STABLE MOLYBDENUM ISOTOPES 188

6.3.4 A.-P. Leppänen: DETERMINING ^{7}BE PRODUCTION RATE BY COSMIC RAYS USING WATER TARGET 189

6.3.5 H. Holopainen, H. Niemi and K.J. Eskola: ELLIPTIC FLOW IN HYDRODYNAMICS WITH FLUCTUATING INITIAL CONDITIONS 190

6.3.6 A. Hietanen, T. Karavirta, A-M. Mykkänen, J. Rantaharju, K. Rummukainen and K. Tuominen: SU(2) GAUGE THEORY WITH TWO ADJOINT DIRAC FLAVORS ON THE LATTICE 191

6.4 Poster session I, Thursday 11 March 16:30-18:30 192

6.4.1 P. Aarnio, A.A. Andreev and R. Salomaa: FEASIBILITY STUDIES OF LASER-ENHANCED RADIOACTIVE DECAY OF NUCLIDES 192

6.4.2 O. Antipin and K. Tuominen: RESIZING THE CONFORMALWINDOW: A BETA FUNCTION ANSATZ 193

6.4.3 J. Auvinen, K. J. Eskola and T. Renk: MONTE-CARLO SIMULATION FOR ELASTIC ENERGY LOSS OF HIGHENERGY PARTONS IN A HYDRODYNAMICAL BACKGROUND 194

6.4.4 T. Eronen, V.-V. Elomaa, J. Hakala, J. C. Hardy, A. Jokinen, A. Kankainen, I.D. Moore, M. Reponen, J. Rissanen, A. Saastamoinen, C. Weber and J. Äystö: HIGH-PRECISION QEC VALUES OF SUPERALLOWED BETA EMITTERS FOR TESTING THE STANDARD MODEL 195

6.4.5 A. Ferrantelli: CONSTRAINTS ON THE REHEATING TEMPERATURE FROM GRAVITINO DARK MATTER PRODUCTION AFTER INFLATION . . . 196

6.4.6 V. Föhr, A. Bacquias, V. Henzl, A. Kelic, V. Ricciardi, K.-H. Schmidt, J. Äystö: HIGH-PRECISION MOMENTUM MEASUREMENTS OF PROJECTILE FRAGMENTS IN ^{112,124}SN + ^{112,124}SN COLLISIONS AT 1 AGEV 197

6.4.7 J. Hakala, J. Rissanen, V.-V. Elomaa, T. Eronen, A. Jokinen, J. Kurpeta, I. D. Moore, A. Kankainen, P. Karvonen, A. Plochocki, H. Penttilä, S. Rahaman, M. Reponen, A. Saastamoinen, J. Szerypo, W. Urban, C. Weber and J. Äystö: NUCLEAR STRUCTURE STUDIES OF NEUTRON-RICH NUCLEI PERFORMED BY JYFLTRAP 198

6.4.8 P. Heikkinen: THE JYVÄSKYLÄ MCC30/15 CYCLOTRON PROJECT 199

6.4.9 T. Kähärä and K. Tuominen: EFFECTIVE MODELS OF TWO-FLAVOR QCD: FROM SMALL TOWARDS LARGE m_q 200

6.4.10 T. Eronen, J. Hakala, A. Jokinen, A. Kankainen, P. Karvonen, V. S. Kolhinen, I.D. Moore, H. Penttilä, J. Rissanen, M. Reponen, A. Saastamoinen, V. Sonnenschein and J. Äystö: THE PROSPECTS OF THE IGISOL SHIFT . . 201

6.4.11 S. Kasi: EXPONENTIALLY DECAYING NUMBER ALWAYS OBEYS A BINOMIAL DISTRIBUTION 202

6.4.12 V.S. Kolhinen, V.-V. Elomaa, T. Eronen, J. Hakala, A. Jokinen, M. Kortelainen, J. Suhonen, J. Äystö: Accurate Q value for the ^{74}Se double-electron-capture decay 203

6.4.13 S. Kurki: THE TRANSVERSE SHAPE OF THE ELECTRON 204

6.4.14 T. Räihä, L. Bezrukov, T. Enqvist, H. Fynbo, L. Inzhechik, P. Jones, J. Joutsenvaara, T. Kalliokoski, J. Karjalainen, P. Kuusiniemi, K. Loo, B. Lubsandorzhiev, L. Olanterä, V. Petkov, J. Sarkamo, M. Slupecki, W.H. Trzaska, A. Virkajärvi: TRACK RECONSTRUCTION AND VISUALISATION IN EMMA 205

6.4.15 A. Räty: HOMOGENISATION OF GROUP CONSTANTS IN REACTOR PHYSICS 206

6.5 Poster session II, Friday 12 March 16:00-18:00 207

6.5.1 S. Rinta-Antila, P.T. Greenlees, A. Jokinen, R. Julin, V.S. Kolhinen, M. Leino, I.D. Moore, H. Penttilä, J. Sarén, C. Scholey and J. Äystö: FAIR ACTIVITIES AT JYFL; HISPEC/DESPEC, MATS AND LASPEC 207

6.5.2 P. Ruotsalainen, C. Scholey, B.S. Nara Singh, R. Wadsworth, D.G. Jenkins, C.J Barton, M.A. Bentley, L. Bianco, J.E. Brown, P.J. Davies, P.T. Greenlees, U. Jakobsson, P. Jones, D.T. Joss, R. Julin, S. Juutinen, S. Ketelhut, M. Leino, M. Nyman, R.D. Page, P. Peura, P. , P. Sapple, J. Sarén, J. Sorri, M.J. Taylor, J. Uusitalo: RECOIL-BETA TAGGING STUDY OF N=Z NUCLEUS 66As . 208

6.5.3 A. Saastamoinen, L. Trache, A. Banu, M. A. Bentley, T. Davinson, V. E. Iacob, D. Jenkins, A. Jokinen, M. McCleskey, B. Roederb E. Simmons, G. Tabacaru, R. E. Tribble, P. J. Woods, J. Äystö: EXOTIC DECAYS FOR ASTROPHYSICS BY IMPLANTATION TECHNIQUE 209

6.5.4 J. Sarén, J. Uusitalo and M. Leino: MEASURING ABSOLUTE TRANSMISSION VALUES OF THE RITU GAS-FILLED SEPARATOR 210

6.5.5 J. Alanen, E. Keski-Vakkuri and V. Suur-Uski: ASPECTS OF HOLOGRAPHIC QUANTUM HALL TRANSITION 211

6.5.6 W. H. Trzaska: FINNISH KNOW-HOW BEHIND THE FIRST PUBLISHED LHC EVENT 212

6.5.7 E. Edelmann, K. Happonen, J. Klem, J. Koivumäki, T. Lindén, A. Pirinen and J. Välimaa: DISTRIBUTED DATA-ANALYSIS WITH ADVANCED RESOURCE CONNECTOR MIDDLEWARE IN THE COMPACT MUON SOLENOID EXPERIMENT 213

6.5.8 M. Vepsäläinen: HEAVY QUARK-ANTIQUARK POTENTIALS IN HOT QCD 214

6.5.9 T. Enqvist, J. Joutsenvaara, T. Kalliokoski, P. Kuusiniemi, K. Loo, J. Maalampi, G. Nuijten, J. Roinisto, K. Rummukainen, T. Räihä, J. Sarkamo, W.H. Trzaska: LAGUNA – LARGE UNDERGROUND INFRASTRUCTURES FOR NEUTRINO ASTROPHYSICS AND PROTON DECAY 215

6.5.10 T. Kalliokoski, L. Bezrukov, T. Enqvist, H. Fynbo, L. Inzhechik, P. Jones, J. Joutsenvaara, J. Karjalainen, P. Kuusiniemi, K. Loo, B. Lubsandorzhiev, L. Olanterä, V. Petkov, T. Räihä, J. Sarkamo, M. Slupecki, W.H. Trzaska and A. Virkajärvi: KNEE IN COSMIC RAY PHYSICS 216

6.5.11 J. Karjalainen, T. Enqvist, J. Joutsenvaara, P. Kuusiniemi, K. Loo , L. Olanterä,T. Räihä, J. Sarkamo P. Jones, T. Kalliokoski, M. Slupecki, W.H. Trzaska, A. Virkajärvi, L. Bezrukov, L. Inzhechik, B. Lubsandorzhiev, V. Petkov, H. Fynbo: SIMULATIONS OF SCINTILLATOR RESPONSE FOR EMMA-EXPERIMENT 217

6.5.12 K. Loo, T. Enqvist and W. H. Trzaska: REACTOR NEUTRINOS AS A BACKGROUND FOR LOW ENERGY NEUTRINO ASTRONOMY IN THE LAGUNA-PROJECT 218

6.5.13 T. Räihä, T. Enqvist, J. Sarkamo, W.H. Trzaska: EVENT-BY-EVENT BASED COSMIC-RAY PHYSICS IN LHC EXPERIMENTS 219

6.5.14 J. Sarkamo, T. Enqvist, J. Joutsenvaara, J. Karjalainen, P. Kuusiniemi, K. Loo, L. Olanterä, T. Räihä, P. Jones, T. Kalliokoski, M. Slupecki, W.H. Trzaska, A. Virkajärvi, L. Bezrukov, L. Inzhechik, B. Lubsandorzhiev, V. Petkov, H. Fynbo: COSMIC-RAY EXPERIMENT EMMA: UNDERGROUND MUON TRACKING UNIT 220

7 Nanophysics and new materials 221

7.1 Oral session I, Thursday 11 March 15:00-16:30 222

7.1.1 L. Costelle, T.T. Järvi, M. Räisänen, J. Räisänen: FORMATION MECHANISMS OF GOLD CLUSTERS PRODUCED BY MAGNETRON SPUTTERING ON THIOL SELF-ASSEMBLEDMONOLAYERS 222

7.1.2 A. Kaskela, A. G. Nasibulin, M. Y. Zavodchikova, B. Aitchison, Y. Tian, Z. Zhu, D. P. Brown and E. I. Kauppinen: QUICK AND EASY PREPARATION OF CONDUCTIVE AND TRANSPARENT SWCNTFILMS 223

7.1.3 J.T. Korhonen, T. Verho, P. Rannou, and O. Ikkala: SELF-ASSEMBLY AND HIERARCHIES IN PYRIDINE-CONTAINING HOMOPOLYMERS AND BLOCK COPOLYMERS WITH HYDROGENBONDED CHOLESTERIC SIDE-CHAINS 224

7.1.4 S. Paavilainen, Tomasz Róg, J. Järvinen and I. Vattulainen: MODELING CELLULOSE NANOFIBRILS WITH NON-CRYSTALLINE PARTS 225

7.1.5 P. Sievilä, N. Chekurov and I. Tittonen: NANOSCALE PATTERNING OF SILICON WITH FOCUSED ION BEAM AND ANISOTROPIC WET ETCHING 226

7.1.6 J. Vapaavuori, A. Priimagi and M. Kaivola: LIGHT-INDUCED SURFACE PATTERNING OF DYE-POLYMER THIN FILMS 227

7.2 Oral session II, Saturday 13 March 9:00-10:30 228

7.2.1 P. Myllyperkiö, O. Herranen, J. Rintala, H. Jiang, A. Johansson, P.R. Mudimela, Z. Zhu, A.G. Nasibulin, E.I. Kauppinen, M. Ahlskog and M. Pettersson: FEMTOSECOND FOUR-WAVE-MIXING SPECTROSCOPY OF FREELY SUSPENDED AND FULLY CHARACTERIZED SINGLE-WALL CARBON NANOTUBES 228

7.2.2 T.K. Hakala, V. Linko, A.-P. Eskelinen, J.J. Toppari, A. Kuzyk, and P. Törmä: FIELD INDUCED NANOLITHOGRAPHY (FINAL) 229

7.2.3 V. Linko, A. Kuzyk, B. Yurke, S.-T. Paasonen, P.Törmä, and J.J. Toppari: CHARACTERIZATION OF THE CONDUCTANCE MECHANISMS OF DNA ORIGAMI BY AC IMPEDANCE SPECTROSCOPY 230

7.2.4 M. Nevala, I. Maasilta, K. Senapati, and R. Budhani: DC CHARACTERISTICS OF NbN/TaN/NbN SNS JOSEPHSON JUNCTIONS GROWN BY PULSED LASER ABLATION 231

7.2.5 R. H. A. Ras and I. Díez: FEW-ATOM SILVER CLUSTERS AS FLUOROPHORES: COLOUR TUNABILITY AND ELECTROCHEMILUMINESCENCE . . . 232

7.2.6 F. X. Wang, F. J. Rodriguez, W. M. Albers, and M. Kauranen: ENHANCED BULK-TYPE MULTIPOLAR SECOND-HARMONIC GENERATION FROM THIN METAL FILMS 233

7.3 Poster session I, Thursday 11 March 16:30-18:30 234

7.3.1 A. Aho, V.-M. Korpijärvi, A. Tukiainen, V. Polojärvi, M. Guina and M. Pessa: MOLECULAR BEAM EPITAXY AND ANNEALING OF 1 eV GaInNAs FOR HIGH-EFFICIENCY MULTI-JUNCTION SOLAR CELLS 234

7.3.2 S. Chaudhuri, M. R. Nevala and I. J. Maasilta: HIGH PERFORMANCE MATERIAL FOR SINIS TUNNEL JUNCTION THERMOMETRY AND COOLING 235

7.3.3 Z. Sun, I. Swart, W. Evers, D. Vanmaekelbergh and P. Liljeroth: HOLE-INDUCED ELECTRON TUNNELING IN CORE-SHELL QUANTUM DOTS 236

7.3.4 A. Harjunmaa, K. Nordlund, A. Stukowski and K. Albe: STRUCTURE OF SI/GE NANOCLUSTERS AS STUDIED BYMOLECULAR DYNAMICS AND SEMI-GRAND-CANONICAL MONTE CARLO METHODS 237

7.3.5 M.J. Hashemi and M.J. Puska: THE EFFECT OF CLUSTERING AND PERIODICITY OF ADSORBATE ATOMS ON ELECTRONIC PROPERTIES OF CARBON NANOTUBES 238

7.3.6 O. Herranen, K. Hannula, A. Johansson, T. Lahtinen, M. Ahlskog: FABRICATION OF FREELY SUSPENDED CARBON NANOTUBE AND GRAPHENE DEVICES FOR ADVANCED APPLICATIONS 239

7.3.7 L. Korhonen, Qi Hang Qin, and S. van Dijken: FABRICATION OF ALL-OXIDE TUNNEL JUNCTIONS WITH SPINFILTERING FERRITE TUNNEL BARRIERS 240

7.3.8 T. Haatainen, T. Mäkelä and J. Ahopelto: 3D UV-STAMPS BY COMBINED THERMAL AND UV-IMPRINTING 241

7.3.9 T. Mäkelä, T. Haatainen, J. Ahopelto and Y. Kawaguchi: ROLL-TO-ROLL UV NANOIMPRINTING 242

7.3.10 S. Malola, H. Häkkinen and P. Koskinen: INVESTIGATIONS OF NON-IDEAL GRAIN BOUNDARIES OF GRAPHENE 243

7.3.11 K. Mustonen, A. Nasibulin and E. Kauppinen: A PHENOMENOLOGICAL STUDY OF CARBON NANOTUBE GROWTH IN HOT WIRE GENERATOR UNDER CO / CO_2 ATMOSPHERE 244

7.3.12 O. H. Pakarinen, M. Backholm, F. Djurabekova and K. Nordlund: NANOCLUSTER MODIFICATION BY SWIFT HEAVY ION TRACKS, STUDIED WITH MOLECULAR DYNAMICS 245

7.3.13 A. Schramm, A. Tukiainen, J. Tommila, V. Polojärvi, T.V. Hakkarainen, A. Aho, M. Guina, and M. Dumitrescu: GROWTH STUDIES OF SELF-ASSEMBLED InAs QUANTUM DOTS ON PATTERNED SUBSTRATES . . . 246
7.4 Poster session II, Friday 12 March 16:00-18:00 247
7.4.1 M. Ahlskog and J. Lievonen: LATERAL FORCES AND INFLUENCE OF HUMIDITY IN ATOMIC FORCE MICROSCOPY 247
7.4.2 H. Husu, J. Mäkitalo, J. Laukkanen, M. Kuittinen, J. Turunen, and M. Kauranen: RESONANCES IN L-SHAPED GOLD NANOPARTICLES 248
7.4.3 R. Khakimov, A. Shevchenko, A. Havukainen, M. Kaivola: LEVITATION OF COLLOIDAL PARTICLES ON AN EVANESCENT OPTICAL WAVE . . . 249
7.4.4 T. Lahtinen and S. van Dijken: STRONG COUPLING BETWEEN FERROELECTRIC AND FERROMAGNETIC DOMAINS IN THIN Fe FILMS ON $BaTiO_3$ 250
7.4.5 J. Puustinen and J. Lappalainen: MECHANICAL PROPERTIES OF PZT THIN FILMS STUDIED USING NANOINTENDATION TECHNIQUE 251
7.4.6 A. Lindell, A. Latvala, T. Nevanpää, L. Taskinen and J. Viiri: NANOSCHOOL DEVELOPS INQUIRIES FOR SCIENCE EDUCATION 252
7.4.7 D. Mtsuko and M. Ahlskog: NONLINEAR TRANSPORT IN POLYPYRROLE NANOLAYERS ON DISCONTINUOUS ULTRATHIN GOLD FILMS . . . 253
7.4.8 M. Zdanowicz, S. Kujala, H. Husu, and M. Kauranen: EFFECTIVE MEDIUM MULTIPOLAR TENSOR ANALYSIS OF SECONDHARMONIC GENERATION FROM METAL NANOPARTICLES 254

8 Nanophysics and quantum matter 255
8.1 Oral session, Friday 12 March 14:30-16:00 256
8.1.1 J. P. Pekola, V. Brosco, M. Möttönen, P. Solinas and A. Shnirman: DECOHERENCE IN ADIABATIC QUANTUM EVOLUTION - APPLICATION TO COOPER PAIR PUMPING 256
8.1.2 J. Tuorila, M. Silveri, M. Sillanpää, E. Thuneberg, Y. Makhlin and P. Hakonen: EXTREME DRIVING OF A JOSEPHSON QUBIT IN CIRCUIT CAVITY QUANTUM ELECTRODYNAMICS 257
8.1.3 J.-M. Pirkkalainen, P. Solinas, J. P. Pekola, and M. Möttönen: PROPOSAL FOR A GROUND STATE GEOMETRIC QUBIT IN SUPERCONDUCTING CIRCUITS 258
8.1.4 F. Giazotto, J.T. Peltonen, M. Meschke and J.P. Pekola: SUPERCONDUCTING QUANTUM INTERFERENCE PROXIMITY TRANSISTOR 259
8.1.5 J.K. Julin, P.J. Koppinen and I.J. Maasilta: REDUCING 1/F NOISE IN AL-ALO_X-AL TUNNEL JUNCTIONS BY THERMAL ANNEALING 260

8.1.6 T.K. Hakala, J.J. Toppari, M. Pettersson, H. Kunttu, A. Kuzyk, and P. Törmä: VACUUM RABI SPLITTING AND STRONG-COUPLING DYNAMICS FOR SURFACE-PLASMON POLARITONS AND RHODAMINE 6G MOLECULES 261
8.2 Poster session, Friday 12 March 16:00-18:00 262
8.2.1 V. Apaja, H. Lauter and E. Krotscheck: LOCALIZED SUPERFLUID PHASESWITHIN SOLID HELIUM 262
8.2.2 K. Gloos and E. Tuuli: SIZE-DEPENDENCE OF THE KONDO EFFECT IN NANOCONTACTS OF THE PURE METALS 263
8.2.3 T.V. Hakkarainen, A. Schramm, A. Tukiainen, R. Ahorinta, and M. Guina: LATERAL ORDERING OF SELF-ASSEMBLED InAs QUANTUM DOTS ON STRAINED GaInP 264
8.2.4 S. Kafanov, S.J. MacLeod, and J.P. Pekola: FLUCTUATIONS OF TEMPERATURE IN A SMALL METALLIC PARTICLE 265
8.2.5 E. Tuuli and K. Gloos: SUPERCONDUCTIVITY IN THE FERROMAGNETICMETALS Co, Ni AND Fe 266
8.2.6 N. Zen, T. Isotalo and I. Maasilta: FABRICATION OF PHONONIC CRYSTALS WITH NORMAL METAL-INSULATOR-SUPERCONDUCTOR (NIS)TUNNEL JUNCTION THERMOMETERS 267

9 Atomic and molecular physics 269
9.1 Oral session, Friday 12 March 14:30-16:00 270
9.1.1 M.O.J. Heikkinen, F. Massel, J. Kajala, M.J. Leskinen, G.-S.Paraoanu and P. Törmä: SPIN ASYMMETRIC JOSEPHSON EFFECT 270
9.1.2 E. Itälä, D.T. Ha, K. Kooser, S. Granroth and E. Kukk: PHOTOFRAGMENTATION OF CORE IONIZED MOLECULES 271
9.1.3 P. Kuopanportti, E. Lundh, J. A. M. Huhtamäki, V. Pietilä, and M. Möttönen: DYNAMICS OF GIANT VORTICES IN DILUTE BOSE-EINSTEIN CONDENSATES 272
9.1.4 S. Maniscalco, F. Francica, and F. Plastina: OFF-RESONANT QUANTUM ZENO AND ANTI-ZENO EFFECTS ON THE ENTANGLEMENT 273
9.1.5 P. Manninen: PROSPECTS OF EMERGING PROCESSOR TECHNOLOGIES IN COMPUTATIONAL MOLECULAR SCIENCE 274
9.1.6 I. Kylänpää and T.T. Rantala: QMC SIMULATION OF THERMAL DISSOCIATION OF DIPOSITRONIUM 275
9.2 Poster session, Friday 12 March 16:00-18:00 276
9.2.1 P. Haikka and S. Maniscalco: DRIVEN QUBIT IN A STRUCTURED RESERVOIR 276

9.2.2 R. Vasile, S. Olivares, M.G.A. Paris and S. Maniscalco: CONTINUOUS VARIABLE ENTANGLEMENT DYNAMICS IN STRUCTURED RESERVOIRS 277
9.2.3 J. Kajala and P. Törmä: DYNAMICS OF ONE DIMENSIONAL FERMI GASES 278
9.2.4 L. Mazzola, J. Piilo and S. Maniscalco: PHASE TRANSITION BETWEEN CLASSICAL AND QUANTUM DECOHERENCE 279
9.2.5 J. Paavola and S. Maniscalco: DECOHERENCE CONTROL IN DIFFERENT ENVIRONMENTS 280
9.2.6 M. Borrelli, N. Piovella, M.G.A. Paris: QUANTUM PROPERTIES OF A THREE-LEVEL SUBRADIANT SYSTEM 281
9.2.7 I. Juurinen, M. Hakala, S. Galambosi, A. G. Anghelescu-Hakala and K. Hämäläinen: SELF-ASSEMBLY OF THERMALLY SWITCHABLE POLYMER p(NIPAM) 282
9.2.8 V. Keränen, E. Keski-Vakkuri, S. Nowling and K. P. Yogendran: SOLITONS IN A HOLOGRAPHIC MODEL OF A SUPERFLUID 283
9.2.9 J. Lehto and K.-A. Suominen: APPROXIMATIVE APPROACHES TO THE PARABOLIC MODEL 284
9.2.10 L. Nykänen, J. Andersin and K. Honkala: SURFACE AND SUBSURFACE C ON Pd(111) AND Pd(211) SURFACES: A COMPUTATIONAL STUDY . . 285
9.2.11 S. Parviainen, F. Djurabekova, K. Nordlund: IMPLEMENTATION OF ELECTRONIC PROCESSES INTO MOLECULAR DYNAMICS SIMULATIONS OF NANOSCALE METAL TIPS UNDER ELECTRIC FIELDS 286
9.2.12 H.-P. Breuer, E.-M. Laine, and J. Piilo: MEASURE FOR THE NON-MARKOVIANITY OF QUANTUM PROCESSES 287
9.2.13 J. Schultz: DENSITY MATRIX RECONSTRUCTION FROM DISPLACED PHOTON NUMBER DISTRIBUTIONS 288

Industrial exhibition **299**

0 Plenary sessions

0.1 Plenary session I, Thursday 11 March 13:00-14:30
0.2 Plenary session II, Friday 12 March 9:00-10:30
0.3 Plenary session III, Friday 12 March 11:00-13:15
0.4 Plenary session IV, Saturday 13 March 11:00-12:30

X-RAY TOMOGRAPHY OF MATERIALS

Philip Withers

School of Materials
The University of Manchester
PO Box 88, Manchester M60 1QD
United Kindom

LHC – NEW ERA IN HIGH ENERGY PHYSICS

J. Tuominiemi

Helsinki Institute of Physics
POB 64, FI-00014 University of Helsinki
Finland

The Large Hadron Collider at CERN started its operation at the end of 2009 with the collision energy of 1.18+1.18 TeV. First data were collected by the LHC experiments and physics results were promptly produced. The experiments will be continued in March 2010 with 3.5+3.5 TeV collision energy. The present plan is to run LHC with this energy in 2010-2011, before taking it up to the design energy of 7+7 TeV. One of the main goals of the LHC project is to clarify the mechanism of the spontaneous braking of the electroweak symmetry in the Standard Model, searching for the Higgs boson(s). The Standard Model of the basic structure of matter, a result of half a centenary of experimental and theoretical work has been tested to a high precision at CERN, Fermilab and at B-factories in USA and Japan. However, an increasing amount of theoretical work has accumulated on the limitations and problems of the Standard Model, particularly on the difficulties to extrapolate it to higher energies in the interactions of the elementary particles. At present, new experimental results at higher energies are badly needed to make progress in building a more general theory. LHC will eventually study elementary particle interactions at an energy of an order of magnitude larger than at present facilities. It will produce new experimental results that will help to clarify the Higgs sector of the Standard Model and to decide between the new theoretical developments and possibly reveal new phenomena - to open a new era in the study of elementary particle physics. The status of LHC and its experiments is reviewed and the prospects and plans for future are discussed in detail.

TAMING OPTICAL NONLINEARITIES: FROM FEW-FEMTOSECOND BEAM DELIVERY TO FILAMENT SELF-COMPRESSION

G. Steinmeyer

Optoelectronics Research Center, Tampere University of Technology, P.O. Box 692, 33101 Tampere, Finland
email: gunter.steinmeyer@tut.fi

All-solid-state laser technology has advanced and matured in the recent decade to make femtosecond laser pulses with durations down to a few femtoseconds commercially available. The optical pulses emitted by these laser systems only comprise few cycles of the underlying electrical field. With pulse energies reaching into the millijoule regime, such systems display peak powers up to several gigawatts. Focusing these powers to a small volume exceeds inneratomic binding forces and can destroy virtually any optical medium brought into the focal volume. Advanced femtosecond laser sources therefore enable all sorts of nonlinear optical effects ranging from relatively simple perturbative effects like second-harmonic generation up to highly-nonlinear optical effects, in which harmonics at more than hundred times the frequency of the input wave may appear.

One example for exploitation of nonlinear optical processes is pulse compression. These techniques normally involve a combination of an optical nonlinearity, typically self-phase modulation, with subsequent equalization of timing differences encountered in the nonlinear process. Compression of an optical pulse therefore typically requires two successive steps. We have recently shown that simply focusing a multi-millijoule pulse into a gas cell can immediately result in pulse shortening, provided only that a suitable input parameter range is met. This pulse self-compression is highly versatile and has been demonstrated by directly compressing 45 fs input pulses to 7.3 fs output duration [1,2].

For other applications, however, avoidance of optical nonlinearities is of paramount importance. One such application is the delivery of femtosecond pulses through an optical fiber without distorting temporal shape of the pulses and without sacrificing peak power of the pulses. Together with researchers in Saratov, Russia, we have recently developed a novel type of fiber with a hollow core that enables such pulse transport over meter length down to pulse durations in the 20 fs regime [3].

These two examples just illustrate the vast range of applications that have been made accessible by modern femtosecond laser technology, which is considered a key technology of the emerging decade.

[1] G. Stibenz *et al.*, Opt. Lett. **31**, 274 (2005).
[2] S. Skupin *et al.*, Phys. Rev. E **74**, 056604 (2006).
[3] J. Skibina *et al.*, Nature Photonics **2**, 679 (2008).

ANALYSIS AND CONTROL OF ELECTRONIC MOTION ON THE FEMTO-SECOND TIME SCALE

E.K.U. Gross

Max-Planck Institute for Microstructure Physics, Weinberg 2, D-06120 Halle, Germany
e-mail: hardy@mpi-halle.mpg.de

Modern density functional theory is based on the surprising fact that knowledge of the density alone is sufficient to calculate all physical observables of a quantum many-body system. In this lecture, the time-dependent generalization of density functional theory will be employed to visualize, analyse and, ultimately, control electronic motion on the femto-second time scale. After an overview of the basic concepts of time-dependent density functional theory, three recent developments beyond the linear-response regime will be presented: (**i) The time-dependent electron localization function (ELF).** This quantity is derived from the conditional probability of finding an electron in the vicinity of a point **r** if one knows with certainty that there is another electron with the same spin at **r**. The shape of the ELF (as function of **r**) provides a topological classification of the different types of chemical bonds. In the time-dependent case, the ELF allows one to visualize the formation and breaking of chemical bonds in a laser field in real time. The sequence of snapshots below shows a laser-induced π-π^* transition in acetylene. Questions like: "How much time needs an electron to complete a transition from one state to another? " can be addressed in this way.

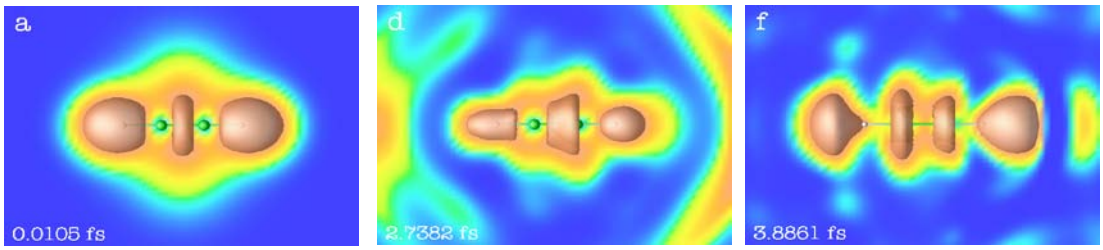

(ii) In the second part of the lecture, questions like "By which laser pulse can one make an electronic wave packet follow a given trajectory in real space or a given path in Hilbert space?" will be addressed. **Quantum optimal control theory** will be presented as a method to compute such laser pulses that are optimized to achieve a given goal. As examples we will calculate the laser pulse needed to break a chosen preselected bond in a molecule, and we will study how the chirality of the electronic current in a quantum ring can be controlled. Finally, we will turn to the field of molecular electronics: **(iii) Time-dependent features of the electronic current through nano-structures** will be studied such as electron pumps and molecular optical switches.

SUPERCONDUCTING X-RAY AND GAMMA-RAY SPECTROMETERS: FROM MATERIAL SCIENCE TO NUCLEAR SECURITY

Stephan Friedrich

Lawrence Livermore National Laboratory
7000 East Ave., L-188, Livermore, CA 94550
USA

Superconducting single photon and particle detectors have been developed over the last decades because of the high energy resolution that operation at temperatures below 1K enables. Among the different detector technologies, superconducting tunnel junctions (STJs) are based on measuring the increase in tunneling current, and superconducting transition edge sensors (TES) measure the increase in temperature upon photon absorption. STJs tend to be smaller and faster, and are therefore primarily used for optical and soft X-ray science. TESs are slower but have higher resolution and can be made larger, and are therefore preferred for high-energy astrophysics and nuclear science.
This talk will provide an overview about the different superconducting detector technologies, their relative advantages and the science that drives their development. As representative applications, we will discuss the use of STJ X-ray detectors at the synchrotron for material science, e. g. to develop novel semiconductor materials for high-speed electronics. Applications for TES Gamma-detectors include their use in safeguards to precisely measure the isotopic composition of nuclear materials. Current research focuses on increasing sensitivity by developing detector arrays, and on improving user-friendliness by developing liquid-cryogen-free refrigerators for automated detector cooling.

THE ICECUBE NEUTRINO OBSERVATORY: OPENING A NEW WINDOW ON THE UNIVERSE

C. Finley

Oskar Klein Centre, Stockholm University, Stockholm
Sweden

Enormous progress in astronomy during the last century has come from extending our observations of the sky across the whole range of the electromagnetic spectrum, from radio waves to gamma rays. The principal mission of the IceCube Observatory is to extend our vision again with a new messenger particle: the abundant but elusive neutrino. IceCube is located at the geographic South Pole, and it consists of over 5,000 light-detecting modules deployed up to 2.5 km deep into the Antarctic ice sheet. The array monitors the dark, clear ice for the bright aftermath of particles created on the rare occasions when a passing neutrino interacts with an atom in the ice. Next winter, the 7-year construction of the observatory will be completed, and the challenge begins in earnest: to discover suspected sources of high energy neutrinos within and outside of our galaxy. I will describe the promising results obtained so far with the early stages of the detector, and what we might learn with the full observatory in the not-too-distant future.

PROBING NUCLEI AT THE EDGE OF STABILITY

P. Butler

Department of Physics, University of Liverpool, Liverpool L69 7ZE, United Kingdom

Much of our traditional understanding of nuclear structure physics has been turned upside down by the discovery of unexpected phenomena, such as nuclei containing nucleons orbiting a central core like a halo, nuclei that can rapidly switch between different shapes, unexpected re-arrangement of the nuclear shells, superheavy nuclei that can rotate at high frequencies, etc. These discoveries have been made possible by major advances in technology that have greatly expanded the variety of atomic beams (both stable and radioactive) used in nuclear physics experiments and have increased the sensitivity of the experimental measurements by several orders of magnitude. These improvements are required in order to access and probe rare, exotic nuclei far from the line of stability. In my talk I will select a few examples that illustrate how new discoveries have, in some cases, caused paradigm shifts in the conventional wisdom of describing nuclear behaviour. I will also describe the plans for major new accelerator facilities that offer exciting opportunties for discovery in this new decade.

EVIDENCE BASED PHYSICS EDUCATION

Jouni Viiri

Department of Teacher Education, University of Jyväskylä, Finland

It is noticed internationally that physics does not attract as many young students as is needed for science and technology education and research. Students' real motivation does not follow e.g. from some interesting demonstrations during the lectures. Instead, real motivation might follow if teaching and learning is more meaningful for the students. Physics education research (PER) aims to evidence based physics education. PER studies cover both theoretical studies and studies which have concrete implications for physics instruction. In the lecture I give an overview of PER and concentrate on some concrete examples. Research results dealing with teaching and learning the 'simple' force concept are described more detailed.

PHYSICS OF INSECT VISION

Matti Weckström

Department of Physics, University of Oulu, Finland
email: matti.weckstrom@oulu.fi

Vision is one of the oldest meeting points of physics and biology, and it has therefore been – and still is – an active area of biophysical research and related computational physics. The study of physics of vision encompasses biological optical systems, photon absorption by light-sensitive molecules, electrical excitation of photoreceptor cells, information processing and transmission, and coding and decoding of light-related sensory messages by neurons. In the present review of physics relevant to insect vision I shall shortly go through all of these processes and where the research now stands in the most active sub-fields. Insect eyes utilize different types of optical systems to focus light on the light-sensitive photoreceptor cells. The absorption of a photon by the π-electrons in the vitamin-A like chromophore of the photopigment molecule, the rhodopsin, triggers a cascade of biochemical events. This leads eventually to changes in conductance of the cell membrane, created by activation of Na^+ and Ca^{2+} permeable TRP (Transient Receptor Potential) ion channels. The photoreceptor cell's voltage signal arises from an intricate play of the light-gated conductance and nonlinear, voltage-dependent conductances based on potassium permeable ion channels. The photoreceptor signals are conducted to deeper neurons in the insect brain with further processing in several neural assemblies, including temporal differentiation and reduction of spatially redundant signals. The evolution of visual systems as information processors have been dictated to a large extent by the statistical structure of the natural scenes, and therefore also the spatio-temporal properties of the flow of photons striking the photoreceptors. The signals generated in photoreceptors also contain noise, essentially photon shot noise, which defines how the information processing takes place in order to extract information in each insect species in an energetically optimal manner.

1 Applied physics, instrumentation and optics

1.1 Oral session I, Thursday 11 March 15:00-16:30
1.2 Oral session II, Friday 12 March 14:30-16:00
1.3 Oral session III, Saturday 13 March 9:00-10:30
1.4 Poster session I, Thursday 11 March 16:30-18:30
1.5 Poster session II, Friday 12 March 16:00-18:00

BOUNDARY ENGINEERING FOR SINIS BOLOMETERS WITH INTEGRATED TUNNEL JUNCTION COOLERS

T.J. Isotalo and I.J. Maasilta

Nanoscience Center, Department of Physics, University of Jyväskylä, P.O. Box 35, FIN-40014 University of Jyväskylä, Finland
email: tero.isotalo@phys.jyu.fi

The feasibility of boundary engineering for the improvement of bolometric detectors and tunnel junction coolers is investigated. It can be shown, by comparing results of suspended and bulk tunnel junction coolers, that ballistic phonon transport dominates heat flow at low temperatures in suspended nanostructures. This allows the control of cooling and heating properties through contact boundary engineering.

Nanoscale beams and membranes form the basis for a host of ultra sensitive low–temperature devices such as bolometers and calorimeters. Cooling of both electrons and phonons in suspended nanomechanical beams has recently been demonstrated with normal metal–insulator–superconductor (NIS) tunnel junctions [1, 2]. By using suspended structures, cooling performance was greatly increased over bulk cooler results. We propose the use of contact boundary engineering to increase the sensitivity of bolometers and enhance the performance of tunnel junction coolers. At low temperatures, bulk impurity and phonon–phonon scattering become weak, leading to the possibility of ballistic transport [3]. In this regime, the scattering of phonons at abrupt interfaces should dominate.

Fabrication issues for suspended structures include the mechanical stability of the structure and material specific limitations. Additionally, device operation is a complicated mix of factors which in turn, affect the materials and geometries available. A solution to fabrication issues in the structural release of tunnel junction coolers is demonstrated by a change of materials. These modified structures show phonon cooling of suspended structures from 115 mK down to 70 mK confirming their functionality.

Boundary engineering of complex, suspended silicon nitride structures has been demonstrated with integrated Al/AlO_x/Ti/Au tunnel junctions. Additionally, we have demonstrated the possibility of using suspended tunnel junction structures for bolometry. Finally, we predict that boundary engineering of suspended structures can lead to a significant reduction of the noise equivalent power (NEP) of such devices. Such reduction could be put to use in space based applications. One particular target is the SAFARI/SPICA far-infrared instrument which will fly on the joint JAXA-ESA telescope project.

[1] P. J. Koppinen and I. J. Maasilta, Phys. Rev. Lett. **102** (2009) 165502.
[2] P. J. Koppinen and I. J. Maasilta, J. Phys.: Conf. Series **150** (2009) 012025.
[3] I. J. Maasilta and T. Kühn, J. Low Temp. Phys. **151** (2008) 64-69.

VIDEO-RATE TERAHERTZ IMAGING USING SUPERCONDUCTING BOLOMETERS

M. Grönholm[1], L. Grönberg[1], P. Lappalainen[1], M. Leivo[1], P. Helistö[1], A. Rautiainen[1], H. Seppä[1], H. Sipola[1], C. R. Dietlein[3], E. N. Grossman[3] and A. Luukanen[2]

1) VTT Technical Research Center of Finland, Tietotie 3, 02044 Espoo, Finland
2) Millimetre-wave Laboratory of Finland – MilliLab, Tietotie 3, 02044 Espoo, Finland
3) National Institute of Standards and Technology, Boulder, CO, U.S.A.

We demonstrate passive THz video imaging with a system developed at VTT and NIST.

Terahertz range covers a part of the electromagnetic spectrum between microwaves and infrared, usually 300 GHz - 3 THz. This region is also called far infrared or submillimetre range. Because of the longer wavelength, terahertz radiation has better transmission than infrared through clothing. The lack of compact and low-cost sources and detectors for this range has created a need for new technologies and innovations.

The detectors used in this camera are antenna-coupled superconducting air-bridge bolometers [1], where a log-spiral antenna is coupled to a small NbN air-bridge. When the radiation heats the bridge, this can be observed as a change in the electrical resistance. The bridge is kept at the transition using a special feedback bias circuit [2].

A linear array of 64 detectors is cooled with a closed-cycle cryocooler. A conical scanner and a folded Schmidt telescope are used to form a 2D image. Observed noise level is close to theoretical and imaging at 6 frames per second has been achieved with temperature resolution of 0.98 K. Applications for this kind of camera are for example detecting concealed weapons and explosives from stand-off range and because this camera is passive, neither privacy nor health is threatened [3].

[1] A. Luukanen, J. P. Pekola, *Appl. Phys. Lett.*, V. 82, No. 22. (2003), pp. 3970-3972.

[2] Jari S Penttilä et al., *Supercond. Sci. Technol.* **19** 319-322, 2006

[3] A. Luukanen, L. Grönberg, P. Helistö, J. S. Penttilä, H. Seppä, H. Sipola, C. R. Dietlein and E. N. Grossman, Proc. of SPIE Vol. 6548 654808-1, 2007

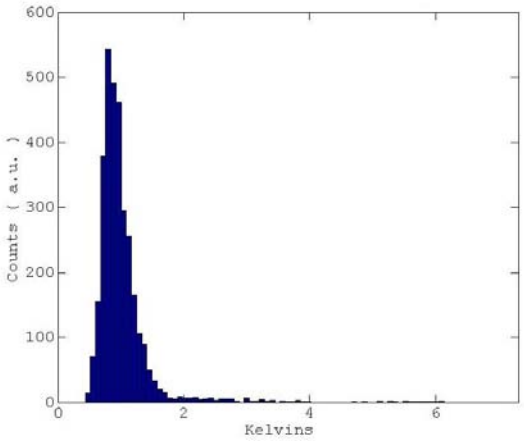

Temperature resolution histogram at 7 ms integration time

MEASUREMENTS OF InGaN QUANTUM WELL RELAXATION WITH PULSED UV-LASER EXCITATION

O. Kimmelma, S. Suihkonen, I. Tittonen, M. Sopanen, and H. Lipsanen

Department of Micro and Nanosciences, Aalto University, Micronova,
P.O.B. 13500, 00076 Aalto, Finland
email: Ossi.Kimmelma@tkk.fi

The III-N material system is currently the only practical solution for blue and near UV LEDs. Although III-N materials have been under extensive study there still exist several contradictory theories for the dislocation resistant light emission mechanisms of InGaN quantum wells (QW). Closely related to the emission mechanism in InGaN QWs is the LED efficiency roll-off at high current density. All InGaN QW based LEDs exhibit an efficiency droop at high operating currents. The reason for the efficiency drooping is still unclear. In this work we present our studies on time resolved photoluminescence measurements on InGaN QWs.

A luminescence response of InGaN quantum wells to an laser pulse at 374 nm is measured with varied exciting optical intensity. These measurements provide information about different radiative and nonradiative relaxation mechanisms of excited electrons. Time traces of incoming laser pulse and luminescence signals from the InGaN quantum wells with low and high intensity excitation are shown in Figure 1.

The exciting laser source is a laser diode pumped, passively Q-switched Nd:YAG laser at 1123 nm frequency tripled to 374 nm [1]. The pulse width at 374 nm is 10 ns (FWHM).

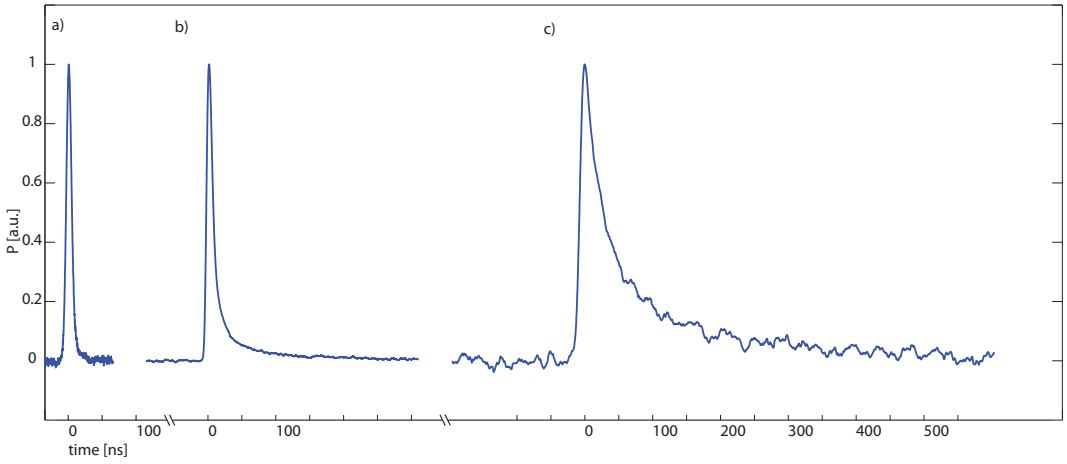

Figure 1: Time traces of a) incoming laser pulse and InGaN quantum well luminescence signal b) with high intensity and c) low intensity showing the close to exponential decay.

[1] O. Kimmelma, I. Tittonen, and S. C. Buchter, "Passively Q-switched Nd:YAG pumped UV lasers at 280 and 374 nm," Optics Communications **282** 2930-2933 (2009).

FIELD-TOLERANT SQUID SENSORS FOR A COMBINED MEG-MRI SYSTEM

J. Luomahaara[1], J. Hassel[1], J. Penttilä[2], M. Kiviranta[1] and L. Grönberg[1]

[1]VTT, Tietotie 3, 02150 Espoo, Finland
[2]Aivon Oy, Tietotie 3, 02150 Espoo, Finland
email: juho.luomahaara@vtt.fi

The simultaneous use of Magnetoencephalography (MEG) and low-field Magnetic Resonance Imaging (MRI) enables one to image the electrical activity of human brain with both high temporal and spatial accuracy, respectively. Recent research [1] has shown that the detection of MEG and MRI signals could be performed with Superconducting QUantum Interference Device (SQUID). SQUID, based on the phenomena of Josephson tunneling and flux quantization, is an ultrasensitive sensor of magnetic flux traditionally employed in MEG. However, when exposed to high magnetic fields of MRI, the SQUID operation becomes complicated as large amount of flux enters the structures of the SQUID. Field tolerance can be enhanced with technological improvements in design, such as linewidth reduction, superconducting shielding, modifying pickup geometry and using flux dams.

Field tolerance of SQUIDs equipped with and without flux dams was measured by placing the SQUID in perpendicular magnetic field. It was found that flux dams are able to reduce the field captured by the pickup loop to a negligible level even with a magnetometer. Tolerance was further enhanced by placing superconducting shields on both sides of the SQUID. Measurements show that current SQUID models are able to function in a homogeneous magnetic field of several hundreds μT and recover independently from pulses of at least 11 mT. Thus, SQUID sensors can be used in the hybrid MEG-MRI device presently under development [2]. To obtain a theoretical understanding, measurement results were compared with the theory of geometrical barrier [3]. A theoretical threshold field for the flux penetration of about 1.5 mT was calculated for our devices. This is in reasonable agreement with the measurements. A new fabrication process based on projection lithography was developed. Now, SQUIDs with narrow linewidths have been manufactured and the field tolerance is expected to be enhanced even further.

[1] J. Clarke, M. Hatridge and M. Mößle, Annual Review of Biomedical Engineering 9 (2007) 389413.
[2] http://www.megmri.net/
[3] E. Zeldov, A. I. Larkin, V. B. Geshkenbein, M. Konczykowski, D. Majer, B. Khaykovich, V. M. Vinokur and H. Shtrikman, Phys. Rev. Lett. 73 (1994) 1428.

PERFORMANCE IMPROVEMENTS OF A SINGLE ELECTRON TURNSTILE

V. F. Maisi[1,*], S. Kafanov[2], Yu. A. Pashkin[3], A. Kemppinen[1], N. Chekurov[4], O.-P. Saira[2], M. Möttönen[2,5], J. S. Tsai[3], A. Manninen[1], J. P. Pekola[2]

[1]Centre for Metrology and Accreditation (MIKES), P.O. Box 9, 02151 Espoo, Finland
[2]Low Temperature Laboratory, Aalto University School of Science and Technology, P.O. Box 13500, FI-00076 AALTO, Finland
[3]NEC Nano Electronics Research Laboratories and RIKEN Advanced Science Institute, 34 Miyukigaoka, Tsukuba, Ibaraki 305-8501, Japan
[4]Department of Micro and Nanosciences, Aalto University School of Science and Technology, P.O. Box 13500, FI-00076 AALTO, Finland
[5]Department of Applied Physics/COMP, Aalto University School of Science and Technology, P.O. Box 15100, FI-00076 AALTO, Finland
*email: ville.maisi@mikes.fi

Accurate current standard based on charge pumping has been pursued internationally over two decades. The main motivation of the work is to improve the basis of the SI unit system by defining the ampere in terms of the number of electrons transported in a known time period. A successful current standard would enable comparisons against other electrical standards in the so-called quantum metrological triangle experiment and allow the redefinition to take place in SI unit system.

A single-electron turnstile, presented here, is a novel candidate for obtaining charge pumping with a high accuracy [1]. Yet, the device is simple enough for parallel operation which enables higher output currents needed in applications. We have demonstrated parallel operation up to ten pumps yielding high enough output current for the quantum metrological triangle experiment [2].

On the other hand, the accuracy of the pumps has not been as good as predicted by higher order tunneling processes. The excess leakage has typically been modelled successfully with a lifetime broadened density of states of the the superconductor, known as the Dynes-model [3]. In our case, the model can be addressed to the electromagnetic environment of the junctions and it is not the property of the superconducting material itself [4]. The parameter values of the analysis match well to the ones reachable with experiments. Further on, we have shown experimentally that the leakage current can be suppressed by an order of magnitude by minimizing the impact of the environment. This is not only advatageous for the charge pump but also for other applications.

[1] J. P. Pekola et. al., Nature Phys. **4**, 120-124, (2008).
[2] V. F. Maisi et. al., New J. Phys. **11** 113057 (2009).
[3] R. C. Dynes et. al., Phys. Rev. Lett. **41**, 1509-1512 (1978).
[4] J. P. Pekola et. al., Paper in preparation, (2010).

SINGLE-ATOM TRANSISTOR

M. Möttönen,[1,2,3] K. Y. Tan,[1] K. W. Chan,[1] A. Morello,[1] C. Yang,[4] J. van Donkelaar,[4] A. Alves,[4] J.-M. Pirkkalainen,[1,2] D. N. Jamieson,[4] R. G. Clark,[1] and A. S. Dzurak[1]

[1]Centre of Excellence for Quantum Computer Technology, School of Electrical Engineering, University of New South Wales, Sydney NSW 2052, Australia.
[2]Department of Applied Physics/COMP, Aalto University, School of Science and Technology, P.O. Box 15100, FI-00076 Aalto, Finland.
[3]Low Temperature Laboratory, Aalto University, School of Science and Technology, P.O. Box 13500, FI-00076 Aalto, Finland.
[4]Centre of Excellence for Quantum Computer Technology, School of Physics, University of Melbourne, Melbourne VIC 3010, Australia.

email: mikko.mottonen(ät)tkk.fi

We have developed nano-scale double-gated field-effect-transistors (nanoFETs) for the study of electron transport through single deliberately-implanted phosphorus donors [1]. The devices provide a high-level of control of key parameters required for potential applications in nanoelectronics. For example, the reservoir density of states in the source and drain leads can be controlled in-situ [2]. The current through the nanoFET can be suppressed or allowed by tuning a gate voltage. Since all the current flows in this device through a single phosphorus donor potential in silicon, it has recently been referred to as a single-atom transistor.

For the donors, we resolve transitions corresponding to two charge states successively occupied by spin-down and spin-up electrons. The charging energies and the Landé g-factors are in agreement with the expectations for donors in gated nanostructures.

(a) SEM image and (b) a schematic cross section of the nanoFET. The top gate is used to induce the electron layer at the Si–SiO_2 interface connecting the transistor source (S) and drain (D). The barrier gate depletes the gas at the donor and controls the single-electron tunneling.

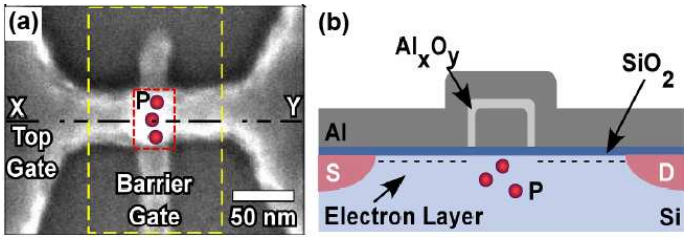

[1] K. Y. Tan, K. W. Chan, M. Möttönen, A. Morello, C. Yang, J. van Donkelaar, A. Alves, J.-M. Pirkkalainen, D. N. Jamieson, R. G. Clark, and A. S. Dzurak, Nano Letters 10 (2010) 11.

[2] M. Möttönen, K. Y. Tan, K. W. Chan, F. A. Zwanenburg, W. H. Lim, C. C. Escott, J.-M. Pirkkalainen, A. Morello, C. Yang, J. A. van Donkelaar, A. D. C. Alves, J.-M. Pirkkalainen, D. N. Jamieson, L. C. L. Hollenberg, and A. S. Dzurak, arXiv:0910.0731 (2009).

DEVELOPING A MODEL FOR FAST ION DETECTION IN FUSION REACTORS

E. Hirvijoki, S. Jämsä, T. Kurki-Suonio

Aalto University, Department of Applied Physics, P.O.Box 14100 FI-00076 AALTO
email: eero.hirvijoki@tkk.fi

Harvesting thermonuclear fusion energy is taking a step forward as the construction of ITER reactor has begun. In ITER, energy is released in deuterium-tritium fusion which produces 14.7 MeV neutrons and 3.5 MeV alpha particles. These alphas, together with fast deuterium and tritium ions produced by external heating of the plasma, provide a massive source of free energy. Therefore their distribution should be monitored. In future tokamaks the influence of this energy to the stability of the plasma and to the reactor walls is a key issue.

At the moment there are no ITER relevant methods to observe the distribution of fusion alphas and other particles heated up to MeV range. The most promising candidates for diagnostics are NPA (Neutral Particle Analyzer), CTS (Collective Thompson Scattering), FIDA (Fast Ion Deuterium alpha radiation detector), neutron diagnostics and probes like FILD (Fast Ion Loss Detector).

In this paper we briefly present the operating principles of these different diagnostics. The focus is on the latest numerical development concerning NPA and FIDA where neutral particle density from neutral beam injections (NBI) plays a crucial role. Our aim is to integrate a model that calculates neutral particle density from NBI according to atomic physics together with a Monte Carlo particle following code ASCOT and obtain a synthetic diagnostics tool for NPA and FIDA modelling.

NEW HIGH RESOLUTION SPECTROMETER FOR NANOMETER LEVEL ELEMENTAL DEPTH PROFILING

M. Laitinen, M. Rossi, P. Rahkila, H.J. Whitlow and T. Sajavaara

University of Jyväskylä, Department of Physics, P.O. Box 35, 40014, Finland
email: mikko.i.laitinen@jyu.fi

A new time-of-flight-energy spectrometer for Elastic Recoil Detection Analysis (ToF-ERDA) has been constructed in JYFL Pelletron Laboratory. The new spectrometer is able to quantitatively depth profile all elements, especially the light ones, with good sensitivity.

Thin films with thickness less than 10 nm are nowadays a common practice in many applications. Among different deposition techniques, Atomic Layer Deposition (ALD) is becoming more and more popular in wide range of applications. In the deposition process development, reliable elemental depth profiling tool is crucial, and TOF-ERDA can provide both film composition stoichiometry and impurity concentrations. Hydrogen is a very common impurity in thin films but it is either impossible or difficult for most of the analysis techniques.

Here we describe the newly developed spectrometer and report the first results of the spectrometer's elemental depth profiling performance for thin ALD oxides, nanolaminates and metal films having thickness of less than 10 nm. Surface resolution better than 2 nm was achieved with this first setup for the Al_2O_3 film on silicon (Fig. 1). Further improvement in depth resolution is expected when the first timing gate is modified to be position sensitive. This enables kinematic correction for detected ions flying through the spectrometer. Angular corrected data as well as planned improvement for the energy detection will be shown and discussed.

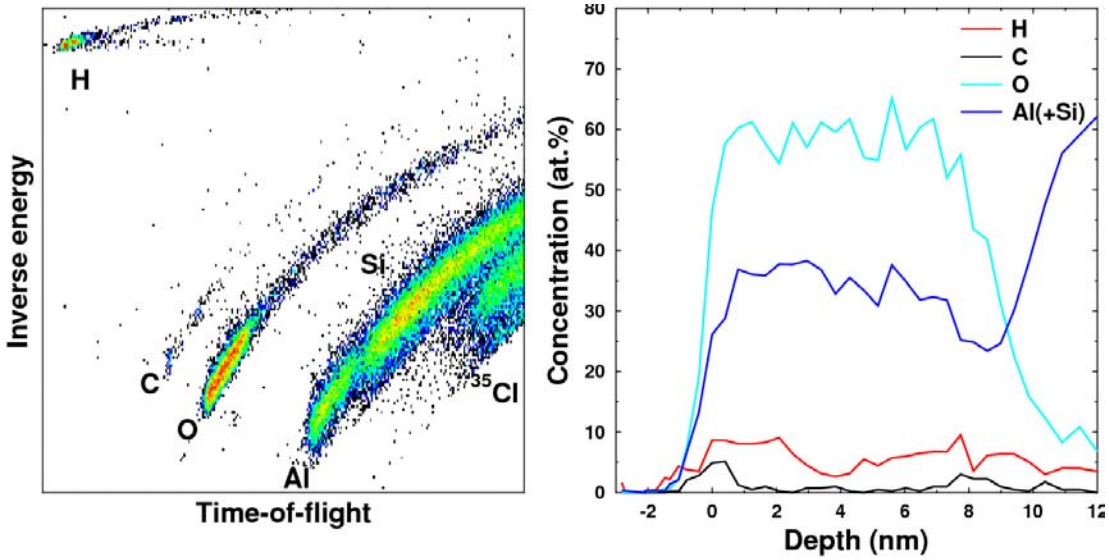

Figure 1. The first high resolution spectrum from the new spectrometer. Raw ToF-E data (left) and the elemental depth profiles for 8.6 nm Al_2O_3 film on Si (right) measured with 5 MeV $^{35}Cl^{+}$ ions.

TRANSPORT OF TRACE IMPURITIES INSIDE A TOKAMAK PLASMA

T. Makkonen[1], T. Kurki-Suonio[1], K. Krieger[2], M. Groth[1], L. Aho-Mantila[1], and A. Hakola[1]

[1]Aalto University, Department of Applied Physics, P.O.Box 14100, FI-00076 AALTO, Finland
[2]Max–Planck–Institut für Plasmaphysik, Euratom Assoc., 85748, Garching, Germany
email: toni.makkonen@tkk.fi

Fusion plasmas would ideally consist only of deuterium and tritium. The presence of other atomic species, called impurities, is unfortunately unavoidable. At the very least, helium ash from the D–T reaction will be present. Another challenge is imposed by impurities originating from erosion of the plasma exposed reactor walls. Key issues include 1) predicting how much of the impurities penetrate into the core plasma lowering fusion performance, 2) controlling co–deposition and implantation of radioactive tritium fuel on the walls, and 3) understanding long–term material migration.

The transport of the impurity ions along the magnetic field lines is mainly determined by Coulomb collisions with the background plasma ions. This gives rise to somewhat counter–intuitive forces, such as the ion temperature gradient force. The cross section for Coulomb collisions decreases strongly as the relative velocity of the colliding particles increases. Even though the ions from the hot side carry more momentum, the net effect is surprisingly that plasma impurities experience a net force towards hotter regions.

Impurity transport is in general a complicated process to model, and already early on it was learned that the observations cannot be explained by solely by Coulomb collisions and classical models. In particular, the transport across the magnetic field lines is likely due to small–scale turbulence and is best accounted for by a diffusive model [1].

In this work, the 2007 carbon–13 impurity injection experiment from the ASDEX Upgrade tokamak is simulated with the objectives of interpreting the experimental results. Also, the physical model used in the simulation program DIVIMP [2] is critically reviewed. This serves to improve the understanding of impurity transport in tokamaks.

[1] E. S. Marmar et al. Nucl. Fusion **22** (1982) 1567–1575.
[2] Peter C Stangeby, The Plasma Boundary of Magnetic Fusion Devices (2000) IOP Publishing.

APPLICATIONS AT THE IGISOL FACILITY

T. Eronen, J. Hakala, A. Jokinen, A. Kankainen, P. Karvonen, V.S. Kolhinen, I.D. Moore, H. Penttilä, J. Rissanen, M. Reponen, A. Saastamoinen, V. Sonnenschein and J. Äystö

Department of Physics, P.O.Box 35 (YFL), FI-40014 University of Jyväskylä, Finland
email: penttila@jyu.fi

The basic goal of the IGISOL mass separator facility [1] at the Accelerator Laboratory of the University of Jyväskylä, JYFL, is the research of the nuclear landscape in its extremes. However, the capability of production of mass separated ion beams of any element, combined with the outstanding performance of JYFLTRAP double Penning trap, capable to produce mass separated sources of atoms of a single isotope or even a single isomer, also gives boost for applied research. The development and use of the applications has taken place in close collaboration with the local accelerator based materials physics group, as well as several other laboratories, including for example STUK (Helsinki), IFIC(Valencia, Spain), GSI (Darmstadt, Germany) and PNPI (Gatchina, Russia).

The mass separated radioactive ions from IGISOL implanted in material samples can be used to study properties of the samples [2]. As an example, radioactive atoms are the only way to study self-diffusion. At IGISOL, radioactive ions of any element can be implanted.

The studies of isotopically purified samples of fission products with a Total Absorption Spectrometer (TAS) give information of the reactor decay heat [3]. In recent years, practically all the experiments defined as “requested TAS measurements” by OECD Nuclear Energy Agency [3] have taken place at IGISOL. Independent fission product yields for a variety of particle-induced fission reactions have been measured at IGISOL [4]. These, as well as the measurements of beta-delayed neutron probabilities, also performed at IGISOL, are important for the design of the advanced nuclear reactors.

It is also possible to produce isomerically purified sources using advanged and up-to-date purification techniques of JYFLTRAP. These sources are planned to be collected and provided to the Comprehensive Nuclear-Test-Ban Treaty Organisation CTBTO for calibration purposes [5].

[1] P. Karvonen, *et al.*, Nucl. Instr. and Meth. B 266, 4454 (2008).
[2] J. Ekman, *et al.*, Nucl. Instr. and Meth. B 249, 544 (2006).
[3] M.A. Kellett, *et al.*, Assessment of Fission Product Decay Data for Decay Heat Calculations, report No. 6284, NEA/WPEC-25, OECD/NEA, Paris, 2007.
[4] H. Penttilä *et al.*, submitted to Eur. Phys. J. A.
[5] K. Peräjärvi *et al.*, Appl. Radiat. Isot., in print.

ELECTRICAL RESISTANCE TOMOGRAPHY IMAGING OF CONCRETE

A. Seppänen[1], K. Karhunen[1], A. Lehikoinen[1], J. Blunt[2], J.P. Kaipio[1,3] and P.J.M. Monteiro[2]

[1]Department of Physics and Mathematics, University of Eastern Finland, FI-70211, Kuopio, Finland
[2]Department of Civil and Environmental Engineering, University of California, Berkeley, USA
[3]Department of Mathematics, University of Auckland, Auckland 1142, New Zealand
email: Aku. Seppanen@uef.fi

Concrete is distinctly the most extensively used construction material in the world – twice as much concrete is used in construction around the world than the total of all other building materials, including wood, steel, plastic and aluminum. During the life-cycle of concrete, there are several situations necessitating measurement and analysis of the structural integrity and other properties of concrete structures. Many of the existing methods for assessment of concrete conditions are destructive in nature. Non-destructive modalities exist but most of them are inaccurate and prone to uncertainties of the models.

Electrical Resistance Tomography (ERT) is an imaging modality in which the internal (3D) conductivity distribution of the target is reconstructed on the basis of electrical measurements acquired from the surface of the target. The reconstruction problem of ERT is an ill-posed inverse problem, the solutions require accurate modeling of the measurements and state-of-the-art inversion methods [1]. In our recent studies we have demonstrated the feasibility of ERT for assessment of different properties of concrete [2]. The results have indicated that ERT holds potential for localization of reinforcing bars and cracks, and estimation of moisture distributions in concrete.

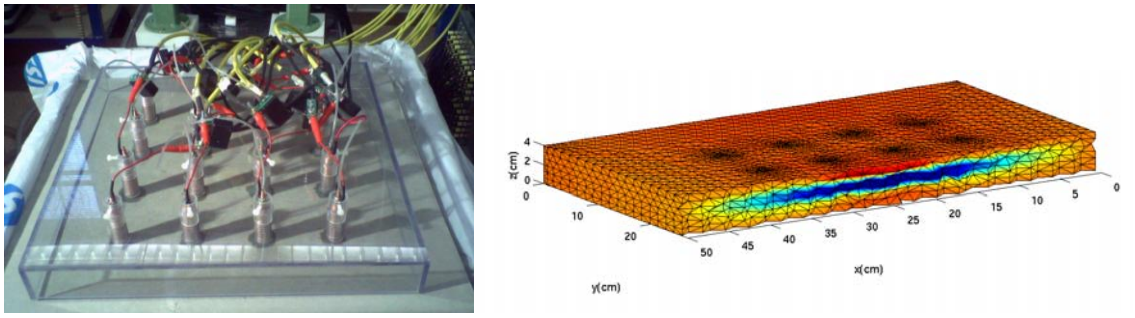

Figure 1: ERT measurements from the top surface of a concrete slab (left) and reconstructed 3D conductivity distribution in the slab (right).

[1] J.P. Kaipio and E. Somersalo, Statistical and computational inverse problems. Springer Science+Business Media, Inc. 2005.

[2] K. Karhunen, A. Seppänen, A. Lehikoinen, P.J.M. Monteiro, J.P. Kaipio, Electrical resistance tomography imaging of concrete, Cement and Concrete Research, 40: 137-145, doi:10.1016/j.cemconres.2009.08.023, 2010.

AUTOMATED MEASUREMENT SYSTEM FOR VALIDATION OF ACOUSTICAL SIMULATION RESULTS

S.-P. Simonaho and T. Lähivaara

University of Eastern Finland/Kuopio Campus, P.O.B. 1627, FIN-70211 Kuopio, Finland
email: simo-pekka.simonaho@uef.fi

Acoustical simulations can provide more information than measurement. Before using any simulation method, its performance should be validated. Usually validation can be made using a known benchmark problem and/or comparing simulations to analytic solutions or measurements. In latter case, a great number of measurement points are needed especially in 3 dimensional cases. Thus, measurements can be extremely laborious when done manually. In addition, the location of each measurement point should be known accurately. Thus, these measurement can be extremely laborious when done manually.

In this study, we introduce automated measurement system which is composed of 3 dimensional positioning system, microphone array and data acquisition hardware. The microphone array can be moved inside $2.2\ \mathrm{m} \times 2.2\ \mathrm{m} \times 1.7\ \mathrm{m}$ with 0.1 mm spatial accuracy. Data acquisition hardware makes measurements and moves the microphone array in desired measurement locations. With this system its possible to make measurements in single or multiple measurement points with high spatial accuracy and repeatability. This system is used to measure pressure fields in different 2D planes.

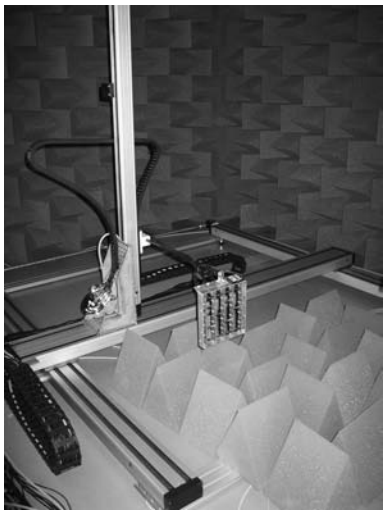

The high-order discontinuous Galerkin (DG) method is used to model the acoustic wave propagation in time domain. Detailed description of the DG can be found in [1] and references therein. Simulation results are compared to the measured pressure fields. The agreement between simulations and measurements was found to be very good.

[1] T. Lähivaara, M. Malinen, J.P. Kaipio and T. Huttunen, (2008), Computational aspects of the discontinuous Galerkin method for the wave equation, Journal of Computational Acoustics, 16 507-230 (2008).

SOLITON COLLISION INDUCED DISPERSIVE WAVE GENERATION

M. Erkintalo[1], G. Genty[1], and J. M. Dudley[2]

[1]Tampere University of Technology, Optics Laboratory, FI-33101 Tampere, Finland
[2]Université de Franche-Comté, Institut FEMTO-ST, 25030 Besançon, France
email: goery.genty@tut.fi

Photonic crystal fibers (PCF) with two zero-dispersion wavelengths (ZDW) have recently been shown to be associated with pulse propagation dynamics unobservable in ordinary fibers [1]. A particular effect that occurs when a femtosecond soliton is propagating in the PCF is the stabilization of the Raman-induced soliton self-frequency shift as the soliton approaches the second ZDW. This effect arises because the soliton sheds energy into the long-wavelength normal dispersion regime in the form of Cherenkov-like dispersive radiation [2].

In this work we use stochaistic numerical simulations to study shot-to-shot fluctuations in the properties of dispersive radiation generated during noise-driven supercontinuum (SC) generation in a PCF with two ZDWs. Specifically, we simulate the propagation of 1000 transform-limited 4 ps pulses in a commercially available PCF and find that in a small number of outputs the SC spectrum consists of dispersive waves with extraordinary spectro-temporal properties such as abnormally high amplitude and long wavelength.

The origin of these peculiar dispersive waves can be understood upon inspection of the trajectories of individual solitons emerging from the pulse envelope shown in Fig. 1(a). Specifically, approximately at distance of 1.7 m two solitons collide and a strong dispersive wave component can be seen to be shed exactly at the moment of collision as illustrated in the zoomed view in Fig. 1(b). In addition to numerical simulations, experimental signatures of these collision-induced dispersive waves will be shown.

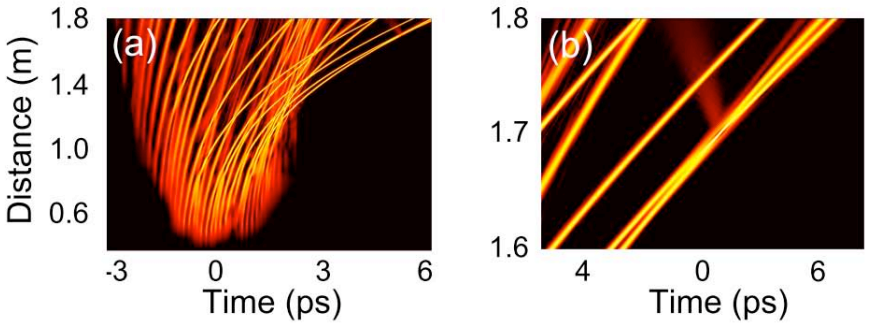

Figure 1: (a) Time domain trajectories of the individual solitons emerging from the pulse envelope. (b) Zoomed view shows that the collision event of two solitons generates a strong dispersive wave component.

[1] J. M. Dudley and J. R. Taylor, Nat. Photonics 3, (2009) 85–90.
[2] N. Akhmediev and M. Karlsson, Phys. Rev. A 51, (1995) 2602–2607.

DETERMINING THE CHRONOLOGICAL ORDER OF CROSSING LINES USING SCANNING WHITE LIGHT INTERFEROMETRY

V. Heikkinen[1], I. Kassamakov[1, 2], J. Aaltonen[2] and E. Hæggström[1]

[1]Department of Physics, P.O.B. 64, FIN-00014 University of Helsinki, Finland
[2]Helsinki Institute of Physics, P.O.B. 64, FIN-00014 University of Helsinki, Finland
email: ville.heikkinen@helsinki.fi

In forensics it may be important to determine the chronological order of crossing lines. This can be difficult if the lines are made with a similar tool and pressure or if the surface exhibits other features. 3D imaging using 3D laser profilometry has been used to determine order of crossing lines on paper [1]. We apply Scanning White Light Interferometer (SWLI) and 3D image processing to study 1-5 crossing lines on a copper surface. Our SWLI setup quantitatively measures the height profiles with the accuracy needed in forensic applications [2]. Image processing methods allow us to remove unimportant features, such as surface form, roughness and measurement noise, from the measured profiles. This allows us to see more clearly the features in the crossing area, such as the ridges and bumps across the older line seen in fig. 1, needed to determine the chronological order of the lines. We provide analysis of correct classification from a statistically significant set of cases.

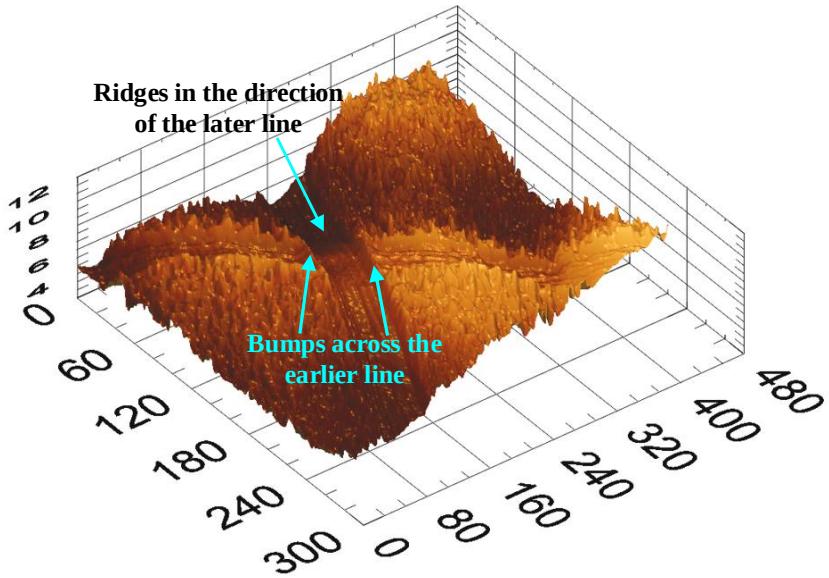

Figure 1. Surface of a printed circuit board with crossing lines measured using our SWLI setup.

[1] G. Spagnolo, Forensic Science International 164, (2006) 102-109.
[2] P. Ahvenainen, et al., QNDE 2009, Rhode Island, USA, (2009).

PHYSICAL MODELLING OF THE INTERFEROMETRIC CANTILEVER MICROPHONE USED IN PHOTOACOUSTIC GAS DETECTORS

Jyrki Kauppinen[1], Tom Kuusela[1], Pekka Malmi[1] and Jussi Raittila[2]

[1]Department of Physics and Astronomy, University of Turku, FI-20014 Turku, Finland, e-mail: jyrki.kauppinen@utu.fi
[2]Gasera Ltd., Tykistökatu 4, FIN-20520 Turku, Finland

The sensitivity of the microphone in photoacoustic trace gas detection systems is an essential parameter. In practice the sensitivity of the detector is mainly limited by the noise characteristics of the whole system. The signal-noise-ratio determines the lowest gas concentration, which can be reliably measured. Therefore it is most important to understand both the signal response and the noise characteristics of the microphone.

The detection limit of the system with commonly used condenser microphones is limited by the electrical noise of the microphone amplifiers. The best condenser microphones work at the physical limits and therefore there is no way to further improve their sensitivity. The interferometric cantilever microphone [1, 2, 3] can be constructed in such a manner that the electrical and laser noise are well below the level of Brownian noise of the cantilever mediated by random collisions between the molecules in the gas medium and the cantilever.

There are several physical mechanisms involved in the cantilever microphone system. Although the dynamics of the cantilever itself can be modelled by 1-dimensional harmonic oscillator, the situation is much more complex when the cantilever is attached into the photoacoustic cell. The effects of the finite volumes, the pressure and energy leak through the gap between the cantilever and the frame, thermal conductions mechanisms and various relaxation processes must be carefully described in order to achieve realistic and useful model, which can be used to estimate the properties of the system. We have created a cantilever-based photoacoustic model, which include all essential physical mechanisms.

The pectral properties of Brownian noise are critical when optimising the sensitivity of the cantilever microphone. The spectrum has typically a clear local maximum around the resonance frequency of the gas-damped cantilever since the system can be modelled as a damped 1-dimensional harmonic oscillator. However, there is also another frequency range typically on the very low frequencies where the level of noise is significant or even dominant. The last one is due to leak of the gas between the cantilever and its frame. We have modelled these noise components and compared them with experimental spectra measured in real photoacoustic cells. The results indicate that parameters can be optimised in order to minimize the noise level on the photoacoustic modulation frequency.

[1] J. Kauppinen, K. Wilcken, I. Kauppinen, V. Koskinen, Microchem. J. 76, 151 (2004)
[2] T. Kuusela, J. Kauppinen, Appl. Spectrosc. Rev. 42, 443 (2007)
[3] V. Koskinen, J. Fonsen, K. Roth, J. Kauppinen, Appl. Phys. B 86, 451 (2007)

THE ULTRA WEAK VARIATIONAL FORMULATION WITH BESSEL BASIS FUNCTIONS

T. Luostari[1a], T. Huttunen[1] and P. Monk[2]

[1]University of Eastern Finland, Department of Physics and Mathematics, Kuopio Campus, P.O. Box 1627, 70211 Kuopio, Finland
email: [a]teemu.luostari@uef.fi
[2]Department of Mathematical Sciences, University of Delaware, Newark, DE 19716, USA

The accurate full-wave modeling at high wave numbers requires a lot of computer memory and CPU time. The ultra weak variational formulation (UWVF) is a potential numerical method for solving wave modeling problems in fields of acoustics, electromagnetism and elasticity. The UWVF is a special form of an upwind discontinuous Galerkin method (DGM) and it uses finite element (FE) type meshes. However, the UWVF uses non-polynomial basis functions such as plane wave and/or Bessel basis functions. These basis functions are also called physical basis functions. The UWVF was first introduced and analyzed by Cessenat and Deprés [2] and they applied it to the Helmholtz equation and Maxwell's equations.

The UWVF uses originally plane wave basis functions and in this case the UWVF integrals can be computed efficiently in closed form. However, in the case of plane wave basis ill-conditioning may occur if the elements are small compared to the wavelength. Moreover, methods based on non-polynomial bases may suffer a reduced accuracy near sharp corners (also known as corner singularities). Motivated by [1] and [3], we apply Bessel basis functions in the UWVF in order to enhance the accuracy of singular wave field problems.

We shall investigate time-harmonic 2-D Helmholtz problems. As a first model problem we consider a plane wave propagation and evanescent waves in a rectangular domain to show the feasibility of the Bessel basis functions in the UWVF. In the second model problem we consider an L-shaped domain problem with a corner singularity where we use the coupling of plane wave and Bessel basis functions in the same mesh [4].

[1] A.H. Barnett and T. Betcke, An exponentially convergent nonpolynomial finite element method for time-harmonic scattering from polygons. Submitted.
[2] O. Cessenat and B. Després,Application of an ultra weak variational formulation of elliptic PDEs to the two-dimensional Helmholtz problem. SIAM Journal on Numerical Analysis 35(1):255–299, 1998.
[3] C. Gittelson, R. Hiptmair and I. Perugia, Plane wave discontinuous Galerkin methods: Analysis of the h-version. ESAIM: M2AN Mathematical Modelling and Numerical Analysis 43(2):297–331, 2009.
[4] T. Luostari, T. Huttunen and P. Monk, The ultra weak variational formulation using Bessel basis functions. Submitted.

High bandwidth measurements of large area 2-Dimensional systems using rf reflectometry

L.J. Taskinen[1,3], R.P. Starrett[1], T.P. Martin[1], J. C. H. Chen[1], A.P. Micolich[1], A.R. Hamilton[1], M.Y. Simmons[1], D.A. Ritchie[2] and M. Pepper[2]

[1] School of Physics, University of New South Wales, Sydney NSW 2052, Australia.
[2] Cavendish Laboratory, University of Cambridge, Cambridge CB3 0HE, United Kingdom.
[3] Current address: Department of Physics, PL 35 (YFL) , FI-40014 University of Jyväskylä.
email: lasse.taskinen@jyu.fi

There is a growing interest in studying non-equilibrium and noise properties of 2D systems, e.g., in context of the still controversial metal insulator transition [1] and glassy dynamics [2]. These studies would benefit from sensitive large bandwidth measurement methods, such as the rf reflectometry widely used with mesoscopic devices such as single electron transistors and quantum point contacts [3]. Initially one would expect that it is not possible to use the rf reflectometry technique with large area gated 2D systems because the large capacitance results in a negligible sensitivity at high resistances. However, our experimental results and a simple model show that rf reflectometry is a sensitive method to measure the device resistance up to several hundreds of k$\Omega/\Box$ with a bandwidth up to tens of MHz [4].

To test how rf reflectometry works with large area devices we embedded a 2D hole system (2DHS) in an AlGaAs/GaAs heterostructure (a Hall bar with a $80\ \mu\text{m}\times800\ \mu\text{m}$ metal top gate) into an impedance matching LC circuit that terminates a transmission line, and used rf reflecetometry to measure temporal changes in the resistance of the device at mK temperatures.

Our method enables rapid measurements of 2D systems, e.g., fast mapping of the Landau level evolution in a 2DHS as a function of magnetic field and gate voltage [4]. In addition, we show how the rf response depends on the device geometry [5]. We have also used rf reflectometry to study non-equilibrium relaxation processes in AlGaAs/GaAs heterostructures by measuring 2DHS resistance changes with sub-millisecond time resolution.

[1] S. V. Kravchenko and M. P. Sarachik, Rep. Prog. Phys. **67**, 1, (2004).
[2] J. Jaroszyński and D. Popović, Phys. Rev. Lett. **96**, 037403, (2006).
[3] R. J. Schoelkopf, P. Wahlgren, A. A. Kozhevnikov, P. Delsing and D. E. Prober, Science **280**, 1238, (1998).
[4] L. J. Taskinen, R. P. Starrett, T. P. Martin, A. P. Micolich, A. R. Hamilton, M. Y. Simmons, D. A. Ritchie and M. Pepper, Rev. Sci. Inst. **79**, 123901, (2008).
[5] L. J. Taskinen, R. P. Starrett, T. P. Martin, J. C. H. Chen, A. P. Micolich, A. R. Hamilton, M. Y. Simmons, D. A. Ritchie and M. Pepper, Physica E, accepted (2009).

PERFORMANCE OF A THERMOACOUSTIC METAL WIRE ARRAY LOUDSPEAKER

V. Vesterinen[1], A.O. Niskanen[1], L. Grönberg[1], P. Helistö[1], M. Tikander[2], P. Maijala[1] and J. Hassel[1]

[1] VTT, Tietotie 3, P.O.B. 1000, FIN-02044 VTT, Espoo, Finland
[2] Aalto University School of Science and Technology, Department of Signal Processing and Acoustics, P.O.B 13000, FIN-00076 AALTO, Finland
email: visa.vesterinen@vtt.fi

We have designed and fabricated air-bridge arrays comprising hundreds of thousands of aluminum wires [1]. Thermally decoupled from the underlying silicon substrate, the wires act as thermoacoustic sound sources. Periodic heating occurs in the resistive wires due to Joule's law when AC signal is driven through an array. In the surrounding air, rapidly attenuating thermal waves excite pressure oscillations which we understand as sound waves.

We have investigated the highly frequency-dependent factors that limit acoustic performance. While the thermoacoustic coupling of temperature and pressure improves with rising frequency, the heat capacity of wires becomes a major limiting factor at the same time. We have measured sound pressure levels produced by the arrays as a function of frequency and seen that the arrays can reproduce both audible and ultrasonic frequencies. It has been recently proven that carbon nanotube thin films can be operated thermoacoustically as well [2].

We have also developed a simulation model to solve the partial differential equations of linear thermoacoustics. Utilizing axisymmetric finite element method, the model where circular metal wires are heated periodically has given results which are in good agreement with the experiments at least at frequencies up to 40 kHz. We are currently studying theoretically and experimentally the high frequency properties of the loudspeakers.

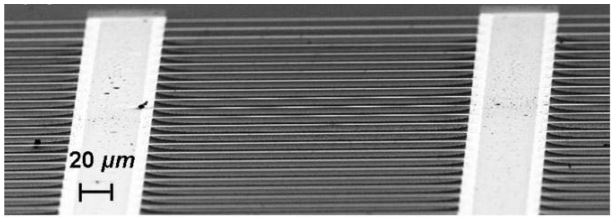

Figure 1: A close-up of the photolithographically fabricated array of wires

[1] A. O. Niskanen, J. Hassel, M. Tikander, P. Maijala, L. Grönberg, and P. Helistö, Applied Physics Letters 95, 163102 (2009).
[2] Xiao L. *et al.*, Nano Letters 8, 4539-4545 (2008).

LASER-ULTRASONICS CHARACTERIZES LAYERED POLYMERS

T. Fabritius, J. Eskelinen and E Hæggström

Department of Physics, P.O.B. 64, FIN-00014 University of Helsinki, Finland
Email: tom.fabritius@helsinki.fi

There is currently no method for rapid non-destructive analysis of the structural quality of layered extruded polymers (thickness, elasticity, inner defects). Laser-ultrasonics has been used [1] [2] [3] in material characterization, but not on polymers in the <1 mm size range, mainly due to problems with laser absorption and ultrasound attenuation.

Laser-ultrasonics uses a pulsed excitation laser to create an acoustic pulse in the sample. The absorbed laser pulse creates thermoelastic expansion, which generates a mechanical wave. This wave then propagates in the sample and can be picked up with an interferometer at some distance from the excitation.

We have developed laser-ultrasonic measurement methods to measure polymer layer thickness, evaluate elasticity and detect delaminated areas. We have measured acoustic signals normally to the surface probing the layer thickness and tangentially along the surface at various detection distances to determine the sound velocity in the layer, which is linked to the elasticity of the material.

[1] J.-P. Monchalin, et. al., Advanced Performance Materials 5 (1998)
[2] J. Rogers, et al., Annual Review of Material Science 30 (2000)
[3] D. Hutchins and A. Tam, IEEE Transactions on Ultrasonics, Ferroelectrics and Frequency Control 33 (1986) 5.

PERFECT CLOAKING IN FIRST BORN APPROXIMATION

T. Setälä[1], T. Hakkarainen[1], A. T. Friberg[1,2], and B. J. Hoenders[3]

[1] Department of Applied Physics, Aalto University, P.O.B. 13500,
FI-00076 Aalto, Finland
[2] Department of Physics and Mathematics, University of Eastern Finland, P.O.B. 111,
FI-80101 Joensuu, Finland
[3] Centre for Theoretical Physics and Zernike Institute for Advanced Materials,
University of Groningen, Nijenborg 4, 9747 AG Groningen, The Netherlands
email: ari.friberg@tkk.fi

Recent progress in the research of metamaterials has enabled one to control light in extraordinary ways as evidenced, e.g., by negative refraction, reversed Doppler shift, and the phenomenon of perfect focusing [1]. In particular, cloaking of objects making them invisible or less detectable has received much attention due to its potential applications. Several approaches for cloaking have been proposed, such as coordinate transformations, reduction of scattering cross-section, use of embedded arrays of holes and dielectric particles in metal films, and utilization of anomalous resonances in certain systems. However, the methods normally necessitate the use of strong scatterers.

In this work we consider the possibility of object-dependent cloaking in weak scattering. We investigate a geometry in which the object and the cloak are slabs, both of which scatter (scalar) light in the first-order Born approximation. For the cloaking to occur in such a system, we require that [2]

$$\int_0^a F_o(z',\omega)\mathrm{d}z' = -\int_{a_1}^{a_2} F_c(z',\omega)\mathrm{d}z', \quad \text{for} \quad z \geq a_2, \tag{1}$$

$$\int_0^a F_o(z',\omega)e^{2ik_0mz'}\mathrm{d}z' = -\int_{a_1}^{a_2} F_c(z',\omega)e^{2ik_0mz'}\mathrm{d}z', \quad \text{for} \quad z \leq 0, \tag{2}$$

where $F_o(z,\omega)$ and $F_c(z,\omega)$ are the scattering potentials of the object and cloak slabs, respectively. The field propagates along the positive z axis, the object slab is located within the interval $[0,a]$, whereas the cloak slab is positioned at $[a_1,a_2]$, with $a_1 > a$. The parameter k_0 is the free space wave number and m denotes the (normalized) z component of light's wave vector. The solution is given by $F_c(z,\omega)$, a_1, a_2, and the values of m that satisfy the above equations, when $F_o(z,\omega)$ and a are known.

Equation (1) implies that perfect cloaking in the forward direction is achieved for any incident field and object slab with transversally invariant optical properties. The cloak slab has two possibilities: positively refractive and amplifying slab or a lossy, negative-index metamaterial slab. Instead, solutions to Eq. (2) are found to be self-imaging fields. In both cases the refractive-index distribution and dispersive properties of the cloak slab resemble those of the object slab.

[1] L. Solymar and E. Shamonina, *Waves in Metamaterials* (Oxford UP, 2009).
[2] T. Setälä, T. Hakkarainen, A. T. Friberg, and B. J. Hoenders, submitted.

UNAMBIGUOUS PROBE OF SURFACE CHIRALITY BASED ON FOCUSED CIRCULAR POLARIZATIONS

M. J. Huttunen,[1] M. Virkki,[1] M. Erkintalo,[1] E. Vuorimaa,[2] A. Efimov,[2] H. Lemmetyinen[2] and M. Kauranen[1]

[1]Department of Physics, Tampere University of Technology, FIN-33101, Finland
[2]Department of Chemistry and Bioengineering, Tampere University of Technology, FIN-33101, Finland
email: mikko.j.huttunen@tut.fi

Chiral objects, e.g. molecules, lack reflection symmetry. Chiral molecules occur in two enantiomers, which are mirror images of each other. Nonlinear optical phenomena offer sensitive tools to probe chirality, i.e., handedness, of molecules, surfaces and solutions [1, 2, 3]. For example, second-harmonic generation (SHG) can detect chirality based on measuring SHG intensity differences when the handedness of the probing fundamental light is reversed [2, 3]. Typically circular polarizations (CP), collimated beams and oblique angles of incidence are used. For samples with in-plane anisotropy, however, these typical techniques may give rise to ambiguous and false chiral signatures even for achiral samples, which arise from the chirality of the setup due to sample anisotropy [4].

In this Paper, we present a new technique to measure surface chirality based on SHG that is not compromised by the anisotropy of the sample. The technique relies on focused CP beams at normal incidence as recently proposed [5]. The ambiguity due to the breaking of the reflection symmetry of the setup is avoided by the normal incidence. In addition, focused fundamental beams are used to couple the light to the surface nonlinearity of the sample. We measured SHG responses from achiral and chiral anisotropic thin films as a function of the rotation angle of a quarter-waveplate (QWP), where the achiral sample acted as reference. The results are shown in Fig. 1 where different response from oppositely handed CP signifies surface chirality.

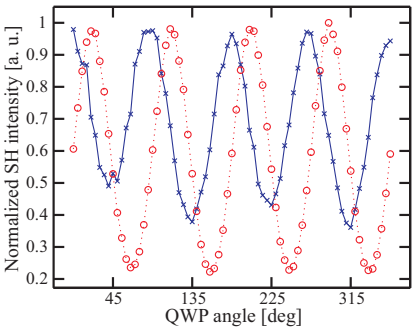

Figure 1. SHG responses from anisotropic thin films of chiral (x) molecules and achiral molecules (o) as a function of rotation angle of the QWP. Angles 45°, 135°, 225° and 315° correspond to CP with varying handedness.

[1] P. Fischer and F. Hache 2005, Chirality **17** (2005) 421.
[2] J. J. Maki, T. Verbiest, M. Kauranen, S. Van Elshocht and A. Persoons, J. Phys. Chem. **105** (1996) 767.
[3] M. Kauranen, T. Verbiest and A. Persoons, J. Mod. Opt. **45** (1998) 403.
[4] T. Verbiest, M. Kauranen, Y. Van Rompaey and A. Persoons, Phys. Rev. Lett. **77** (1996) 1456.
[5] M. J. Huttunen, M. Erkintalo and M. Kauranen, J. Opt. A: Pure Appl. Opt. **11** (2009) 034006.

FRONTIERS IN FUSION ENERGY RESEARCH – A REVIEW

S. Jämsä

Aalto University, Department of Applied Physics, P.O.Box 14100, FI-00076 AALTO
email: simppa.jamsa@tkk.fi

The purpose of this work is to present a short review of recent developments and state of the art in fusion energy research. The main focus is in magnetically confined fusion, but most significant results from inertial confinement fusion are also included.

A SHORT INTRODUCTION TO THE PRINCIPLES OF FUSION ENERGY PRODUCTION

The fuel must be maintained hot and dense for a sufficient time period for enough fusions to occur. There are two main approaches: In magnetic confinement the fuel is in plasma state and confined for seconds, but the density is low. The tokamak is the leading concept for the magnetic confinement device. In inertial confinement the fuel is originally solid, and is then compressed into high density with a short, high intensity lasers pulse, but the confinement time is less than nanoseconds.

In either case, the released energy is captured into the reactor walls, where water is heated. The resulting steam is used in the same way as in conventional power plants. A fusion power plant would have the following advantages: Nearly unlimited fuel reserves, high power density, no long-lasting nuclear waste, no CO_2 emissions. The disadvantages are due to the advanced technology and materials needed in a reactor. A power plant is still decades in the future, but closer than ever.

THE FOLLOWING TOPICS ARE PROJECTED FOR THE REVIEW:

- Most significant scientific results in the field.
- Current state of ITER, the large international tokamak reactor being build in Cadarache, France.
- Current state of NIF, the large inertial confinement experiment in operation at The Lawrence Livermore National Laboratory, in USA.
- Major remaining challenges.

CORROSION OCCURING IN THE FOOD PROCESSING INDUSTRY

P. Junell, J. Alarinta and M. Kärkkäinen

Seinäjoki University of Applied Sciences, P.O.B. 64, FIN-60101 Seinäjoki, Finland
email: pasi.junell@seamk.fi

Corrosion has been a subject of numerous investigations during the last hundred years. Different corrosion mechanisms on different metals are more or less understood by now. However, the corrosion of metals under industrial environments has received less attention. More recently, corrosion in food processing industry has been a subject of increasing interest due to its impact on hygiene and product safety [1].

Food processing industry is the fourth largest industry branch in Finland including variety of different types of processes. Figure on the left below illustrates in general the diversity of food industry and its link to different corrosion phenomena. The food processing machinery is exposed to physically and chemically demanding circumstances because of the processes themselves and due to high hygienic requirements that are set to the field of industry. Therefore, machines in direct contact with products are typically made from stainless steel. Other metals are also used in machines and structures that are not in contact with food. However, there are exceptions to this thump rule as hygiene requirements differ from application area to another.

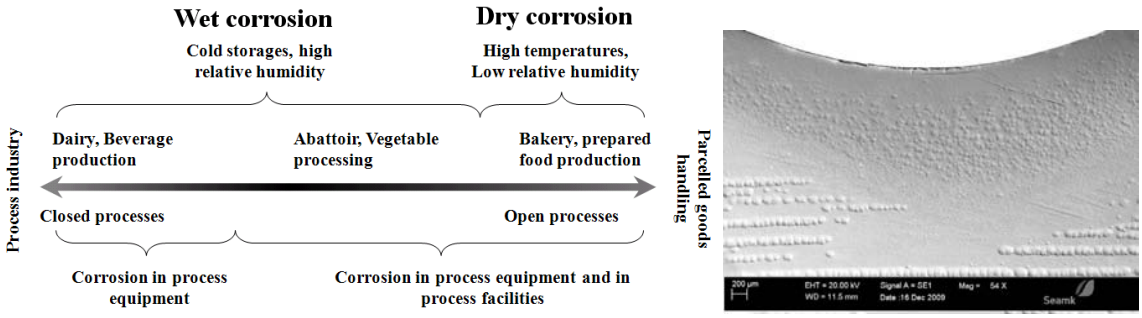

In this study, we have investigated the corrosion occurrence in food industry by interviewing technical personnel from six food processing plants representing the different areas of food industry. By interviewing we were able to achieve comprehension of corrosion occurrence on selected fields of food processing industry. However, the technical personnel were typically not able to distinguish the corrosion mechanisms or the reason behind the corrosion. After the interviews we collected representative corroded steel samples for analysis with scanning electron microscope (SEM) equipped with energy dispersive X-ray spectrometer (EDS). As a result from SEM/EDS analyses, we were able to identify different corrosion mechanisms and determine probable reasons for corrosion of several representative cases. As an example, SEM image of corroded cutting blade from bakery is shown on figure right above indicating two different corrosion mechanisms at different parts of the blade. The complete results of the analyses of different samples will be shown in our presentation.

[1] M. Jellesen, A. Rasmussen and L. Hilbert, Materials and Corrosion 57 (2006) 387.

PRINTABLE POLYANILINE-ALUMINUM THIN FILM BATTERIES

S. Jussila, M.Valkiainen, K. Solehmainen and S. Kielosto*

VTT Technical Research Centre of Finland, Printed Functional Solutions, PO BOX 1000, FI-02044 VTT, Finland
*Aalto University, School of Science and Technology, Department of Automation and Systems Technology, PO BOX 15500, FI-00076 AALTO, Finland
email: salme.jussila@vtt.fi

Electroactive polymers like polyaniline (Pani) can be used as battery electrodes in both disposable (primary) and rechargeable (secondary) batteries [1]. They have high energy content with respect to unit weight and volume as well as low manufacturing costs. Commercial polyaniline dispersions are also printable on various substrates with standard printing methods such as flexography [2]. Here we report the fabrication and testing of thin flexible batteries utilizing doped polyaniline as the cathode, aluminium foil as the anode and ion conducting hydrogel as the electrolyte. We have measured these batteries with different constant current loads in a potentiostat and in a periodical pulse testing arrangement.

The most essential step of the fabrication process involves impregnating paper or board material with toluene based polyaniline dispersion. When the solvent has evaporated the polyaniline cathode is combined with the aluminium foil anode coated with the electrolyte. In the test procedure the open circuit voltage (OCV) was first measured and then the battery was discharged with a constant current load (20, 50 or 100 µA) and the battery voltage was registered as a function of time. Typically OCV was at first 1.0 Volts (Fig. 1) and dropped to 0.7-0.8 Volts during stabilization. During 80 hours of discharge with 50 µA current the voltage decreased to 0.507 Volts. The area of the tested battery was 25 cm^2 and this gives the current density value of 2 $\mu A/cm^2$ and the capacity of 113 $\mu Wh/cm^2$ in this voltage range. Some batteries were charged with a constant current by using the same system, but the operation could be repeated only once.

Figure 1.
Open circuit voltage of the fresh Pani-aluminum battery is typically between 0.9 – 1.0 Volts.

[1] P. Novak et al., Chemical Reviews **97** (1997) 207.
[2] T. Mäkelä et al, Synth. Metals **153** (2005) 285.

THE HELSINKI POSITRON LIFETIME BEAM – PRESENT STATUS AND DATA ANALYSIS TECHNIQUE

E. Korhonen, F. Reurings and F. Tuomisto

Department of Applied Physics, Aalto University, P.O.Box 11100, FI-00076 Aalto, Finland
email: esa.korhonen@tkk.fi

Positron annihilation spectroscopy is an experimental method for probing the atomic structure and local electron density of a sample at the point chosen by the electrostatic interaction of the positron. Information about the annihilation environment is carried by the time and energy spectra of the annihilation radiation. Positron lifetime is a measure of defect concentration and the size of lattice vacancies, whereas the Doppler broadening spectrum is dependant on the electron momentum distribution. By measuring these quantities several types of localized structures of the bulk material can be investigated.

To measure positron lifetime in thin surface layers, a slow positron beam with accurate timing is required. This is achieved by modulating the slow positrons obtained from a Na-22 source and moderator with a three-stage radio frequency pulsing system. The resulting positron pulses are less than 200 ps FWHM with a peak-to-background ratio of 1000:1 and a 30% pulsing efficiency. After bunching the beam is accelerated to the desired energy between 2 and 30 keV. Detector signal is collected by a high-speed digitizer and the lifetimes extracted by an in-house developed program. The overall time resolution of the system is 270 ps.

Since positron diffusion effects are significant when measuring thin layers, the usual method of fitting exponential decay components to the lifetime event distribution is no longer valid. Furthermore, the pulsing distorts the positron time distribution leading to a non-gaussian resolution function [1]. Another method for analyzing the lifetime data is required.

We present the current status of the pulsed positron beam and the data-analysis method developed for the device. Measurement data is analyzed by fitting a theoretical lifetime distribution to the observed data. The distribution is calculated starting from material parameters such as trapping rate and diffusion coefficient. The non-linear fitting procedure is carried out by a Matlab program.

[1] F. Reurings and A. Laakso, Physica Status Solidi C 4 (2007) 3965.

APPLICATION OF R-FUNCTIONS FOR GAMMA-RAY DETECTION EFFICIENCY WHEN MEASURING ACTIVITY OF RADIOACTIVE SAMPLES WITH COMPLEX SHAPES

O. Korniyenko[1], T.Enqvist[2], K.Loo[1,2] and W.H.Trzaska[1]

[1]University of Jyväskylä, Finland
[2]University of Oulu, Finland
email: oleg.kornienko@luukku.com

The **R** –function theory developed by Ukrainian mathematician V.L. Rvachev [1], describes the complex shape figures and bodies analytically. The logical equation of the boundary domain $W = W_1 \cup W_2 \cap ... \cup W_m$ is constructed, using Boolean algebra, by the support sets, $W_i = (x : \omega_i(x) \geq 0)$, known from analytical geometry. **R**-function $\omega(x) = \omega_1 \vee_\alpha \omega_2 \wedge_\alpha \cdots \vee_\alpha \omega_m$ is defined as a continuous real function, with following conditions: $\omega(x) > 0,\ x \in W$; $\omega(x) = 0,\ x \in \partial W$; $\omega(x) < 0,\ x \notin W$.

To integrate over a complicated volume W , find N point $x_1, x_2, \ldots, x_N$ randomly selected in an easier multidimensional volume Ω , $W \subseteq \Omega$. Then using Monte Carlo integration technique

$$\int_W f\ dV = \int_\Omega f \cdot \chi_W\ dV \approx \int_\Omega dV \times \frac{1}{N} \sum_{i=1}^{N} f(x_i)\, \chi_W(x_i),$$ where

the indicator function $\chi_W = \max\left(\frac{\omega(x)}{|\omega(x)|}, 0\right) = \begin{cases} 1, x \in W \\ 0, x \notin W \end{cases}$

MATLAB codes are made finding solid angels for evaluation of gamma-ray detection efficiency [2].

The results have been applied, for instance, for the activity study of the rock samples collected from the Pyhäsälmi mine. The results are relevant to the cosmic ray experiment EMMA and to the LAGUNA project.

[1] L. Rvachev: *Methods of Logic Algebras in Mathematical Physics*, Naukova dumka, Kiev, 1974.

[2] G.F.Knoll Radiation Detection and Measurements. 1979, p.p 92- 95

UNIVERSITY OF JYVÄSKYLÄ

Dynamic Mechanical Analysis testing of Norwegian spruce

J. Lääkkö, A. Salmi, F. Gates, T. Karppinen and E. Hæggström

University Of Helsinki / Department of Physics
Electronics Research Unit
Gustaf Hällströmin katu 2
FI-00014 University of Helsinki
Tel. 09 191 50693

The dynamic properties of wood are of interest to the industry. There is strong frequency dependence in mechanical properties of wood. These properties have been widely studied using static tests and in the MHz range with ultrasound. However, these frequencies are considerably different from those of most industrial processes, which tend to be in the kHz range.

Dynamic Mechanical Analysis (DMA) is an instrument which is widely used to measure rheological properties of polymers. In this study the dynamic elastic modulus of wood in the longitudinal wood direction was measured at frequencies between 1 and 200 Hz using DMA. The samples were block-shaped dry Norwegian spruce (Picea abies). Prior to this experiment, they were tested by a standardized three-point bending test to obtain the static longitudinal modulus of elasticity in longitudinal wood direction.

These results will be used with data from previous static and ultrasonic measurements to verify the Pritz five-parameter derivative model [1], which gives a prediction on the frequency dependency of the dynamic elastic modulus.

[1] T. Pritz, *Five-parameter fractional derivative model for polymeric damping materials*, Journal of Sound and Vibration, 265(5), pp. 935-952, 2003

NEW HEAVY ION SOURCE, MODIFIED INJECTOR AND NEW TOF-ERDA BEAMLINE FOR PELLETRON ACCELERATOR

M. Laitinen, V. Nieminen, O. Vaittinen, L. Mättö, A. Arcot, J. Julin, M. Napari, H.J. Whitlow and T. Sajavaara

University of Jyväskylä, Department of Physics, P.O. Box 35, 40014, Finland
email: mikko.i.laitinen@jyu.fi

During the year 2009 accelerator based material physics group at JYFL constructed a new heavy ion-source, rebuilt the injector and installed a new beamline for the ToF-ERDA spectrometer at the 1.7 MV Pelletron accelerator (Fig. 1).

A sputtering heavy ion source was commissioned and put to operation for wide range of negative ions from hydrogen up to gold. Also the whole injector with Alphatross RF-source was rebuilt.

On the high energy side of the accelerator, a new ToF-ERDA beamline was constructed for high resolution elemental depth profiling and resolution better than 2 nm at the surface has already been achieved. The vacuum in the spectrometer was designed to reach the UHV region so for fast sample change a load lock was designed and constructed.

In the time-of-flight-energy (TOF-E) spectrometer we used commercially available microchannel plate detectors for the time-of-flight signal and a standard implanted silicon detector for detecting particle energies. Labview based data acquisition system enables list-mode data collection via NI's FPGA card with 25 ns resolution time stamps for each event. In the near future, first timing gate will be modified to be position sensitive in order to further improve the depth resolution. Furthermore, solid state energy detector will be replaced by gas ionization detector with much better energy resolution for low energy heavy ions.

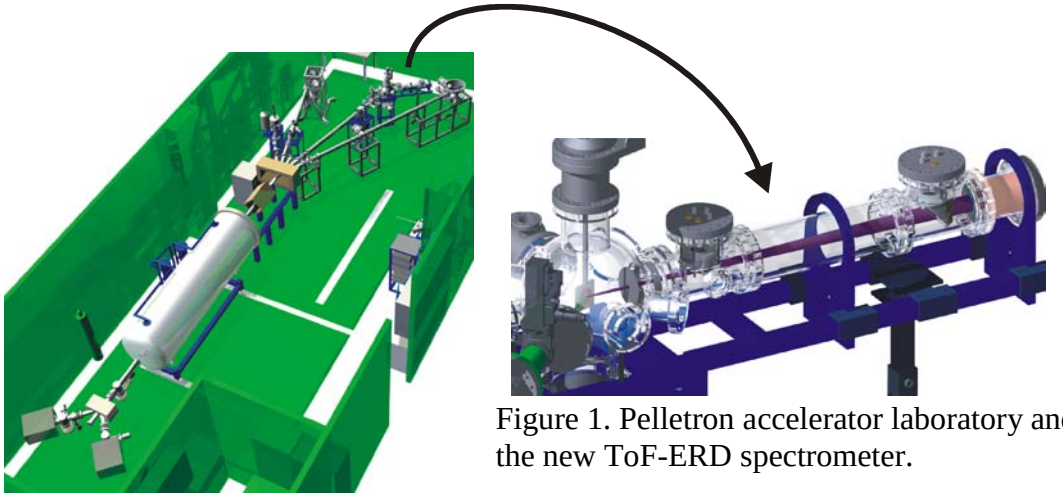

Figure 1. Pelletron accelerator laboratory and the new ToF-ERD spectrometer.

SEITSEMÄN IHMETTÄ – SEVEN MIRACLES OF PHYSICS ROAD SHOW

Anssi Lindell, Anna-Leena Latvala and Jouni Viiri

Dept. of Teacher Education, P.O. Box 35, FIN-40014 University of Jyväskylä, Finland
email: anssi.lindell@edu.jyu.fi

Seitsemän Ihmettä (Seven Miracles) is a low budget science road show for small schools and institutes that are located far from the main national science centers and museums in southern Finland. It is annually re-designed and realized by voluntary Physics teacher students in co-operation with the Departments of Physics and Teacher Education of University of Jyväskylä. The approach can vary from a stage presentation to table demonstrations and workshops and combinations of these.

Each year, the theme of the road show is selected to include current topics. Seitsemän ihmettä started in 2007 with an energy theme. In the international year of astronomy, 2009, the show introduced pupils to conditions in stars and space [1]. The next tour in spring 2010 will concentrate on senses.

The target audience of the show is not only the pupils of the schools, but also their teachers. While the pupils' main interests are in the phenomena, the teachers are instructed to the content knowledge and pedagogy of the topics. Seitsemän ihmettä is also suitable for entertainment or an ice-breaker in meetings, celebrations or exhibitions.

In this poster we shall introduce the highlights of the previous road shows and give a peek into the miracles in science which will have their premiere on March 2010.

[1] A. Lindell and J. Varsaluoma, Dimensio 4 (2009).

UNIVERSITY OF JYVÄSKYLÄ

EXPERIMENTAL PHYSICS FOR ADVANCED STUDENTS

A. Lindell[1)], A. Latvala[1)], J. Lauros[2)], T. Nevanpää[3)] and J. Viiri[1)]

1) Department of Teacher Education
2) Department of Physics
3) Teacher Training School
P.O. Box 35, FIN-40014 University of Jyväskylä, Finland.
email: anssi.lindell@jyu.fi

The practical and problem-solving skills of upper secondary school graduates in Physics are not on par with requirements for degree studies. To bridge the gap, we encourage the students to take on more demanding physics in the form of Physics competitions and weekend camps.

The International Physics Olympiads is one of the greatest international Physics happenings with more than 400 students from 90 participating countries. The upper secondary students compete in problem solving and experimental work. Finland has taken part in the Olympiad since 1976. The Olympic teams have received training in theoretical problem-solving as well as experimental work.

Experimental equipment has been collected throughout the years from the previous Olympiads. The experiments have been carefully developed by teams of scientists of the organizing countries and reviewed by the international board of the participating countries. We have a comprehensive collection of the Olympiad equipment and are offering it for interested students also outside the Olympic team. To reach these students, we have organized an upper secondary school experimental Physics course and a Physics training camp. In both outreaches we are using six experiments ranging from mechanics to modern physics, covering the upper secondary school curriculum.

As a showcase of this work, we present an optics experiment from the 2009 Olympiad [1], focusing on measuring the wavelength of a laser beam using a diffraction pattern from the interference of light from a lens and a razor blade. The experiment includes designing the setup, completing the measurements and calculating the result using graphical analysis.

[1] A. Lindell, L. Franti and M. Ahtee, Dimensio 4 (2009).

UNIVERSITY OF JYVÄSKYLÄ

PROCESS TOMOGRAPHY UNDER NONSTATIONARY VELOCITY FIELDS

A. Lipponen[1], A. Seppänen[1] and J.P. Kaipio[1,2]

[1] Department of Physics and Mathematics, University of Eastern Finland, FI-70211 Kuopio, Finland
[2] Department of Mathematics, University of Auckland, Auckland 1142, New Zealand
email: Antti.Lipponen@uef.fi

Process tomography (PT) refers to a variety of imaging techniques used in process industry. The applications of PT include monitoring, control and design of mixing and foaming processes, mass transport in pipelines, and chemical reactors. Typical imaging modalities used in PT are based on the use of radiation, ultrasound, or electric currents, and the suitable imaging modality naturally depends on the physical properties of the target.

In 2001, Seppänen et al. developed an image reconstruction technique for PT based on the state estimation approach [1]. In the state estimation approach, the temporal evolution of the target is modelled and the model is employed in the reconstruction. This enables accurate imaging of rapidly varying targets and also the inference of the evolution model parameters, such as the velocity field.

In our recent studies, we employed flow model based on convection-diffusion and Navier-Stokes equations as the evolution model, and evaluated the accuracy of the state estimation approach with simulations. Electrical impedance tomography (EIT) was used as the imaging modality. Also, the errors due to the model reduction used in the state estimation were taken into account by employing the recently introduced approximation error approach [2]. A snapshot of the true (simulated) and estimated concentration distribution and velocity fields are depicted in Figure 1, see [3] for more details. Further, experimental evaluation of the state estimation approach in process tomography with approximation error approach and EIT was carried out.

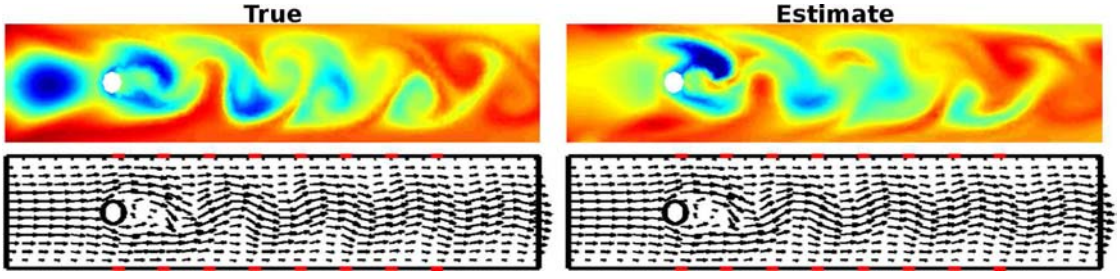

Figure 1: Simulated (left column) and estimated (right column) concentration distributions and velocity fields for one instant of time. Thick red lines depict locations of the electrodes.

[1] A. Seppänen et al., Inverse Problems 17 (2001) 467-483.
[2] J.P. Kaipio and E. Somersalo, (2005) Springer-Verlag, New York.
[3] A. Lipponen, A. Seppänen, and J.P. Kaipio, Inverse Problems (2010). In review.

MODELING THE OPTICAL PROPERTIES OF METAL NANOPARTICLES WITH THE FINITE DIFFERENCE TIME DOMAIN METHOD

J. Mäkitalo, H. Husu and M. Kauranen

Department of Physics, Optics Laboratory, P.O.B. 692, FI-33101 Tampere University of Technology, Finland
email: jouni.makitalo@tut.fi

The rapid development of nanofabrication techniques, such as electron beam lithography, during recent years has enabled the experimental research of sub-wavelength metamaterials. Especially the study of metal nanostructures has spawned many novel applications and research branches, such as second-harmonic generation and surface-enhanced Raman scattering. These phenomena benefit from the substantial field enhancement due to plasmonic resonances that characterize metal nanoparticles. Usually, the symmetry of the local electric field plays a vital role in the process efficiency.

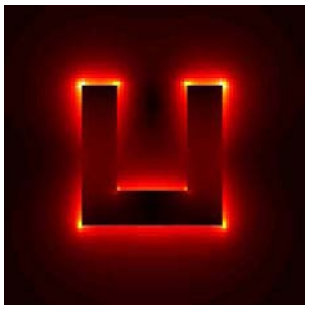

Figure 1: Electric field amplitude in a gold split-ring resonator.

To rigorously understand the yield in the afore-mentioned processes, the governing electromagnetic problem must be solved. By analyzing the distribution of local elecric fields, one is able to make qualitative predictions and optimize materials without the need to build a physical sample at each step. For large size parameters, a full wave solution to the Helmholtz equation is only obtainable in closed form for ellipsoidal particles and thus one needs to resort to numerical methods.

The Finite Difference Time Domain (FDTD) method has been used to solve electromagnetic wave problems since 1966 when first reported by Yee [1]. This method scales extremely well to electrically large problems, since no system matrix generation nor solving systems of linear equations is involved. Using massively parallel computing via Message Passing Interface, it is possible to model the optical and electromagnetic properties of metal nanoparticles with spatial resolution down to parts of a nanometer. We developed a parallel FDTD solver with state-of-the-art features, such as Convolutional Perfectly Matched Layer absorbing boundary conditions [2] and combined Drude-Lorentz formulation of dispersive media [3], to investigate the plasmonic modes in non-centrosymmetric gold nanoparticles (Fig. 1). Spectral properties of fabricated samples could be reproduced with numerical computation with reasonable accuracy and FDTD results proved to give a significant aid in the characterization of resonances.

[1] K. S. Yee IEEE Transactions on Antennas and Propagation 14 (1966) 302.
[2] J. A. Roden and S. D. Gedney, Microwave and Optical Technology Letters 27 (2000) 334.
[3] M. Okoniewski and E. Okoniewska, Electronics Letters 42 (2006) 503.

THE ANALYSIS OF HYBRID ELECTROMAGNETIC-SPIN WAVES PROPAGATION IN SLOT TRANSMISSION LINE

A. Nikitin[1,2], A. Semenov[1], S. Karmanenko[1] and E. Lähderanta[2]

[1]Saint Petersburg Electrotechnical University "LETI", Professor Popov str. 5, St.Petersburg, 197376, Russia
[2]Lappeenranta University of Technology, P.O.Box 20, FIN-53851 Lappeenranta, Finland
email: and.a.nikitin@gmail.com

The interest to layered structures comprising the materials of nonlinear physical properties is enhanced during recent years. Basing on the ferrite-ferroelectric layered structures one can develop principally novel frequency-agile microwave devices possessing the combined electrical and magnetic tunability.

Spin waves (SW) can propagate in the ferromagnetic films with low wave energy dissipation, such as yttrium iron garnet (YIG). These magnetization waves are widely used in tunable mutual and non-mutual devices. The advantages of spin waves are diversity of the dispersion characteristics, low phase and group velocities and wide frequency range of tunability. However spin waves devices have a serious disadvantage. This disadvantage is connected with necessity to use variable magnetic fields to tune spin wave devices. Magnetic tunability method has serious lacks, such as a large-size magnetic system, low tuning velocity and high power consumption. Another kind of the materials possessing nonlinear physical properties is ferroelectrics. Dielectric permittivity of ferroelectric materials is changing under action of applied electric field. Ferroelectric layers could be included in the combined devices. Fast tunability (nanoseconds), low energy consumption and small mass and dimensional parameters of the electrical systems are able to improve the parameters of the tunable microwave devices based on ferroelectric-ferromagnetic structures. Most practical interest is connected with the planar film layered structures.

Ferrite-ferroelectric layered structures can be combined with microwave slot transmission line. In this case thin ferroelectric film could be used. This work presents the theory of the hybrid electromagnetic-spin waves propagation in the slot transmission line based on the ferrite-ferroelectric layered structure. The dispersion equation and characteristics of the hybrid waves have been obtained. Theoretical and experimental investigations were performed. It has been demonstrated that slot line with thin ferrite and ferroelectric films filling could be considered as the microwave tunable resonator or phase shifter with the dual tuning by external magnetic and electric fields.

MODELING OF PROCESSES IN THE MAGNETRON SPUTTERING SYSTEM WITH HIGH CURRENT DENSITIES

N. Nikitina[1,2], V. Barchenko[1], E. Lahderanta[2]

[1]Saint Petersburg Electrotechnical University "LETI", Professor Popov str. 5, St.Petersburg, 197376, Russia
[2]Lappeenranta University of Technology, P.O.Box 20, FIN-53851 Lappeenranta, Finland
email: natalia.nikitina@lut.fi

In this work we construct a model for processes in magnetron sputtered systems (MSS) at high cathode current densities. Earlier was introduced a number of assumptions [1]:
1. If the discharge current density is strong, larmorovkiy radius of the electron can be several times greater than the width of the cathode potential drop. This gas ionization will occur in the positive column plasma. The primary role to maintain the discharge is the stream of ions from the cathode positive column plasma. 2. Pressure and the currents are very low, so that the area involved in the discharge is more than the thickness of the cathode space. Then the layer can be considered as flat and one dimensional. 3. The potential distribution in the cathode drop, in general, obeys the Poisson equation. 4. According to the continuity law of the current in a stationary process, the discharge current density in any section x is constant. 5. In the area of the cathode potential drop the following conditions apply: $n_i >> n_e$; $j_i >> j_e$ and $\rho_i >> \rho_e$
6. Primary electrons from the cathode and the newly formed electrons, move on cycloid directions along the surface from the cathode to the anode and move only because of collisions with neutrals. The whole target area is bounded by the magnetic field lines when the discharge current density in the sputtering is strong. Therefore, the calculation of the compound sputtering was adopted in the whole area [2].
We made modeling of a theoretical I-V curve and a charged experimental copper target. Their difference was 20% for selected values of pressure and magnetic field. These differences may be explained by the inaccuracy in determining the approximation coefficients A_f and B_f, which are proportional to the number of ionizing collisions in the mean free path and to the ionization voltage drop, respectively.
To make the model applicable to a particular MSS, it is required preliminary comparison of the banding changes p_{eff} and approximation of the coefficients A_f and B_f. In other case, the model is simple enough to estimate the I-V, if one knows the complexity of the processes occurring at high current densities at the cathode MSS.
When constructing the theoretical I-V characteristics for certain values of the discharge current, a characteristic voltage drop is observed.

[1] Данилин Б. С., Сырчин В. К., Магнетронные распылительные системы.- М.: Радио и связь, 1982.- 72 с., ил.
[2] Кузьмичев А. И., Магнетронные распылительные системы. Книга 1. Введение в физику и технику магнетронного распыления.- Киев.: Аверс, 2008.- 244 стр., ил.

Development of research with an accelerater microbeam (DREAM)

Rattanaporn Norarat , Harry J. Whitlow, Timo Sajavaara and Mikko Laitinen

Department of Physics, P.O. Box 35(YFL), FIN-40014 University of Jyväskylä, Finland
email : ranorara@jyu.fi

Varpu Marjomäki and Leona Gilbert

Department of Biological and Environmental Science, P.O. Box 35 (YA; Survontie 9)
FIN-40014 University of Jyväskylä, Finland

MeV ions offer many advantages for materials and biomedical imaging, such as mapping spacial distributions of trace elements and sub-optical diffraction limit imaging of fluorescent labelled biomolecules. The *Jyväskylä MeV ion beam lithography system* at the Pelletron Accelerator is being adapted to develop a state-of-the-art ion beam imaging. Here we present a short presentation of the DREAM project which is a flexible tool for development of a MeV-ion nanobeam for imaging and lithography [1]. The system will initially be based on focussing with a so-called quadrupole doublet in a Heidelberg microbeam configuration [2], but also retain the capability of Programmable Proximity Aperture Lithography (PPAL). The system can easily be extended to a higher order quadrupole muliplet later to achieve true nanometre resolution. The sample holder is computer controlled and will hold three standard samples that are mounted on electron microscope grids. The imaging signals that will be available are direct-Scanning Transmission Ion Microscopy, (direct-STIM), secondary electron, fluorescence photons and PIXE. The data system will, in contrast to conventional systems, use a total data collection approach which allows dynamic changes to be studied. This is based on using LabView with a Field Programmable Gate Array (FPGA) board. This will be provided with an interface to BioImageXD to facilitate sophisticated multidimensional image rendering.

[1] H. J. Whitlow, M. Ren, J. A. van Kan, F. Watt, D. White.Nucl. Instrum. Methods B 260 (2007) 28
[2] G. W. Grime and F. Watt, *Beam optics of quadrupole probe-forming systems*, (Adam Hilger, Bristol, 1984)

NANOPROBER AS A TOOL FOR ELECTRICAL MEASUREMENTS OF NANOSTRUCTURES

L. Olanterä[a], K. Arstila[a], T. Hantschel[a], S. Palanne[b], and T. Sajavaara[b]

[a] IMEC, Kapeldreef 75, B-3001 Leuven, Belgium
[b] Department of Physics, P.O. Box 35, 40014 University of Jyväskylä, Finland

The nanoprober is a tool which combines nanomanipulation, scanning electron microscopy (SEM) and electrical measurements using a parameter analyzer. Four nanomanipulators and a linear xyz sample stage allow to position several tips independently on a selected structure at the sample surface with nanometer precision. Contacting with a 100-nm diameter tungsten tip allows to measure e.g. electrical properties of individual CNTs (Fig. 1a).

Electrical measurements for semiconductors require a very high pressure ($\sim$10 GPa for Si) to obtain an ohmic contact between the tip and the structure. In these conditions metallic tips wear rapidly and reliable measurements are in most cases impossible. To overcome this limitation, we have designed and manufactured an in-plane conductive diamond tip which allows for high-contact force electrical measurements with accurate positioning and good visibility of the contact point (Fig. 1b) [1].

To achieve good repeatability in high-contact force measurements, a force control system is essential. We present here a force control solution based on an optical-lever principle, used in atomic force microscopy. In this design the laser, the detector and the tip are integrated in one slim and light-weight unit (only $\sim$3.5 g) which can be attached to a nanomanipulator allowing precise positioning in a SEM (Fig. 1c) [2].

Currently an automated electrical measurement system is developed using a Labview-based control system and applying force control with diamond tips in a nanoprober.

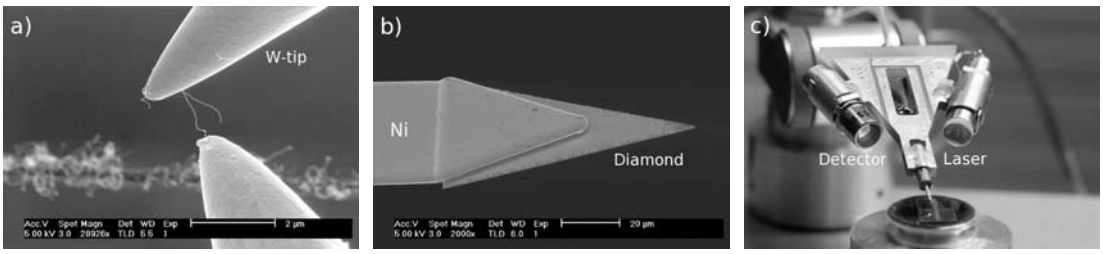

Figure 1: a) Electrical measurement of a single MWCNT. b) In-plane diamond tip for high contact force electrical measurements. c) Optical force measurement system attached to a nanomanipulator.

[1] K. Arstila, T. Hantschel, C. Demeulemeester, A. Moussa, W. Vandervorst, Microelectronic Engineering 86 (2009) 1222.
[2] K. Arstila, T. Hantschel, S. Kleindiek, J. Sterr, Q. Vaquette, C. Demeulemeester, W. Vandervorst, Microelectronic Engineering, in press.

TOWARDS A HIGH POWER ULTRASHORT-PULSE CARRIER-ENVELOPE PHASE STABLE HIGH REPETITION LASER SYSTEM

L. Orsila, C. Grebing and G. Steinmeyer

Optoelectronics Research Centre, Tampere University of Technology, P.O.Box 599, FIN-33101 Tampere, Finland
email: lasse.orsila@tut.fi

Carrier-envelope phase (CEP) stabilization [1] has opened an avenue towards frequency metrology with unprecedented precision [2] and optical pulse generation on the previously inaccessible attosecond time scale [3]. Such laser sources have recently become even commercially available for novel scientific experiments, but quite clearly, there is a major gap between oscillators and amplified sources in the region between 10 kHz and 1 MHz repetition rate. In this paper we present a scheme and work in progress towards a 100-kHz source of few-cycle microjoule pulses, clearly advancing the limits of amplified laser sources. The system consists of four main sections as shown in Fig. 1. The first section is a nearly octave-spanning 6-fs Ti:sapphire oscillator with roughly 78 MHZ repetition rate and 200–300 mW average power. The next part is a novel CEP stabilization scheme, which utilizes the difference frequency of the far ends of the broad fs-oscillator spectrum. This signal is then electronically filtered and sent to the feedback loop with an AO shifter that shifts the signal to zero CEP. After pulse-picking with a Pockel's cell the beam enters a multi-pass cryogenically cooled Ti:sapphire amplifier, where the pulses are intensified to reach the microjoule level. The last stage is pulse compression. This may require high-pressure gas cells, using special photonic crystal fibers, special ducts, or creation of a filament. An alternative could be supercontinuum generation in liquid media such as water.

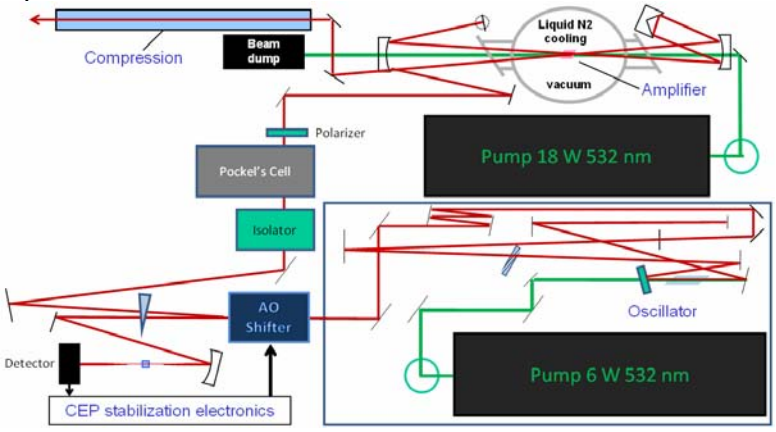

Fig. 1: Schematic of a 100-kHz repetition rate μJ-level CEP stable laser system.

[1] H. R. Telle, G. Steinmeyer, A. E. Dunlop, J. Stenger, D. H. Sutter and U. Keller, Applied Physics B 69, 327–332 (1999)
[2] T. W. Hänsch, Nobel Lecture, Rev. Mod. Phys. 78, 1297–1309 (2006)
[3] A. Baltuška, T. Udem, M. Uiberacker, M. Hentschel, E. Goulielmakis, C. Gohle, R. Holzwarth, V. S. Yakovlev, A. Scrinzi, T. W. Hänsch and F. Krausz, Nature 421, 611–615 (2003)

GEOENGINEERING WITH SEA SPRAY EMISSIONS

A.-I. Partanen[1,2], H. Kokkola[2] and H. Korhonen[1]

[1] Department of Physics and Mathematics, University of Eastern Finland,
Kuopio Campus, P.O.B. 1627, FI-70211 Kuopio
[2] Finnish Meteorological Institute, Kuopio Unit, P.O.B. 1627, FI-70211 Kuopio
email: antti-ilari.partanen@uef.fi

In recent years deliberately altering the climate system has been a target of extensive research. One of these geoengineering ideas is to inject sea spray aerosol in selected regions over the oceans to provide additional cloud condensating nuclei (CCN) for low-level clouds. Previous model studies have assumed a fixed cloud droplet number concentration (CDNC) in the modified marine regions without any microphysical calculations [2]. In this study we use aerosol-climate model ECHAM5-HAM to get a better view on the cloud droplet activation and the microphysical processes that affect the injected sea salt particles and cloud droplets. The second main goal is to calculate the radiative forcing caused by the cloud modification. We perform simulations with five different wind-speed dependent sea spray fluxes (baseline flux and its multiples.) These fluxes fall roughly into the range of previous estimates of the required injection rates [1]. Four marine regions are selected for cloud modification.

Increase in cloud top cloud droplet concentration with the baseline flux is only about 20 % at maximum and over most regions the increase is much lower. Three times the baseline flux is enough to double the cloud top concentrations near the coasts, but the effect is weaker further to the oceans. The effects on the clouds are fairly similar to each other in all regions except on the coast of Australia. The effect of the added particles doesn't properly reach the cloud level there. We calculate the radiative forcing by comparing 10-year mean values for the top of the atmosphere total radiation from the geoengineered climate with the control simulation. Global mean value of this Radiative Flux Perturbation (RFP) was -0.44 Wm^{-2} for the baseline simulation. With double, triple, quadruple and quintuple fluxes the RFPs were -0.90, -1.72, -2.44, -3.12 Wm^{-2}, respectively. Local RFPs were much higher: in the baseline simulation they were about 3-4 Wm^{-2} and in the simulation with twice the baseline flux the RFPs were around 8-10 Wm^{-2}.

These results show that aerosol microphysics and cloud activation must be explicitly calculated when studying marine stratocumulus cloud modification schemes. Otherwise the regional differences might be left unnoticed and the number concentration of activated cloud droplets could be over or under estimated.

This work was supported by Nessling Foundation under grant 2009152.

[1] J. Latham, Atmospheric Science Letters, 3 (2002) 52
[2] A. Jones, J. Haywood and O. Boucher, Journal of Geophysical Reasearch, 114 (2009) D10106

TRANSIENT CURRENT TECHNIQUE FOR THE STUDY OF RADIATION HARDNESS OF SEMICONDUCTOR DETECTORS

T. Peltola[1)], J. Aaltonen[1)], S. Czellar[1)], J. Härkönen[1)], I. Kassamakov[1),2)], and E. Tuominen[1)]

[1)] Helsinki Institute of Physics, P.O.B. 64, FIN-00014 University of Helsinki, Finland
[2)]University of Helsinki, Department of Physics, Electronics Research Laboratory, P.O.B. 64, FIN-00014 University of Helsinki, Finland
email: timo.peltola@helsinki.fi

Transient Current Technique (TCT) is a tool to measure the charge collection efficiency of an irradiated silicon-detector. It is based on the detection of the dominant type of charge carriers, electrons or holes, which are getting trapped by the radiation induced defects while drifting through the detector thickness. The excitation of the electron-hole pairs is achieved either by picosecond laser pulse or by radioactive source.

Electrical part of a novel TCT measurement system was manufactured and tested at the Helsinki Detector Laboratory. AutoCAD design of the vacuum chamber including the sample holder is shown in Fig.1. The Helsinki TCT system is being operated were performed with red laser (670 nm) and pulse generator. The Helsinki TCT resembles the CERN RD39 cryogenic TCT [1], e.g. the 3 GHz oscilloscope and the operating software are identical.

Fig.1. AutoCAD design of the Helsinki TCT vacuum chamber including the sample holder.

[1] J. Härkönen et al., Nuclear Instruments and Methods in Physics Research A 583 (2007) 71-76.

HIGH INTENSITY AIRBORNE ULTRASOUND SOURCE FOR SENSING AND MACHINING

J. Pentikäinen, I. Lassila, E. Hæggström

Electronics Research Laboratory, Department of Physics, P.O.B. 64, FIN-00014 University of Helsinki, Finland
e-mail: juha.ao.pentikainen@helsinki.fi

We present research into ionic high-intensity (120+ dB SPL), high-bandwidth (5 kHz to 100+ kHz) ultrasound sources. The ultrasound is produced by modulating a high-voltage ion flame on an electrode. The operating principle promises powerful and versatile transducer designs due to improved acoustic coupling into gas compared to previous piezoelectric and capacitive transducers. The modulated ion flame is also nearly massless and practically a point source.

We describe the design, building and testing of this type of transducer and its power supply. The bandwidth, sound pressure level, transient response, directivity and stability of the system are reported as well as the electric characteristics of the resonance coil and the required feedback.

The end-use of these transducers could be non-destructive evaluation in a multitude of environments, shaping granules for pharmaceutical purposes, measuring nonconductive materials and samples that laser-acoustic excitation would alter. Higher sound pressure levels and high spatial resolution can be achieved by focusing the ultrasound with parabolic mirrors.

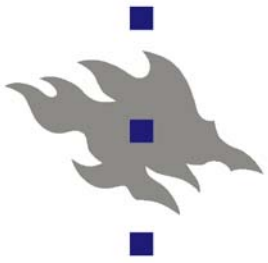

UNIVERSITY OF HELSINKI

SUB WAVELENGTH NANOSTRUCTURES FOR BROAD BAND SOLAR CELLS ANTI-REFLECTION COATINGS

V. Polojärvi, J. Tommila, J. Salmi, A. Aho, A. Tukiainen, A. Schramm, J. Viheriälä, and M. Guina

Optoelectronics Research Centre, Tampere University of Technology, P.O.B. 692, FIN-33101 Tampere, Finland
email: ville.polojarvi@tut.fi

The deployment of high efficiency solar cells (SC) to terrestrial systems have attracted increasing interest during past few years owing to development of advanced solar concentrators able to meet grid parity requirements. Multi-junction III-V compound semiconductor SCs have the highest conversion efficiencies (η) in photovoltaic systems: three-junction III-V cells have reached $\eta \approx 41$ % in concentrator applications [1]. Due to exploitation of three different band structures, such devices have a wide absorption spectrum ranging from 300 nm to 1800 nm. Theoretical calculations have revealed that efficiencies of about 70 % can be reached if the entire solar spectrum would be collected [2]. To reach higher η, novel SC material systems must be developed to absorb as much from the solar spectrum as possible.

In addition, advanced designs should be devised to mitigate the high discontinuity of refractive index at semiconductor SC/air interface, leading to high back reflection. To avoid unwanted reflection, dielectric multilayer interference structures can be used as an anti-reflection (AR) coating. An optimization of multilayer dielectric structure is challenging, and yet, this type of coating works only at limited wavelength bands and exhibits highly angular dependent reflection. Another method to make AR coating is to exploit so called moth-eye AR structures [3], consisting of sub wavelength nanostructures (Fig. 1). This type of nanostructures provides a graded transition of refractive index between the air and the semiconductor SC, and thus, decreases the amount of reflected light at broad band and at all angles. Moth-eye AR structures have been successfully applied, e.g., on silicon [4], GaAs [5], and GaSb [6] substrates.

Here we demonstrate sub-wavelength AR moth-eye nanostructures (Fig. 1) on molecular-beam epitaxy grown AlInP/GaAs(100) semiconductors. Moth-eye structures are fabricated by nanoimprint lithography [7] on AlInP, which is commonly used as a window layer material in III-V semiconductor SCs. Average reflection of less than 3 % is demonstrated at the wide spectral range from 450 nm to 1650 nm and at normal incidence.

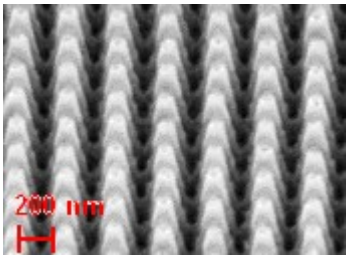

Fig. 1. Scanning electron microscope image of moth- eye nanostructures etched on AlInP.

[1] W. Guter *et. al.*, Appl. Phys. Lett. **94**, 223504 (2009).
[2] A. De Vos, H. Pauwels, Appl. Phys. **25**, 119 (1981).
[3] P. Clapham, M. Hutley, Nature **244**, 281 (1973).
[4] Q. Chen *et. al.*, Appl. Phys. Lett. **94**, 263118 (2009).
[5] C.-H. Sun *et. al.*, Opt. Lett. **33**, 2224 (2008).
[6] W.-L. Min *et. al.*, Appl. Phys. Lett. **92**, 141109 (2008).
[7] J. Kontio *et. al.*, Opt. Lett. **34**, 1979 (2009).

NOVELL TECHNIQUES FOR HOT CAVITY CATCHERS AND GAS CELLS AT IGISOL

M.Reponen , V. Sonnenschein, I. Pohjalainen, M. Savonen I.D. Moore and J. Äystö

University of Jyväskylä, Department of Physics, Survontie 9, 40500 Jyväskylä, Finland
email: mikael.h.t.reponen@jyu.fi

Two projects are underway in the IGISOL group at the JYFL accelerator laboratory that aim to improve the existing recoil catcher systems. Though the projects approach recoil catching from different directions, they both share the ion production mechanism, namely resonant laser ionization.

Traditionally thermal ionizers and hot cavity catchers have been heated using resistive heating or electron bombardment [1,2]. We present a novel approach, using well know method of induction heating, for achieving temperatures exceeding 2000 degrees Celsius. The catcher is based on the catchers used in FEBIAD systems albeit very much simplified. The simple designs omits nearly all the complicated insulations required in the other hot cavities and allows the heating system to be completely decoupled from the catcher.

In normal gas cells at IGISOL significant fraction of the reaction products remain in a +1 charge [3]. Upon exiting the ion guide trough an exit nozzle they are caught with a sextupole ion guide. Other way to create ions is to let the initially created ions to neutralize and selectively re-ionize the ions of interest with resonant laser ionization. Currently the aim is to improve the shape of the gas jet emerging from the ion guide. Traditionally used exit holes have no jet shaping properties, but exit nozzles such as De Laval nozzle have. These types of converging diverging nozzles can be shaped to provide well collimated jets with high pressure ratios. Well collimated jet is one of the criterion for efficient use of a LIST, Laser Ion Source Trap, method where the atoms of interest are ionized within the sextupole structure rather than in source.

We present data from hot cavity and jet shaping development.

[1] A. R. Kirchner, K.H. Burkhard, W. Huller, O. Kleppner, Nucl. Instrum. Methods 186, 295 (1981).
[2] M. Reponen, T. Kessler, I. D. Moore, S. Rothe, and J. Äystö. EPJ A,2009.
[3] J. Arje, K. Valli, Nucl. Instrum. Methods, 1981

UNIVERSITY OF JYVÄSKYLÄ

ELECTRICAL IMAGING MODALITIES IN PHARMACEUTICAL APPLICATIONS

V. Rimpiläinen[1], L. M. Heikkinen[1], M. Vauhkonen[1] and J. Ketolainen[2]

Department of Physics and Mathematics[1], School of Pharmacy[2], University of Eastern Finland, P.O.B. 1627, FIN-70211 Kuopio, Finland
email: ville.rimpilainen@uef.fi

This research focuses on applying electrical imaging modalities in pharmaceutical processes. The two modalities used are electrical impedance tomography (EIT) and electrical capacitance tomography (ECT). In both methods, an array of electrodes is attached on the surface of the studied object, and two- and/or three-dimensional tomograms depicting the electrical properties of the interior of the object are constructed with the help of electrical measurements at the electrodes and computational algorithms. The topic is divided into cases of which two are presently under research.

In the first case, the drug release properties of pharmaceutical tablets are monitored with EIT during release test. In this test, a tablet is dropped on the bottom of a vessel filled with dissolution medium. The medium is agitated with a paddle, and traditionally the process is monitored by taking small samples from the medium, and analyzing their drug content off-line with, for example, UV/VIS spectrophotometer. With EIT, it is possible to monitor in-line the whole three-dimensional drug concentration distribution inside the vessel. This way, the drug release properties can be more comprehensively examined. The technique is detailed in [1] and its characteristics are evaluated in [2].

In the second case, the high-shear granulation is monitored with ECT. In the granualtion, pharmaceutical ingredients that are commonly different kinds of powders are processed to granules of certain size. The granules are beneficial because they are easier to use and handle, and because they do not cause dusting problems. In high-shear granulator, the material is agitated with impeller, and at the same time binding fluid is sprayed along. The success of the process is traditionally based on trial-and-error knowledge, and the degree of success would be far better if novel monitoring methods such as ECT would be used. This research is further introduced in [3].

[1] V. Rimpiläinen, L. M. Heikkinen, M. Kuosmanen, A. Lehikoinen, A. Voutilainen, M. Vauhkonen and J. Ketolainen, An electrical impedance tomography-based approach to monitor *in vitro* sodium chloride dissolution from pharmaceutical tablets, Rev. Sci. Tech. 80 (2009) 103706
[2] V. Rimpiläinen, M. Kuosmanen, J. Ketolainen, K. Järvinen, M. Vauhkonen and L. M. Heikkinen, Electrical impedance tomography for three-dimensional drug release monitoring, Eur. J. Pharm. Sci. *under review*
[3] V. Rimpiläinen, S. Poutiainen, L. M. Heikkinen, T. Savolainen, M. Vauhkonen and J. Ketolainen, In-line monitoring of high-shear granulation with electrical capacitance tomography, *manuscript in preparation*

Realistic calculation of ITER wall loads including finite orbit effects

A. Snicker, S. Sipilä and T. Kurki-Suonio

Aalto University, Department of Applied Physics, P.O.Box 14100, FI-00076 AALTO
email: antti.snicker@tkk.fi

The power load on ITER walls is a major concern since the power and heat flux may severely damage the plasma facing components. One major cause of the losses is magnetic field ripple - due to the discrete nature of its toroidal field coils, a tokamak's magnetic field is non-axisymmetric. Until now, the power loads have been evaluated using guiding centre simulations, see e.g. [1] and references therein, in which the fast gyration of the charged particle around the magnetic field line is averaged out. Moreover, it has been assumed that the effects caused by the finite Larmor radius of the fast ions are small and thus can be neglected. This assumption should be tested by simulations including finite Larmor radius effects.

In the presence of a strong magnetic field ripple, the gradient of the magnetic field becomes large. Due to this and the large Larmor radius of the fast ion, the magnetic field properties at the guiding centre may substantially differ from those at the full orbit location. This gives rise to some phenomena that are not taken into account in the guiding centre approximation. The main differences are 1) a significant difference in toroidal precession and 2) enhanced diffusion coefficients [2]. The former is caused by the variable mirror point of the charged particle, while the latter is due to the cyclotron resonance, also called gyroresonance, Ref. [2].

We present an accurate full orbit integration procedure for the particle tracing. At the heart of the procedure is the leap frog Boris method which is used to advance the particle's velocity and location in time. Moreover, we recalculate the ITER wall loads with the full orbit method and compare the results with the traditional guiding centre simulation. It is found that the wall load distribution is very similar to the one obtained by guiding centre simulation but in the presence of a strong ripple the overall wall load will slightly increase. The full orbit scheme also provides a tool to accurately evaluate the point where the particle collides with a plasma facing component.

Taking the finite Larmor effects into account comes with a significant cost - the CPU consumption with the full orbit calculation is roughly 50 to 100 times (depending on several details) that of the guiding centre calculation. This makes it impossible to follow a large ensemble of fast ions throughout the whole slowing down process, i.e. around 0.1 s, using the full orbit procedure. To solve this problem, we discuss the possibility to use a hybrid method where the guiding centre and full orbit integration are combined, preserving the best properties of both approaches.

[1] T. Kurki-Suonio *et al*, Nucl. Fusion, **49** (2009) 095001.
[2] H. Mimata *et al*, Progress in Nuclear Energy, **50** (2008) 638.

WAVELET-BASED INVERSE METHOD AS A TOOL IN PAPER QUALITY ASSESSMENT

J. Takalo and J. Timonen

Department of Physics, University of Jyväskylä, P.O.B 35, FI-40014 University of Jyväskylä, Finland
email: jouni.j.takalo@jyu.fi

J. Sampo, S. Siltanen and M. Lassas

Department of Mathematics and Statistics, University of Helsinki, P.O.B 68, FI-00014 University of Helsinki, Finland
email:samuli.siltanen@helsinki.fi

Using orientation analysis we show that the optical formation of a sheet of paper is biased because of light scattering effects. This is particularly true for thick paper grades like cardboard. Thus the standard optical analysis does not necessarily reveal the real areal mass distribution of paper.

Convolution models are applied to properly map optical transmission data into x-ray transmission data which are believed to describe the true material distribution in the sample (very little scattering). We use the Barzilai-Borwein minimization to enhance the information content of the optical transmission map.

For getting the prior information to be used in the Bayesian approach we apply wavelet transformation based methods. The Besov-space classification of the samples is based on their two- and three-dimensional x-ray tomographic reconstructions.

.

UNIVERSITY OF JYVÄSKYLÄ

ULTRA-PURE ^{133M}XE STANDARD FOR SENSITIVE DETECTION OF NUCLEAR WEAPONS TESTS

J. Turunen[1], K. Peräjärvi[1], T. Eronen[2], V.-V. Elomaa[2], J. Hakala[2], A. Jokinen[2], H. Kettunen[2], V.S. Kolhinen[2], M. Laitinen[2], I.D. Moore[2], H. Penttilä[2], J. Rissanen[2], A. Saastamoinen[2], H. Toivonen[1] and J. Äystö[2]

[1] STUK - Radiation and Nuclear Safety Authority, P.O. Box 14, FI-00881 Helsinki, Finland
[2] Department of Physics, University of Jyväskylä, P.O.Box 35 (YFL), FI-40014 University of Jyväskylä, Finland
email: jani.turunen@stuk.fi

Radioactive noble gases produced in nuclear weapons tests offer a sensitive probe for the verification of the compliance with the Comprehensive Nuclear-Test-Ban Treaty [1]. Even in the case of underground detonation it is probable that noble gases are released into the atmosphere [2, 3]. In practise, the detection effort is focused on ^{131m}Xe ($T_{1/2}$ = 11.84 d), ^{133m}Xe ($T_{1/2}$ = 2.19 d), ^{133}Xe ($T_{1/2}$ = 5.243 d) and ^{135}Xe ($T_{1/2}$ = 9.14 h) [4]. Their relative amounts in the sample, the ratio of ^{133m}Xe to ^{133}Xe in particular, are the key indicators [5] to reveal the origin of the sample, i.e., to prove the attribution to a nuclear test or to releases of nuclear reactors or isotope production plants.

Even though noble gas detection instruments are routinely used for nuclear monitoring, the exact calibration of such devices has so far been difficult. This is due to the lack of pure ^{133m}Xe calibration sources. Naturally, if available, such samples would also be valuable for the quality control and for further development of noble gas samplers and spectrometers. Here we discuss a method initially reported in [6] for the production of pure ^{133m}Xe samples. The isomeric ^{133m}Xe source is the most complicated xenon signature to prepare, since the isomeric state lies only 233 keV above the ground state of ^{133}Xe. The purification process developed is based on a highly sophisticated Penning-type mass separator having a relative mass resolution of about 1 ppm. If desired, pure ^{133}Xe, ^{131m}Xe and ^{135}Xe sources are also possible to manufacture using the developed method. In this contribution, we also present that the implanted xenon atoms remain in an aluminium matrix meaning that the produced surface sources are easy to manipulate. The xenon can be released to the gas phase simply by heating the sample.

[1] T. W. Bowyer et al., J. Environ. Radioact. 59 (2002) 139.
[2] Nuke sniffer, New Scientist Vol. 196 No. 2627 (2007) 4.
[3] A. Ringbom et al., J. Radioanal. Nucl. Chem. 282 (2009) 773.
[4] B. Wernsperger and C. Schlosser, Radiat. Phys. Chem. 71 (2004) 775.
[5] P.L. Reeder and T.W. Bowyer, Nucl. Instrum. Methods Phys. Res. A 408 (1998) 573.
[6] K. Peräjärvi et al., Appl. Radiat. Isot., doi:10.1016/j.apradiso.2009.12.020.

OPTIMIZING STABILITY OF ALL-OPTICALLY POLED MATERIALS

M. Virkki,[1] A. Priimägi[2], M. Kauranen[1]

[1]Department of Physics, Tampere University of Technology, FIN-33101, Finland
[2]Department of Applied Physics, Helsinki University of Technology, FIN-02015, Finland
email: matti.virkki@tut.fi

All-optical poling is a method that can be used to induce noncentrosymmetric polar order in a originally centrosymmetric material [1]. Spin coated films with nonlinear organic molecules embedded into a polymer matrix are originally centrosymmetric. Applying a dual frequency beam into such a sample film leads to selective excitation and reorientation of the nonlinear molecules. The main problem with optically poled materials is the lack of stability of the induced noncentrosymmetry since the molecules spontaneously reorient in a random fashion. By choosing the active molecule and the supporting matrix carefully the stability of the noncentrosymmetry can be significantly enhanced.

We present results of optical poling with nonlinear molecules in different matrices and show that strong interactions between the polymer matrix and the active molecules leads to significantly increased stability of the induced noncentrosymmetry. Furthermore, we show that with certain combinations the stability is significantly increased by extending the time used for the poling process. The samples we used were thin films with 30 wt-% of Disperse Red 1 (DR1) azobenzene embedded into polystyrene (PS) and polyvinylphenol (PVPh) matrices. The poling was achieved by applying a superposition of an infrared beam and its second-harmonic (SH) into the sample. The monitoring of the growth and decay of the noncentrosymmetry was carried out by periodically applying only an infrared beam into the sample and measuring the SH radiation produced by the sample.

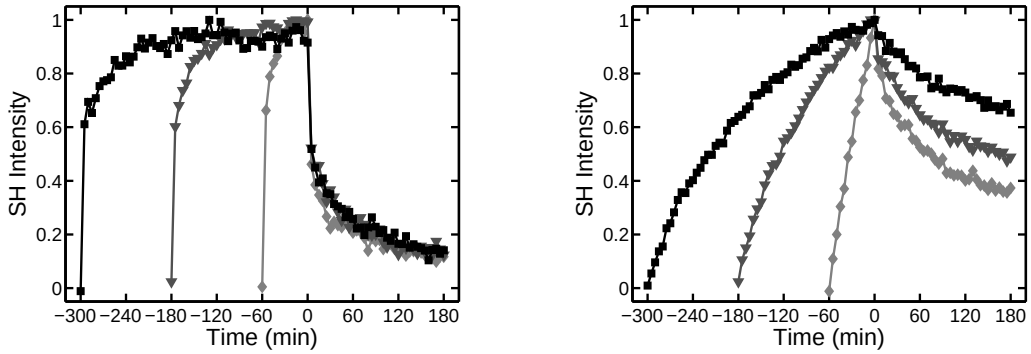

Figure 1. Normalized growth and relaxation of the SH signal in all-optical poling experiments for DR1 in PS (left) and DR1 in PVPh (right) with different poling times. The poling process is ceased at 0 min.

[1] C. Fiorini, F. Charra, Nunzi, M. J, and P. Raimond, J. Opt Soc. Am. B **14** (1997) 1984–2003.

CHARACTERIZATION OF POLARIZATION DYNAMICS IN RANDOM THREE-DIMENSIONAL ELECTROMAGNETIC FIELDS

T. Voipio[1], T. Setälä[1], A. Shevchenko[1], and A. T. Friberg[1,2]

[1] Department of Applied Physics, Aalto University, P.O.B. 13500,
FI-00076 Aalto, Finland
[2] Department of Physics and Mathematics, University of Eastern Finland, P.O.B. 111,
FI-80101 Joensuu, Finland
email: timo.voipio@tkk.fi

Electromagnetic fields generated by any source, whether natural or artificial, exhibit fluctuations in their polarization state, due to e.g. randomness of the emission process or random variations in the propagation medium. Characterization of the polarization fluctuations of light may enable such information to be extracted on the source and medium that otherwise would be impossible. An important concept related to the polarization state is the degree of polarization, which has been defined for both paraxial (2D) and nonparaxial (3D) fields. A more complete characterization is obtained by examining the dynamical behavior of the instantaneous polarization state. The polarization dynamics of 2D fields has been investigated recently via two approaches, one based on the Poincaré vector formalism [1] and the other on the use of Jones vectors [2]. In this work, we extend both methods to nonparaxial electromagnetic fields and define a polarization time for them.

The first method is based on introducing the correlation function $\gamma_{3,\mathrm{P}}(\tau)$, characterizing the correlation between 3D instantaneous Poincaré vectors, $\mathbf{\Lambda}(t)$, at two times. The second approach relies on the function $\gamma_{3,\mathrm{J}}(\tau)$ defined in terms of the 3D Jones vectors, $\mathbf{E}(t)$. The two correlation functions are explicitly given by

$$\gamma_{3,\mathrm{P}}(\tau) = \frac{\langle \mathbf{\Lambda}(t) \cdot \mathbf{\Lambda}(t+\tau) \rangle}{3\langle \Lambda_0(t)\Lambda_0(t+\tau) \rangle}, \quad \text{and} \quad \gamma_{3,\mathrm{J}}(\tau) = \frac{\langle |\mathbf{E}^*(t) \cdot \mathbf{E}(t+\tau)|^2 \rangle}{\langle I(t)I(t+\tau) \rangle}, \tag{1}$$

where τ denotes a time difference, $\Lambda_0(t) = I(t)$ is the instantaneous intensity, and the angle brackets stand for the time average. The polarization time can be defined as a time interval over which the correlation functions decay significantly.

We show that in the case of Gaussian statistics the correlation functions can be expressed in terms of the 3D degree of polarization and two quantities that characterize electromagnetic coherence. The formalism is illustrated with three examples: a uniformly partially polarized, temporally Gaussian correlated 3D field, black-body radiation in a cavity, and a superposition of three orthogonally propagating and orthogonally polarized beams whose mutual correlation is varied.

[1] T. Setälä, A. Shevchenko, M. Kaivola, and A. T. Friberg,
Phys. Rev. A 78 (2008) 033817.
[2] A. Shevchenko, T. Setälä, M. Kaivola, and A. T. Friberg,
New J. Phys. 11 (2009) 073004.

2 Astrophysics, cosmology and space physics

2.1 Oral session, Saturday 13 March 9:00-10:30

2.2 Poster session, Friday 12 March 16:00-18:00

LARGE PLASMOIDS IN GLOBAL MHD SIMULATIONS: SOLAR WIND DEPENDENCE AND IONOSPHERIC MAPPING

I. Honkonen, M. Palmroth, T.I. Pulkkinen and P. Janhunen

Finnish Meteorological Institute, P.O. B. 503, FIN-00101, Finland
email: ilja.honkonen@fmi.fi

The energy from the solar wind drives magnetospheric dynamics. An important, but the most difficult to measure, factor is the energy released in plasmoids. Plasmoids are large magnetic structures that form in the Earth's magnetotail during substorms, which are the main mechanism of extracting and releasing solar wind energy from the magnetosphere. During plasmoid formation the 3-d structure of the magnetotail becomes complicated, with spatially alternating closed and open magnetic topologies. While the formation and the release of plasmoids are unresolved, they are classically thought to detach from the magnetotail at the substorm onset.

Using our global magnetohydrodynamic (MHD) simulation GUMICS-4, we investigate how different parameters of the solar wind affect the formation of plasmoids. Specifically we concentrate on the role of the solar wind magnetic field parameters. We also investigate the solar wind dependence of plasmoid foot points, which are the end points of the plasmoid magnetic field in the ionosphere. Preliminary results suggest that plasmoid formation and plasmoid foot point location in the ionosphere strongly depend on the solar wind magnetic field parameters. Our work may be of importance when interpreting some observed, but unexplained, ionospheric phenomena. We also present an operational definition of plasmoids, which enables their automatic detection in simulations.

The project has received funding from the European Research Council under the European Community's Seventh Framework Programme (FP7/2007-2013) / ERC Starting Grant agreement number 200141-QuESpace. The work of IH and MP is supported by the Academy of Finland.

MAGNETOSPHERIC FEEDBACKS IN SOLAR WIND ENERGY TRANSFER: IMPLICATIONS FOR THE SUBSTORM CYCLE

M. Palmroth[1], T. I. Pulkkinen[1], C. R. Anekallu[1], I. Honkonen[1], H. E. J. Koskinen[2,1], E. A. Lucek[3], and I Dandouras[4]

[1]Finnish Meteorological Institute, P. O. Box 503, 00101 Helsinki, Finland
[2]University of Helsinki, Helsinki, Finland
[3]Imperial College, London, UK
[4]Université de Toulouse, Toulouse, France
email: minna.palmroth@fmi.fi

The solar wind kinetic energy fuels all dynamical processes within the near-Earth space, including magnetic storms and substorms during which spectacular auroral displays are frequently observed. The solar wind energy is extracted by a dynamo process at the magnetopause converting kinetic energy into magnetic energy utilized in magnetospheric processes. We investigate the magnetopause energy transfer using both Cluster observations as well as three-dimensional global magnetohydrodynamic (MHD) simulation GUMICS-4. In the simulation, the spatial distribution of the energy transfer exhibits a dependence on the interplanetary magnetic field (IMF) orientation, which is shown to agree with observational local estimates from Cluster spacecraft recordings. In both sythetic runs with artificial solar wind input as well as in reproductions of the observed solar wind we observe a "hysteresis" effect, where the magnetopause energy input stays enhanced longer than the traditional energy transfer proxies (e.g., epsilon) indicate. Specifically we focus in the simulation of a substorm sequence on Feb 18, 2004, during which an exceptional agreement between the simulation results and spacecraft recordings was observed on several orbits within the near-Earth space. In this event, we again observe the hysteresis effect and investigate the processes causing it at the magnetopause. We argue that since GUMICS-4 reproduces the observed signatures of the substorm sequence, the simulation results represent physical processes within the magnetosphere. We conclude that as the simulation energy input exhibits delays already at the magnetopause, the delays in the classical substorm loading - unloading cycle may be interpreted in a new light.

The project has received funding from the European Research Council under the European Community's Seventh Framework Programme (FP7/2007-2013) / ERC Starting Grant agreement number 200141-QuESpace. The work of MP and IH is supported by the Academy of Finland.

ELECTRIC SOLAR WIND SAIL PROPULSION: TOWARDS TEST MISSIONS

P. Janhunen[1] and P. Toivanen[1]

(1) Finnish Meteorological Institute, P.O.B. 503, FIN-00101, Helsinki, Finland
email: pekka.janhunen@fmi.fi

The electric solar wind sail (E-sail) is a way of using the momentum flux of the solar wind for spacecraft propulsion. The physical idea was conceived in 2004 [1] and a practical implementation scheme was invented in 2006 [2]. In the recent year, very significant progress has been made on multiple fronts. It was shown that due to a specific electron orbit chaotisation effect, trapped electrons are naturally removed from the potential wells of the positively charged tethers although the plasma is collisionless, resulting to $\sim$500 nN/m E-sail thrust per tether length [3] which is about five times higher than earlier estimates.

We have also discovered a new mechanical concept of the E-sail which has no moving parts during flight and solves the spinup question without additional arrangements. We connectsthe tips of the centrifugally stretched tethers by nonconducting auxiliary tethers. The centrifugal force acting on the auxiliary tethers provides a restoring force which stabilises the flight without the need for active tether length fine-tuning.

ESTCube-1 is an Estonian 1 kg nanosatellite which will be launched in 2012 to deploy a 10 m tether in low Earth orbit to experimentally measure the E-sail effect (Coulomb drag effect) induced on a charged wire by flowing plasma. The satellite is designed and built by an Estonian team led by the University of Tartu and the E-sail test payload by Finnish and German groups. Drafting of real solar wind test missions is also underway.

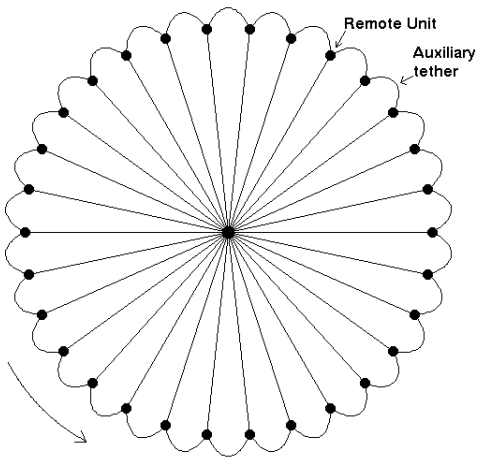

The new E-sail concept with auxiliary tethers and Remote Units. The Remote Units contain the auxiliary tether reels and gas thrusters for producing the initial angular momentum and for modifying the spin during flight if needed.

[1] P. Janhunen, J. Propulsion Power, 20 (2004) 763.
[2] P. Janhunen, U.S. Pat. 11/365875 (2006), accepted.
[3] P. Janhunen, Ann. Geophysicae 27 (2009) 3089.

The status of Planck

E. Keihänen, H.Kurki-Suonio, T. Poutanen, M. Savelainen and A.-S. Sirviö

Department of Physics, P.O.B. 64, FIN-00014 University of Helsinki, Finland
email: anna-stiina.sirvio@helsinki.fi

The European Space Agency's Planck Observatory was launched on the 14th of May along with the Herschel Space Observatory from Europe's spaceport in Kourou, French Guiana. It is designed to map the Cosmic Microwave Background (CMB) – the relic radiation from the Big Bang – with three times the accuracy of previous satellites. By measuring the CMB more accurately than ever before, our ultimate goal is to determine the geometry and contents of the Universe, and to conclude which theories describing the birth and evolution of the Universe are correct [1].

To detect minute temperature anisotropies in the CMB, Planck uses two instruments, one for high frequencies (HFI) and one for low (LFI). The radiometer-based LFI has three frequency bands, covering the range of 30–70 GHz, while the bolometer-based HFI has six frequency bands, between 100 and 857 GHz. All frequency bands are sensitive to linear polarization, except the two highest bands which are not [1].

The first observation period, the "First Light Survey" (FLS), to assess performance of the two instruments began on the 13th of August after cooling and tuning of the two instruments in space. The first maps of the FLS were released in mid September yielding promising results. The Planck team at the University of Helsinki is responsible for producing these maps for the Low-Frequency Instrument. Preliminary analysis indicates that the quality of the data is excellent [2].

We will discuss up to date status of the mission and go through the important milestones since the launch in May.

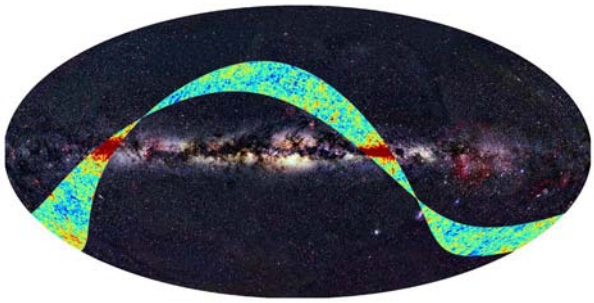

Figure 1: The frequency map at 70 GHz measured by Planck during the FLS superposed on an all-sky map at optical wavelengths. Copyright: ESA, LFI & HFI Consortia (Planck), Background image: Axel Mellinger.

[1] The Planck Collaboration, astro-ph/0604069.
[2] The Planck Collaboration, Press release on ESA web page (17 September 2009).

ADJOINT DARK MATTER

K. Kainulainen, K. Tuominen and J. Virkajärvi

Department of Physics, P.O.B. 35 (YFL), FIN-40014 University of Jyväskylä, Finland
email: jussi.virkajarvi@jyu.fi

Minimal technicolor theory [1], when supplemented with certain extra matter fields uncharged under Technicolor gauge group, leads to MSSM-like one-loop unification of the standard model coupling constants [2]. We consider the possibility that some of these new matter fields with electroweak charges provide a source for the dark matter in the universe [3]. Concretely, we have studied the case where lightest neutral fermion in the adjoint representation of $SU_L(2)$ mixes with a neutral gauge singlet fermion. Our results show that, in addition to a non-supersymmetric solution of electroweak hierarchy problem and unification of the standard model couplings, this model also provides correct dark matter abundance. The dark matter candidate is stabilized by a discrete symmetry and will be difficult to detect at colliders and in cryogenic direct dark matter search experiments due to suppressed weak interactions.

[1] F.Sannino and K.Tuominen, Phys. Rev. D 71 (2005) 051901.
[2] S.B. Gudnason, T.A. Ryttov and F. Sannino, Phys. Rev. D 76 (2007) 015005.
[3] [3] K.Kainulainen, K.Tuominen and J.Virkajärvi, "Naturality, Unification and Dark Matter" Work in progress.

TESTING GENERAL RELATIVITY WITH THE BINARY BLACK HOLE SYSTEM OJ287

M.Valtonen[1,2] , S. Mikkola[2], H. Lehto[2] and A.Gopakumar[3]

1. Helsinki Institute of Physics, P.O.B. 64, FIN-00014 University of Helsinki, Finland,
2. Department of Physics and Astronomy, Tuorla Observatory, 21500 Piikkiö, Finland
3. Tata Institute of Fundamental Research, Mumbai, India
email: mvaltonen2001@yahoo.com

Binary black hole system OJ287 forms a unique system for testing General Relativity. In this system the two bodies are in a 9 year orbit around each other, with the closest approach at the separation of only 10 Schwarzschild radii of the primary. This system tests the curvature of spacetime much deeper in the potential well than e.g. the binary pulsars. The timing of the orbital motion is achieved by studying the optical light curve of the system. So far we have determined that the system loses energy at the rate which agrees with the energy loss to gravitational waves in General Relativity with the accuracy of 6% [1,3] . The value of the spin of the primary is 0.28, with the accuracy of 10%, in relative units where the maximum value is 1.0 [2]. We have further calculated the value of the quadrupole moment of the primary; it can be determined only with 30% accuracy (1 sigma) at present [2,3]. However, it is important that even with this accuracy the result agrees with General Relativity, and it proves so called “no-hair” theorem of black holes. In other words, our result is consistent with the concept of a black hole in the primary, and excludes the possibility of other kinds of material bodies. This is the first time that the “no-hair theorem” has been proven with any accuracy, and is an essential step in showing that General Relativity applies to strong gravitational fields. It is possible to improve the accuracy of the measurement of the quadrupole moment in 2019 when the two black holes are close to each other again. However, this will require a space born measurement, possibly from an interplanetary probe [3].

[1] M.Valtonen et al., Nature 452 (2008) 1851.
[2] M.Valtonen et al., Astrohys.J. 709 (2010) Jan20.
[3] M.Valtonen et al., CelMechDynAstr. (2010) in press.

VENUS IN THE SOLAR WIND: A HYBRID MODELLING OVERVIEW

R. Järvinen[a], E. Kallio[a], S. Dyadechkin[a], P. Janhunen[a] and I. Sillanpää[b]

a) Finnish Meteorological Institute, P.O. Box 503, FI-00101 Helsinki, Finland
b) Southwest Research Institute, San Antonio, Texas
email: riku.jarvinen@fmi.fi

By spring 2010, the Venus Express mission has provided among other things four years of in situ observations of the Venusian plasma environment. We present an overview of our Venus research carried out during these years. Our aim has been to study the Venus-solar wind interaction with a 3-dimensional hybrid plasma simulation (HYB-Venus) and, thereby, interpret the new particle and magnetic observations in a global context. In our studies we have demonstrated that the hybrid model can reproduce the observed large scale structures of the induced magnetosphere. Further, we have studied the escape rates of the planetary oxygen and hydrogen ions which are energized by the solar wind. Our simulations suggest that in the present Solar System conditions Venus is not losing considerable amounts of ionic oxygen compared to its atmospheric reserves.

[1] Kallio E., Jarvinen R., Janhunen P., Venus-solar wind interaction: Asymmetries and the escape of O^+ ions, Planet. Space Sci. 54 (13-14), 1472-1481, 2006

[2] Jarvinen R., Kallio E., Sillanpää I., Janhunen P., Hybrid modelling the Pioneer Venus Orbiter magnetic field observations, Adv. Space Res. 41 (9), 1361-1374, 2008

[3] Liu K., Kallio E., Jarvinen R., Lammer H., Lichtenegger H.I.M., Kulikov Yu.N., Terada N., Zhang T.L., Janhunen P., Hybrid simulations of the O^+ ion escape from Venus: Influence of the solar wind density and the IMF x component, Adv. Space Res. 43 (9), 1436-1441, 2009

[4] Jarvinen R., Kallio E., Janhunen P., Barabash S., Zhang T.L., Pohjola V., Sillanpää I., Oxygen ion escape from Venus in a global hybrid simulation: role of the ionospheric O^+ ions, Ann. Geophys. 27 (11), 4333-4348, 2009

SHOCK OBLIQUITY AND PRE-HEATED PARTICLE POPULATIONS IN SELF-CONSISTENT PARTICLE SHOCK ACCELERATION

M. Battarbee[1], T. Laitinen[1,2], R. Vainio[3] and N. Agueda[4]

[1]Department of Physics and Astronomy, University of Turku, Finland
[2]email: timo.laitinen@utu.fi
[3]Department of Physics, University of Helsinki, Finland
[4]Space Sciences Laboratory, University of California, Berkeley, CA, USA.

Acceleration in coronal and interplanetary CME-driven shocks is currently considered the primary source of large solar energetic particle (SEP) intensities. In large SEP events, the particles accelerated at the shock generate Alfvénic turbulence in the ambient medium, which facilitates particle trapping and repeated shock crossings, thus bootstrapping the acceleration process. In order to study this process, we have developed a Monte Carlo simulation method, where particles are traced in prescribed large-scale electromagnetic fields utilizing the guiding center approximation.

In our simulations, particles are scattered in the turbulence according to quasilinear theory, with the scattering amplitude directly proportional to the intensity of Alfvén waves at gyro-resonant wavenumbers. The Alfvén waves are traced simultaneously with the particles, so that the wave field is propagated outwards from the Sun using WKB propagation supplemented with a phenomenological wavenumber diffusion term and a growth rate computed from the net flux of the accelerated particles.

We have previously reported on effects of decreasing shock velocity and shocks propagating with various shock-normal angles. In these studies, we have discovered that the injection energy of particles clearly affects the efficiency of the acceleration process, which complicates the effort of isolating the effects of other parameters in the overall structure of the shock and the coronal environment the shock travels through. We now extend our study by varying the spectral and radial injection profile, specifically injecting pre-heated particles, allowing us to better assess the separate effects of shock obliquity and injection energy on SEP acceleration.

TOWARDS MULTI-SCALE AURORAL OBSERVATIONS

N. Partamies, M. Syrjäsuo and E. Donovan

Finnish Meteorological Institute, P.O.B. 503, FIN-00101 Helsinki, Finland
email: noora.partamies@fmi.fi

The core of ground-based auroral observations is all-sky imaging. The largest camera networks in the northern hemisphere are: MIRACLE network (8 stations) in Fennoscandia and Svalbard, NORSTAR network (8 stations) in Canada, and THEMIS network (20 stations) in Canada and Alaska. These instruments take either whitelight images, colour images or images filtered for a certain wavelength. The data rate varies from 20 to 3-second cadence and the large field-of-view with overlapping field-of-views of the neighbouring stations allow a good coverage for monitoring large-scale (10–100 km) evolution and morphology of the aurora. Imaging is automatic for a full winter season at a time. A nominal spatial resolution for all-sky cameras is about 0.5 km.

Another widely used imaging system is a video rate TV camera that typically uses a narrow field-of view optics. Its main focus is to study auroral fine-scale structures of 10–100 m. Due to the huge data rate, TV cameras are usually campaign instruments and thus, operated for short periods and at central or otherwise easily accessible sites.

The two imaging types provide information on very different scale sizes. Statistical studies exist on both the large-scale auroral structures (e.g. [1, 3]) as well as on fine-scale structures (e.g. [2, 4]). But what happens in the scale size area in between? How are the different scale sizes spatially and temporally coupled?

This study is one of the first steps forward on studying the multiple scales of the auroral structures. A new imaging system was designed for studying the "in-between" sizes of the aurora to complete the observations of the scale size spectrum. The system has been in campaign-based operation since 2007. We present results of the scale size study including all the available observations and discuss the importance of multi-scale auroral observations.

[1] D. J. Knudsen, E. F. Donovan, L. L. Cogger, B. J. Jackel, and W. D. Shaw, Geophysical Research Letters 28 (2001) 705.
[2] J. E. Maggs and T. N. Davis, Planetary and Space Science 16 (1968) 205.
[3] N. Partamies, K. Kauristie, T. I. Pulkkinen and M. Brittnacher, Journal of Geophysical Research 106 (2001) 15,415.
[4] T. Trondsen and L. L. Cogger, Journal of Geophysical Research 103 (1998) 9405.

Exact 2-point Wightman functions and cQPA

J. Pasanen, K. Kainulainen and P. M. Rahkila

Department of Physics, P.O. Box 35 (YFL), FIN-40014 University of Jyväskylä, Finland
Helsinki Institute of Physics, P.O. Box 64, FIN-00014 University of Helsinki, Finland
email: joni.j.pasanen@jyu.fi

We have calculated numerically the 2-point Wightman functions in Wigner representation for free fermionic fields in presence of CP-violating mass wall. Direct space wave functions are well known from the work of Ayala *et. al.*[1], but complete mixed representation correlators have not been calculated before. We compare the full 2-point correlator to new cQPA shell ansatz derived in [2, 3] and find good agreement in cases relevant to electroweak baryogenesis. The 2-point functions indeed have large contributions with expected spatial structure in particular close to the new singular shell at zero momentum $k_z = 0$. As a direct application to electroweak baryogenesis we calculate the spatial variation of densities of observables in different parts of the phase space.

[1] A. Ayala, J. Jalilian-Marian and L. McLerran,
Phys. Rew. D 49 (1995) 10
[2] M. Herranen, K. Kainulainen and P. M. Rahkila,
Nucl. Phys. B 810 (2009) 389 [arXiv:0807.1415 [hep-ph]].
[3] M. Herranen, K. Kainulainen and P. M. Rahkila,
arXiv:0912.2490 [hep-ph]

ON THE DEFLECTION OF CORONAL MASS EJECTIONS IN THE SOLAR CORONA

J. Pomoell, R. Vainio, E.K.J. Kilpua and R. Kissmann

Department of Physics, P.O.B. 64, FIN-00014 University of Helsinki, Finland
email: jens.pomoell@helsinki.fi

Coronal mass ejections (CMEs) are eruptions in the solar corona that drive large amounts of plasma with a high velocity into interplanetary space. Observations by the Solar and Heliospheric Observatory (SOHO) spacecraft have unambiguously revealed that CMEs often do not propagate radially outwards with respect to the position of their source regions. It is commonly believed that coronal holes (CHs) – regions where the solar magnetic field is opened out into interplanetary space – play a significant role in the deflection of CMEs. For instance, it has been proposed that the presence of CHs near the eruption region of a CME can explain why some interplanetary shocks arrive at Earth without a discernible ejecta behind them. Further, it has recently been suggested that the relative contribution of deflecting CMEs to the near-ecliptic interplanetary CME rate could be significant at solar minimum conditions. Despite these important implications, the dynamics of the deflection itself has not received much attention.

In this work, we study the deflection of CMEs in the low corona by simulations and observations. We focus especially on the role of magnetic environment of the source region as well as the size of the erupting structure on determining wether the CME experiences a deflection or not. Finally, we compare our simulation results to high-cadence Solar Terrestrial Relations Observatory (STEREO) observations of CME deflection in the low corona.

ELECTRIC SAILING AND SOLAR WIND VARIATIONS

P. K. Toivanen and P. Janhunen

Finnish Meteorological Institute, P.O.B. 503, FIN-00101, Helsinki, Finland
email: petri.toivanen@fmi.fi

The electric sail is a novel propellantless spacecraft propulsion concept. It is based on positively charged tethers that are centrifugally uncoiled and stabilised to extract the solar wind momentum by repelling the solar wind protons. This study addresses both the navigation and sail control under observed solar wind conditions. Steering of an electric sail ship is realised either by changing the tether voltage or the sail spin plane similarly to helicopter flight maneuvers. To model the solar wind, we use spacecraft observations for the density and wind speed at 1 AU and assume that the speed is constant and density decreases in square of the distance from the Sun. We show that passive navigation based only on the statistical properties of the solar wind is far too inaccurate for planetary missions and active navigation is required. As a conclusion, the electric sail is highly navigable and it suits for targeting planets and asteroids, in addition to broad targets such as the heliopause. The control of the sail configuration consideres the rotation phase and spin plane of each tether to prevent tether collisions and to maintain the desired thrust angle. To avoid moving mechanical components, the aim is to use only the tether voltage as the control routine parameter. Primary results show that non-radial components of the solar wind cause hazardous drift in the tether rotation phase and it can only be removed if the tether spin plane is let slowly drift instead.

SPACE WEATHER AND STRATOSPHERIC OZONE

Pekka T. Verronen[1], Annika Seppälä[2], Craig J. Rodger[3], Mark A. Clilverd[2], Carl-Fredrik Enell[4], Antti Kero[4], Sanna-Mari Salmi[1], Thomas Ulich[4], Johanna Tamminen[1], Erkki Kyrölä[1], and Esa Turunen[5]

[1] Finnish Meteorological Institute, P.O.B. 503, FIN-00101 Helsinki, Finland
[2] British Antarctic Survey, Physical Sciences Division, Cambridge, UK
[3] University of Otago, Department of Physics, Dunedin, New Zealand
[4] University of Oulu, Sodankylä Geophysical Observatory, Sodankylä, Finland
[5] EISCAT Scientific Association, Kiruna, Sweden

E-mail: pekka.verronen@fmi.fi

Earth's atmosphere is under the influence of a highly-varying flux of energetic particles from space. Driven by the solar wind, i.e. space weather, the magnitude of electron and proton precipitation is connected to the activity of Sun. For example, solar proton events are most frequent during solar maximum while relativistic electron precipitation tends to peak during declining phase of the solar cycle. Because of the protection provided by Earth's magnetic field, charged particles are guided into atmosphere in the polar regions. The energy range of these particles is such that ionization of atmospheric gases increases, typically at mesospheric and stratospheric altitudes (10–100 km). As a result, electron density is affected and ion as well as minor neutral composition changes. One of the most interesting effects of particle precipitation is the decrease of ozone in the upper stratosphere and above. Whether of not particle precipitation can, through changing the amount of ozone, significantly affect the thermal balance and general circulation of the atmosphere or tropospheric conditions remains an open question.

We present some highlights of the particle precipitation research conducted during the last five years at Finnish Meteorological Institute. Both ionospheric and atmospheric changes have been studied, using a wide range of satellite and ground-based instruments. Our results point out the importance of ion chemistry modelling in understanding the changes in the amounts of such important atmospheric species as ozone, NO_2, HNO_3, and OH. The significance of winter-time polar vortex in transporting the affected air mass into lower altitudes is demonstrated with satellite observations and modelling.

Energy conversion at the Earth's magnetopause: Validating single spacecraft methods

C.R. Anekallu. ,Minna Palmroth, Tuija Pulkkinen, Elizabeth Lucek, Iannis Dandouras

Finnish Meteorological Institute, P.O.B. 503, FIN-00101 Helsinki Finland
email: chandrasekhar.anekallu@fmi.fi

Energy transfer from the solar wind occurs at the outer boundary of the magnetosphere, the magnetopause, where solar wind kinetic energy is converted to magnetic energy in a dynamo process. Presently, the conditions of global energy transfer and conversion can be estimated using observational proxies and global three-dimensional magnetohydrodynamic (MHD) simulations, while locally spacecraft data can be used. To achieve an observation-based global estimate of the magnetopause energy transfer, a large statistical data base must be developed. Here, we investigate both multi-spacecraft and single-spacecraft methods to estimate the local magnetopause energy conversion rates. Cluster-II is the first mission to fly 4 satellites in a tetrahedral formation with which one can derive three dimensional vectors from four point measurements and also can distinguish the spatial signatures from the temporal variations. While the multi-scpacecraft methods are proved to give the best results by applying on Cluster II data, the small number of suitable magnetopause crossings becomes a limitation while aiming for the final large statistics. Hence, we need to depend on single spacecraft methods such as recently developed Generic Residue Analysis method. We test and validate the single-spacecraft methods against the multispacecraft methods using Cluster observations and conclude that they can be used in quantitative analysis. We present a subset statistics of the magnetopause crossings and interpret the results in light of the magnetopause dynamo converting the solar wind energy. The results are also compared with those from the GUMICS-4 global MHD simulation.

3 Biological and medical physics

3.1 Oral session, Thursday 11 March 15:00-16:30
3.2 Poster session I, Thursday 11 March 16:30-18:30

PATIENT EXPOSURE MONITORING AND RADIATION QUALITIES IN DIGITAL X-RAY IMAGING

P. Toroi

Radiation and nuclear safety authority, STUK, P.O.B. 14, FIN-000881 Helsinki, Finland
email: paula.toroi@stuk.fi

In digital x-ray imaging excessive patient exposures may remain undetected. The useful dose range of digital detector is large and image does not reveal too high doses. Therefore, real-time monitoring of radiation exposure is important. The methods for estimating patient exposure in x-ray imaging are based on the measurement of radiation incident on the patient. According to international recommendations, the measurement uncertainty should be lower than 7% (confidence level 95%).

The kerma-area product (KAP) is a measurement quantity used for monitoring patient exposure to radiation. A proper calibration of KAP meter is important to be able to achieve the recommended accuracy level. A practical calibration method was examined and evaluated for this purpose. A KAP meter cannot be used to determine the radiation exposure of patients in mammography. The use of digital detector signal was proposed for this purpose. In mammography part of the radiation beam is always aimed directly at the detector without attenuation produced by the tissue. Detector signal from this area could be used to monitor the radiation beam incident on the patient. This method was tested and concluded to be useful and the uncertainty lower than 7% can be achieved with the studied method.

The clinical range of used x-ray energy spectra (radiation qualities) is larger than the choices typically used in dose meter calibrations. The status of radiation quality was studied trough the whole chain of dosimetry from SSDL calibrations to clinical measurement and optimisation. The impact of the use of different radiation quality in calibration and clinical situation was studied. It was concluded to be a major issue when dose meter with high energy dependence, like a conventional KAP meter, is the one in question. Clinical radiation qualities have been optimised for film-screen imaging and new optimisation is needed for new digital detectors. In this study optimal radiation qualities for digital mammography were under specific interest and spectrum with higher mean energies than traditionally used was concluded to be optimal.

The work described in this abstract is based on the doctoral dissertation of author [1].

[1] P. Toroi, STUK-A239 (2009), Helsinki.

PATIENT SPECIFIC MONTE CARLO DOSE SIMULATIONS: INTERNAL EMITTERS

E. Hippeläinen

Department of Physics, University of Helsinki, POB 64, 00014 Helsinki University, HUSLAB Helsinki University Central Hospital, POB 340, 00029 HUS

email: eero.hippelainen@helsinki.fi

With an increasing number of targeted radionuclide therapies and new potential pharmaceuticals, detailed patient dosimetry for internal emitters has got more interest lately. It is known, that an accurate calculation of the patient specific absorbed dose leads to the best clinical response in radionuclide therapy.

Aims of the research: Verify the capability of the PENELOPE[1] monte carlo (MC) code to evaluate dose distribution of internal emitters. *Materials and methods:* The computer code system PENELOPE performs MC simulation of coupled electron-photon transport in arbitrary materials for a wide energy range. Auxiliary functions Internal Source (IS) and Voxel-penelope were coded to control PENELOPE in voxel space. Particles are simulated according activity distribution in medical images (SPECT or PET). Simulation materials are determined by segmented computer tomography images (CT). Segmentation was done using MATLAB®. Code was tested in two different geometries simulating three different activity distributions: 1) one simple iron point source (1 voxel) in cylindrical water phantom 2) five iron point sources in cylindrical water phantom distributed in 3 dimensions and 3) Lung tumour model using patient CT and one artificial active nodule. Point sources were mono-energetic photon emitters and in tumour model active nodule was electron emitter. In all cases real CT-images were used, but activity distributions image stacks were artificial.

Results and conclusion: Preliminary results indicates that auxiliary functions works and dose distributions behaves naturally. In figure is represented CT image overlaid with one point source dose distribution and dose curves from centre of source to adjacent slices. Auxiliary functions presented in this study, gives a flexible package to calculated dose distributions based on CT and activity distribution images.

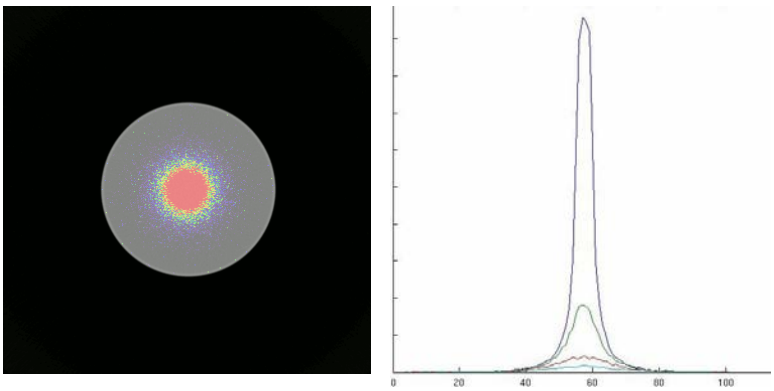

[1] F. Salvat, J. M. Fernández-Varea, J. Sempau,PENELOPE-2008: A Code System for Monte Carlo Simulation of Electron and Photon Transport Workshop Proceedings, Barcelona, Spain, 2008

NOVEL COMPUTED TOMOGRAPHY METHOD FOR DIAGNOSTICS OF ARTICULAR CARTILAGE DEGENERATION

T.S. Silvast, A.S. Aula, H.T. Kokkonen, J.S. Jurvelin and J. Töyräs

University of Eastern Finland, Department of Physics and Mathematics, PO Box 1627, FI-70211 Kuopio, Finland
email: tuomo.silvast@uef.fi

Articular cartilage consists 60-80% of water and cannot be directly visualized with traditional x-ray radiography due to low attenuation of cartilage at clinical x-ray energies. Cartilage damages such as osteoarthritis may be diagnosed indirectly, but unfortunately insensitively, by x-ray imaging on the grounds of narrowed joint space. An innovative use of x-ray contrast agents could provide improvement in diagnostics. In theory, the distribution of charged contrast agent molecules reaches the Gibbs-Donnan equilibrium with the distribution of negatively charged proteoglycan (PG) macromolecules in cartilage [1-2]. Since decrease of PGs is among the first signs of cartilage degeneration, the change in equilibrium distribution of contrast agent could provide valuable diagnostic information. Furthermore, mechanical damage increases the permeability of cartilage tissue, which may increase the diffusion of the contrast agent into the cartilage.

The potential of contrast enhanced computed tomography (CECT) was evaluated with enzymatically or spontaneously degenerated, or mechanically damaged cartilage tissue. The cartilage samples were exposed to a clinically used, iodine based anionic contrast agent. The diffusion and equilibrium distribution of the contrast agent were determined using a peripheral computed tomography device [3], combined also with the FE model analysis of the diffusion.

After application of the contrast agent the cartilage tissue was clearly visible, and the tissue thickness and superficial fissures could be sensitively detected from the images. Furthermore, both diffusion rate and equilibrium distribution were indicative to compositional or structural degeneration of the tissue. Further, it was found that mechanically induced damage could be sensitively detected with CECT.

The present results suggest that the CECT technique could significantly enhance the detection of early osteoarthritis and mechanical cartilage injuries. Optimally, this technique has potential for a breakthrough in clinical diagnostics of cartilage injuries and osteoarthritis.

[1] A. Bashir, M.L. Grey and D. Burstein,
Magnetic Resonance in Medicine 36 (1996) 665-673.
[2] M.D. Cockman, C.A Blanton, P.A. Chmielewski, L. Dong, T.E. Dufresne, E.B. Hookfin, M.J. Karb, S. Liu and K.R. Wehmeyer, Osteoarthritis and Cartilage 14 (2006) 210-214.
[3] T.S. Silvast, H.T. Kokkonen, J.S. Jurvelin, T.M. Quinn, M.T. Nieminen and J. Töyräs,
Physics in Medicine and Biology 54 (2009) 6823-6836.

FINITE ELEMENT APPROXIMATION OF THE FOKKER-PLANCK EQUATION FOR DIFFUSE OPTICAL TOMOGRAPHY

O. Lehtikangas[1], T. Tarvainen[1,2], V. Kolehmainen[1], S.R. Arridge[2], and J. P. Kaipio[1,3]

[1]Department of Physics and Mathematics, University of Eastern Finland, P.O. Box 1627, 70211 Kuopio, Finland

[2]Department of Computer Science, University College London, Gower Street, London WC1E 6BT, United Kingdom

[3]Department of Mathematics, University of Auckland, Private Bag 92019, Auckland Mail Centre, Auckland 1142, New Zealand

E-mail: Ossi.Lehtikangas@uku.fi

In diffuse optical tomography (DOT), the goal is to reconstruct the optical properties of tissues using transmission measurements of scattered near-infrared light on the boundary of the object. The imaging modality has potential applications in detection of breast cancer, neonatal brain imaging and functional brain activation studies [1]. The image reconstruction in DOT is a nonlinear ill-posed inverse problem. The iterative solution of this problem requires several solutions of the forward problem. Moreover, due to ill-posedness of the reconstruction problem, even small errors in the modelling can produce large errors into the reconstructions. Therefore, an accurate and computationally feasible forward model is needed.

The most often used forward model in DOT is the diffusion approximation (DA). The DA is computationally feasible but it has limitations in accuracy [1]. The idea of using the Fokker-Planck equation as the forward model in DOT was introduced in [2]. The Fokker-Planck equation can be used to describe light propagation accurately when scattering is forward-peaked which is the case in biological tissues.

In this work, the Fokker-Planck equation is solved with the finite element method (FEM) [3]. The approach is tested with simulations and compared with the FE-solution of the DA and Monte Carlo (MC) simulations. The simulation geometry and solved photon density on the boundary of the object are shown in Figure 1 for two different cases. The results show that the Fokker-Planck equation describes light propagation accurately when the scattering is forward-peaked.

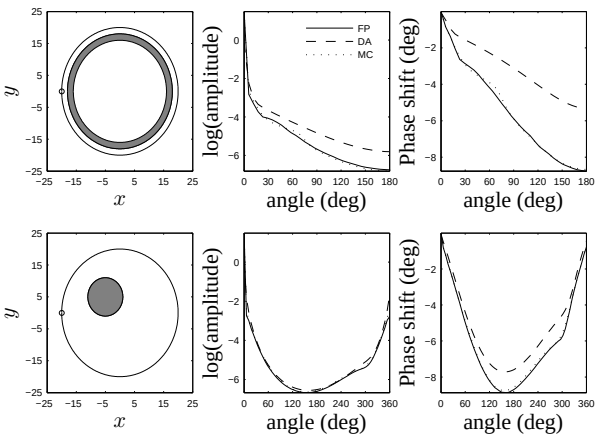

[1] S.R. Arridge, “Optical tomography in medical imaging,” Inverse Problems **15**, 41-41 (1999).

[2] A.D. Kim and J.B. Keller, “Light propagation in biological tissue,” JOSA A **20** 92-98 (2003).

[3] O. Lehtikangas, T. Tarvainen, V. Kolehmainen, A. Pulkkinen, S.R. Arridge, and J.P. Kaipio, “Finite element approximation of the Fokker-Planck equation for diffuse optical tomography”. J Quant Spectrosc Radiat Transf (Submitted, 2009).

Simulation approach to quantitative FRAP analysis

T. Kühn, T. O. Ihalainen, J. Hyväluoma, J. Timonen and M. Vihinen-Ranta

NanoScience Center, P.O.B. 35, FIN-40014 University of Jyväslylä, Finland
email: thomas.h.kuehn@jyu.fi

Photobleaching techniques on the laser scanning confocal microscope (LSCM) have in recent years become important tools for studying protein dynamics in living cells. One of these methods, Fluorescence Recovery After Photobleaching (FRAP), monitors the redistribution of fluorescent particles within the cell after a region of the cell has been bleached. The conventional way of data analysis is to fit the average fluorescense instensity of the bleached region as function of time to a mathematical model to distinguish between pure diffusion, reaction-diffusion, and directed transport, and to extract relevant parameters. In many cases, however, the strong assumptions used to derive these mathematical models do not conform to the experimental setup, introducing large systematic errors to the results.

To overcome these problems, we have developed a numerical method of FRAP data analysys. In this method we simulate the fluorescence redistribution after the photobleach in a three-dimensional (3D) digital model cell which is derived from an initial 3D LSCM scan of the sample cell before the FRAP measurement. The digital model cell takes the internal structure of the cell into account. This structure includes well distinguished cell segments like nucleus and vesicles as well as finer structures like the cytoskeleton and many membraneous structures which are not resolved by the LSCM but nonetheless reduce particle mobility.

Here we applied this method to determine the cytoplasm and cytosol diffusion coefficients of a freely diffusing model protein, enhanced yellow fluorescent protein (EYFP) in NLFK and HeLa cells. The results where in good agreement with those obtained by Fluorescence Fluctuation Spectroscopy on the same cells, while conventional FRAP analysis yielded much smaller diffusion coefficients.

OBSERVATION OF BURIED WATER MOLECULES IN PHOSPHOLIPID MEMBRANES BY SURFACE SFG SPECTROSCOPY

M. Sovago[1], E. Vartiainen[2] and M. Bonn[1]

[1]FOM Institute for Atomic and Molecular Physics, Kruislaan 407, 1098 SJ, Amsterdam, The Netherlands.

[2]Dept. of Mathematics and Physics, P.O.B. 20, FIN-53851 Lappeenranta University of Technology, Finland, email: erik.vartiainen@lut.fi

Biological membranes are the barrier between the interior and the exterior of the cell, and support many proteins involved in important cell functions. It is becoming increasingly clear that water plays a key role in their structure, stability, function and dynamics. Herein, we have studied the structure and orientation of water molecules at the water-lipid interface, using vibrational Sum-Frequency Generation (SFG) spectroscopy. We have found that interfacial water molecules have an orientation opposite to that predicted by electrostatics and thus are likely localized between the lipid headgroup and its apolar alkyl chain. In other words, our results strongly suggest the existence of 'buried' water molecules located within phospholipid headgroups, but absent in structurally simpler surfactants [1]. This illustrates, once again, the complexity of biological aqueous interfaces.

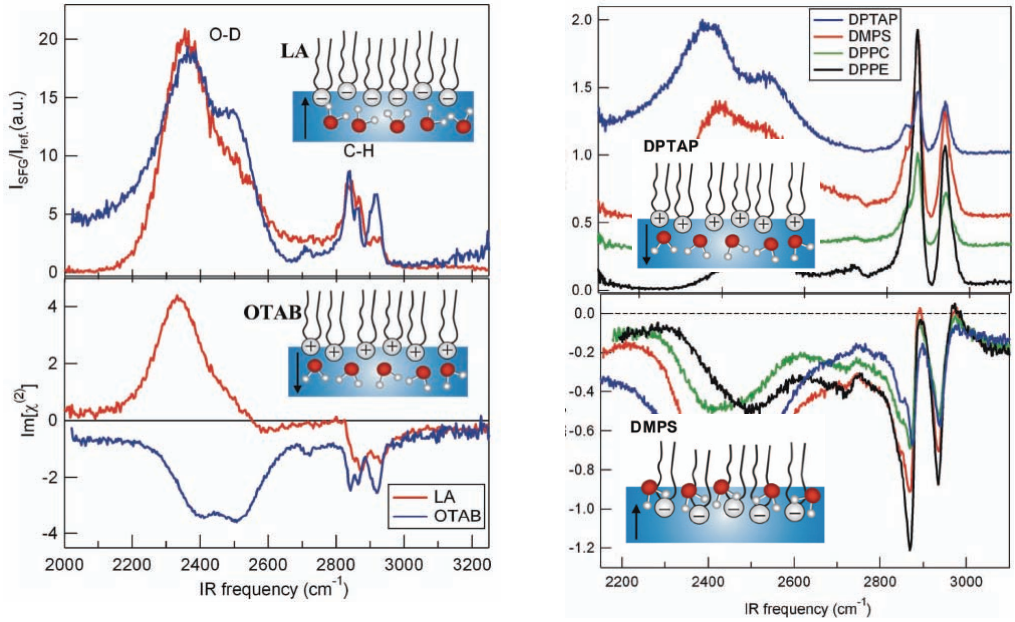

Figure 1. Top panel on right: the $|\chi^{(2)}|^2$ spectra for lauric acid (LA, red) and octadecyl trimethyl ammonium bromide (OTAB, blue), respectively. Bottom panel on right: the corresponding imaginary part of the nonlinear susceptibility, $Im[\chi^{(2)}]$, obtained by our analysis. Top panel: the $|\chi^{(2)}|^2$ spectra for DPTAP (blue), DMPS (red), DPPC (green) and DPPE (black), respectively. Data are offset for clarity. Bottom panel: the corresponding imaginary part of the nonlinear susceptibility, $Im[\chi^{(2)}]$, obtained by our analysis. Insets: schematic representation of water orientation at surfactant-water interface. The arrow indicates the orientation of the electric field below the headgroup region.

[1] M. Sovago, E. Vartiainen and M. Bonn, J. Chem. Phys. 131 (2009) 161107-1.

PROMIS CENTRE – MULTIDISCIPLINARY RESEARCH CONSORTIUM AS A LINK BETWEEN PHYSICS AND PHARMACEUTICS

L.M. Heikkinen[1,2], J. Aaltonen[1], S.-P. Simonaho[1,2], E. Nippolainen[2], R. Pellinen[1], M. Vauhkonen[2], V.-P. Lehto[2], K. Järvinen[1], and J. Ketolainen[1]

School of Pharmacy[1] and Department of Physics and Mathematics[2], P.O.B. 1627, FIN-70211, University of Eastern Finland, Finland
email: Lasse.Heikkinen@uef.fi

Promis Centre is a multidisciplinary research consortium that develops and uses new physical methods for analysis and optimization of pharmaceutical processes. Promis Centre consists of three research partners (University of Eastern Finland, Savonia University of Applied Sciences, and VTT Technical Research Centre of Finland) and several industrial partners ranging from large global to small local enterprises. Promis Centre connects people doing the basic and applied research, sensor/measurement technology providers and pharmaceutical manufacturers.

The driving force for Promis Centre is the changing needs of pharmaceutical industry. The current quality control of drug manufacturing is badly outdated, and therefore, regulatory guidelines are promoting application of new and more rational methods. The focus of Promis Centre is not only on development of rapid and cost-efficient methods, but also on the overall understanding and knowledge of the drug products and manufacturing processes. This is where the combined multidisciplinary expertise is needed; when we combine the newest methods of physical, chemical and mathematical analysis, understanding of fundamental physics and knowledge of the complex pharmaceutical processes, the benefits of the collaboration can be realised.

The research from the physical point of view at Promis Centre include development of novel monitoring technologies (electrical tomography techniques, acoustics emission, non-destructive testing using ultrasound, colour recognition, spectroscopic methods, optical sensors), as well as development of computational modelling and simulation technologies (finite and discrete element methods, estimation methods, inverse problems, data mining and chemometrics).

The web pages of Promis Centre can be found www.promiscentre.fi.

LATERAL DIFFUSION IN LUNG SURFACTANT

M. Javanainen, L. Monticelli and I. Vattulainen

Department of Physics, P.O.B. 692, FIN-33101,
Tampere University of Technology, FINLAND
email: matti.javanainen@tut.fi

Lung surfactant is a thin membrane lining the interior of the alveoli in the mammalian lung. Its main function is to prevent the alveoli from collapsing during exhaling. Despite the fact that lung surfactant has been studied rather extensively by a number of experimental and computational methods, its dynamics and functions have remained largely unclear.

One of the relevant dynamical processes associated with lung surfactant is the diffusive motion of lipids in a membrane, as it is crucial in many processes such as signalling and domain formation. The latter is involved in the formation of highly ordered cholesterol-rich domains – lipid rafts. It has been suggested that rafts in lung surfactant act as sites where vesicles fuse to the lipid interface [1].

The goal of our study is to provide insight into the diffusion processes occurring in lung surfactant. To this end, we employ both atomistic and coarse-grained simulations. We consider seven systems whose molecular composition models the one in lung surfactant, and where the physical state of the lung surfactant describes different stages of the breathing cycle. First, we consider the diffusion mechanisms associated with lipid motion in a lung surfactant membrane. Second, we investigate the validity of the so-called free area theory for lipid diffusion [2, 3, 4].

The results indicate that the diffusive motions in the lung surfactant are largely collective with features of both random rattling and flow-like motion. The dynamical correlations last for at least 100 nanoseconds. This qualitative behaviour is very different from the one suggested by the free area theory. Further, while the description given by the free area theory fits the diffusion data quite well, thorough considerations show that the values of the parameters emerging from the fit lack a physically meaningful interpretation. Overall, our results are in good agreement with recent studies of diffusion in lipid bilayers [3, 4].

[1] M. Gugliotti and M. Politi, Biophys. Chem. **89**, 243 (2001).

[2] P. Almeida, W. Vaz, and T. Thompson, Biochemistry **31**, 6739 (1992).

[3] T. Apajalahti, P. Niemelä, P. Govindan, M. Miettinen, E. Salonen, S. Marrink, and I. Vattulainen, Faraday Discuss. **144**, 411 (2010).

[4] E. Falck, T. Rog, M. Karttunen, and I. Vattulainen, JACS **130**, 44 (2008).

COMPARISON OF MCNP5 ELECTRON TRANSPORT WITH EGSnrc AND PENELOPE: ENERGY-LOSS DISTRIBUTION AND DOSE CALCULATION IN A SMALL GAS CAVITY

H. Koivunoro[1], T. Siiskonen[2], P. Kotiluoto[3], E. Hippeläinen[1], I. Auterinen[3] and S. Savolainen[1,4]

[1]Department of Physics, University of Helsinki, P.O. Box 64, 00014 Helsinki University, [2]STUK - Radiation and Nuclear Safety Authority, [3]VTT Technical Research Centre of Finland, [4]HUS Medical Imaging Centre, Helsinki University Central Hospital
email: hanna.koivunoro@helsinki.fi

Ionization chamber (IC) measurements are used as a reference dosimetry method for absorbed dose determination in external beam radiotherapy. Accurate computer simulation of the IC response is an important, while a challenging task for Monte Carlo (MC) codes. The MC code must simulate correctly the interface between two media of very different densities, boundary crossing and backscatter from the chamber wall.

The MC codes PENELOPE and EGSnrc can simulate the IC chamber response within an accuracy of 0.2% or better [1, 2]. In neutron beam dosimetry, like in boron neutron capture therapy (BNCT), a code with ability to simulate coupled neutron-photon-electron transport, like MCNP, is required.

The electron transport simulation results obtained with the physics models available in versions of MCNP earlier than MCNP5 release 1.40, have shown to include unphysical artifacts in the case of small geometry zones. With release 1.40, the electron transport algorithm is improved by applying approach of the Landau model [3] for electron energy straggling.

Purpose of this study was to evaluate ability of the MCNP5 code version 1.4 to provide reliable electron dose calculation results and ultimately its suitability for IC response simulations. The calculations using the EGSnrc and PENELOPE codes are used as benchmark. The electron dose distributions in water are compared using various mono-energetic (50 keV, 100 keV, 1 MeV and 10 MeV) electron beams. To study the IC response simulation, the absorbed dose and the electron fluence were calculated in a low-density cavity, comparable to IC gas volume, placed in water phantom and exposed to ^{60}Co photon beam.

A good agreement is observed between the calculated depth dose distributions obtained with the three codes in case of the 10 MeV electron beam. Some differences are found with the 1 MeV and 100 keV electron beams and the most notable differences with the 50 keV beam. The dose calculation result in the gas cavity is found to be dependent on the gas material.

[1] I. Kawrakow Med. Phys. 33 (2006)
[2] C. Y., S. H. Hah and M. S. Yeom Med. Phys. 33 (2006)
[3] L. Landau. J. Phys. USSR 8 (1944)

NATURAL PATTERNS OF ENERGY DISPERSAL

T. Mäkelä and A. Annila

Department of Physics, P.O.B. 64, FIN-00014 University of Helsinki, Finland
email: teemu.makela@helsinki.fi

The 2nd law of thermodynamics is recognized to underlie ubiquitous spatial patterns such as power-laws, skewed distributions, tree-like and spiral structures as well as temporal patterns such as sigmoid growth, diversification by bifurcations and chaos. Also emergence of natural standards such as the common genetic code and chirality of amino acids are understood as consequences of energy dispersal in least time.

The principle of increasing entropy, when derived from statistical physics of open systems as an equation of motion [1,2], is identified as the common cause of the universal patterns [3]. Intriguingly the self-similar evolutionary equation in general cannot be solved because the flows of energy and their driving forces are inseparable from each other. Evolving systems are non-Hamiltonian and evolutionary processes with three or more degrees of freedom are inherently non-deterministic. However, to consume free energy in least time the flows of energy naturally select paths of least action, known also as geodesics. The natural law impinges on processes at all scales of space and time and leaves its characteristic tracks that are recognized as the scale-invariant spatial structures and temporal courses.

[1] V. Sharma and A. Annila, Natural process – Natural selection. Biophys. Chem. 127 (2007) 123–128.
[2] P. Tuisku, T.K. Pernu, A. Annila, In the light of time. Proc. R. Soc. A. 465 (2009) 1173–1198.
[3] T. Grönholm and A. Annila, Natural distribution. Math. Biosci. 210 (2007) 659–667.

NON-OPTIMAL FOCUSING OF ULTRASOUND DOES NOT AFFECT DUAL FREQUENCY ULTRASOUND MEASUREMENT OF BONE

M.K.H. Malo, O. Riekkinen, J.P. Karjalainen, H. Isaksson, J.S. Jurvelin and J.Töyräs

Biophysics of Bone and Cartilage, P.O.B. 1627, FIN-70211 University of Eastern Finland, Finland
email: markus.malo@uef.fi

In pulse-echo (PE) ultrasound measurements, the use of focused transducers is essential for quantitative assessment of bones because of the strong attenuation in soft tissues and bone. Furthermore, if the ultrasonic field has a large spatial focal area (e.g. non-focused fields), the natural curvature of the cortical bone surface can distort the measurements. Variable thickness and composition of soft tissues overlying the bone affect the focal depth and may mislead the selection depth in reference measurement from a known reflector. A dual frequency technique (DFUS) was recently introduced for compensation of soft tissue derived errors in the ultrasound measurements [1, 2]. The aim of this study was to numerically simulate the effect of non optimal focal depth of the ultrasound beam on the integrated reflection coefficient (IRC) of bone as well as on the DFUS based correction of the IRC. When the soft tissue–bone surface was out of focus, the errors in the determination of the soft tissue composition increased dramatically (2% - 100%) due to over- and underestimation of lean and fat tissue contents. Attenuation compensation with correct composition of soft tissue resulted average relative error of 28.7% in the IRC values. Interestingly, the attenuation compensation with the DFUS technique was successful, and only a minor bias error (average relative error 8.9%) was observed in the corrected IRC values.

[1] O. Riekkinen et al., Ultrasound in Medicine & Biology 2008;34:10:1703-08.
[2] J. Karjalainen et al., Acta Radiol. 2008;49:1038-41.

UNIVERSITY OF EASTERN FINLAND

B-MODE ULTRASOUND QUALITY ASSURANCE: PHANTOM MEASUREMENTS

V. Mannila , O. Sipilä

Medical Imaging Center, Meilahti Hospital P.O.B. 340, FIN-00029 HUCH, Finland
email: vilma.mannila@hus.fi

Purpose: Many national and international organizations have been involved in the definition and methods for the assessment of the quality of medical ultrasound (US) equipment [1,2,3]. Still diagnostic US is lacking widely accepted technical quality assurance (QA) standards**.** Purpose of this project was to specify which of typical phantom based image-quality parameters were best suited for a routine QA protocol.

Methods and Materials: A phantom based QA protocol was used to measure 54 US-scanners with altogether 163 probes from 6 different suppliers. The scanners were purchased during the years 1998 to 2008, and the probe models range from typical linear probes to sector probes. The project was carried out by the same person in the period of three months. Measurements were done with the CIRS General Purpose Multi-tissue Ultrasound phantom. Similar probes were measured using identical protocols. Measured image-quality parameters were depth of penetration, uniformity, beam profile, vertical and horizontal caliber accuracy, near field resolution, axial and lateral resolution and size of anechoic and high scatter masses. Differences between similar scanners and probes were studied.

Results: Only slight differences between similar probes were found. The uniformity showed bad channels in some probes. The depth of penetration and the resolution measurements gave useful information only in few probes. The beam profile, caliber accuracy or measuring the size of the masses did not give any additional information to the preceding parameters.

Conclusions: Almost half the parameters used in the phantom based QA protocol did not provide any further information compared with the other parameters. The uniformity measurement turned out to be the most useful parameter for routine quality control.

[1] American Institute of Ultrasound in Medicine. The AIUM 100 mm test object and recommended procedures for its use. Rockville, MD: American Institute of Ultrasound in Medicine; 1974.

[2] Goodsitt MM, Carson PL, Witt S, Hykes DL, Kofler JM. Real time B-mode ultrasound quality control test procedures. Med Phys 1998;25:1385-406.

[3] Hill CR. Methods of measuring the performance of ultrasonic pulse-echo diagnostic equipment (Discussion document: IEC Working Group). Ultrasound Med Biol 1977;2:343-50.

T2* MAPS TO ASSESS TISSUE IRON CONCENTRATION

M. Nyrhinen[1,2], O. Sipilä[1]

[1]HUS Helsinki medical imaging center, P.O. Box 340, 00029 HUS, [2]Dept. of Physics, University of Helsinki POB 64, 00014 Helsinki University, Finland
email: mikko.nyrhinen@hus.fi

The *T2** value computed from magnetic resonance gradient multi-echo images has been shown to decrease when tissue iron concentration increases [1]. However, there is no full consensus about the best approach for the analysis of the images. The purpose of this work was to examine the effect of different computational models and algorithms on the results with different myocardial and liver iron concentrations. Also, the differences between ROI-based and pixel-wise methods, two MRI devices and sequences were analyzed.

Liver and cardiac multi-echo *T2** sequences were imaged with 1.5 T Siemens Avanto and Philips Achieva MRI devices. Altogether, 57 images of the liver and 9 images of the heart were analyzed. Two different kinds of curve fitting algorithms (linear and non-linear) and a total of five different decay models (monoexponential, noise correction, baseline, offset and truncation model) were compared [2]. In addition to ROI-based analysis, *T2** maps were acquired with pixel-wise analysis using 3 x 3 and 5 x 5 pixel averaging to reduce noise and artefacts [3]. Spatial variation of the *T2** value was also estimated from the maps.

Pixel-wise and ROI-based methods showed no statistically significant differences. The offset model and the monoexponential model with linear regression showed significant differences compared to the other models. There were no significant differences between different sequences, devices or ROI-areas. Good linear correlation (R = 0,954) was found for the standard deviation and average derived from the *T2** maps for the offset model.

Besides estimating the *T2** value, *T2** maps showed the iron distributions and areas were motion artefacts and blood vessels affected *T2** times. Non-linear regression resulted in more accurate fitting than linear. The offset model gave the most accurate fitting, but the results differed from the other models. Increase in iron concentration seemed to make the *T2** value spatially more homogenous.

[1] Westwood M, Anderson LJ, Firmin DN, Gatehouse PD, Charrier CC, Wonke B, Pennell DJ, Journal of Magnetic Resonance Imaging 18 (2003).

[2] He Taigang, Peter D. Gatehouse, Paul Kirk, Raad H. Mohiaddin, Dudley J. Pennell and David N. Firmin, Magnetic Resonance in Medicine 60 (2008).

[3] Positano V., B. Salani, A. Pepe, M. Santarelli, D. De Marchi, A. Ramazzotti, B. Favilli, E. Cracolici, M. Midiri, P. Cianciulli, Magnetic Resonance Imaging 27 (2009).

REVEALING THE MICROSTRUCTURAL CHANGES IN TISSUES IN-SITU WITH POSITRON ANNIHILATION SPECTROSCOPY

P.Sane[1], F.Tuomisto[1], I. Vattulainen[2] and J. Holopainen[3]

[1] Department of Applied Physics, Aalto University , P.O. Box 11100 00076 Espoo, Finland
[2] Department of Physics, Tampere University of Technology, Finland
[3] Department of Ophthalmology, University of Helsinki, Finland

In this work we present a novel and promising tool for characterizing the microstructural changes in biomaterials, namely mammalian lens. Positron annihilation lifetime spectroscopy (PALS) is a widely used tool to study atomic scale defects in semiconductors and routinely used to study the voids in polymer materials [1]. Through the increased understanding of the biomolecular materials via biophysics research by Molecular Dynamics simulations, the results from PALS experiments can now be compared with these simulations and further analysis of the results is possible. Recently we have showed that PALS can be applied to study and characterize free volume changes in lipid bilayers and the results are in full agreement with MD simulations [2]. In biomolecular material, a thermalized positron forms a meta-stable bound state, Positronium (Ps), with an electron from the material. This o-Ps-atom can be used as a probe, due to the Ps lifetime in the material being strongly affected by the free volume characteristics of the probed material. Hence the PALS studies in biomaterials are concentrated almost solely on studying the changes in o-Ps lifetime.

Here we present results obtained by studying the temperature dependent changes in free volume parameters in mammalian lenses, lipids separated from the lenses and controlled Spingomyelin-cholesterol mixtures [3]. All the measurements provide strong evidence towards a minor structural reorganization near 35°C, far below strict phase transition temperatures. This change indicates a transition to liquid order phase and is not visible with conventional experimental methods used in the study, probably due to the microstructural scope of the change which does not provide strong enough signal for e.g. DSC.

[1] O. E. Mogensen, *Positron annihilation in Chemistry* Springer-Verlag, Heidelberg, (1995)
[2] P. Sane et al, J. Phys. Chem. B: **113**:1810-12 (2009)
[3] P.Sane et al, *"Temperature Induced Structural Transition in-situ in Porcine Lens - Changes Observed in Void Size Distribution"*, submitted to BBA Biomembranes on 4.1.2010

THE FINNISH BORON NEUTRON CAPTURE THERAPY (BNCT) - 87.00 PROJECT

S. Savolainen

Dept. of Physics, Univ. of Helsinki, POB 64, 00016 Helsinki University &
HUS Helsinki Medical Imaging Center, Helsinki University Central Hospital, POB 340, 00029 HUS

email: sauli.savolainen@hus.fi

Clinical trials on BNCT in Finland started in May 1999. In BNCT protocol P01, the patients exhibited newly diagnosed glioblastoma multiforme (GBM) and BNCT was given as the first postoperative radiation treatment. No other concomitant or adjuvant treatments were offered. In the BNCT protocol, P03 patients showed recurrent or progressing GBM or anaplastic astrocytoma gradus III, and had undergone prior cranial conventional external beam radiotherapy. Patients in head and neck (HN) protocol had inoperable, recurrent, histologically confirmed head and neck cancer. Detailed criteria for protocols P01 and P03 appear in a paper by Joensuu *et al.* [1], and for protocol HN in a paper by Kankaanranta *et al.* [2]. Altogether, 190 patients have been treated with BNCT since May 1999 in Finland.

Detailed physical quantities for BNCT dosimetry have previously been presented in doctoral theses in the Dept. of Physics, Univ. of Helsinki [3-10].

Several studies have examined, the suitability of positron emission tomography (PET) for treatment planning purposes. Prompt gamma spectroscopy has also been investigated for boron determination. ^{11}B or ^{10}B MR imaging and MR spectroscopic methods have been reported for boron detection. The possibility of applying clinically widely used proton MRS for selective BPA-F detection has been studied in the doctoral thesis by M. Timonen [10].

One area of future research and development is still a search for optimal blood-tumour ^{10}B –concentration, and the methods to detect the boron distribution *in vivo*.

[1] H. Joensuu *et al.*, J of Neuro-Oncology, 2003 (62) 1027-39.
[2] L. Kankaanranta *et al.*, IJROBP 2007 (69) 475-82.
[3] C. Aschan (1999): http://urn.fi/URN:ISBN:951-45-8686-7
[4] A. Kosunen, University of Helsinki, thesis, STUK-A164 (1999) 50 p.
[5] M. Kortesniemi (2002): http://urn.fi/URN:ISBN:951-45-8955-6
[6] T. Seppälä (2002): http://urn.fi/URN:ISBN:952-10-0570-X
[7] P. Ryynänen (2002): http://urn.fi/URN:ISBN:952-10-0568-8
[8] P. Kotiluoto (2007): http://urn.fi/URN:ISBN:978-951-38-7016-4
[9] J. Uusi-Simola (2009): http://urn.fi/URN:ISBN:978-952-10-4232-4
[10] M. Timonen (2010): http://urn.fi/URN:ISBN:978-952-10-5649-9

PROTON MAGNETIC RESONANCE SPECTROSCOPY OF BNCT ^{10}B-CARRIER, L-*P*-BORONOPHENYLALANINE-FRUCTOSE COMPLEX

M. Timonen[1,2], L. Kankaanranta[3], N. Lundbom[2], S. Savolainen[1,2] and S. Heikkinen[4]

[1]Dept of Physics, P.O.B. 64, FIN-00014 University of Helsinki, Finland
[2]HUS Helsinki Medical Imaging Center, P.O.B. 340, FIN-00029 HUS, Finland
[3]Dept of Oncology, P.O.B 180, FIN-00029 HUS, Finland
[4]The Laboratory of Organic Chemistry, P.O.B. 55, FIN-00014 University of Helsinki, Finland.
email: sauli.savolainen@hus.fi

Boron neutron capture therapy (BNCT) has been used to treat malignant brain tumours, melanomas, head and neck cancer, and liver metastases. In BNCT, boronophenylalanine fructose (BPA-F) is widely used as the ^{10}B-carrier. Proton magnetic resonance spectroscopy (^{1}H MRS) can be used for selective BPA-F detection and quantification since aromatic protons of BPA resonate in the spectral region clean from brain metabolite signals [1-5].

In this study, we investigated validity of MRS as a tool for BPA detection. In an *in vivo* study, the acquisition weighted MRSI and/or single voxel MRS was performed for ten patients (pts 1-10) on the day of BNCT. ^{1}H MRS/3D ^{1}H MRSI measurements were conducted for nine patients at 1.5 T and ^{1}H MRS for one patient at 3.0 T. PRESS localization with CHESS water suppression scheme was used. Three patients had glioblastoma multiforme (GBM), five patients had a recurrent or progressing GBM or anaplastic astrocytoma gradus III, and two patients had a head and neck cancer. For nine patients (pts 1-9), MRS/MRSI was performed 70-140 min after the second irradiation field, and for one patient (pt 10) MRSI study was started 11 min before the end of the BPA-F infusion and ended 6 min after the end of the infusion. As a comparison, a single voxel MRS was performed before BNCT for two patients (pts 3 and 9), and for one patient (pt 9), MRSI was done also one month after the treatment. For one patient (pt 10), MRSI was performed also four days before infusion. In three patients (pts 1, 9, and 10), the signals in the aromatic region of tumour spectrum were detected on the day of BNCT, indicating that in favourable cases, it is possible to detect BPA *in vivo* in the brain after BNCT treatment or at the end of BPA-F infusion.

[1] C. Zuo *et al.* Med Phys 1999; 26(7):1230-1236
[2] S. Heikkinen *et al.* Phys. Med. Biol. 2003; 48(8):1027-1039
[3] M. Timonen *et al.* EJR 2005;56(2):154-159
[4] P. Bendel *et al.* Magn Reson Med 2005;53(5):1166-1171
[5] M. Timonen *et al.* J Radiat Res 2009;50(5):435-440

COMPARISON BETWEEN VOXEL BASED AND DOUBLE FOLDED INTEGRAL CALCULATION METHODS FOR CELLULAR DOSIMETRY

P. Välimäki, A. Kuronen and S. Savolainen

University of Helsinki, Department of Physics, Finland
Boneca Oy, Helsinki, Finland
email: Petteri.Valimaki@Helsinki.fi

In internal radiotherapies for cancer treatment a cell cluster model is needed for the estimation of the absorbed dose on the cellular level. Up to this day the cluster models have been mainly constructed from simple geometrical shapes like spheres and cubes mimicking biological cells and nuclei. The most common model has been the closed packed cubic lattice model with spheres. However, quantitative verification of the lattice models against biological data has not been carried out and the analysis of the ranges of their usability has been missing.

To create a realistic setting for the cell-level dose estimation and cell cluster validation we developed voxel-based **RealCluster** software – to our knowledge the world's first dose calculation system enabling dose calculations in 3D clusters of arbitrary cell shapes. The software calculates doses on voxel-by-voxel basis using Monte Carlo based dose point kernels.

To verify the calculations of the software and to measure its accuracy we calculated radiation doses in simple spherical structures by the voxel method and by a method based on double folded integration utilizing Fourier-Bessel expansion. The spherical source cell was filled with homogeneously distributed radionuclide (Fig 1). Radiation doses to the neighbouring cells at various distances were calculated with both methods (Fig 2). The doses calculated by the **RealCluster** software compared well with the values of the double folded integration calculations differing by about 3 percent at maximum.

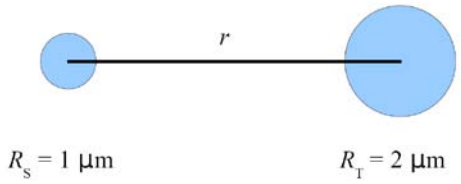

Fig 1: Geometry of the test calculations.

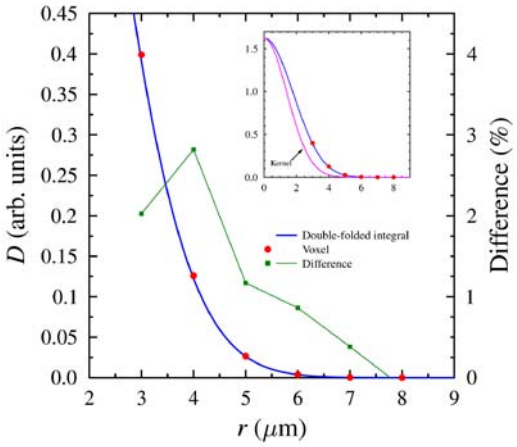

Fig 2: Dose as a function of source-target distance.

LACTOBACILLUS BREVIS S-LAYER STUDIED BY SAXS AND ELECTRON MICROSCOPY

Pentti Jääskeläinen[1], Peter Engelhardt[2], Mika Torkkeli[3], Ulla Hynönen[4], Heikki Vilen[4], Jukka Heikkonen[5], Airi Palva[4] and Ritva Serimaa[3]

[1] Department of Biomedical Engineering and Computational Science, Aalto University School of Science and Technology, Finland[2] Department of Pathology, Haartman institute, University of Helsinki, Finland[3] Department of Physics, University of Helsinki, Finland[4] Department of Basic Veterinary Sciences, Division of Microbiology and Epidemiology, University of Helsinki, Finland
email: pentti.jaaskelainen@helsinki.fi

Lactobacillus brevis is a Gram-positive, probiotic bacterium that could potentially be developed into a probiotic vaccine. [1] *L. brevis* surface (S) layer proteins (SlpA) bind to a polysaccharide receptor within the cell wall, forming a crystalline, two dimensional surface layer that forms the outermost layer of the cell wall. In this poster, we have studied S-layer of *L. brevis* both in native state and reassembled on cell surface using small- angle X-ray scattering (SAXS) and electron microscopy.[2]
SAXS intensities show that the structure of native S-layer differs from the layer formed by recombinant SlpA (rSlpA) reassembled on purified *L. brevis* cell wall fragments (CWF): The same peaks that are present in the reassembled S-layer are not present in the native one. The diffraction peaks observed at higher values of the length of scattering vector *k* are sharper, indicating that the structure of the reassembled S-layer is more crystalline than that of the native one. Results obtained with electron microscopy show that *L. brevis* S-layer proteins are arranged in rows separated by pore rows in both native and reassembled S-layers.

SAXS intensities of rSlpa reassembled on CWF show the same diffraction peaks as SlpA reassembled on surface of L. brevis cells from which native S-layer has been stripped with 5M guanidium hydrochloride. This indicates that the reassembly results to essentially same structures in both of these cases [2]. We have also reached similar results by comparing the CWF reassembly of wild type rSlpA and rSlpA mutants, in which one of the amino acids has been replaced with a cysteine [3].

References
[1] S. Åvall-Jääskeläinen, U. Hynönen, N. Ilk, D. Pum, U. B. Sleytr and A. Palva., BMC Microbiology,8 (2008) 165
[2] P. Jääskeläinen et al., Manuscript in preparation
[3] H. Vilén, U. Hynönen, H. Badelt-Lichtblau, N. Ilk, P. Jääskeläinen, M. Torkkeli and A. Palva, Journal of Bacteriology 191 (2009) 3339

4 Condensed matter: Structural properties

4.1 Oral session, Friday 12 March 14:30-16:00
4.2 Poster session I, Thursday 11 March 16:30-18:30
4.3 Poster session II, Friday 12 March 16:00-18:00

EXOTIC DENSE ICES

T. Pylkkänen[1,2], V. M. Giordano[2], A. Sakko[1], M. Hakala[1], J. A. Soininen[1], K. Hämäläinen[1], G. Monaco[2] and S. Huotari[2]

[1]Division of Materials Physics, P.O.B. 64, FIN-00014 University of Helsinki, Finland
[2]European Synchrotron Radiation Facility, B.P. 220, F-38043 Grenoble, France
email: tuomas.pylkkanen@helsinki.fi

Water, one of the most common substances and certainly the most significant for life, has a variety of unusual features ranging from thermodynamical anomalies to an impressive polymorphism. At least 15 crystalline and multiple amorphous phases have been characterized [1] and more may follow. These exotic phases of ice have interesting properties such as proton ordering and densities up to twice that of the common hexagonal phase.

Exploring the phase diagram of ice requires access to high pressures and low temperatures. Studying materials in extreme conditions of pressure and temperature is currently generating new results across the field of condensed matter physics, ranging from the discovery of novel ultrahard materials to the understanding of the properties of the Earth's core and mantle. X-ray methods have had an important role in this development, since they facilitate studies of the often microscopic samples that are embedded in high-pressure sample environments such as the diamond anvil cell.

We report studies of ice phases Ih, VI, VII and VIII using inelastic x-ray scattering at the European Synchrotron Radiation Facility. X-ray spectroscopies provide information on the electronic structure and dynamics of materials. Core-level spectroscopies, such as x-ray Raman scattering (XRS), give access to the local density of empty electronic states in the vicinity of a chosen chemical element. The detailed interpretation of the spectra can provide valuable structural information that complements diffraction studies. There is considerable interest in obtaining more detailed structures of disordered hydrogen-bonded liquids and solids. In this context, high-pressure ice phases can be used as model systems with different local structures to study the effect of hydrogen bonding on near-edge spectra. We compare the measurements with calculations using density-functional theory.

Recently, the near-edge spectra of water and ices have been studied intensively. The spectra have been shown to be sensitive to broken and distorted hydrogen bonds and increased disorder in the hydrogen bond network [2, 3, 4]. We find a new behavior in which increased density leads to strong systematic changes in the spectra, similar to the effect of broken bonds. We connect the spectral changes, however, to increased coordination from non-hydrogen-bonded neighbors, whose influence has been previously neglected.

[1] C. G. Salzmann *et al.*, Phys. Rev. Lett. 103 (2009) 105701.
[2] Ph. Wernet *et al.*, Science 304 (2004) 705.
[3] Y. Q. Cai *et al.*, Phys. Rev. Lett. 94 (2005) 025502.
[4] J. S. Tse *et al.*, Phys. Rev. Lett. 100 (2008) 095502.

COMPRESSING A THIN-WALLED ELASTIC BOX

T. Tallinen[1], J. A. Åström[2] and J. Timonen[1]

[1]Department of Physics, P.O. Box 35, FI-40014 University of Jyväskylä
[2]CSC - IT Center for Science, P.O. Box 405, FIN-02101 Esbo
email: tuomas.tallinen@jyu.fi

Vertical compression of an elastic thin-walled box is explored. Such a compression displays three successive regimes: linear, buckled and collapsed. Analogy of the buckled regime to thin-film blisters [1] is demonstrated. The compression force is shown to reach its maximum at the end of that regime, after which the box collapses displaying features (e.g. ridges) typical of crumpling of thin sheets [2, 3]. These qualitative findings are confirmed by numerical simulations based on a discrete element method, and implications are drawn on the box compression strength.

Thin-walled box compressed by 1 % (left) displays focusing of compressive stress at the vertical edges. Under further compression the box collapses and stretching ridges form (right).

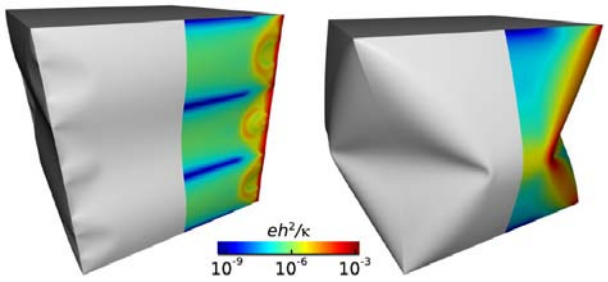

[1] S. Conti, A. DeSimone, S. Müller, Self-similar folding patterns and energy scaling in compressed elastic sheets. *Comput. Methods Appl. Mech. Engrg.* **194**, 2534 (2005).
[2] T. Tallinen, J. A. Åström, J. Timonen, The effect of plasticity in crumpling of thin sheets. *Nature Mater.* **8**, 25 (2009).
[3] T. A. Witten, Stress focusing in elastic sheets. *Rev. Mod. Phys.* **79**, 643 (2007).

DENSITY FUNCTIONAL STUDY ON ETHYLENE DECOMPOSITION ON FLAT AND STEPPED PALLADIUM

J. Andersin[1], K. Honkala[1,2]

[1]Department of Chemistry, Nanoscience Center, P.O. Box 35, University of Jyväskylä, FIN-40014 Jyväskylä, Finland
[2] Department of Physics, Nanoscience Center, P.O. Box 35, University of Jyväskylä, FIN-40014 Jyväskylä, Finland
email: jenni.andersin@jyu.fi

Ethylene (CH_2CH_2) adsorption and decomposition to atomic carbon and hydrogen over Pd(111) and Pd(211) surfaces have been studied with the aim to unravel the complex chemistry of this industrially relevant reaction [1, 2]. We have constructed a potential energy surface containing information of the energetics of ethylene decomposition pathway (see Figure 1). In unison with the experiments our calculations show that ethylidyne (CCH_3) is the most stable molecule among the ethylene decomposition residues. Our results also support the experimental findings indicating that decompositions come into action in a progressive order with increasing temperature: Calculated activation barriers related to ethylidyne decomposition to atomic carbon are around 0.5 eV higher compared to ethylene-ethylidyne conversion on flat Pd. Step edges scramble the picture by offering active sites for adsorbates and facilitating certain reaction mechanisms. The reaction and activation energies for processes involving the activation of C-H bond are directly proportional, and the linear response is outstanding for the flat surface.

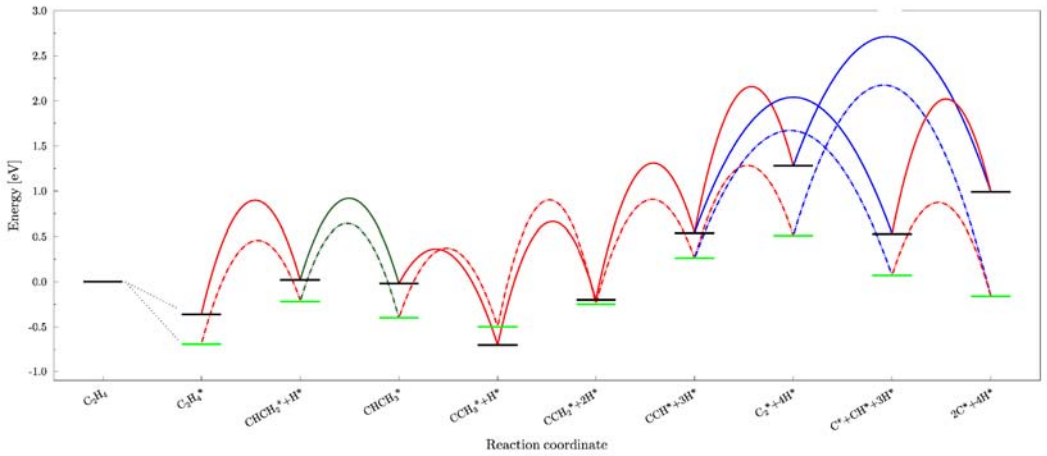

Figure 1: Potential energy diagram for ethylene decomposition on Pd(111) and Pd(211) surfaces. Black (green) line represents the adsorption energies of the different hydrocarbon species on Pd(111) (Pd(211)). Transition state energies are illustrated with curved lines. The zero of energy is ethylene far away from the clean surface.

[1] J. Andersin and N. Lopez and K. Honkala, J. Phys. Chem. C 113 (2009) 8278.
[2] J. Andersin and K. Honkala, Surface Science, article submitted.

THE EFFECT OF ENZYMATIC HYDROLYSIS ON THE SUB-MICROMETER STRUCTURE OF MICROCRYSTALLINE CELLULOSE

P. Penttilä[1], A. Várnai[2], K. Leppänen[1], M. Peura[1], A. Kallonen[1], P. Jääskeläinen[3], J. Lucenius[1], A. Nykänen[4], M. Siika-aho[5], L. Viikari[2], and R. Serimaa[1]

[1]Department of Physics, POB 64, FI-00014 University of Helsinki, Finland
[2]Department of Food and Environmental Sciences, University of Helsinki, Finland
[3]Department of Biomedical Engineering and Computational Science, Aalto University, Finland
[4]Department of Applied Physics, Aalto University, Finland
[5]VTT Technical Research Centre of Finland, Finland
Email: paavo.a.penttila@helsinki.fi

Cellulose is the most abundant polymer in the world and thus has a great potential for renewable energy production. The utilization requires the depolymerisation of cellulose into glucose, which can be done with the aid of enzymatic hydrolysis. However, the enzymatic hydrolysis is the rate-limiting step in the whole process, since it always tends to slow down with time.

In order to clarify the reasons behind the slowing down of the reaction, we used wide- and small-angle x-ray scattering (WAXS and SAXS), x-ray microtomography (µCT), and transmission electron microscopy (TEM) to characterize the sub-micrometer changes in microcrystalline cellulose during enzymatic hydrolysis. The cellulose was hydrolyzed with the well-known *Trichoderma reesei* enzyme system for different time periods and the freeze-dried hydrolysis residues were measured with WAXS, SAXS, and µCT. Additionally, some of them were re-wetted for wet SAXS and TEM measurements.

The µCT measurements showed a clear decrease in particle size in scale of tens of micrometers. Despite of that, in all the TEM pictures similar cylindrical and partly ramified structures were observed, independent of the hydrolysis time. The SAXS results showed a change in the structure of wet samples in scale of 10–30 nm. According to the WAXS results, the degree of crystallinity and the crystal sizes remained unchanged. The gained results support the assumption, that cellulosic particles are hydrolyzed mostly on their surface, since the enzymes are unable to penetrate into the nanopores of wet cellulose.

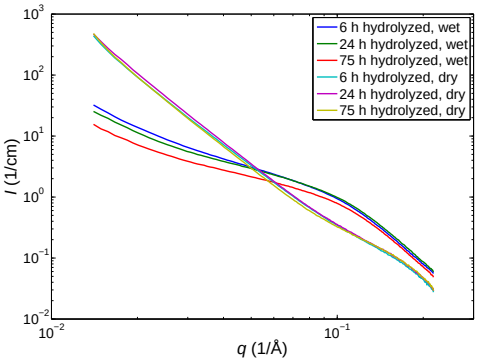

Figure 1: SAXS curves of enzymatically hydrolyzed microcrystalline cellulose in dry and re-wetted state. Porod's q^{-4} law was fitted on larger q-values and other power laws on smaller q-values. Specific surface, average chord length, and fractal dimensions were calculated.

ANDREEV REFLECTION FROM VORTICES IN SUPERFLUID ^{3}He-B

J. Hosio, V.B. Eltsov, R. de Graaf, and M. Krusius

Low Temperature Laboratory, Aalto University, PO BOX 15100, 00076 Aalto, Finland
email: jaakko.hosio@tkk.fi

The energy spectrum of the elementary excitations in superfluid ^{3}He-B, the quasiparticles and quasiholes, is characterized by an energy gap Δ similarly to electrons and holes in superconductors. At very low temperatures, in the ballistic regime of transport, the mean free path of the excitations is long and collisions between them can be neglected. The rotatory flow associated with quantized vortices, however, can constrain their trajectories.

In the ballistic regime the thermal damping of oscillating objects in a quiescent bath of ^{3}He-B is proportional to the density of thermal quasiparticles, with a temperature dependence given by the Boltzmann factor $\rho_{qp} \propto e^{-\Delta/k_BT}$. In the rest frame of the condensate the dispersion curve of excitations is symmetrical. In the presence of superfluid flow with velocity $\mathbf{v}$ excitations with momentum $\mathbf{p}$ undergo the Galilean transformation $E \rightarrow E + \mathbf{p} \cdot \mathbf{v}$. Thus, an excitation propagating through the superfluid flow field may not find a forward-propagating state and therefore retraces its trajectory and changes flavor from quasiparticle to quasihole. This mechanism is called Andreev reflection. It has been widely used to study quasiparticle dynamics in the presence of a turbulent vortex tangle with unknown density [1]. Previously we have measured the Andreev reflection of thermal quasiparticles in a quiescent bath of ^{3}He-B using one quartz tuning fork oscillator as a generator of flow and a second as detector [2].

Recently, we measured Andreev reflection of quasiparticles from a cluster of rectilinear vortex lines in the rotating state. These are the first direct measurements of Andreev scattering from a well-defined vortex configuration with a known density and spatial extent. Our measurements with rotation velocities up to $\Omega = 1.7$ rad/s show that the effective area of the bolometer orifice, which is inversely proportional to the fraction of the retro-reflected quasiparticles, decreases linearly as a function of Ω or the density of vortices in the cluster. The results can now be compared to direct analytic calculations [3], in order to refine quasiparticle beam techniques for the visualization of different vortex configurations and measuring their densities.

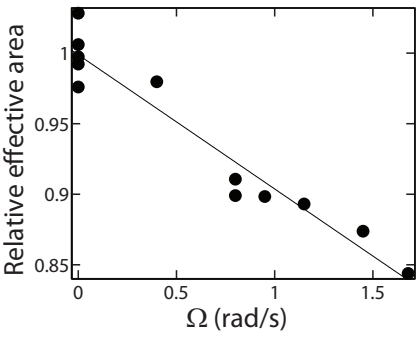

Fig. 1: Relative effective area of the bolometer orifice or the fraction of non-reflected quasiparticles as a function of rotation velocity.

[1] D.I. Bradley *et al.*, PRL **93**, 235302 (2004).
[2] M. Blaŝková *et al.*, J. Low Temp. Phys. **146**, 537 (2007).
[3] C.F. Barenghi, Y.A. Sergeev, and N. Suramlishvili, Phys. Rev. B **77**, 104512 (2008).

EFFECT OF SURFACE HYDROXYL CONCENTRATION ON THE BONDING AND MORPHOLOGY OF AMINOPROPYLSILANE THIN FILMS ON AUSTENITIC STAINLESS STEEL

H. Ali-Löytty, P. Jussila, K. Lahtonen, M. Hirsimäki, and M. Valden

Surface Science Laboratory, Department of Physics, Tampere University of Technolgy, P.O.B. 692, FIN-33101 Tampere, Finland
email: harri.ali-loytty@tut.fi

Stainless steels (FeCr-based alloys) are employed in many fields of technology due to their excellent mechanical properties and corrosion resistance. In addition to established applications in construction, transportation, and process industry, novel applications include medical and biofunctional materials such as orthopedic implants and vascular stents. The favourable surface properties of stainless steels stem from a protective chromium-containing oxide film, which forms spontaneously under oxidizing conditions. The morphology and chemical composition of this film are crucial to the corrosion resistance of stainless steel and to the adhesion of functional coatings which are used to further extend the range of applications. [1]

Organofunctional silanes are attractive for assembling such coatings, because they allow for tailoring of surface properties via selection of their specific molecular structure and functional groups. It is well established that hydroxylated silica is one of the most favourable substrates for silane depositions, whereas stainless steel materials are generally considered difficult. One reason for this is that knowledge of the interaction between silanes and metal oxide structures on stainless steel remains limited. [1]

In our recent study the adsorption of 3-aminopropyltrimethoxysilane thin films on Fe-18Cr-7Mn-3Ni was investigated by X-ray photoelectron spectroscopy (XPS) and inelastic electron background analysis. The bonding and morphology of the films were strongly dependent on the surface hydroxyl concentration, which was controlled by the oxidation pretreatment of the substrate. In particular, an aminopropylsilane monolayer with high degree of bonding to the substrate was obtained on an electrochemically passivated surface with very high hydroxyl concentration. On the other hand, the deposition of weakly bound aminopropylsilane clusters was observed on substrates having relatively low hydroxyl concentrations. The adsorption occurred initially via hydrogen bonding, whereas heating to 373 K resulted in the formation of covalent Si–O–M bonds at the silane/metal oxide interface. The results suggest that high quality silane films could be obtained even on stainless steel substrates given the proper pretreatment of the surface. [1]

[1] P. Jussila, H. Ali-Löytty, K. Lahtonen, M. Hirsimäki, and M. Valden, Surface and Interface Analysis (in press).

HYDROGEN IN FePd:$L1_0$: SOLUBILITY AND MIGRATION

M.G.Ganchenkova

COMP/Department of Applied Physics, School of Science and Technology, Aalto University, P.O.Box 11100, FIN-00076 AALTO, Finland
e-mail: mganchen@cc.hut.fi

E.A.Gonzales, P.V.Jasen, A.Juan

Departamento de Fisica, Universidad Nacional del Sur, Avda.Alem 1253, Bahia Blanca 8000, Argentina

Binary intermetallic compounds with the order L10 structure, such as FePt, FePd, etc., are of considerable interest for both structural and functional applications ranging from advanced gas-turbine and combustion engines to permanent magnet micro-devices and data-storage media. Despite extensive investigations there are still a lot of open questions about defect and impurity behavior in these systems.

This work is dedicated to the study of hydrogen solubility and its migration in FePd:$L1_0$ matrix. Calculations are performed using density-functional theory approximations as implemented in VASP code. All the possible interstitial hydrogen positions in the lattice have been studied. The most energetically favorable interstitial hydrogen configuration among the six considered high-symmetry configurations found to be the octahedral one having four Fe atoms and two Pd atoms as its neighbors. All the probable pathways for H migration are considered and discussed. In particular, it is shown that the most favorable diffusion pathway for hydrogen atoms in the bulk involves the exchange of octahedral positions with the effective migration energy of ~ 0.6 eV.

NONLINEAR MICRORHEOLOGY OF DENSE COLLOIDAL SUSPENSIONS

I. Gazuz[1], A. M. Puertas[2] and M. Fuchs[3]

[1]Department of Applied Physics, Aalto University, P.O. Box 11000, FI-00076 AALTO, Finland
email: igor.gazuz@tkk.fi
[2]Departamento de Fisica Aplicada, Universidad de Almeria, 04.120 Almería, Spain
email: apuertas@ual.es
[3]Fachbereich Physik, Universität Konstanz, P.O. Box M671, 78457 Konstanz, Germany
email: matthias.fuchs@uni-konstanz.de

The motion of a colloidal tracer particle, pulled through a colloidal suspension by means an external force is investigated. We are interested in the nonlinear response of the system. We start with the formally exact expressions and adopt the *intergration through transients* [1] approximation method, developed for sheared suspensions, for our case.

The key quantity of the approach is the time and external force dependent density correlator of the tracer. By means of mode-coupling approximations, a self-consistent equation is established for it [2], exhibiting many new properties (e.g. the correlator is, in general, complex) due to the non-hermiticity of the Smoluchowski operator for an open system.

The mobility of the tracer strongly changes with applied force as surrounding particles are pushed aside for strong forces. The competition between internal diffusion and external drive leads to the thinning behaviour with increasing external force on the tracer. For a glassy suspension, our approach yields that the tracer can only move if the external force exceeds a certain threshold value. This yielding behaviour is in agreement with experiments and simulations. [2, 3].

[1] Fuchs M., Cates M. E., J. Phys.: Condens. Matter **17** (2005) S1681-S1696.
[2] I. Gazuz, A. M. Puertas, Th. Voigtmann, M. Fuchs (2009), Phys. Rev. Lett. **102**, 248302 (2009)
[3] Weeks E. et. al., Europhys. Lett. **67** (3), pp. 4

BOSE-EINSTEIN CONDENSATION OF MAGNONS IN SUPERFLUID ^{3}He-B

P. J. Heikkinen, Yu. M. Bunkov, V. B. Eltsov, R. de Graaf, M. Krusius, and G. E. Volovik

Low Temperature Laboratory, Aalto University, P.O.B. 15100, FI-00076 AALTO, Finland
email: petri.heikkinen@tkk.fi

Spin waves, or magnons, are collective excitations obeying Bose-Einstein statistics and existing in magnetically ordered systems. In superfluid ^{3}He a magnon condensate can be formed in a homogeneous system, where it forms a spin superfluid, or at low temperatures in a magnetic trap. As seen in Fig. 1, in ^{3}He-B a potential well can be formed in the cylindrically symmetric "flare-out" texture which in the axial direction has a superposed minimum in the polarizing magnetic field.

This is achieved by confining the ^{3}He-B sample at temperatures below $0.4\,T_{\rm c}$ within a cylindrical container in an axial homogeneous magnetic field which is supplemented by the localized field from a pinch coil. The radial width of the trap can be modified by rotating the sample. The depth of the field minimum is adjusted by the current in the pinch coil. Using continuous-wave NMR techniques one can populate either the ground state or different excited levels (m,n) of the approximately harmonic trap. The low-amplitude spin wave spectrum, in the limit of small number N of magnons, has the form

$$\omega_{\rm mn}(N) = \omega_{\rm L}(0) + \omega_r\,(\mathrm{m}+1) + \omega_z\,(\mathrm{n}+1/2) - \lambda_{\rm mn}\,N\,.$$

Two spectra at different rotation velocities Ω in a state of vortex-free superfluid counterflow are shown in Fig. 2 as a function of frequency shift between the Larmor frequency f_0 and the applied RF pumping frequency f. By increasing Ω, the superfluid velocity field $v_{\rm s} = |\mathbf{\Omega} \times \mathbf{r}|$ changes and the potential well becomes steeper in the radial direction. This increases the radial oscillator frequency ω_r and the spectral distance between the radial eigenvalues m. By increasing the depth of the magnetic field minimum, the axial oscillator frequency ω_z can be increased, which, in turn, increases the spacing of the axial eigenvalues n. The NMR signal from the condensate can be used to investigate the low temperature limit of ^{3}He-B – the vacuum state of a Fermi superfluid.

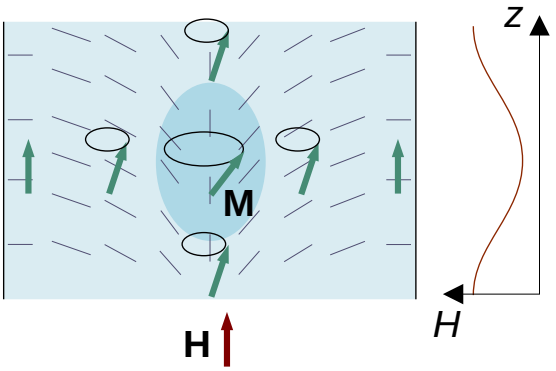

Figure 1: Magnetic trap in the order parameter texture of ^{3}He-B.

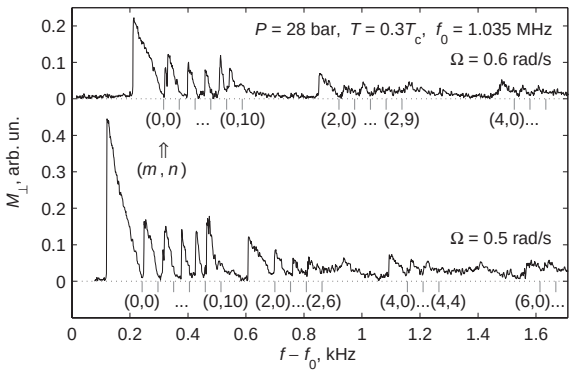

Figure 2: Formation of magnon condensates on different excited levels (m,n).

MD SIMULATIONS ON CUTTING ICE WITH A NANOSCALE WIRE USING 3D MERCEDES-BENZ MODEL

Vili Heinonen, Teemu Hynninen, Tapio Ala-Nissilä and Adam Foster

Department of Applied Physics, Aalto University School of Science and Technology, P.O.B. 11000 FI-00076 Aalto, Finland
email: vili.heinonen@tkk.fi

Cutting ice with a wire is an interesting experiment and yet another example of the complex nature of water and its intermolecular interactions. In this work a MD simulation for cutting ice with a nanoscale wire is set using 3D Mercedes-Benz model for ice. The motion of the wire through ice is distinguished into three different modes and corresponding ranges of driving forces are determined. Also a phase transition is observed in the ice under the pressure induced by the force driving the wire through ice.

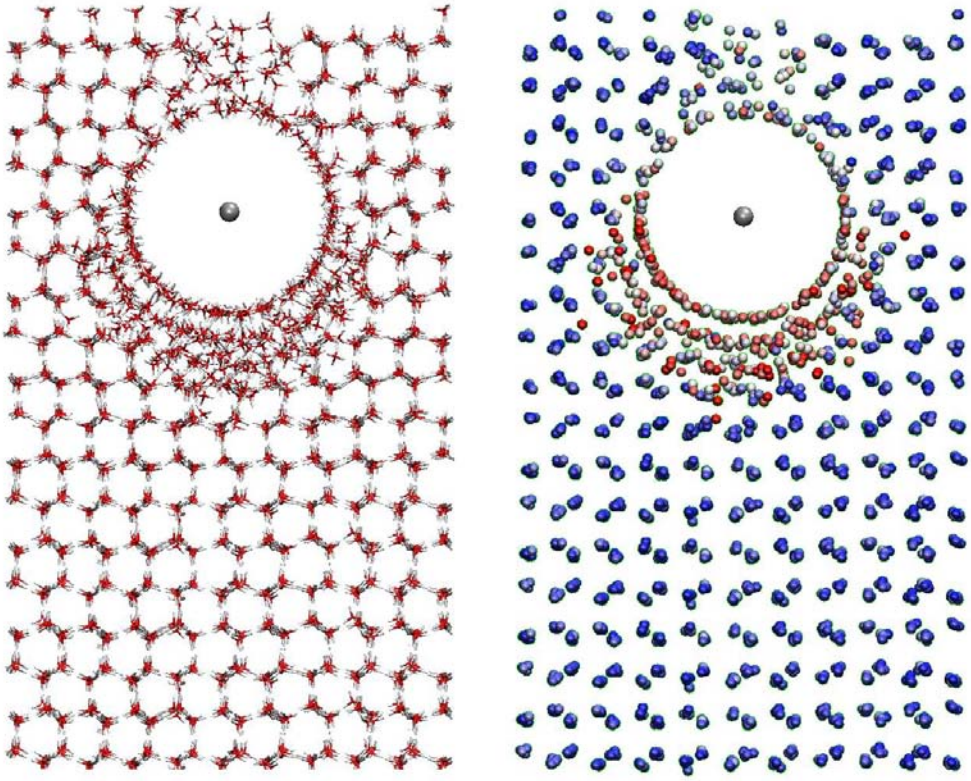

Figure 1: Wire cutting through ice. On the left a tetrahedral representation of the Mercedes-Benz molecules and on the right corresponding picture where the colours scaling from red to blue indicate the number of bonds of a single molecule.

FERROMAGNETISM IN CARBON NANOPOWDER

E. Hujala[1], A. Pulkkinen[1], E. Lähderanta[1], A.V. Lashkul[1] and R. Laiho[2]

[1] Lappeenranta University of Technology, Department of Mathematics and Physics, P.O.B. 20, FIN-53851 Lappeenranta, Finland
[2] Wihuri Physical Laboratory, University of Turku, Finland

Nowadays researchers are more and more interested in light magnets. One way to obtain light magnets is by utilization of the properties of nanocarbon. Therefore, these materials are interesting, not only for fundamental science, but also for practical applications.

Nanocarbon powder sample with randomly distributed pores was manufactured by decomposition of polyvinyl spirit in inert atmosphere. In this work we report preliminary investigation of magnetic properties of nanocarbon powder which demonstrate ferromagnetic features even at room temperature. The dc magnetization $M(B)$ was measured using a SQUID magnetometer at temperatures $3\,\mathrm{K}$, $15\,\mathrm{K}$, $40\,\mathrm{K}$, $100\,\mathrm{K}$ and $300\,\mathrm{K}$ in magnetic fields B up to $5\,\mathrm{T}$.

In Fig 1 is presented the magnetic field dependence of magnetization of not doped nanocarbon powder, which demonstrates hysteresis loop up to 300 K. It is visible, that remanent magnetization $M_r = 10^{-4}\,\mathrm{A\,m^2/g}$ and coercive field $B_c = 30\,\mathrm{mT}$ at low temperatures and $M_r = 5 \cdot 10^{-5}\,\mathrm{A\,m^2/g}$ and $B_c = 10\,\mathrm{mT}$ at room temperature. In our system the magnetization of nanocarbon is probably not caused by impurities but by non-compensated spins of π-electrons. Similar results have been reported for proton- and iron-implanted graphite [1].

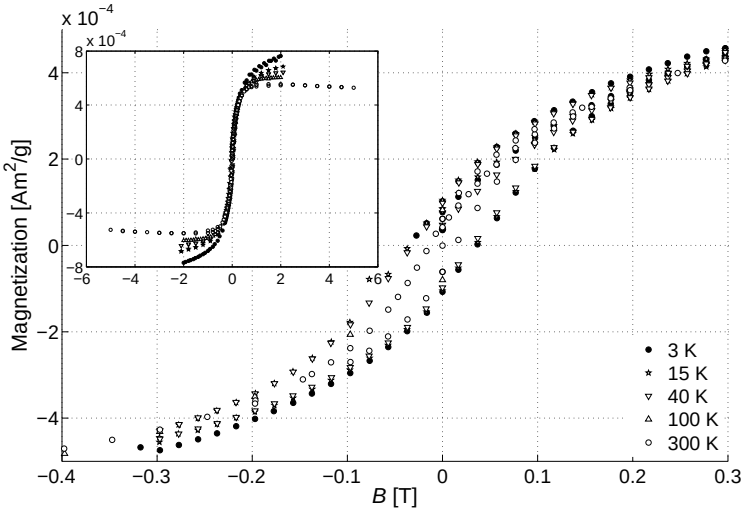

Figure 1: Magnetization measurement of pure carbon nanopowder.

[1] J. Barzola-Quiquia, R. Höhne, M. Rothermel, A. Setzer, P. Esquinazi and V. Heera, 2008, *Eur. Phys. J. B*, **61**, 127-130.

DIFFUSION BETWEEN EVOLVING INTERFACES

Janne Juntunen and Juha Merikoski

Department of Physics, P.O.B. 35 (YFL), FI-40014 University of Jyväskylä, Finland
janne.k.juntunen@jyu.fi

Diffusion phenomena are ubiquitous in nature. Familiar examples are heat transfer by conduction in a metals and osmosis. Often diffusion occurs in a random environment as it does, for example, in heat transfer in the presence of mobile or immobile lattice imperfections. Due to the complexity of real-world environments, transport has been considered within different theoretical frameworks, often utilizing the random-walk picture to describe some assumed underlying microscopy. The study of random walks in a random environment (RWRE) has a long history [1, 2] (rewiev [3]). In general, theoretical studies have been limited to models, where the environment is stationary.

We consider continuos-time random lattice walks in a spatially evolving restricting environment produced by the dynamics of BCSOS2-model introduced in [4]. Thus due to the interface dynamics, the actual transition rates of diffusing particles become dependent on time and position when diffusive jumps are possible only inside the "bubbles" between the interfaces. To be more specific, we consider the symmetric case where both intefaces are driven with equal force towards each other. In [4] we observed that there is a dip in the rouhgness of the interfaces as a function of this drive parameter which we denoted by f. However, this dip does not affect the dynamics of diffusive particles. In fact the particles experience the strucure of the interfaces at a somewhat bigger value of drive parameter, actually close the point $f = f_k$ where the kink-density reach its minimum. In addition to continuos-time Monte Carlo simulations, we develop an adiabatic theory for the diffusion coefficient for $f > f_k$.

[1] F. Solomon, Ann. Prob. 3 (1975)
[2] H. Kesten, M. V. Kozlov and F. Spitzer, Comp. Math. 33 (1975)
[3] Ofer Zeitouni, J. Phys. A: Math. Gen. 39 (2006) R433
[4] J. Juntunen, O. Pulkkinen and J. Merikoski, Phys. Rev. E. 76 (2007) 041607

CHARACTERISATION OF BIOLOGICAL STRUCTURES BY X-RAY ABSORPTION MICROTOMOGRAPHY

A. Kallonen[1], J.-P. Suuronen[1], M. Peura[1], E. Harjunmaa[2], I. Corfe[2], O. Manninen[4], J. Jernvall[2], K. Fagerstedt[3], P. Saranpää[5], A.-E. Lehesjoki[4], R. Serimaa[1] and K. Hämäläinen[1]

[1]Department of Physics, P.O.B. 64, FI-00014 University of Helsinki, Finland [2]Institute of Biotechnology, [3]Department of Biological and Environmental Sciences (U. Helsinki); [4]Folkhälsan Institute of Genetics; [5]Finnish Forest Research Institute
e-mail: aki.kallonen@helsinki.fi, jussi-petteri.suuronen@helsinki.fi

Obtaining structural information in the micrometer scale and below on biological materials is of key interest in understanding their behaviour and growth processes. Time-dependent processes demand non-destructive probing, and many biological materials are also fragile, making traditional physical sectioning methods unsuitable. X-ray absorption microtomography is a non-destructive method whose use in the biological and life sciences is a rapidly developing avenue of scientific study.

On-going research at the University of Helsinki microtomography laboratory includes the characterisation of dental development, wood anatomy and physiology, fossils, and indicators of congenital disease. The open construction of the measurement system enables imaging of biological samples ranging from whole organisms to individual organs. Equipment development is aimed at improving control of the absorbed dose, and combining other x-ray methods with microtomography *in situ*.

Wood research focuses on monitoring variations in the water status of tree saplings. Using microtomography, this information can be obtained together with cellular level images of the xylem structure. Dental structures provide information in developmental and evolutionary biology. X-ray microtomography has been applied for non-destructive study of both organ growth and fossilised remains. Skeletal changes in mice (*Mus musculus*), indicating a congenital disease, have also been quantified using our device.

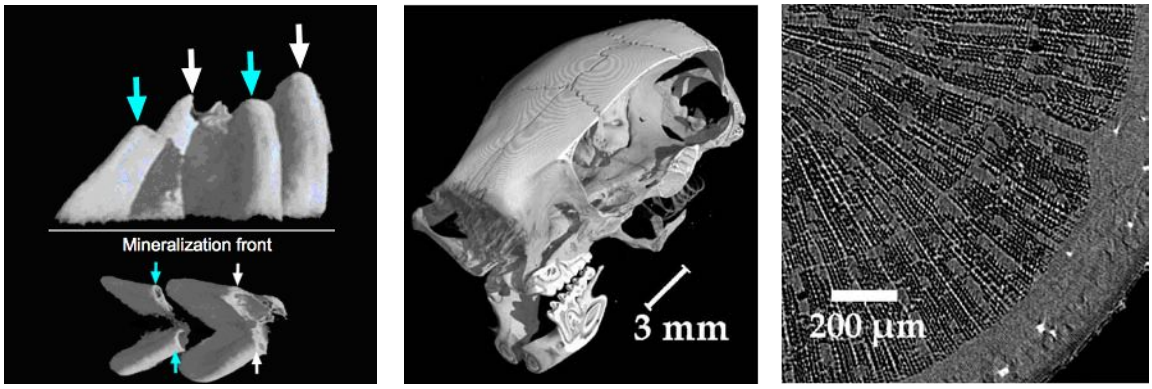

Left: 3D-renderings of a 2-day old mouse molar (length 1 mm) **Middle:** 3D-rendering of a mouse skull **Right:** Axial slice through a birch (*Betula Pendula*) sapling

CHEMICAL AND STRUCTURAL CHARACTERIZATION OF TRIMESIC ACID ON CU(100) AND O/CU(100) STUDIED BY XPS AND STM

L. Kanninen[1], K. Lahtonen[1], N. Jokinen[1], P. Jussila[1], O. Tarvainen[1], M. Kuzmin[2], M. Hirsimäki[1], and M. Valden[1]

[1]Surface Science Laboratory, Department of Physics, Tampere University of Technology, P.O.B 692, FIN-33101 Tampere, Finland, www.tut.fi/surfsci
[2]A.F. Ioffe Physico-Technical Institute, Russian Academy of Sciences, St. Petersburg, Russian Federation
email: leena.kanninen@tut.fi

The self-organization of organic molecules into metallosupramolecular structures on nanostructured metal substrates is an interesting bottom-up method of fabricating functional nanostructures for biomedical applications e.g. biosensors and implants. Biofunctionality of a surface is mainly controlled by the spatial distribution and orientation of the biomolecules on the surface as well as passivation of unspecific adsorption to the surface. Metallosupramolecular surface structures provide a potential template for spatially controlled adsorption of molecules that act as a linker between the substrate surface and biomolecules.

In this study, the chemical and structural properties of trimesic acid (1,3,5-benzenetricarboxylic acid, $C_6H_3(COOH)_3$, TMA) at coverages ranging from low submonolayer to multilayer on Cu(100) and oxygen adsorption induced uniformly reconstructed (Cu(100)-(2√2×√2)*R*45°-O) surfaces [1,2] were examined. The samples were prepared and examined *in situ* in ultrahigh vacuum conditions. The chemical analysis was performed by X-ray photoelectron spectroscopy (XPS) and surface nanostructure was investigated with constant current scanning tunneling microscopy (STM).

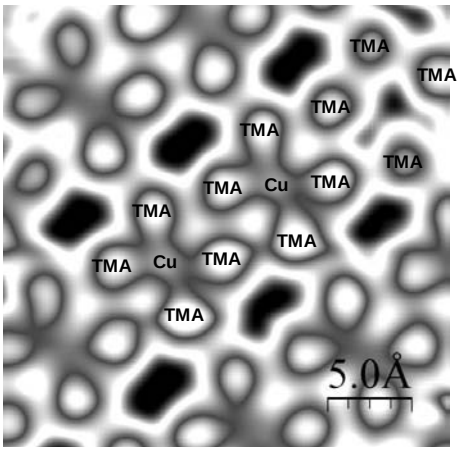

The TMA molecules bond with the surface Cu atoms as one to three of the TMA carboxyl groups deprotonate upon adsorption. The degree of deprotonation depends on the TMA coverage and substrate properties. The presence of oxygen enhances the deprotonation at all TMA coverages. STM images reveal different ordered TMA structures on Cu(100) depending on the TMA coverage. At submonolayer TMA coverage, Cu adatoms act as coordination centers for TMA molecules (right). On O/Cu(100) such ordering is not observed.

[1] K. Lahtonen, M. Lampimäki, M. Hirsimäki, and M. Valden, Journal of Chemical Physics 129 (2008) 124703.
[2] M. Lampimäki, K. Lahtonen, M. Hirsimäki, and M. Valden, Journal of Chemical Physics 126 (2007) 034703.

Ratchet effect for polymers

J. Kauttonen and J. Merikoski

Department of Physics, University of Jyväskylä,
P.O. Box 35, FI–40014 Jyväskylä, Finland
email: janne.kauttonen@jyu.fi

Polymer motion in time-dependent ratchet potentials is considered. We use the discrete space Rubinstein-Duke (RD) model [1] which is a "toy-model" for linear polymers in a restrictive medium and a good prototype model for studying complex molecules in the ratchet. We concentrate on the so called *ratchet effect* that means transport of particles/molecules without biased forces (e.g. electric field) with interplay between non-symmetric potential and random, usually thermal, motion. Such motion is non-trivial and even the direction of the motion is sometimes unexpected (possible current inversions) (e.g. [2]). There has been lots of studies of the ratchet effect with pointlike and other simple objects, but a limited number of studies with complex systems. We use a numerically exact master equation approach [3] to compute several properties of polymers in varying potentials, including long-time drift velocity, diffusion coefficient and efficiency. By varying the model parameters we notice drastic differences in drift direction and magnitude. In some situations long polymers are faster than shorter ones or even single particles. To reveal the leading mechanism responsible for the transport process, we propose a simple graph analysis method to find most probable trajectories of the molecule. We apply this method to the RD model and find it to be very useful when analyzing transport by the ratchet effect.

[1] M. Rubinstein, Phys. Rev. Lett. **59**, 1946 (1987);
T.A.J. Duke, Phys. Rev. Lett. **62**, 2877 (1989)
[2] P. Reimann, Phys. Rep. **57**, 361 (2002)
[3] J. Kauttonen, J. Merikoski, O. Pulkkinen, Phys. Rev. E **77**, 061131 (2008).

THERMAL EVOLUTION OF VACANCY COMPLEXES IN n-TYPE $Si_{1-x}Ge_x$:P

S.Kilpeläinen, K. Kuitunen, F. Tuomisto and J. Slotte

Department of Applied Physics, Aalto University, P.O.Box 11100, FIN-00076 Aalto, Finland
email: simo.kilpelainen@tkk.fi

Silicon germanium ($Si_{1-x}Ge_x$) has attracted major research interest recently due to its promising properties in semiconductor technology. The complete solubility of silicon and germanium makes band gap engineering between pure Si and pure Ge values possible. Additionally, carrier mobilities in Ge are higher than in Si which encourages the use of SiGe-based devices in high frequency applications. Since Si and Ge have similar lattice constants, compatibility with existing Si-based technology is also good.

Positron annihilation spectroscopy is a nondestructive tool for studying neutral and negative vacancy-type defects in semiconductors. Positrons can get trapped in these vacancies, resulting in observable changes in both positron lifetime and the momentum distribution of the annihilating positron-electron pair. In this work we have focused on the latter and used positron Doppler broadening spectroscopy to study defects in $Si_{1-x}Ge_x$.

The defect we have been interested in is the vacancy-group V donor -complex, which is often referred to as the E-center in elemental semiconductors. It is probably the most studied point defect in semiconductors. The E-center in phosphorus-doped $Si_{1-x}Ge_x$ has been studied extensively by positron annihilation spectroscopy (PAS) at TKK [1, 2, 3]. It has been shown that the E-center in P-doped $Si_{1-x}Ge_x$ becomes mobile at 150°C but a new defect type consisting of a vacancy, a phosphorus dopant and a germanium atom is formed after annealing at 150-175°C [1].

In this work, P-doped $Si_{1-x}Ge_x$ was isochronally annealed at temperatures ranging from 250 to 350°C. The obtained results show that the samples recover during the annealing but the state reached after annealing differs from the as-grown one. Theory of annealing kinetics was applied in order to find out the activation energy related to the recovery process. Based on the obtained value of $\sim$1.4 eV we attribute the activation energy to diffusion of the defects via the ring migration mechanism.

[1] S.-L. Sihto, J. Slotte, J. Lento, K. Saarinen, E. V. Monakhov, A. Yu. Kuznetsov, and B. G. Svensson, Phys. Rev. B 68, 115307 (2003).
[2] M. Rummukainen, J. Slotte, K. Saarinen, H. H. Radamson, J. Hallstedt, and A. Yu. Kuznetsov, Phys. Rev. B 73, 165209 (2006)
[3] K. Kuitunen, F. Tuomisto and J. Slotte, Phys. Rev. B 76, 233202 (2007)

DENSITY RESPONSE OF A STRONGLY INTERACTING TRAPPED FERMI GAS

Anna Korolyuk, Jami Kinnunen, and Päivi Törmä

Aalto University, Department of Applied Physics, P.O.Box 15100, FI-00076 AALTO,Finland
email: ankorol@cc.hut.fi

We study collective excitations of a 3D trapped superfluid Fermi gas by using self-consistent Kadanoff-Baym theory in the Bogoliubov-deGennes formulation. We hope to see collective phonon-like modes and study the interplay with the gapped single-particle branch. Furthermore, our approach is applicable also to spin-imbalanced gases opening an interesting possibility of studying the density response of an Fulde-Ferrel-Larkin-Ovchinnikov-type superfluid.

DFT and LEED study of Sn/Cu(100) p(2×6) structures.

M.Lahti, K. Pussi and M. Alatalo

Department of Mathematics and Physics, Lappeenranta University of Technology, PO Box 20, FIN-53581 Lappeenranta, Finland
email: lahti@lut.fi

Cu-based surfaces are very interesting and well studied, because they show very useful properties in particular in catalytical activity. The Cu/Sn system is an excellent example of complex bimetallic surface. With different coverages, Sn adopts a different structures, and with these structures a lot of intresting phenomena occur. The alloy of Cu and Sn is also the base of bronze.

We have studied several possible Sn p(2×6) surface structures with symmetry p2mg on coverage 0.33 monolayer on Cu(100) surface[1][2], and discovered that the structure from [2] is the energetically most favourable, see Fig. [1]. With different coverages Sn adapts different phases. For this study we have used density functional theory (DFT) calculations as implemented in Vienna $ab\ initio$ simulation package (VASP) and the projector augmented wave (PAW) method. We have also used the dynamical low energy electron diffraction (LEED) calculations to interpret the experimetal data. The calculations with both methods support each other.

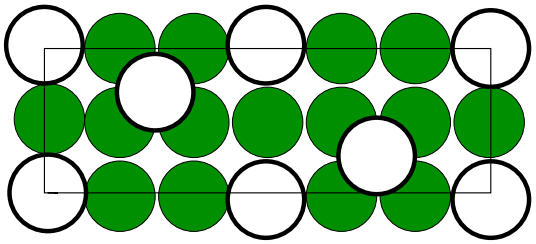

Figure 1: Shcematic figure of the energetically most favourable Sn p(2×6)surface structure with symmetry p2mg on Cu(100) surface.

[1] J. Lallo $et\ al.$, Surface Science 602(2008)2348-2357.
[2] A.A. Cafolla, private communication

X-RAY STUDY ON THE CELL WALL STRUCTURE OF MOSO BAMBOO

K. Leppänen, Y. Wang[1], S. Andersson, R. Serimaa, H. Ren[1] and B.H. Fei[2]

Department of Physics, P.O.B. 64, FIN-00014 University of Helsinki, Finland
[1] Institute of Wood Industry, Chinese Academy of Forestry, Beijing 100091, China
[2] International Centre for Bamboo and Rattan, Beijing 100102, China
email: kirsi.leppanen@helsinki.fi

The application areas of bamboo are versatile: bamboo is used as light but strong constructive material, in paper, textile, cosmetic and medicine industry, and in many leisure and household items. Bamboo is considered as functionally graded material i.e. it has radially varying microstructure due to the non-even fiber distribution [1]. In this study the nanostructure of the cell wall of Moso bamboo ($Phyllostachys\ edulis$) was studied using wide-angle x-ray scattering (WAXS). The aim was to find out the possible dependencies of the structure on the age and on the radial position in the culm by determining the crystallinity, the size of cellulose crystallites and the microfibril angle (MFA) distribution of the selected samples. Bamboo is considered as mature for industrial use at the age of 4-6 years. The focus of this study was on the samples at the age of 0.5 year, 4.5 and 10.5 years.

The WAXS results indicated that the nanostructure of the bamboo cell wall was dependent on the radial position in the culm: the crystallinity and the width and length of cellulose crystallites increased from the inner to outer part of the culm, and the mean MFA decreased [2]. The widths and lengths of the crystallites of 4.5-year-old bamboo were from 2.96 nm (inner) to 3.16 nm (outer) and from 24.7 nm (inner) to 32.8 nm (outer), respectively. The age had effect neither on the width of crystallites nor crystallinity. The only difference at various ages was detected between the lengths of crystallites: the crystallites were 3-4 nm shorter in the outer part of 10.5-year-old sample and in the inner part of the 0.5-year-old sample than in the corresponding parts of the 4.5-year-old sample. It has been known that the mechanical properties of bamboo depend on the radial position [3] and according to our results, the mechanical properties of bamboo may be related to the nanostructure of the cell wall in the same way as those of wood.

[1] A.K. Ray, S.K. Das and S. Mondal, J Mater Sci 39 (2004) 1055-1060.
[2] Y. Wang, K. Leppänen, S. Andersson, R. Serimaa, H. Ren and B.H. Fei, submitted to Wood Sci Technol (2010).
[3] H.Q. Yu, Z.H. Jiang, C.Y. Hse and T.F. Shupe, J Trop For Sci 20 (2008) 258-263.

STUDY OF WILD *POPULUS TREMULA* L. X *TREMULOIDES* MICHX. SEEDLINGS USING WAXS AND X-RAY MICROTOMOGRAPHY

J. Lucenius[1], K. Leppänen[1], P. Penttilä[1], R. Serimaa[1], M. Peura[1]
P. Immerzeel[2], E. Mellerowicz[2]

[1]Department of Physics, POB 64, 00014 University of Helsinki, Finland
[2]Department of Forest Genetics and Plant Physiology, Swedish University of Agricultural Sciences SE, S901-83 Umeå, Sweden
email: jessica.lucenius@helsinki.fi

The cell wall structure of wood fibers in aspen (*Populus tremula* L. X *tremuloides* Michx.) seedlings was studied using wide angle x-ray scattering. In wood cell wall, partially crystalline cellulose microfibrils and their aggregates (macrofibrils) are wound helically around the cell axis. From the diffraction patterns the size of cellulose crystallites, the microfibril angle (MFA) and the crystallinity i.e. the volume fraction of crystalline cellulose in the sample, were determined.

The seedlings were grown in the greenhouse to a height of approximately 1.5 and 2 m in two separate experiments. The younger trees were 73 and older trees 100 days old. The stems segments of internodes 30-31 and 48-49, respectively, had been frozen in liquid N_2 immediately after the seedlings were cut. For a few samples, changes in the crystallite structures were followed during drying. The rest of the samples were measured only in the dry state.

Relative crystallinity, crystal width and MFA were determined using perpendicular transmission geometry and area detector. The length of the crystallites was determined using symmetrical transmission geometry and 4-circle goniometer and scintillation counter as detector. The MFA values were small in all aspen samples, between 2° and 7°. No change in the mean MFA or the width of the crystallites was observed due to drying. The crystallinity of wood in the dry samples varied between 25 and 35 %. The width of the crystallites was 30Å (±1Å) for all samples. The length of the crystallites varied between 260 and 400Å (±20Å) in the dry samples, the average and the standard deviation were 360Å and 52Å for the first series and 310Å and 68Å for the second series, respectively. The results of drying experiments showed that the full width at half maximum (FWHM) of 004 reflection increased 10-20% which indicated increase of strain and disorder of crystallites during drying.

Previous work has shown that the crystallinity and the width of the crystallites varied more strongly in juvenile than in mature wood among trees [1]. We are aiming to compare seedlings to more mature trees grown in forest and to visualize size of cell lumens with x-ray microtomography.

[1] S. Andersson, R. Serimaa, T. Paakkari, P. Saranpää and E. Pesonen. Crystallinity of wood and the size of cellulose crystallites in Norway spruce (Picea Abis,) J Wood Sci (2003) 49:531-537

Vacancy defects in a- and c-plane AlN thin film layers

J.-M. Mäki[1], F. Tuomisto[1], M. von Kurnatowski[2], B. Bastek[2], M. Wieneke[2], T. Hempel[2], F. Bertram[2], A. Dadgar[2], J. Christen[2], A. Krost[2]

[1]Department of Applied Physics, Aalto University, P.O. Box 11100, FI-00076 Aalto
[2]Institute of Experimental Physics, Otto-von-Guericke-University Magdeburg, Germany
email: jmmaki@cc.hut.fi

Aluminium nitride (AlN) is a promising extremely wide bandgap semiconductor material (E_g=6.2 eV), for applications in deep ultraviolet optoelectronics in combination with other nitride semiconductors. AlN has already been applied successfully in AlN/AlGaN heterostructures, but the ability to fully control the purity, structural quality, and luminescent properties of the material is still being developed. The identities and concentrations of native point defects are often related to all of the three above-mentioned material quality issues. Preliminary results on the identification of Al vacancies in AlN already exist [1, 2]. Furthermore, the aim of reducing the internal electric fields in the III-nitride layers has resulted in interest in growing non-polar a-plane AlN in addition to the polar c-plane material.

In this work we study in-grown vacancy-type defects in thin film AlN layers grown by metal-organic vapour phase epitaxy (MOVPE) using positron annihilation spectroscopy, catholuminesence (CL) and scanning electron microscopy (SEM). The samples are grown in a- and c-planes in different conditions in order to find out how the growth temperature and V/III ratio affect the vacancy concentration. Positron Doppler broadening and CL measurements show that vacancy formation is more dependent on the growth temperature and the V/III ratio rather than the crystal orientation of the growth. Increasing the growth temperature generally improves the material quality as shown by the positron measurements and SEM while increasing the V/III ratio has a smaller influence. CL measurements suggest that c-plane growth generally results in slightly better crystal quality.

[1] F. Tuomisto, J.-M. Mäki, T. Yu. Chemekova, Yu. N. Makarov, O. V. Avdeev, E. N. Mokhov, A.S. Segal, M. G. Ramm, S. Davis, G. Huminic, H. Helava, M. Bickermann, and B. M. Epelbaum, J. Crystal Growth 310, 3998 (2008).
[2] J.-M. Mäki, F.Tuomisto, B. Bastek, F. Bertram, J. Christen, A. Dadgar, A. Krost, physica status solidi (c) 6, 2575 (2009).

MODELING CHARGE-IMBALANCED $NaNbO_3/SrTiO_3$ SUPERLATTICES

R. Oja and R. M. Nieminen

COMP/Department of Applied Physics, Aalto University School of Science and Technology, P.O.B. 11100, FI-00076 Aalto, Finland
email: riku.oja@tkk.fi

Structurally simple perovskites exhibit many interesting phenomena, e.g. polarization and dielectric and electromechanic properties very sensitive to small deformations. Perovskite superlattices, stacked epitaxial layers of different perovskites, are used to obtain properties that cannot be achieved in bulk perovskites, e.g. increased polarization and permittivity.

$NaNbO_3$ and $SrTiO_3$ are perovskites with nearly equal lattice parameters. Therefore, in $NaNbO_3/SrTiO_3$ superlattices there is no misfit strain to dominate the structure, and its behavior is determined solely by subtler interface effects. Also, the $NaNbO_3/SrTiO_3$ superlattice is *charge-imbalanced*, i.e. SrO and TiO_2 layers are charge neutral, while $(NaO)^-$ and $(NbO_2)^+$ layers are charged if we considered their preferred ionic charges. Charge-imbalanced interfaces are known to have rich behavior: a high-mobility electron gas has been observed in the $LaAlO_3/SrTiO_3$ interface [1], leading to 2D metallicity. Lattice relaxation from the ideal perovskite positions has been calculated to be considerable in such interfaces (e.g. [2]). $NaNbO_3/SrTiO_3$ superlattices are reported to have anomalous properties such as expansion of volume and decrease of permittivity [3].

Due to charge imbalance, the SrO-NbO_2 interface has one extra electron, while NaO-TiO_2 interface has one extra hole when compared to nominal ionic charges. By simple band theory, extra electrons or holes will result in metallicity. Here, different $NaNbO_3/SrTiO_3$ superlattices are modelled with standard DFT methods: LDA and LSDA+U.

It is found [4] that an ideal superlattice will be either semiconducting or metallic, depending on the types of interfaces present. Relaxation of ionic positions is considerable and has to be taken into account to obtain correct structural and electronic properties. These ferroelectric-like displacements could be the cause of decreased permittivity at the interface [5]. Also, depending on the types of interfaces, a superlattice may have volume larger or smaller than bulk; this is because superlattices with two similar interfaces are nonstoichiometric. The extent of the conducting state and 2D/3D metallicity depends on interface type as well as layer thicknesses, as conduction holes are more localized than conduction electrons. Within LSDA+U, we obtain half-metallicity and ferromagnetic alignment of holes, but not electrons.

[1] A. Ohtomo, D. A. Muller, J. L. Grazul, and H. Y. Hwang, Nature 419 (2002) 378.
[2] S. Okamoto, A. J. Millis, and N. A. Spaldin, Phys. Rev. Lett. 97 (2006) 056802.
[3] J. Narkilahti, M. Plekh, J. Levoska, and M. Tyunina, Phys. Rev. B 79 (2009) 014106.
[4] R. Oja and R. M. Nieminen, Phys. Rev. B 80 (2009) 205420.
[5] M. Tyunina, M. Plekh, R. Oja, and R. M. Nieminen, submitted to Appl. Phys. Lett..

MICROANALYSIS ON TRACHEIDS AND RAY PARENCHYMA CELLS OF FERTILISED NORWAY SPRUCE WOOD

K. Pirkkalainen, J. Lucenius, A. Meriläinen, A. Salmi, A. Kallonen, M. Peura and R. Serimaa

Department of Physics, P.O.B. 64, FIN-00014 University of Helsinki, Finland
email: kari.pirkkalainen@helsinki.fi

In the structure of Norway spruce (*Picea abies* [L.] Karst.) wood, about 90 - 95 % of cells are tracheids. Tracheids support the structure of the tree stem and provide means of transportation of water and nutrients up the tree stem. On the other hand, the nutrients are stored mainly in parenchyma cells, which are mostly found in rays that extend in the radial direction from the pith to the bark. [1]

We have studied samples of fertilised and untreated Norway spruce with x-ray fluorescence spectroscopy (XRF) and x-ray diffraction (XRD). The sample material was obtained from a nutrient optimisation field trial at Asa, situated in southern Sweden. The measurements were made at the microanalysis beamline ID18F of the European Synchrotron Radiation Facility (ESRF). The beamline provides for an x-ray beam small enough to probe the different cell types separately. The purpose of the experiment was to determine the effect of fertilisation on the nutrient element content of ray parenchyma cells and tracheids around these cells as a function of the annual ring from pith, combined to the cellulose microfibril angle (MFA) distribution and the crystallite dimensions in the same cells. In addition, the microstructure of the cells was imaged using several complementary microscopic techniques, including optical microscopy (OM), scanning electron microscopy (SEM) and x-ray microtomography (μCT).

[1] M. Peura *et al.*, Trees - Structure and Function 22 (2008) 499.

AB-INITIO STUDY OF MECHANICAL PROPERTIES OF AUSTENITIC STAINLESS STEEL ALLOYS

H. Pitkänen[1], M. Alatalo[1], A. Puisto[2], M. Ropo[3,4,5], K. Kokko[3] and L. Vitos[5,6,7]

[1]Department of Mathematics and Physics, Lappeenranta University of Technology, P.O.Box 20, FIN-53851 Lappeenranta, Finland, [2]Helsinki University of Technology, Department of Applied Physics, P.O. Box 1100, FI-02015 HUT, Espoo, Finland, [3]Department of Physics and Astronomy, University of Turku, FIN-20014, Turku, Finland, [4]Department of Information Technology, Åbo Akademi, Fin-20500 Turku, Finland, [5]Applied Materials Physics, Department of Materials Science and Engineering, Royal Institute of Technology, Stockholm SE-100 44, Sweden, [6]Division for Materials Theory, Department of Physics and Materials Science, Uppsala University, SE-75121 Uppsala, Sweden, [7]Research Institute for Solid State Physics and Optics, Budapest H-1525, P.O. Box 49, Hungary

email : htpitkan@lut.fi

Stainless steels are the most widely used maintenance free and safe engineering materials. In this work, the ideal cleavage energies of austenitic Fe-Cr-Ni alloys were calculated in order to deduce their mechanical strength. The three low index surfaces, (100), (111) and (110) were studied, because it can be assumed that the material is more easily cleaved in those directions than high index directions.

Cr was chosen as the other admetal, because alloying Fe with Cr makes it stainless. Cr also represents many other admetals (Mo, Si, Nb, V, Al). To be able to address the problem with the chosen method, we consider a homogenous Fe-Cr-Ni alloy, without interstitials and precipitates. Also the effects of short range order and relaxation effects are omitted. It is well known that insterstitial C and N have a strong effect on stabilising the austenitic phase. However, modeling the effect of interstitials from the first principles theory is very cumbersome especially in the chemically and magnetically disordered matrix. Since Ni also has a stabilising effect on the austenitic phase, we can represent the interstitials, as well as other austenite stabilisers, with Ni.

For this problem the exact muffin-tin orbital (EMTO) method was applied with coherent potential approximation (CPA) which enables one to study random alloys from first principles. The EMTO method provides very accurate total energies and the CPA enables one to study the whole concentration range of alloys consistently using a minimal size unit cell.

A DATA BANK APPROACH TO MULTISCALE MODELLING OF MICROSTRUCTURE FORMATION IN POLYMER CASTING

T. Pitkänen, S. Majaniemi and T. Ala-Nissila

Department of Applied Physics, COMP center of excellence, Aalto University School of Science and Technology, P.O. Box 11000, FI-00076 Aalto, Espoo, Finland
email: timo.pitkanen@tkk.fi

A data bank approach to multi-scale modelling of polymer solidification under flow and holding conditions is presented with applications to injection molding. The solidification of supersaturated polymer melt can be described via the time-dependent Ginzburg-Landau formalism. A phase field model called Model C under the classification of Hohenberg and Halperin [1] is applied in the present work.

The latent heat of solidification, which acts as an input parameter for large scale simulations, is determined as a function of different process dependent parameters such as the flow speed, supersaturation and geometric properties including the seed density of emerging spherulitic microstructures. Supersaturation and flow velocities are obtained from the larger scale simulation code as input values. The released latent heat can be obtained from the pre-computed data bank as function of the supersaturation and flow velocity thereby offering a possibility to circumvent the spatial and temporal coarse-graining problem associated with large scale simulations.

The results [2] demonstrate the plausibility of the data bank approach to multi-scale modelling of polymer solidification using 2D phase field simulations. It is noted that increasing seed density at constant supersaturation causes a collapse of the time dependent latent heat production onto a single master curve thereby making the velocity a redundant parameter at high enough densities where sufficient self-averaging takes place. These types of observations can be used to simplify the parametrisation of the data bank.

[1] Theory of dynamic critical phenomena, Hohenberg, P. C. and Halperin, B. I., Reviews of Modern Physics, 49 No. 3, 1977
[2] Multiscale Modelling of Microstructure Formation in Polymer Casting, T. Pitkänen, S. Majaniemi and T. Ala-Nissilä, accepted to be publsihed in Technische Mechanik

DISLOCATIONS EMITTED FROM VOID UNDER STRESS - GROWTH ON SURFACE

A.Pohjonen, S. Fitzgerald, F. Djurabekova, K. Nordlund

Helsingin Yliopisto, P.O.B. 43, FIN-00014 University of Helsinki, Finland
Culham Centre for Fusion Energy, Abingdon OX14 3DB, Great Britain
email: aarne.pohjonen@iki.fi

The development of future linear colliders requires the use of high electric field. The testing of prototypes has shown that a severe limitation to the operation of the collider is vacuum sparks occuring in the accelerating structures. The first step to increase the efficiency of the accelerating structures is therefore to understand the initiation of the spark. Experiments have shown that the electric field applied to metal surface is enhanced locally at random spots. This field enhancement can only be explained by the formation of sharp features on the surface. Currently these sharp features and the mechanism which leads to their formation remains a scientific mystery. A possible way of tip formation under stress is proposed.

It has been earlier experimentally observed that a void inside aluminum grows under shock loading. MD simulations have previously shown that the mechanism for void growth in bulk is dislocation emission from the void.[1] If a void is located near surface, the dislocation emission may lead to mass transport resulting in grow to the surface. On the other hand surface nanoscale objects tend to flatten to a one monolayer above room temperature. Given the number of phenomenona involved, it is clear that research is needed to describe the possibility of this feature growth mechanism.

Our MD simulations show that such growth on surface can indeed happen. A void is placed inside copper below the surface at 600 K temperature and a pulling force is exerted on surface atoms. Dislocations are emitted from the void and glide to the surface, causing a protrusion to form. Simulations are carried out to give an estimate of the dependence of growth time on the applied force, void size, void depth and surface orientation.

[1] D. C. Ahn, P. Sofronis, Journal of Applied Physics, 101, 063514 2007: *Void growth by dislocation-loop emission*.

MULTISCALE SIMULATION FOR LIQUID POLYMER USING MD/CONTINUUM HYBRID METHOD

Y. Senda[1], J. Blomqvist[2] and R. M Nieminen[2]

[1] Department of Applied Science, Yamaguchi University, Yamaguchi-Ube, 755-8611, Japan, email: senda@yamaguchi-u.ac.jp
[2] COMP/Department of Applied Physics, Aalto University School of Science and Technology FIN-00076 AALTO, Finland

Polymeric material has been interested as a promising material due to its valuable properties. To understand mechanical and thermodynamics properties of the materials it would be highly desirable to use a multiscale approach covering atomistic and macroscopic behavior. We have developed computational method coupling atomic model and continuum model, which enables us to analyze properties of the polymer from wide rage of scales[1].
In this paper, we have applied our hybrid method to liquid polymer. The polymer molecule is coarse-grained into meso-scopic model, and its model is coupled with an elastic continuum model using our hybrid method (figure). Long-chain polymer consisted of 500 monomers is calculated as a test model, and the calculated mean square end-end distance shows fast convergence to the equilibrium. This result shows that our hybrid model can be useful in a large-scale system.

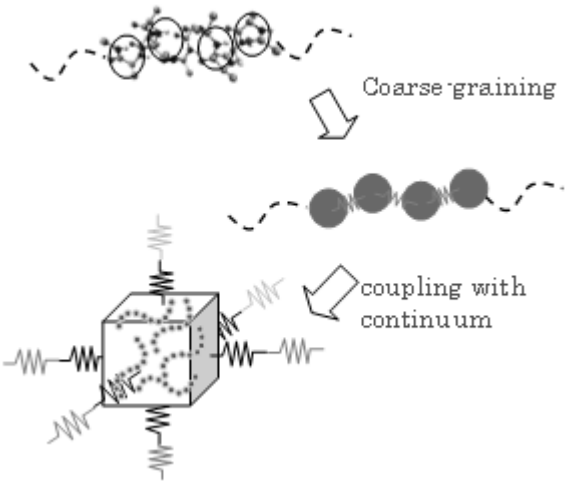

Polymer model using coarse-graining and MD/continuum hybrid method

[1] G. Kim and Y. Senda, *Journal of Physics: Condensed Matter* **19** 246203 (2007)

X-RAY STUDIES ON THE PORE STRUCTURE OF BARLEY EXTRUDATES

J.-P. Suuronen[1], P. Penttilä[1], S. Kirjoranta[2], M. Peura[1], K. Jouppila[2], M. Tenkanen[2], and R. Serimaa[1]

[1]Department of Physics, University of Helsinki, Finland
[2]Department of Food and Environmental Sciences, University of Helsinki, Finland
email: jussi-petteri.suuronen@helsinki.fi

Barley is the fourth most cultivated cereal crop worldwide (2008 statistics on quantity produced and area of cultivation) [1]. It is mainly used as animal feed and for malting purposes, but it also provides health benefits in food. Extrusion cooking is a technique for processing barley flour into edible snack products. It produces solid, foamy extrudates, whose nutritional value and structural properties can be tailored by additives, such as whey protein isolate (WPI) and polydextrose (PD). In this study, we have combined x-ray microtomography (μCT) with small- and wide-angle x-ray scattering (SAXS and WAXS) to quantify the micro- and nanostructural changes caused by these additives.

In the microtomography experiment, short pieces of the extrudates were scanned with a voxel size of 6.25 μm, and microscale porosities and wall thicknesses were calculated from the reconstructions using gray value thresholding and the Euclidean distance transform (figure). Additionally, smaller pieces from each sample were scanned with resolutions of 0.7–1 μm. The SAXS measurements were conducted in the 0.015–0.22 1/Å q range, and Porod's law was fitted to the data on angles corresponding to structures of approximately 3–5 nm. From the fitting parameters, the specific surface and the average chord length of each phase were calculated. In addition to Porod's law, other power laws were fitted to the data in order to analyze the possible fractal structure.

Structural changes caused by WPI and PD were observed with both methods. With μCT, WPI was found to increase sample porosity and reduce the mean thickness of walls between pores. In the SAXS results, the nanoscale specific surface increased and the average chord length of the solid phase decreased with the introduction of WPI. Compared to the sample with pure barley, an opposite effect was observed for PD with both methods. Since both porosity and crispness are desirable qualities in snack products, WPI is concluded to improve the structural quality of the final product.

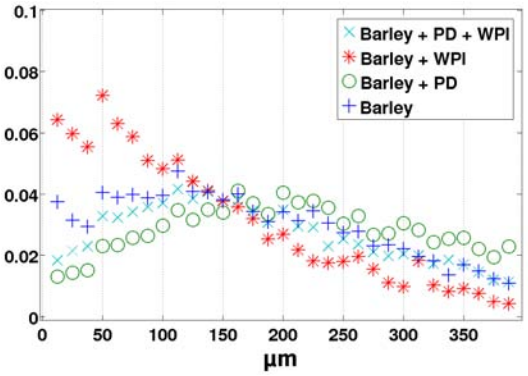

Figure: Normalized wall thickness distributions of the samples.

[1] FAOSTAT database, Food and Agriculture Organization of the United Nations, http://faostat.fao.org/site/567/default.aspx#ancor Retrieved 14.1.2010

PORE SPACE ANALYSIS OF HETEROGENEOUS POROUS MATERIALS USING X-RAY TOMOGRAPHY

Tuomas Turpeinen, Viivi Koivu, Markku Kataja and Jussi Timonen

Department of Physics, University of Jyväskylä, P.O. Box 35, FI-40014 Jyväskylä, Finland. Email: firstname.surname@phys.jyu.fi

The transport properties of heterogeneous porous materials are largely defined by their pore space. Traditionally the structural analysis of porous materials has been based on modeling the structure of such materials. Now that computed microtomography (µCT) has reached the resolution which makes characterization of many porous materials possible, µCT imaging can be used to evaluate also transport properties of these materials. To this end one needs however advanced image analysis tools.

µCT is an imaging method which provides a digitalized 3D representation of the sample such that each voxel represents the local density of the material (when absorption contrast is used). For structural analysis this 3D representation must be segmented into solid material and void. The void is the pore space which must further be segmented into individual pores separated by pore throats. This is a highly nontrivial task.

The resulting network of pores and pore throats allows determination of e.g. the volume, shape, orientation, surface area and coordination number of each individual pore and pore throat. It also allows analysis of the tortuosity and connectivity of the pore network, and it can be used to realistically simulate the intrusion of liquids or diffusion in that material.

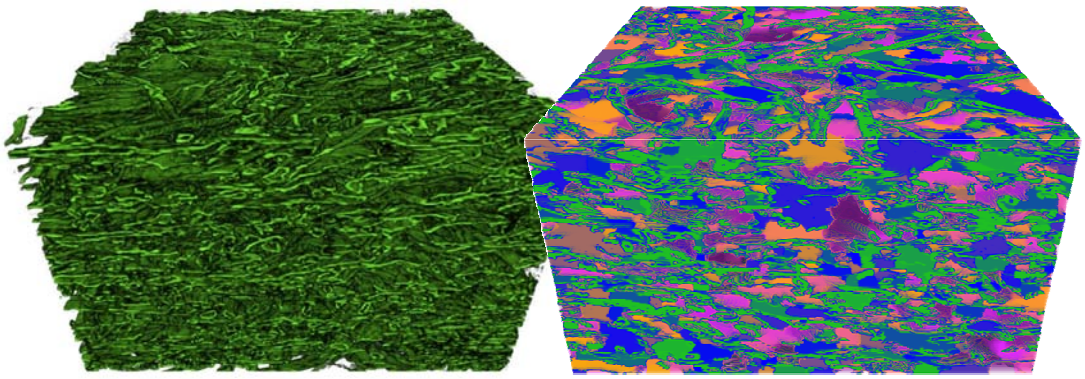

Figure 1: Visualization of a tomographic reconstruction of a cardboard sample (left), and the individual pores of that sample colour coded (right). The size of the sample is 700 x 700 x 520 µm3.

Results will be shown for a structural analysis and tortuosity of cardboard, and for intrusion of mercury in a granular packing of calcium carbonate pigments.

UNIVERSITY OF JYVÄSKYLÄ

FERMI LIQUID THEORY APPLIED TO VIBRATING WIRE IN ^{3}HE-^{4}HE MIXTURES

T. H. Virtanen and E. V. Thuneberg

Department of Physics, P.O.B. 3000, FIN-90014 University of Oulu, Finland
email: timo.virtanen@oulu.fi

We study vibrating wire resonators (VWR) in ^{3}He-^{4}He mixtures at such low temperatures, that all of ^{4}He is superfluid. The ^{3}He part can be treated as degenerate Fermi liquid, using Landau's Fermi liquid theory in the form suggested by Khalatnikov [1] for mixtures of ^{3}He in ^{4}He. We solve the linearized Landau-Boltzmann equation for quasiparticle distribution $\psi(\mathbf{r}, \hat{\mathbf{p}})$ numerically in a discrete grid near the wire. The mechanical properties of helium mixtures are largely determined by the quasiparticle mean free path ℓ, which behaves as $\ell \propto T^{-2}$. At $T > 10$ mK the fluid's motion can be described by hydrodynamic theory, but at lower temperatures a kinetic approach is required. In the ballistic limit of infinite mean free path simple kinetic arguments give dissipation of correct magnitude, but fail to explain the recently observed decrease in wire's inertia[2]. We present numerical results for full scale of the quasiparticle mean free path, ranging from the hydrodynamic region to the ballistic limit.

We can numerically reproduce the peculiar decrease of inertia in the ballistic limit, by taking into account that the ^{3}He quasiparticle energy depends on the superfluid ^{4}He motion and on the Fermi interactions through the Landau parameters F_l^s and the effective mass m^*. We show that in the ballistic limit, the beam of quasiparticles generated by the moving wire alters the quasiparticle distribution incoming on the wire. When a quasiparticle trajectory crosses the beam of quasiparticles, it experiences a potential change $\delta\epsilon$ caused by the beam. We show that this leads to a reduction of the inertia experienced by the wire. We also show that the presence of container walls near the wire further decreases the inertia in the ballistic limit, in comparison to its high-temperature value.

We plot the force on wire in terms of impedance $Z = Z' + iZ'' = -F/u$, where Z'' and Z' correspond to the inertia and dissipation of the wire, respectively. Here we show a fit to one of the experimental curves in ref. [2]. We have used $S = 0.8$ for the fraction of specular scattering from the wire, and an absorbing container of radius $b = 14a$, where a is the wire radius. For other data, we may need to consider asymmetry in experimental geometry, as well as second sound resonances.

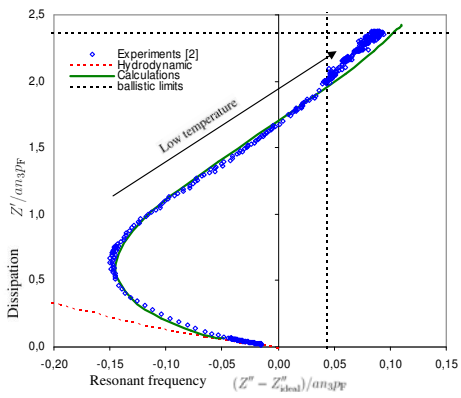

[1] I. M. Khalatnikov, Sov. Phys. JETP **28**, 1014 (1969).
[2] J. Martikainen, J. Tuoriniemi, T. Knuuttila, and G. Pickett, J. Low Temp. Phys. **126**, 139 (2002).

MOLECULAR DYNAMICS SIMULATIONS OF PRIMARY RADIATION DAMAGE IN Fe-Cr

K. Vörtler[a], C. Björkas[a], D. Terentyev[b], L. Malerba[b], and K. Nordlund[a]

[a] Association Euratom-TEKES, Department of Physics, P.O.B. 43, FIN-00014 University of Helsinki, Finland
[b] Structural Materials Group, Institute of Nuclear Materials Science, SCK·CEN, Boeretang 200, B-2400 Mol, Belgium

email: katharina.vortler@helsinki.fi

High-Cr ferritic/martensitic steels, typically with 5 to 15% chromium content, are of technological interest as nuclear reactor materials. They are applied in both future (advanced) fission and fusion reactors as structural materials. Therefore their irradiation properties need to be studied. The first step in doing so is to study the primary damage state produced by a displacement cascade. Computer simulations, mainly molecular dynamics (MD), are suitable to study cascades because of their length and time scales.

Displacement cascades were studied using MD in Fe-Cr alloys, which are the simplest model materials for steels. We studied random Fe-5Cr, Fe-10Cr, and Fe-15Cr alloys using two versions of a two-band embedded atomic model potential [1]. The defect production of single cascades and their clustered fraction was previously analyzed, comparing the results with pure Fe [2,3]. We now analyzed the size distribution of the clusters. Moreover, the effect of overlapping cascades on changes in the ordering of the alloys and the Frenkel pair production was studied.

[1] P. Olsson, J. Wallenius, C. Domain, K. Nordlund, and L. Malerba, Phys. Rev. B 72 (2005) 214119.
[2] C. Björkas, K. Nordlund, L. Malerba, D. Terentyev, and P. Olsson, J. Nucl. Mater. 372 (2008) 312.
[3] K. Vörtler, C. Björkas, D. Terentyev, L. Malerba, and K. Nordlund, J. Nucl. Mater. 382 (2008) 24.

FIRST PRINCIPLES STUDY OF DIFFUSION OF ATOMIC COPPER IN SILICON DIOXIDE

M. Zelený[1], J. Hegedus[1], A. Foster[2], and R. M. Nieminen[1]

[1]Department of Applied Physics, Aalto University, P.O. Box 11100, Fin-00076 Aalto
[2]Department of Physics, Tampere University of Technology, P.O. Box 692, Fin-33101 TUT Tampere
email: zeleny@cc.hut.fi

Non-volatile memory chips based on resistive switching have attracted much interest due to their high performance, low power consumption and high storage capacity. Their switching mechanism is based on electrochemical metallization occurring due to migration of Ag or Cu ions in oxide glasses as for example silicon dioxide. This process consists of two steps: 1) electro-chemical formation of a metallic filament ("SET" step) and 2) its electro-chemical dissolution ("RESET" step). One of the main problems in developing new non-volatile memory materials is the lack of microscopic understanding of these processes.

In order to clarify the mechanism underlying these processes, we have performed theoretical calculations of copper diffusion in SiO2. All calculations in our study are carried out based on first-principles density-functional theory (DFT) using planewave basis sets and the projector augmented-wave method as it is implemented in the Vienna Ab initio Simulation Package (VASP). For exchange-correlation energy we have used the Local Density Approximation (LDA). The minimum-energy path and the corresponding energy barriers are determined by the Nudged Elastic Band (NEB) method.

In this work, we present a total-energy calculation of the barrier along a diffusion path of copper between two equivalent interstitial positions in α-cristobalite. The α-cristobalite is a crystalline polymorph whose density is close to that of amorphous SiO2. The shape of the path strongly depends on charge of the system, but the height of the migration barrier stays between 0.15-0.2 eV.

5 Condensed matter: Electronic properties

5.1 Oral session I, Thursday 11 March 15:00-16:30
5.2 Oral session II, Saturday 13 March 9:00-10:30
5.3 Poster session I, Thursday 11 March 16:30-18:30
5.4 Poster session II, Friday 12 March 16:00-18:00

MULTISCALE MODELING OF TiO_2 NANOPARTICLES

S. Auvinen[1], M. Alatalo[1], H. Haario[1], J-P. Jalava[2], and R-J. Lamminäki[2]

[1]Lappeenranta University of Technology, P.O.B. 20, FIN-53851 Lappeenranta, Finland
[2]Sachtleben Pigments Oy, FIN-28840 Pori, Finland
email: sami.auvinen@lut.fi

Titanium dioxide is a wide band gap semiconductor which has a very high optical reflectivity at visible wavelengths, while being a strong absorber of ultraviolet radiation. It is also photoactive, and exhibits high surface reactivity with many chemical agents. Due to these properties titanium dioxide is used widely as a white pigment and opacifyer in paints, food dyes, medicines, ceramics and plastics. It also has promising applications for solar cells, batteries, UV protectors, and self-cleaning surface coatings.

The optical and electronic properties of titanium dioxide nanoparticles depend on the size and structure of the particles. Small clusters also exhibit quantum size effects, where particles experience an effective band gap widening. This can also have an effect on the properties of the ultra-fine particles. The main motivation of this study is to know how exactly these properties affect the photoabsorption of particles.

The structures and optical properties of model titanium dioxide nanoparticles are computationally modeled in this work by an *ab initio* DFT method GPAW [1] and a DFT based tight binding method HOTBIT [2]. Starting from the structure of TiO_2 molecule for the smallest particles, and truncated bulk anatase structure for larger particles, the structures for $(TiO_2)_n$ clusters, n={1,2,4,8,16,18,20,28,38}, have been modeled. We have used the time-propagation TDDFT approach, having a focus on the shape changes of the calculated spectra. The results show slight evidence of the quantum-size effect, and a change in the absorption peak position when particle size is changed.

[1] J. J. Mortensen *et al*, Physical Review B 71 (2005) 035109.
[2] P. Koskinen and V. Mäkinen, Computational Materials Science 47 (2009) 237.

TUNABLE MAGNETISM IN QUANTUM RINGS

Gustav Bårdsen, Eero Tölö, and A. Harju

Helsinki Institute of Physics and Department of Applied Physics,
Aalto University, P.O. Box 14100, FI-00076 Aalto, Finland
email: ari.harju@tkk.fi

During the last two decades, there has been an increasing scientific and technological interest in spin related phenomena and in possible application of these in future data processing, communication and storage. Quantum dots have been proposed as components in few-electron spintronics devices, such as spin filters or spin memories, and in spin-based quantum computation devices. In this work, we have numerically studied the spin properties of few-electron circular quantum dot structures that we can tune by an external potential to form quantum rings[1]. The calculations were done using the exact diagonalization method. Our results indicate that ringlike systems can have oscillatory flips between ferromagnetic and antiferromagnetic behaviour as a function of the magnetic field. Knowledge of the nontrivial magnetic phase structure could be very fruitful for the experiments, as this phenomenon opens the possibility for tunability of the magnetism by changing system parameters.

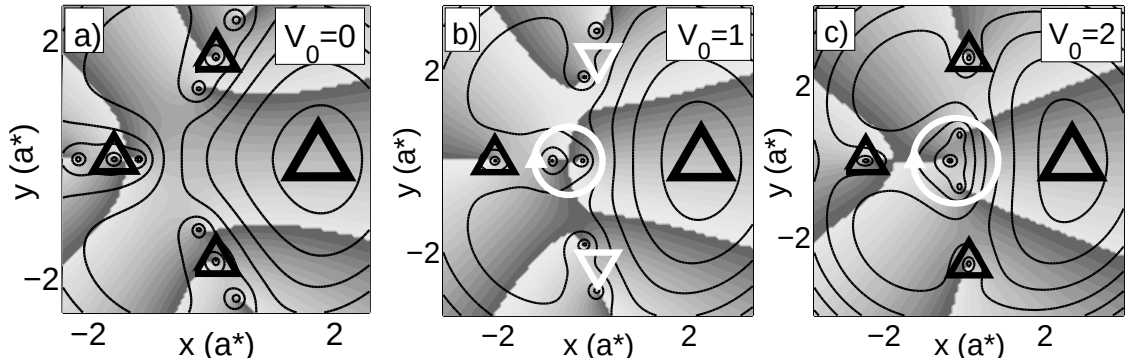

Figure 1: Conditional wave functions consisting of the charge density, plotted with contour lines (logarithmic scale), and the phase of the wave function, illustrated by the gray-scale shading. The fixed spin up electrons are marked with black triangles pointing up, and the spin down electrons with white triangles pointing down. The probe particle is marked with a larger triangle. The clusters consisting of central vortices are denoted by circular arrows. In a) we have a spin-polarized four-electron $\nu = 1/3$ state, and at b) the repulsive impurity at the center of the dot has attracted two vortices, changing the total spin to zero. In c) there is a third vortex at the center, and the system is again spin polarized.

[1] G. Bårdsen, E. Tölö, and A. Harju, Phys. Rev. B. **80**, 205308 (2009).

ELECTRON TRANSPORT IN METALLIC AND SEMICONDUCTING NANOTUBE CROSS JUNCTIONS

P. Havu[1], M. J. Hashemi[1], M. Kaukonen[1], E. T. Seppälä[2] and R. M. Nieminen[1]

1) Aalto University, Department of Applied Physics, P.O. Box 14100, FI-00076 Aalto, Espoo, Finland
2) Nokia Research Center, Itämerenkatu 11-13, FI-00180 Helsinki, Finland
email: Paula.Havu@tkk.fi

Carbon nanotube networks (CNTNs) are promising candidates for many applications in the area of flexible electronics. Modeling their electronic transport properties from first principles however, needs a careful study of carbon nanotubes' (CNTs) relative positions and their electronic tunneling characteristics in CNTs' junctions [1, 2].

In CNTNs there are both metallic and semiconducting nanotubes, which leads to three different basic junctions. While the metallic-metallic (MM) and the semiconductor-semiconductor (SS) junctions have been measured to have a similar contact resistances; metallic-semiconductor (MS) junction has been measured to be two orders of magnitude more resistive [3]. This difference is explained to be originated from charge transfer between metal and semiconductor, which causes extra energy barrier for electrons (a Schottky barrier).

We modeled electronic transport properties of MM, SS and MS junctions using van der Waals corrected density functional theory. In order to model tunneling current through the junctions, we implemented Landauer-Büttiker based transport for the four terminal case to an all electron density functional code FHI-aims. The charge doping of nanotubes were modeled by increasing and decreasing number of electrons in the system with compensating uniform background charge. In our simulations we see a clear charge depletion-accumulation region at the junction in the semiconducting tube close to the MS junction. However, a junction conductance is too complicated to be explained only by simple picture of an extra tunneling barrier. It depends sensitively on the several parameters such as doping of the tubes or the pressure over junctions.

[1] Y.-G. Yoon, M. S. C. Mazzoni, H. J. Choi, J. Ihm, and S. G. Louie, Phys. Rev. Lett. **86**, 688 (2001).
[2] F. A. Bulat, L. Couchman, and W. Yang, Nano Lett. **9**, 1759 (2009).
[3] M. S. Fuhrer, J. Nygård, L. Shih, M. Forero, Young-Gui Yoon, M. S. C. Mazzoni, Hyoung Joon Choi, Jisoon Ihm, Steven G. Louie, A. Zettl, and Paul L. McEuen, Science **288**, 494-497 (2000).

CHARACTERIZING THE PERIPHERY ATOMS OF Au ISLANDS ON MgO THIN FILMS

X. Lin[1], N. Nilius[1], M. Sterrer[1], P. Koskinen[2], H. Häkkinen[2,3], and H.-J. Freund[1]

[1] Fritz-Haber Institut der MPG, Faradayweg 4-6, D14195 Berlin, Germany
Departments of [2]Physics and [3]Chemistry, Nanoscience Center, University of Jyväskylä, P.O. Box 35 (YFL), FI-40014 Finland
email: pekka.koskinen@iki.fi

The perimeter of oxide-supported metal particles plays an important role in various catalytic processes. To understand why, we analyzed the low-coordinated perimeter atoms of planar Au clusters grown on MgO/Ag(001) thin films with scanning tunneling microscopy and electronic structure calculations. The perimeter shows a high density of Au $6s$-derived states at the Fermi level, accommodating electrons transferred from the MgO/Ag substrate. Energies well above the Fermi level, again, accommodate totally delocalized quantum well states with Au $6p_z$-character. The concentration of frontier orbitals at the island perimeter explains the relevance of the cluster perimeter for adsorption and reaction events.

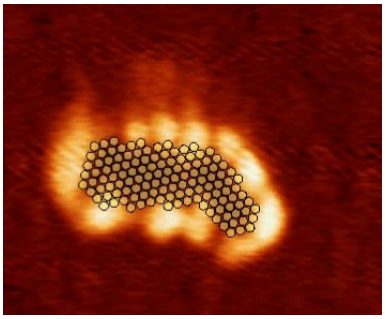

Figure: Filled state STM dI/dV map of an Au island on MgO at -0.1 V bias, together with an overlaid atomic model.

[1] X. Lin, N. Nilius, M. Sterrer, P. Koskinen, H. Häkkinen, H.-J. Freund *(submitted)*.

MANY-ELECTRON AHARONOV-BOHM EFFECT IN QUANTUM RINGS

V. Kotimäki and E.Räsänen

Nanoscience Center, Department oh Physics, University of Jyväskylä, FI-40014, Jyväskylä, Finland
email: ville.kotimaki@jyu.fi

The Aharonov-Bohm (AB) effect is one of the most distinct physical phenomena which illustrates the importance of the quantum mechanical phase [1]. In the AB effect, a charged particle acquires a phase shift $\phi = 2\pi e/h \int_\gamma \mathbf{A} \cdot \mathrm{d}\mathbf{x}$ from the vector potential $\mathbf{A}$ while traveling along a path γ. The existence of this phase shift can be verified, for example, by measuring the current through a quantum ring in a static perpendicular magnetic field.

In this work the many-electron Aharonov-Bohm effect is investigated in a two-dimensional quantum-ring device in magnetic fields by the use of time-dependent density-functional theory with the adiabatic local-density approximation for the exchange and correlation. We show that the AB oscillations are relatively weakly affected by the electron-electron interactions, whereas the ring width has a strong effect on the characteristics of the oscillations. In general, the oscillations are notably reduced when the conduction channels are made wider. We also observe multiple transport loops leading to AB oscillation periods of Φ_0/n.

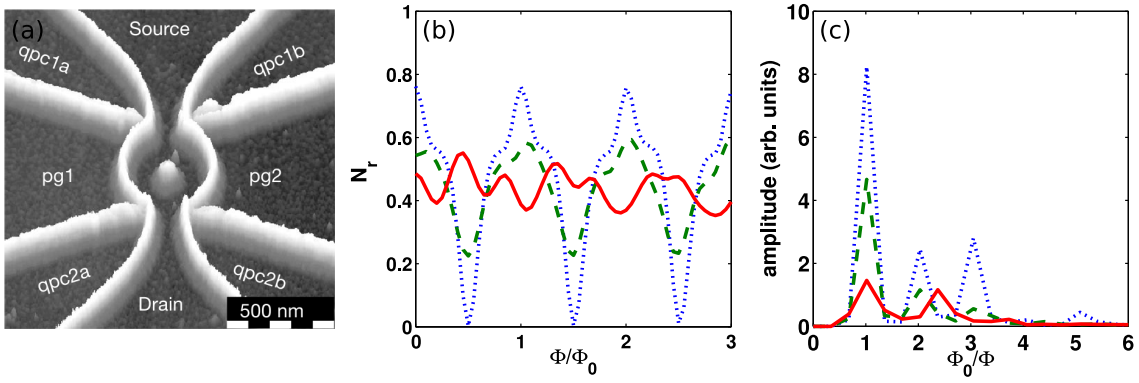

Figure 1: (a) Quantum-ring device from A. Fuhrer *et al.*[2] (b) Transferred density of a single electron at time $t = 2$ as a function of the magnetic flux Φ/Φ_0, where $\Phi_0 = h/e$. Dotted, dashed, and solid lines represent thin, wide, and wider quantum rings, respectively. (c) Fourier spectrum of the situation in (b).

[1] Y. Aharonov and D. Bohm, Phys. Rev. **115**, 485 (1959).
[2] A. Fuhrer, S. Lüscher, T. Ihn, T. Heinzel, K. Ensslin, W. Wegscheider, and M. Bichler, Nature **413**, 822 (2001).

MANIPULATING OPTICAL ACTIVITY OF EXCITONS IN SEMICONDUCTOR QUANTUM RINGS

O. Vänskä[1], M. Kira[2], and I. Tittonen[1]

[1]Department of Micro and Nanosciences, Aalto University, P.O.Box 13500, FI-00076 Aalto, Finland
[2]Department of Physics and Materials Sciences Center, Philipps-University Marburg, Renthof 5, 35032 Marburg, Germany
email: osmo.vanska@tkk.fi

The optical properties of semiconductors and their nanostructures are mainly related to the transitions between electrons and holes. The quantum mechanical many-body problem behind these transitions can be solved by using quasiparticles that are called excitons. Excitons are Coulomb correlated bound states of electron-hole-pairs. Excitonic states can be divided into bright and dark states depending on how strongly they interact with the light field.

Modern fabrication methods can be used to construct wide variety of nanostructures with various geometries. Quantum rings can be made by self-assembly or by lithography. Typical lateral diameter and height of these rings are about 50-300 nm and 2-10 nm, respectively. The nature of electronic states is very characteristic for quantum rings. These torus shaped structures support strongly confined electron and hole states with fully quantized energy spectrum.

In this work we have theoretically modeled semiconductor quantum ring structures resembling those already fabricated. We show that the distinctive properties of electronic states in quantum rings can be used to produce excitonic states with variable optical activity. Excitonic states in modeled rings can be tuned from dark to bright, and vice versa, by adjusting the angle of interacting light field. Although this effect should be seen most clearly in a single ring with perfect crystal structure, we predict that this phenomenon is retained also in multiring systems with considerable impurities and ring size variations.

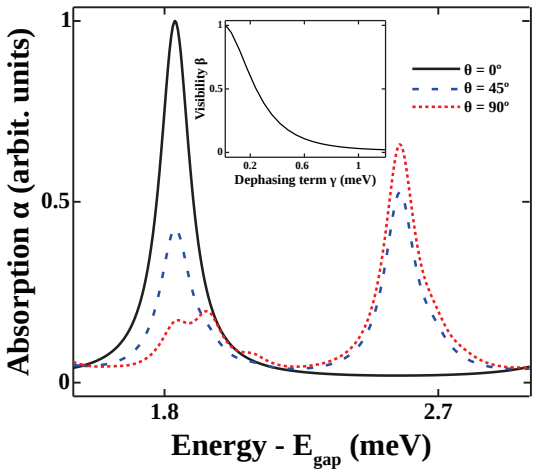

Fig. 1. A part of an absorption spectrum showing how excitonic states are alternating from bright to dark when the angle of light field, θ, is changed. Inset: The visibility of this effect is also seen when dephasing term, γ, is increased. γ-term describes impurities and ring size variations in multiring systems.

DENSITY FUNCTIONAL SIMULATIONS OF PHASE-CHANGE MATERIALS: CHARACTERIZATION OF AMORPHOUS PHASES

J. Akola[1,2,3] and R.O. Jones[3]

[1]Nanoscience Center, Department of Physics, FI-40014 University of Jyväskylä, Finland
[2]Department of Physics, Tampere University of Technology, FI-33101 Tampere, Finland
[3]IFF, Forschungszentrum Jülich, D-52425 Jülich, Germany
E-mail: jaakko.akola@phys.jyu.fi

The technological applicability of phase-change materials (PCM) in DVD media is based on the rapid amorphous-to-crystalline transition and subsequent changes in optical (and electrical) properties. The structure of the amorphous phase poses the main problem for scientists and is difficult to tackle both experimentally and theoretically. We have previously described results for the $Ge_2Sb_2Te_5$ (GST-225, DVD-RAM) and Ge_xTe_{1-x} alloys, which were obtained by performing massively-parallel density functional (DF) / molecular dynamics (MD) simulations on the IBM Blue Gene supercomputers [1-3]. The atoms on GeTe-based materials can be generally classified into atomic types *A* (Ge,Sb) and *B* (Te), with strong *AB* alternation, and that the main structural motif of such materials is a four-membered *ABAB* ring ("*ABAB* square"). Furthermore, a considerable part of the Ge atoms can be described as "tetrahedral" (coexisting with "octahedral"), Sb and Te coordination numbers deviate from the `8-N rule´, and that small cavities (voids, vacancies) are characteristic for these materials. The rapid amorphous-to-crystalline transition can be viewed as a re-orientation (nucleation) of disordered *ABAB* squares which is supported by the free space provided by the cavities, and the metastable NaCl structure corresponds to the perfectly ordered case.

Herein, I shall first discuss the theoretical methods and their limitations, and especially in the context of DF methods and available exchange-correlation functionals. Tellurium is the basis of most PCMs, and it has turned out that elemental Te with an anomalous density maximum at the melting point provides a good example in this context. I also present results for two technologically important PCMs: $Ge_8Sb_2Te_{11}$ (GST-8,2,11, Blu-ray Disc) and $Ag_{3.5}In_{3.8}Sb_{75.0}Te_{17.7}$ (AIST, DVD±RW) alloys [4,5]. The former has been studied by performing a full melt-quench simulation for the pseudobinary GST-8,2,11 alloy (630 atoms, over 400 ps), while AIST has been modeled in its liquid phase (640 atoms, 850 K). Structural details in amorphous GST-8,2,11 are very similar to GST-225, indicating that the addition of only a few percent of Sb changes the properties of GeTe significantly. The structure factor and pair distribution function of liquid AIST agree well with HEXRD measurements at 589°C (862 K). Medium-range order is evident, and Ag and In atoms (dopants) prefer to be near Te atoms rather than Sb.

[1] J. Akola and R.O. Jones, Phys. Rev. B **76** (2007) 235201.
[2] J. Akola and R.O. Jones, J. Phys.: Cond. Matter **20** (2008) 465103.
[3] J. Akola, R. O. Jones, S. Kohara *et al.*, Phys. Rev. B **80** (2009) 020201(R).
[4] J. Akola and R.O. Jones, Phys. Rev. B **79** (2009) 134118.
[5] J. Akola and R.O. Jones, Appl. Phys. Lett. **94** (2009) 251905.

Amorphous defect clusters of pure Si and the type inversion in Si detectors

E. Holmström, M. Hakala and K. Nordlund

Department of Physics, University of Helsinki and Helsinki Institute of Physics, P.O.B. 64, FIN-00014 University of Helsinki, Finland
email: eero.holmstrom@helsinki.fi

A heavily researched problem in materials physics is the effective type inversion of Si detectors as a consequence of energetic particle irradiation. The effect is caused by lattice defects that form upon the interaction between the incident energetic particles and the lattice atoms. The defects trap electrons, and hence negative charge is accumulated in the n-type bulk of the detector. This leads eventually to the inversion of the sign of the space charge and an increase in the full depletion voltage of the device. Ultimately, this phenomenon destroys the functionality of the detector.

The effect is a critically limiting factor in the lifetime of Si detectors in high luminosity colliders such as the LHC and its prospective followers. Traditionally, the effort to identify the main culprits has focused on point-like defects or impurities, such as vacancies and oxygen-related defects. However, that the same effect is observed in a wide range of different types of Si detectors suggests that a specific defect cannot explain the type inversion under all circumstances. Instead, a more generic explanation independent of the type of Si should be sought. Recently, there has been an increasing emphasis on cluster-related defects, which are now believed to be responsible for the phenomenon. Despite much research, the electron traps mainly responsible remain yet unidentified.

In this study, we use large-scale *ab initio* simulations to show that amorphous defect clusters of pure Si, which are intrinsic defects generated by particle bombardment, may alone explain the phenomenon. The presence of these clusters in Si after energetic particle bombardment is well evidenced by many experimental studies. Our results show that they act as powerful electron traps in the lattice.

FROM THE REVISION OF BLOCH'S THEOREM TO SPHERICAL DISTORTIONS OF SINGLE- AND MULTI- LAYER GRAPHENE

O. O. Kit and P. Koskinen

Nanoscience Center, P.O.Box 35, FI-40014 University of Jyväskylä, Finland
oleg.o.kit@jyu.fi

Boosting the computational research, translational symmetry of Bloch theorem have proven its effectiveness for bulk materials. The more to electronic and mechanical properties' research brings the Bloch's theorem revision, introduced here, valid for any symmetry transformation and particularly useful at nanoscale [1, 2]. Since the low-dimensional structures, instead of translational symmetries, often possess some other symmetries (sush as rotational and chiral symmetries for nanotubes and nanotori), Bloch's theorem revision enables proper utilization of these symmetries (e.g. a simulation of a chiral nanotube of any radius from the unit cell of two atoms), leading to considerable economy in computational costs. Moreover, since the effects like bending, twisting and wrapping, being natural attribute of experiment, can be studied from few atoms only (e.g. considering the curvature of bent graphene layer locally), Bloch's theorem revision enables simulation of these structural distortions (e.g. a simulation of twisted nanotube from the unit cell of 2 atoms), providing an easy-access to previously unfeasible systems.

In the presentation, we shall present the revision of Bloch theorem and its quick proof, outline the unified formalism for efficient simulations of systems invariant under more general transformation than translation, and the formalism's recent application to spherical bending of single- and multi- layers graphene sheets (Figure 1).

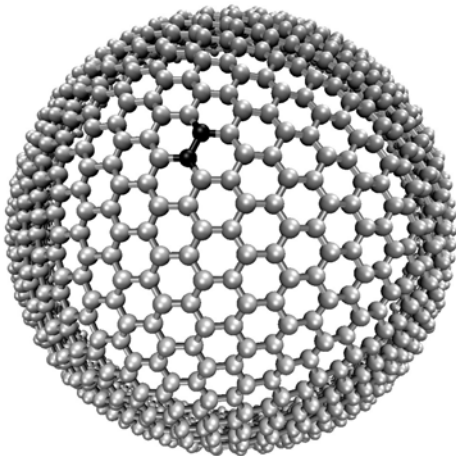

Figure 1. An example illustration of single-layer graphene sheet, bent to the radius of 20 Å. The systems are calculated from the simulation cell of two atoms per layer (depicted in black). The development of easy and efficient simulation formalism naturally follows the work in Ref. 3.

[1] O. O. Kit *Generalized Symmetries in Nanostructure Simulations,* MSc thesis, Department of Physics, University of Jyväskylä (2009), available online
[2] P. Koskinen and O. O. Kit *Electronic structures for distorted nanomaterials: curvature moduli of graphene* (in preparation).
[3] S. Malola, H. Häkkinen and P. Koskinen *Effects of Bending on Raman-active Vibration Modes in Carbon Nanotubes*, Phys. Rev. B **78**, 153409 (2008)

INTERFACE SENSITIVITY OF POSITRONS IN POLAR SEMICONDUCTOR HETEROSTRUCTURES

I. Makkonen,[1] A. Snicker,[2] M. J. Puska,[2] J.-M. Mäki,[2] and F. Tuomisto[2]

[1]Helsinki Institute of Physics and Department of Applied Physics at Aalto University, P.O. Box 14100, FI-00076 Aalto, Espoo, Finland
[2]Department of Applied Physics at Aalto University, P.O. Box 11100, FI-00076 Aalto, Espoo, Finland
email: ilja.makkonen@tkk.fi

Semiconductor heterostructures are the core elements of electronic and especially optoelectronic semiconductor devices, such as light emitting diodes and laser diodes. Ideally, it is the design of the structure that defines the properties of the device at hand, but in practice the structural quality of both the semiconductor materials themselves and the heterointerfaces between them often limit significantly the output. This is the case especially in device structures fabricated out of III-nitrides (AlN, GaN and InN) that are the material family of choice for blue and ultraviolet optoelectronics with potential for covering the whole spectral range down to infrared.

Positron annihilation spectroscopy is a method that is particularly well suited for studying vacancy defects in semiconductors. In this work, we explore its potential in probing nitride heterostructures by using first-principles electronic structure theory supported by positron annihilation experiments for bulk systems. The III-nitrides in their wurtzite crystal structure are characterized by their large spontaneous polarization along with large piezoelectric contributions in device structures formed of these materials. Polarization discontinuities in polar heterostructures result in net interface charges and huge built-in electric fields of the order of MV/cm. We address the implication of these fields on positron annihilation studies of these structures both in the case of ideal defect-free heterostructures and those containing vacancy defects. We discuss especially the potential of positrons in probing interface regions of the polar heterostructures. Our conclusions are not specific to the III-nitride heterostructures only but can be generalized to semiconductor heterostructures formed of other materials such as II-O semiconductors.

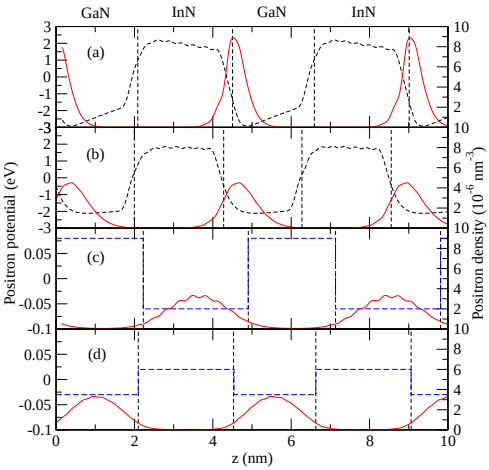

Figure 1: Macroscopic average of positron density (red solid line) in polar [panels (a) and (b)] and non-polar [(c) and (d)] heterostructures formed of GaN and InN, in different strain conditions. The figure also shows schematic macroscopic positron potentials.

EFFECT OF ENVIRONMENTAL FLUCTUATIONS ON SINGLE-ELECTRON PROCESSES IN HYBRID TUNNEL JUNCTIONS

O.-P. Saira[1,2], M. Möttönen[1,2], J. P. Pekola[1]

[1]Low Temperature Laboratory, Aalto University School of Science and Technology, P.O. Box 13500, FI-00076 AALTO, Finland
[2]Department of Applied Physics/COMP, Aalto University School of Science and Technology, P.O. Box 15100, FI-00076 AALTO, Finland
email: ops@ltl.tkk.fi

As demonstrated in [1], a hybrid single-electron transistor (SET) with superconductor-insulator-normal metal (SIN) junctions can be operated as an accurate turnstile for electric current. In the device, interplay between the superconducting energy gap and electrostatic charging energy allows the generation of quantized current levels with a DC bias and a single RF gate voltage. Realization of a quantum standard of elecric current based on the hybrid turnstile may be feasible with present day microfabrication technology [2].

In this work, we use real-time SET electrometry to study single-electron tunneling in SIN-type structures closely related to the hybrid turnstile. Our emphasis is on processes that limit the accuracy of the turnstile in the experiments. Namely, we are interested in tunneling rates at energies that are below the superconducting gap parameter Δ or even negative, i. e., the tunneling happens to an energetically unfavorable direction. The tunneling rates can be determined as a function of energy and temperature by counting the individual tunneling events in the recorded electrometer traces. Two main questions we wish to answer are (1) Is the phenomenological Dynes model used to explain finite sub-gap conductance valid in this context? (2) How do fluctuations of the elecromagnetic environment affect the tunneling rates?

We also demonstrate that the electrometer measurement can be used to study the turnstile error rate in actual pumping operation. This is an important development, as the accuarcy called for metrological applications is of the order of 10^{-8}, which cannot be verified with conventional current amplifiers.

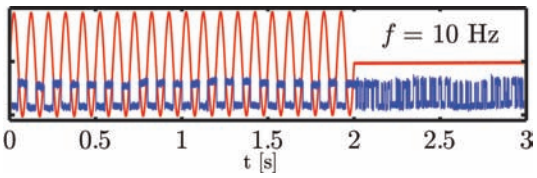

Figure 1: Electrometer signal (blue) showing the charge state of a SIN electron box being controlled by an external gate voltage (red).

[1] J. P. Pekola, J. J. Vartiainen, M. Mottonen, O.-P. Saira, M. Meschke, and D. V. Averin, Nature Phys. 4, 120 (2008).
[2] A. Kemppinen, M. Meschke, M. Möttönen, D.V. Averin, and J.P. Pekola, The European Physical Journal - Special Topics 172, 311 (2009).

TOWARDS IN SITU SPECTROSCOPY OF CHEMICAL REACTIONS: INELASTIC X-RAY SCATTERING FROM GASEOUS N_2O, CO_2, AND N_2

A. Sakko[1], S. Galambosi[1], J. Inkinen[1], J. Röntynen[1], T. Pylkkänen[1,2], M. Hakala[1], S. Huotari[2], and K. Hämäläinen[1]

[1] Department of Physics, P.O.B. 64, FI-00014 University of Helsinki, Finland
[2] European Synchrotron Radiation Facility, B.P. 220, F-38043 Grenoble, France
email: arto.sakko@helsinki.fi

Much of chemical engineering depends on the reactions of small molecules, and thus the detailed understanding of these processes is an important scientific topic. Gas phase molecules also play an important role in atmospheric chemistry and therefore affect the environment in a global sense. However, spectroscopic experiments in controlled conditions, e.g. at high temperatures and pressures, are extremely challenging. On the way towards new *in situ* spectroscopic experiments and the characterization of chemical reactions, we have applied inelastic x-ray scattering for measuring the near-edge spectra of various gaseous molecules.

Core-level spectroscopies, such as x-ray absorption, electron energy-loss spectroscopy and x-ray Raman scattering, are widely used techniques to study the atomic and electronic structure of a wide range of different materials. X-ray Raman scattering (XRS), i.e. non-resonant inelastic x-ray scattering from inner shell electrons, has many intriguing properties. For instance, it enables bulk sensitive experiments at extreme conditions and the study of both dipole and non-dipole electronic transitions. During the last few years significant development has extended the feasibility of XRS and various new applications have emerged. Up to now most XRS studies have focused on crystalline or amorphous materials and liquids. In this pioneering work we demonstrate the technique for several gaseous samples.

The experiment was carried out at beamline ID 16 of the European Synchrotron Radiation Facility (ESRF). We describe the experimental work and present data for the nitrogen, oxygen, and carbon K-edges of gaseous N_2O, CO_2, and N_2. We also discuss the scattering angle (or momentum transfer) dependency of the measured energy loss spectra. The experimental data are analysed using a recently developed density functional theory based computational method [1]. We show how molecular vibrations can be included in the analysis and discuss their relevance to the interpretation. Finally, we discuss the future possibilities that our work opens.

[1] A. Sakko, M. Hakala, J. A. Soininen, and K. Hämäläinen,
Phys. Rev. B 76, 205115 (2007).

MODELING OF POLYMER-METAL HYBRID MATERIALS

J. Blomqvist and P. Salo

Aalto University, Department of Applied Physics,
P.O.Box 11000, FI-00076 AALTO Finland
email: Janne.Blomqvist@tkk.fi

Hybrid materials, where multiple substances are combined, belong to an interesting new class of materials. These materials can be optimized for specific applications, and can provide a more appropriate balance between cost, weight, strength, or some other properties. To understand these materials we must understand the interface between the various substances.

Particularly interesting materials from a practical as well as a scientific perspective are the materials that combine a metal and polymer. Thus, studying the interaction between the metal surface and the molecules in the polymer chains is important. There are multiple adhesion mechanisms that need to be understood, such as mechanical gripping, and multiple phenomena affecting the strength of the interface, such as the surface roughness and wetting. However, in this work we have focused on the microscopic level. The model system we study is bisphenol-A-polycarbonate on an alumina surface.

The interaction of polymers with surfaces present additional challenges to the modeling process. Simulating an entire polymer chain, let alone multiple chains interacting with the surface as well as each other, is far beyond the capability of methods that are able to provide the required accuracy. Thus we simulate fragments along with their nearest neighbor fragments. This provides a more realistic environment for the fragment closest to the surface, both in terms of electronic structure effects as well as limiting the possible conformations. However, these fragments still have many conformational degrees of freedom, with complex non-convex potential energy landscapes. Secondly, these large molecules have filled shells, and thus traditional density-functional theory (DFT) calculations that neglect van der Waals interactions describe these interactions poorly.

We use density functional theory (DFT) calculations with van der Waals corrections to study the binding between fragments of the polymer chain and the oxide surface. These results are used to parametrize interaction potentials for coarse-grained molecular dynamics simulations which we use to study the hybrid material interface on a larger length and time scale. These simulations can be used for providing e.g. boundary coefficients such as friction coefficients that can be used for continuum simulations, or for simulating nanostructured composites where the interface effects dominate the bulk properties of the material.

ROLE OF THE VAN DER WAALS INTERACTION IN FORMATION OF SELF-ASSEMBLED STRUCTURES

A. Gulans[1], O. Pakarinen[2], M. Mura[3], T. Thonhauser[4], M. Puska[1], L. Kantorovich[3] and A. Foster[5]

[1]Aalto University, Department of Applied Physics, PL 11000, 00076 Aalto, Espoo, Finland
[2]Department of Physics and Helsinki Institute of Physics, Helsinki University, Finland
[3]King's College London, UK
[4]Department of Physics, Wake Forest University, USA
[5]Department of Physics, Tampere University of Technology, Finland
email: agl@cc.hut.fi

Self-organisation of organic semiconducting molecules on surfaces is a crucial area in the development of practical molecular electronics. The research in this field relies on a number of experimental and computational techniques, and density functional theory (DFT) calculations take prominent place among them. Unfortunately, the most common approaches to the DFT, namely, the local density and generalised gradient (GGA) approximations, meet difficulties in description of non-covalent bonding, which plays the crucial role in self-assembly. It is clear that the van der Waals interaction increases stability of the molecules on a surface. The same time, there is plenty of space for doubts whether the van der Waals interaction plays any significant role in the diffusion on a surface and in the interaction between the molecules.

In the present work, this question is addressed by computational studies of organic molecules, such as PTCDA, on the KBr (001) and Au (111) surfaces. In order to do so, we apply vdW-DF – a density functional theory based method designed to treat the van der Waals forces in a non-empirical physically justified manner. The calculations of the adsorption energies reveal that the dispersion interaction indeed is crucial in the stabilisation of the molecules on both surfaces at room temperature and contributes to the binding energy up to 95%. On the other hand, the influence of the van der Waals interaction on the diffusion is surface dependent. According to the vdW-DF and GGA calculations the diffusion barrier for PTCDA on Au (111) surface is as small as 0.05 eV. Such an agreement is not observed for KBr(001) surface, where the vdW-DF predicts higher diffusion barriers than the GGA.

[1] M. Dion, H. Rydberg, E. Schröder, D. C. Langreth and B. I. Lundqvist, Phys. Rev. Lett. 92 (2004) 246401

EFFICIENT GRID-BASED OPERATIONS FOR ALL-ELECTRON ELECTRONIC STRUCTURE CALCULATION USING NUMERIC BASIS FUNCTIONS

V. Havu[1] and V. Blum[2] and P. Havu[1] and M. Scheffler[2]

[1] Aalto University, Department of Applied Physics, P.O. Box 11100, FI-00076 Aalto, Finland
[2] Fritz Haber Institute of the Max Planck Society, Faradayweg 4-6, D-14195 Berlin-Dahlem, Germany
email: Ville.Havu@tkk.fi

The increase in computer power in the past decades makes it possible today to study systems of thousands of atoms within the framework of computational electronic structure theory (EST), and in particular density functional theory [1]. In addition to advances in computational hardware, algorithmic developments play even more important role rendering the use of modern day supercomputers feasible for EST calculations.

We consider the problem of developing $O(N)$ scaling grid-based operations needed in many central operations when performing electronic structure calculations with numeric atom-centered orbitals (NAOs) as basis functions [2]. We outline the general formulation of localized algorithms, and focus on the creation of localized grid batches. Due to the complexity of the problem heuristic algorithms must be used.

We show that i) the choice of the grid partitioning scheme plays an important role in the performance and memory consumption of the grid-based operations, ii) top-down partitioning methods achieve essentially the same efficiency as the more rigorous bottom-up approaches and iii) close-to-optimal performance is obtained with the best top-down methods.

Our implementation is a part of FHI-aims [2, 3], a recently developed full-potential / all-electron electronic structure code that uses NAOs as basis functions [4].

[1] P. Hohenberg and W. Kohn, Phys. Rev. 136 (1964) B864
[2] V. Havu and V. Blum and P. Havu and M. Scheffler, Journal of Computational Physics 228 (2009) 8367-8379
[3] http://www.fhi-berlin.mpg.de/th/aims/
[4] V. Blum and R. Gehrke and F. Hanke and P. Havu and V. Havu and X. Ren and K. Reuter and M. Scheffler Computer Physics Communications 180 (2009) 2175-2196

AN EFFICIENT APPROACH TO THE BAND GAP PROBLEM IN DFT

M. Kuisma[a], J. Ojanen[a], J. Enkovaara[b] and T. T. Rantala[a]

[a] Semiconductor Physics Laboratory, Tampere University of Technology P.O. Box 692, FIN-33101 Tampere, Finland
[b] CSC - IT Center for Science Ltd. P.O. Box 405 FI-02101 Espoo, Finland
email: mikael.kuisma@tut.fi

The local and semi-local approximations (LDA and GGA) to the Kohn–Sham density-functional theory (KS-DFT) underestimate the fundamental band gap of semiconductors severely. This is due to omission of the "integer occupation derivative discontinuity" in the functional[1]. There are approaches, which give a good match with experimental band gaps but but they are based mostly on the cumbersome many-body perturbation theory, on optimized effective potential (OEP) methods or both. The OEP requires calculation of complicated functional derivatives of the energy functional wrt. the KS-orbitals and energies for obtaining the KS-potential.

An alternative approach is to approximate KS-potential, directly. The obvious trade-off is, that the energy functional is no longer necessarily consistent with the potential. The OEP-EXX (exact-exchange) potential, for example, can be approximated with KLI, LHF or GLLB potentials, retaining the derivative discontinuity. The draw-back is that the energy functional is known not to exist. The computational effort, however, is substantially reduced. In GLLB this is due to electron gas based approximations.

We have implemented the orbital dependent GLLB-potential [2] to the grid based projector augmented-wave code GPAW [3]. The evaluated KS gaps and discontinuities add up to band gaps close to the experimental ones, as shown in the Fig.1 for AlAs. Other semiconductors and band gap materials are considered, too.

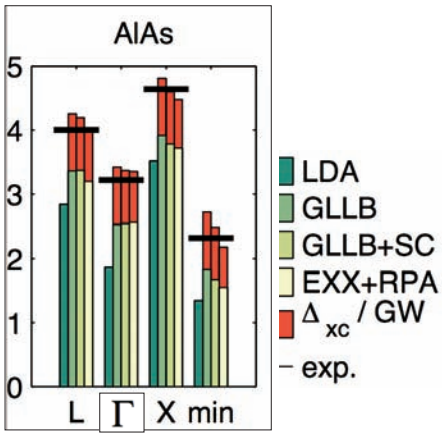

Fig.1. The calculated LDA, GLLB and GLLB+SC (with PBEsol exchange screening and correlation and GLLB-exchange response) KS-gaps and discontinuities compared to what is believed to be accurate GW-based Kohn-Sham potential calculated by solving the linearized Sham-Schlüter equation [4].

[1] L.J. Sham and M. Schlüter, Phys. Rev. Lett., **51**, 1888 (1983).
[2] O. Gritsenko, R. van Leeuwen, E. van Lenthe and E.J. Baerends, Phys. Rev. A **51**, 1944 (1994).
[3] J.J. Mortensen, L.B. Hansen, and K.W. Jacobsen, Phys. Rev. B **71**, 035109 (2005).
[4] R.W. Godby, M. Schlüter, L.J. Sham, Phys. Rev. B **36**, 6497 (1987).

LAGRANGE MESH METHOD APPLIED TO QUANTUM DOTS

O. Kupiainen and A. Harju

Department of Applied Physics,
Aalto University, P.O. Box 14100, FI-00076 Aalto, Finland
email: oona.kupiainen@tkk.fi

Semiconductor quantum dots (QD) have been a subject of both experimental and theoretical research for the last two decades. They can be used to study many-electron quantum physics with a controlled number of electrons ranging from a few to a few hundred. A main issue in the computational study of QDs is to find an efficient method for solving the Schrödinger equation for many interacting particles.

In this work, we have solved the one-particle eigenstates using the Lagrange mesh method. It is an approximately variational method with the simplicity of a mesh calculation. The basis functions are chosen so that all integrals appearing in the Hamiltonian matrix elements can be approximated by summations over grid-points according to a Gauss quadrature. For a smooth enough potential, energy eigenvalues are obtained accurately with significantly less mesh-points than using a finite-differences method.

We computed few-electron groundstates in two-dimensional double QDs using exact diagonalization. The energies were used to study the filling of the QDs as the potentials are varied. Some infra-red excitation spectra were also investigated.

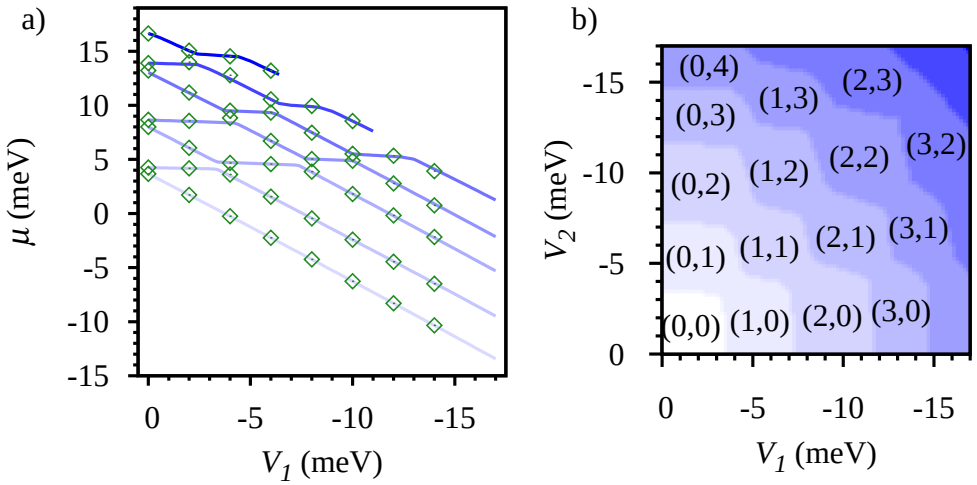

Figure 1: a) Chemical potentials $\mu(N) = E(N) - E(N-1)$ corresponding to the first seven electrons added into a double QD as a function of the potential difference between the minima. b) Ground-state electron numbers of two coupled QDs as a function of their potentials.

TIME-DEPENDENT DENSITY FUNCTIONAL THEORY WITH FINITE ELEMENTS

L. Lehtovaara, V. Havu and M. Puska

Department of Applied Physics, Aalto University School of Science and Technology, P.O.Box 11000, FI-00076 Aalto, Espoo, Finland
email: lauri.lehtovaara@hut.fi

The development of nanotechnology leans strongly on functionalizing materials at the atomic scale. As many forms of functionality, such as light-sensitivity, involve electrons on excited states, it is important to develop computational methods which can provide information on dynamics and phenomena of excited electrons.
The density functional theory (DFT) is the current workhorse of the electronic structure calculations. However, it is bound to model ground state properties. The time-dependent density functional theory (TDDFT) extends DFT to the excited states. TDDFT generally provides accurate results with reasonable computational effort.
We present an all-electron DFT and TDDFT method based on finite-element method. Our mesh generation scheme, in which structured atomic meshes are merged to an unstructured molecular mesh, allows a highly nonuniform discretization of the space. Thus it is possible to represent the core and valence states using the same discretization scheme, i.e., no pseudopotentials or similar treatments are required. The nonuniform discretization also allows the use of large simulation cells, and therefore avoids any boundary effects.

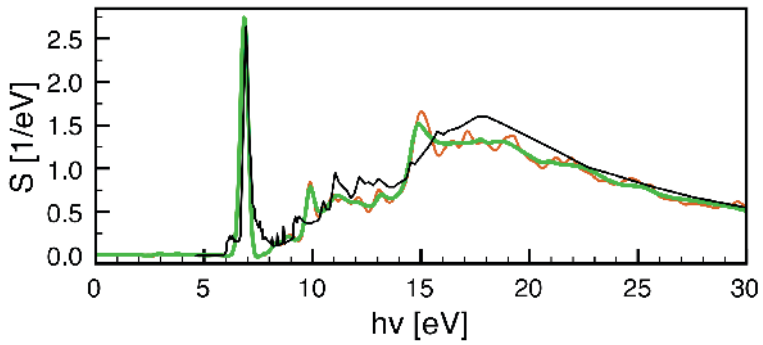

Figure: Photoabsorption spectrum of C_6H_6
green: time-propagation TDDFT with imaginary kinetic energy absorbing boundary conditions
orange: no absorbing boundary, black: experiment

[1] L. Lehtovaara, V. Havu and Martti Puska, J. Chem. Phys. **131**, 054103 (2009).

UNIVERSITY OF JYVÄSKYLÄ

MODELING THIOLATE-PROTECTED Au SUPERATOMS WITH DENSITY-FUNCTIONAL TIGHT-BINDING

Ville Mäkinen and Hannu Häkkinen and Pekka Koskinen

Finnish Physical Society, P.O.B. 64, FIN-00014 University of Helsinki, Finland
email: toimisto@fyysikkoseura.fi

Thiolate-protected gold nanoparticles are complex systems, in which both geometry and electronic structure play an essential role in stabilizing these systems. They have been previously studied[1, 2, 3] theoretically using density-functional theory. It is accurate method but implementations are computationally demanding, and faster methods are needed for example to perform molecular dynamics simulations. We have studied these systems with density-functional tight-binding[4]. We have compared our results to the previously reported ones and found good agreement. The geometry of the clusters relaxes slightly during optimization but the atomic shell structure is preserved. Analysis of the electronic structure showed that we can observe the jellium-like states in the core of these clusters, previosly seen only using density-functional codes. We conclude that tight-binding suits well describing these systems, and because tight-binding is orders of magnitude faster, molecular dynamics studies of these systems are accessible.

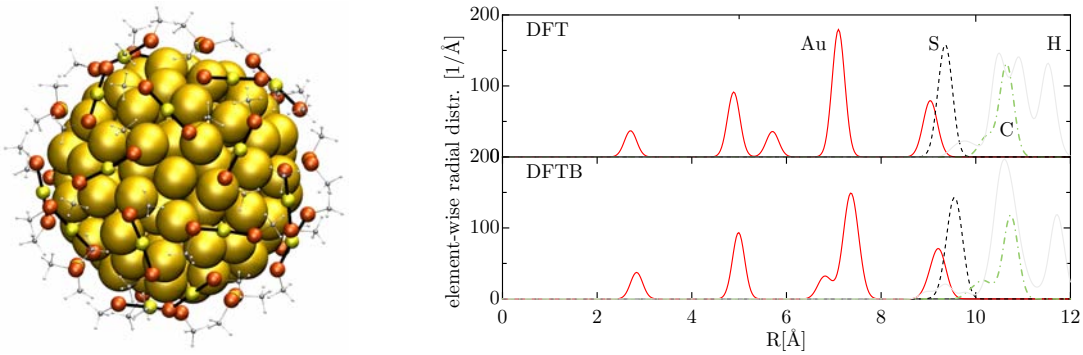

Figure 1: Left: $Au_{144}SMe_{60}$, one of the studied superatoms. Right: The elementwise radial distribution of the DFT- and DFTB-relaxed superatom.

[1] J. Akola, M. Walter, R. L. Whetten, H. Häkkinen, and H. Grönbeck. **On the Structure of Thiolate-Protected Au_{25}** Journal of American Chemical Society (2008), 130:3756-3757

[2] M. Walter, J. Akola, O. Lopez-Acevedo, P. D. Jadzinsky, G. Calero, C. J. Ackerson, R. L. Whetten, H. Grönbeck, and H. Häkkinen. **A unified view of ligand-protected gold clusters as superatom complexes** PNAS (2008), 105(27):9157-9162

[3] O. Lopez-Acevedo, J. Akola, R. L. Whetten, H. Grönbeck, and H. Häkkinen. **Structure and Bonding in the Ubiquitous Icosahedral Metallic Gold Cluster $Au_{144}(SR)_{60}$** The Journal of Physical Chemistry C Letters (2009), 113:5035-5038

[4] P. Koskinen and V. Mäkinen. **Density-functional tight-binding for beginners** Computational Materials Science (2009), 47(1):237-253

Time-dependent quantum transport with the Kadanoff-Baym equations

P. Myöhänen, A. Stan, G. Stefanucci, A-M. Uimonen and R. van Leeuwen

Department of Physics, Nanoscience Center, FIN 40014, University of Jyväskylä, Jyväskylä, Finland.
email: petri.myohanen@jyu.fi

We study theoretically the electronic transport through nanostructures by time-propagating the embedded Kadanoff-Baym equations [1, 2, 3, 4, 5]. The system under consideration consists of a correlated central region coupled to 2D leads which are assumed to be non-interacting. These systems are initially contacted and correlated and are subsequently exposed to time-dependent biases after which we study the time-evolution. The interesting observables for our study are the time-dependent transient currents, densities and dipole moments which we are able to calculate for different subregions in our system. The Kadanoff-Baym equations combined with the conserving approximations (Hartree-Fock,Second Born,GW and T-matrix) for the many-body self-energy [6] offer a powerful tool to study quantum transport in ultrafast (1fs) timescales.

[1] N. E. Dahlen and R. van Leeuwen, Phys. Rev. Lett. 98, 153004 (2007)
[2] P. Myöhänen, A. Stan, G. Stefanucci and R. van Leeuwen, Europhysics Letters, 84, 67001 (2008)
[3] P. Myöhänen, A. Stan, G. Stefanucci and R. van Leeuwen, Phys. Rev. B 80, 115107 (2009)
[4] A. Stan, N. E. Dahlen and R. van Leeuwen, J. Chem. Phys. 130, 114105 (2009)
[5] A. Stan, N. E. Dahlen and R. van Leeuwen, J. Chem. Phys. 130, 224101 (2009)
[6] G. Baym, Phys. Rev. 127, 1391 (1962)

HYBRID FUNCTIONAL STUDY OF VACANCY PROPERTIES IN $CuInSe_2$ AND $CuGaSe_2$

L.E. Oikkonen[1], M.G. Ganchenkova[1], A.P. Seitsonen[2], and R.M. Nieminen [1]

[1] Department of Applied Physics, Aalto University School of Science and Technology, P.O. Box 11100, 00076 Aalto, Espoo, Finland
[2] Physikalisch-Chemisches Institut, University of Zurich, Switzerland
email: loi@fyslab.hut.fi

Cu-based chalcopyrites such as $CuInSe_2$ (CIS) and $CuGaSe_2$ (CGS) have emerged as suitable materials for high-efficiency thin-film solar cells. Since the total conversion efficiency of a solar cell is mainly determined by the material properties, accurate knowledge on them becomes indispensable when CIGS-based solar cell technology is further developed. Despite extensive research, however, this topic is still surrounded by uncertainties. From an experimental point of view, the structural complexity of these materials has complicated the characterization of the defects. At the same time, the most commonly used theoretical approach, density-functional theory (DFT) within the local-density (LDA) or generalized-gradient (GGA) approximation, suffers from an underestimation of semiconductor band gaps. The underestimation is especially pronounced in the case of materials with strongly localized d-states such as CIS and CGS, for which DFT calculations within LDA/GGA give vanishing band gaps. In this work, we have addressed this deficiency by using a hybrid functional [1], where part of the exchange energy is taken from Hartree-Fock. It turns out that the hybrid functional gives band gap values for CIS and CGS in very good agreement with experiment. Following this, we have systematically studied the formation energies and transition levels of the three intrinsic vacancies in these two systems. The results are also compared with those obtained with traditional functionals.

[1] J. Heyd *et al*, Journal of Chemical Physics 118 (2003) 8207

ACOUSTIC PHONON TUNNELING AND HEAT TRANSPORT BETWEEN PIEZOELECTRIC BODIES

M. Prunnila and J. Meltaus

VTT Technical Research Centre of Finland, PO Box 1000, 02044 VTT, Espoo, Finland
email: mika.prunnila@vtt.fi

When two bodies are brought into close proximity (distance *d*) various near-field (NF) effects start to play crucial role in the inter-body heat transport and the well-known Stefan-Boltzmann law is no longer valid. Such photon NF heat transfer effects have been a topic of several theoretical and experimental investigations during the last decades.[1,2] We have recently proposed and demonstrated by analytical and numerical means that similar NF effect can occur also with acoustic phonons if the bodies that are in close proximity pose a property where acoustic phonons couple strongly to electric fields, which can then leak into the vacuum between the bodies [3]. This effect can be particularly strong if the bodies are piezoelectric (PE).

The acoustic phonon NF problem is described in Fig. 1(a) within scattering matrix formalism. The physical idea is that acoustic phonon incoming from PE material 1 invokes an evanescent electric field into the vacuum gap and this field enable the phonon to "tunnel" through the vacuum [see Fig. 1(b)]. Figure 1(c) shows numerically calculated thermal conductance between two PE bodies as a function of normalized thermal wave vector q_T. At small q_T the thermal conductance channel arising from the shear mode is close to the unity transmission thermal conductance, which is the maximal possible thermal conductance.

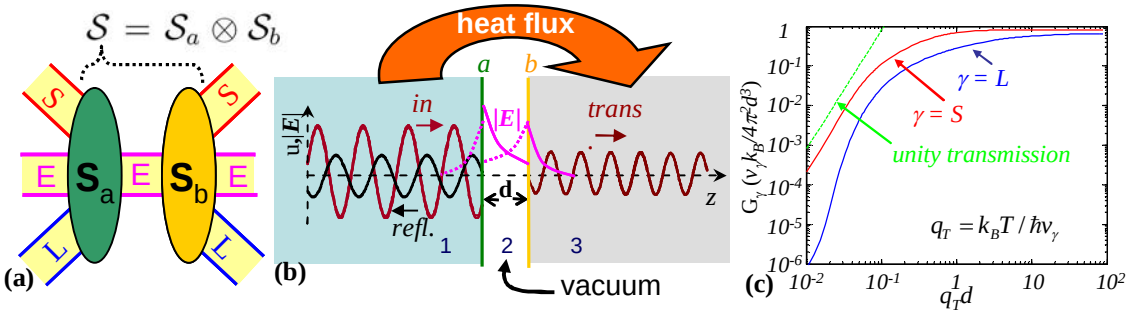

Fig. 1: (a) Diagrammatic illustration of phonon NF transmission through interfaces *a* and *b*. E refers to non-propagating electric field and L (S) to longitudinal (shear) acoustic phonon. S_a and S_b are the scattering matrices of the interfaces and *S* is the total scattering matrix. (b) Illustration of a projection of incoming, reflected and transmitted phonons (*u*) together with evanescent electric fields (*E*). d is the vacuum gap between the PE bodies 1 and 3. (c) Numerically calculated thermal conductance of different modes γ (parameters close to ZnO). The dashed curve is the unity transmission thermal conductance.

[1] A. I. Volokitin and B. N. J. Persson, Rev. Mod. Phys. **79** 1291 (2007).
[2] K. Joulain, J. Quant. Spect. & Rad. Transfer **109** 294 (2008).
[3] M. Prunnila and J. Meltaus, submitted to Phys. Rev. Lett. (2010).

COHERENT CONTROL OF CHARGE IN A DOUBLE QUANTUM DOT

A. Putaja and E. Räsänen

Nanoscience Center, Department of Physics, University of Jyväskylä, Finland
email: antti.putaja@jyu.fi

Theoretical design of a laser pulse to transfer an initial quantum state to a given final quantum state can be achieved with the help of quantum optimal control theory (OCT) [1]. We aim at designing laser-driven quantum bits (qubits) by applying OCT to semiconductor nanodevices such as quantum dots [2] and quantum rigs [3]. As the first application, we have designed a coherent and precise charge-switching scheme on double quantum dots. The charge transfer can be controlled in an arbitrary way by exploiting the superpositions of the eigenstates. For example, we are able to achieve 100 sequential charge-switch operations with more 90% fidelity within the decoherence time. Surprisingly, the fidelity is not dramatically affected by setting realistic constraints, e.g., frequency filters, in the optimization process.

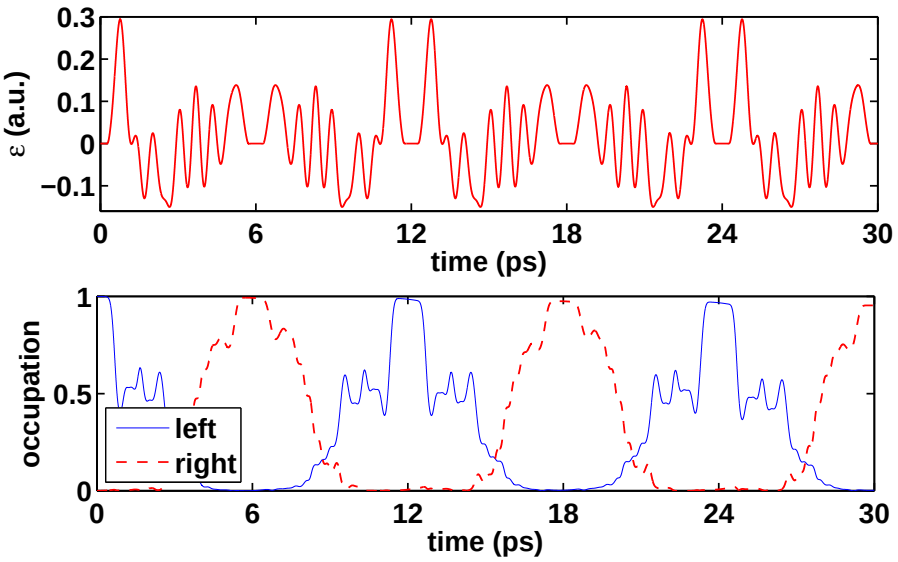

Figure 1: Optimized pulse (upper panel) for the electron transport process $left \rightarrow right \rightarrow ... \rightarrow right$ (lower panel) in a double quantum dot. After five charge-switch operations we obtain a target state occupation of 95.37% with realistic constraints on the spectrum of the laser and on its fluence.

[1] For a review, see, e.g., J. Werschnik and E.K.U. Gross, J. Phys. B: Atom. Mol. Opt. Phys. **40**, R175 (2007).
[2] E. Räsänen, A. Castro, J. Werschnik, A. Rubio, and E. K. U. Gross, Phys. Rev. B. **77**, 085324 (2008).
[3] E. Räsänen, A. Castro, J. Werschnik, A. Rubio, and E. K. U. Gross, Phys. Rev. Lett. **98**, 157404 (2007).

UNIVERSAL EXTENSION TO THE BECKE-JOHNSON EXCHANGE POTENTIAL

E. Räsänen[1], S. Pittalis[2], and C. R. Proetto[3]

[1]Nanoscience Center, Department of Physics, University of Jyväskylä, Finland
[2]Department of Physics and Astronomy, Univ. of Missouri, Columbia, USA
[3]Institut für Theoretische Physik, Freie Universität Berlin, Germany
email: erasanen@jyu.fi

The Becke-Johnson exchange potential [1] has been successfully used in electronic structure calculations within density-functional theory. However, in its original form the potential may dramatically fail in systems with non-Coulombic external potentials, or in the presence of external magnetic or electric fields. Here, we provide a system-independent extension [2] to the Becke-Johnson approximation by (i) enforcing its gauge-invariance and (ii) making it exact for any single-electron system. The resulting approximation is then better designed to deal with current-carrying states, and recovers the correct asymptotic behavior for systems with arbitrary number of electrons. Our approximation is shown to give very good results for atoms, atomic chains, and molecules with and without external electric or magnetic fields.

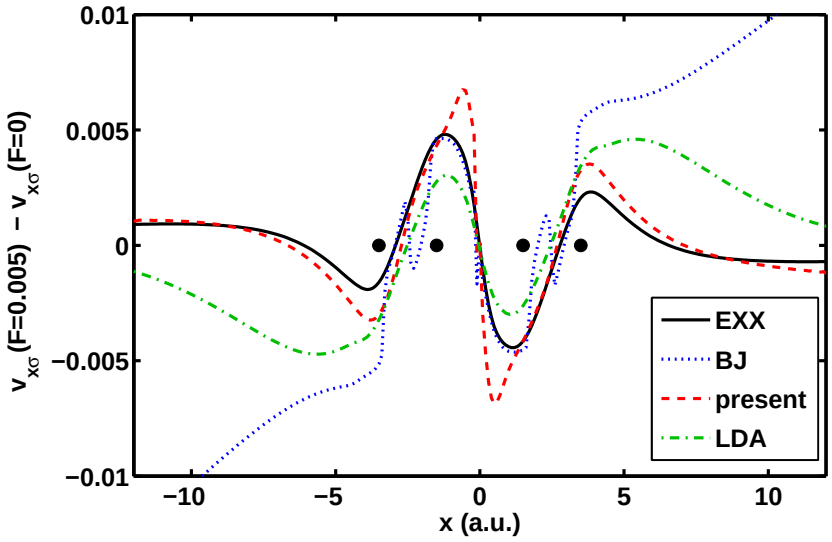

Figure 1: Difference in the exchange potentials for a four-atom hydrogen chain with and without a linear electric field. The exact-exchange (EXX) result has been obtained within the Krieger-Li-Iafrate (KLI) approximation. BJ and LDA correspond to the Becke-Johnson and local-density approximations, respectively. Black dots denote the positions of hydrogen atoms.

[1] A. D. Becke and E. R. Johnson, J. Chem. Phys. **124**, 221101 (2006).
[2] E. Räsänen, S. Pittalis, and C. R. Proetto, J. Chem. Phys. (in print); arXiv:0909.1477.

LOCAL DENSITY FUNCTIONAL FOR THE ELECTRONIC CORRELATION

S. Şakiroğlu[1,2] and E. Räsänen[1]

[1]Department of Physics, Nanoscience Center, P.O. Box 35, FI-40014 University of Jyväskylä, Jyväskylä, Finland
[2]Physics Department, Dokuz Eylül University, 35610 Izmir, Turkey
email: serpil.s.sakiroglu@jyu.fi

Accurate and efficient determination of the electronic correlation is one of the main challenges in quantum chemistry within, e.g., density-functional theory. The Colle-Salvetti (CS) approach [1], which starts with a physically motivated ansatz for the many-body wavefunction, has been widely employed to determine the correlation energies of atoms and molecules [2]. In particular, the CS scheme has been used in the derivation of several popular density functionals for exchange and correlation potentials and energies.

Here we rework the CS scheme with a Gaussian summation for the pair density [2, 3] and derive a *parameter-free* local density functional for the correlation energy. The freedom of fitting parameters is obtained by enforcing the functional to exactly reproduce the correlation energy of the uniform electron gas at arbitrary densities, i.e., with all density parameters r_s. Consequently, the external parameter in the CS scheme, which is usually determined by a semi-empirical fitting procedure, becomes an explicit function of r_s. This function can then be directly incorporated into the correlation-energy functional, where it is applied *locally* in the case of inhomogeneous systems. We obtain promising results for atomic systems and consider also a two-dimensional variant of the scheme [4] to be applied to semiconductor quantum dots.

[1] R. Colle and O. Salvetti, Theor. Chim. Acta **37**, 329 (1975).
[2] F. Moscardó and E. San-Fabián, Int. J. Quantum Chem. **40**, 23 (1991).
[3] F. Moscardó, Theor. Chim. Acta **118**, 631 (2007).
[4] S. Pittalis, E. Räsänen, and M. A. L. Marques, Phys. Rev. B **78**, 195322 (2008).

CHARGE DYNAMICS IN TWO-ELECTRON QUANTUM DOTS

J. Särkkä and A. Harju

Helsinki Institute of Physics and Department of Applied Physics, Aalto University,
P. O. Box 14100, FIN-00076 Aalto, Finland
email: Jani.Sarkka@tkk.fi

The charge and spin states of an electron in a semiconductor quantum dot have become one of the most investigated realizations for a quantum bit. The rapid control of the confining potential has been quite demanding to realize, but recently Kataoka et al.[1] made an experiment with moving single-electron quantum dots defined by surface acoustic waves. This enables changes in the potential in a picosecond time scale. This experiment can be theoretically modeled with a single-electron model.

It is interesting to study charge dynamics for larger electron numbers in the quantum dots, especially the effects that occur when the external potential is rapidly changed. We have modeled the dynamics of the two-electron wave function of a double quantum dot by using exact diagonalization with Krylov subspace methods for the dynamics. For details of our method, see [2-4]. We have studied the dynamics of the wave function with varying time-dependent potentials. In the beginning, both electrons are initialized in the second quantum dot. In the absence of external detuning voltage, the wave function and total charge oscillate between the left and right quantum dots (Fig. 1(a)). When the detuning voltage is adjusted so that the ground state of the second dot is degenerate with the first excited state in the first dot, only one of the electrons oscillates between the dots (Fig. 1(b)).

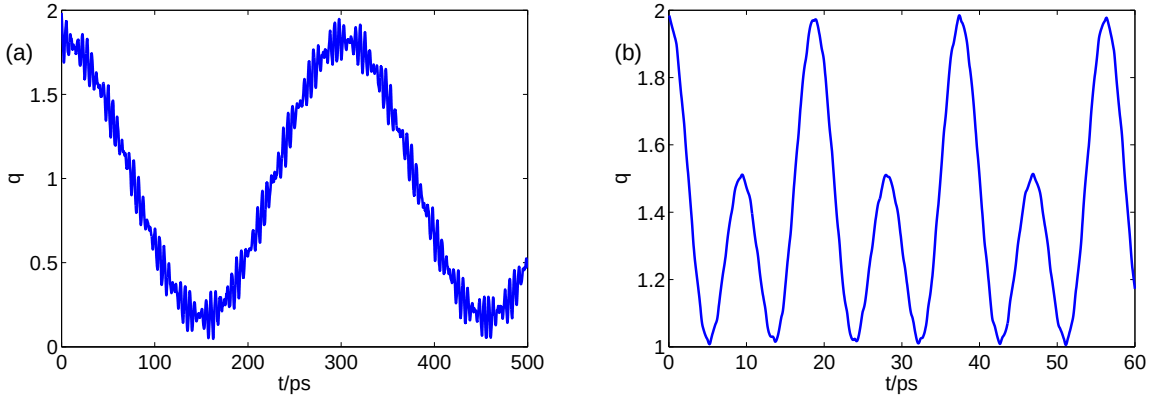

Figure 1: The charge of the second quantum dot as a function of time. The external voltage is zero in Figure (a) and finite in (b).

[1] M. Kataoka et al., Phys. Rev. Lett. 102 (2009) 156801.
[2] J. Särkkä and A. Harju, Phys. Rev. B 77 (2008) 245315.
[3] J. Särkkä and A. Harju, Phys. Rev. B 79 (2009) 085313.
[4] J. Särkkä and A. Harju, Phys. Rev. B 80 (2009) 045323.

MAGNETIC FIELD DEPENDENCE OF VORTEX CORE SIZE IN PNICTIDE SUPERCONDUCTORS

P. Belova[1,2], M. Safonchik[1,3], K.B. Traito[1], E. Lähderanta[1]

[1] Lappeenranta University of Technology, Lappeenranta, Finland
[2] Petrozavodsk State University, Petrozavodsk, Russia
[3] Ioffe Physico-Technical Institute, Saint-Petersburg, Russia

For type II superconductors it has long been known that the low-lying quasiparticles excitations are confined to vortex cores. This size is matching with the superconducting coherence length. This means that the vortex core behaves like a cylinder of normal state materials with radius ξ_h. The presence of magnetic field dependence $\xi_h(B)$ is important for analysis of results of muon-spin rotation and small angle neutron scattering which is interpreted in the London model [1].

In this work the problem of transformation of quasiclassical Eilenberger theory to the London model is considered for the mixed state of pnictide superconductor having s± pairing symmetry. This type of symmetry has been discussed in [2] without microscopical approach. Numerical computations demonstrate that introduction of field-dependent coherence length is enough for description of the magnetic field distribution in the vortex core superconductors. It is found that in pnictide superconductor the shape of $\xi_h(B)$ has strong temperature dependence. Effect of non-magnetic scatters on ξ_h is also considered. The comparison of s± with both s- and d-wave pairing symmetries is done.

[1] J.E. Sonier, Rep. Prog. Phys. 70, 1717 (2007).
[2] A.B. Vorontsov, M.G. Vavilov and A.V. Chubukov, Phys.Ref.B 79, 140507(R) (2009).

WIDE-BAND SUPERCONDUCTING CARBON NANOTUBE FET

P. Häkkinen, A. Fay, P. Lähteenmäki, and P. Hakonen

Low Temperature Laboratory, Aalto University School of Science and Technology
Puumiehenkuja 2 B, Espoo, P.O. Box 15100, FI-00076 AALTO, FINLAND
email: pthakkin@cc.hut.fi

Superconducting carbon nanotube devices provide mesoscopic components that are at the same time low-impedance and charge-sensitive. This is exceptional because typically resistance of a nanosample has to be around the quantum resistance $R_Q = h/e^2$ in order to obtain charge quantization effects. The low impedance nature of such devices makes them very attractive for high frequency electrometry as the matching circuits between samples and the 50 Ohm measuring setup can be avoided.

We have investigated the response of nanotube Josephson junctions at 600-900 MHz using microwave powers corresponding to currents 0 … 10 I_C in the junction. We demonstrate the operation of superconducting FETs as charge detectors at high frequencies *without any matching circuits*. Gate-voltage-induced charge q modifies the critical current, which changes the effective impedance of the junction under microwave irradiation. This change, dependent on the transfer characteristics dI_C/dq, modifies the reflected signal and it can be used for wide-band electrometry. We estimate that a sensitivity of $4 \cdot 10^{-5}$ e/Hz$^{1/2}$ can be achieved in our samples with maximum switching current of I_C = 2.6 nA using this technique. Moreover, we have employed the Josephson inductance for phase-to-frequency conversion, in a similar manner as in a non-hysteretic rf-SQUID.

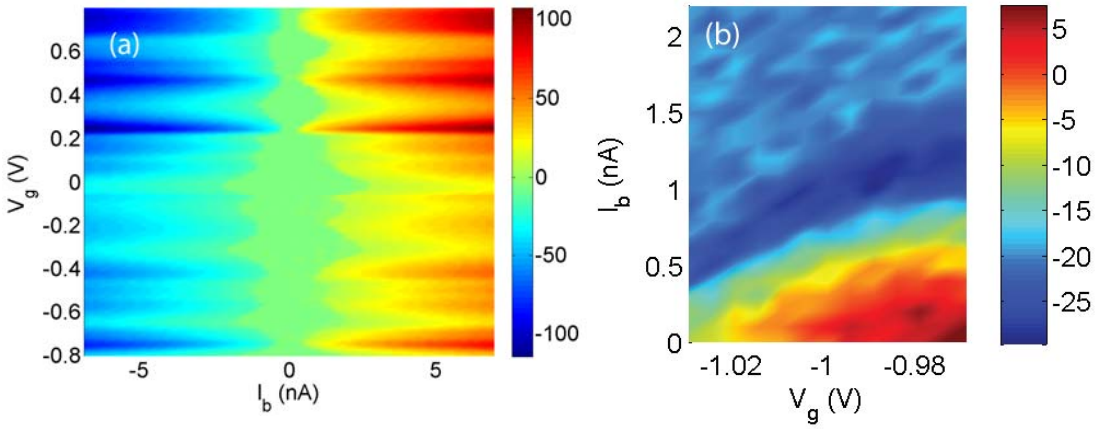

FIGURE**:** (a) Mapping of *IV*-curves measured on a MWCNT sample with Ti/Al contacts for different gate voltages;, the green area denotes the supercurrent regime (the voltages on the scale bar are given in μV). (b) Phase of the reflection signal (in degrees) indicating a change of the Josephson inductance when the Josephson energy is tuned by the gate voltage V_g and the bias current I_b.

THE ROLE OF INJECTION AND CHARGE-CARRIER CONCENTRATION ON ORGANIC MAGNETORESISTANCE

E. Holm[a], S. Majumdar[a,b], H. S. Majumdar[a] , R. Österbacka[a]

[a]Center of Excellence for Functional Materials and Department of Physics at Åbo Akademi University, Porthansgatan 3, 20500 ÅBO, FINLAND
[b]Wihuri Physical Laboratory University of Turku, Vesilinnantie 5, 20014 TURKU, FINLAND
email: erik.holm@abo.fi

Magnetoresistance on the order of 10% has been reported in Organic Light-Emitting Diodes (OLED) [1]. This could provide added functionality to the OLEDs and an enhanced efficiency of the devices. The theoretical understanding of the phenomenon is still incomplete, though previous results have shown that electron-hole pairs seem to play a critical role [2]. Organic magneto-resistance could potentially be used for making printed magnetic sensors for organic electronics applications [3].

The objective of this work is to clarify the dependence of OMAR on carrier polarity and concentration. This is done by studying the magnetoresistive behaviour of multi-layered organic diodes and organic thin-film transistors (OTFT). The diodes are used for clarifying the effect of charge-injection on the magnetoresistance, by using different injecting layers between the electrodes and the semiconductor.

The possibility of a magnetoresistive response in planar structures (see figure 2) is also being investigated. The advantage of planar structures compared to multi-layered structures is that it enables the possibility to study the effect of current modulation, and thus charge carrier concentration, by applying a gate bias.

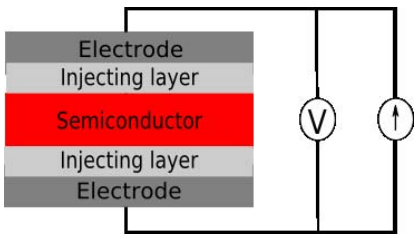

Figure 1: Organic diode

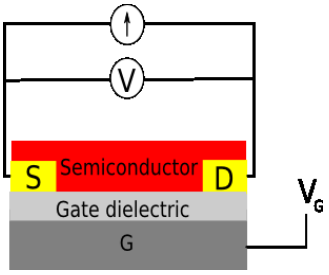

Figure 2: Organic thin-film transistor

[1] T. L. Francis et al., New. J. Phys., **6.** (2004) 9185
[2] S. Majumdar et al., Phys. Rev. B, **79** (2009), 201202
[3] S. Majumdar et al., PSS-A, **206** (2009), 2198-2201

EFFECT OF ELECTRIC FIELD ON DIFFUSION IN DISORDERED MATERIALS

F. Jansson[*,1,2], A. V. Nenashev[3,4], S. D. Baranovskii[5], F. Gebhard[5], R. Österbacka[2]
[*]email: fjansson@abo.fi
[1]Graduate School of Materials Research, Åbo Akademi University, Turku, Finland
[2]Department of Physics and Center for Functional Materials, Åbo Akademi University, Turku, Finland
[3]Institute of Semiconductor Physics, Novosibirsk, Russia
[4]Novosibirsk State University, Novosibirsk, Russia
[5]Department of Physics and Material Sciences Center, Philipps-University, Marburg, Germany

In numerous experimental studies on organic disordered materials, strong deviations from Einstein's relation $eD = \mu kT$, linking the diffusion coefficient D and the mobility μ, have been claimed [1]. Here e is the elementary charge, T is the temperature and k is the Boltzmann constant. Such deviations were also reproduced by numerical simulations [2]. The main source of deviations is the increase of the diffusion coefficient with increasing electric field. We performed extensive numerical and analytical studies of field-dependent diffusion for hopping transport with Gaussian distribution of site energies [3, 4]. The diffusion coefficient is shown to increase with electric field by several orders of magnitude even within the Ohmic regime, where the carrier mobility is almost constant. For hopping transport in three dimensions, our numerical simulations show a quadratic dependence of the diffusion coefficient D on the electric field F: $D(F) = D(0) + AF^2$.

For one-dimensional (1D) hopping, there are two models discussed in the literature: a random-barrier model (RBM), where all sites have equal energies, but are separated by barriers with randomly distributed heights; and a random-energy model (REM), where the site energies are randomly distributed. Unlike our 3D simulation results, the diffusion coefficient in the 1D RBM was claimed to have a linear field dependence in the limit of small fields [5]. To find a reason of this discrepancy, we derived exact analytical expressions for $D(F)$ in the REM. Our results for both the RBM and the REM give a linear field dependence for the diffusion coefficient. Therefore one should conclude that the discrepancy between the linear and the quadratic field dependencies of the diffusion constant reported in the literature is due to the different space dimensionalities considered in the different approaches.

[1] H.-J. Yuh, M. Stolka, Philos. Mag. B 58, 539 (1988).
[2] R. Richert, L. Pautmeier, and H. Bässler, Phys. Rev. Lett. 63, 547 (1989).
[3] F. Jansson, A. V. Nenashev, S. D. Baranovskii, F. Gebhard, and R. Österbacka, Ann. Phys. 18, No. 12, 856 - 862 (2009)
[4] A. V. Nenashev, F. Jansson, S. D. Baranovskii, R. Österbacka, A. V. Dvurechenskii, and F. Gebhard, arXiv:0912.3161 and arXiv:0912.3169
[5] J. P. Bouchaud and A. Georges, Phys. Rev. Lett. 63, 2692 (1989).

THERMAL MODELS OF SUPERCONDUCTING TRANSITION-EDGE SENSORS.

M. Palosaari, K. Kinnunen and I. Maasilta

University of Jyväskylä, Nanoscience Center, Department of Physics
P.O.Box 35, FI-40014 University of Jyväskylä, Finland
email: mikko.palosaari@jyu.fi

Microcalorimeters and bolometers based on superconducting transition-edge sensors (TES) have been under intense research and development during the last decade. A TES can be employed in a broad range of radiation detection applications by coupling it to a suitable absorber of radiation for the desired energy range. TESs provide excellent energy resolution and efficiency but require cryogenic temperatures. TES technology has reached a state of maturity where the focus has shifted from single devices to building large imaging arrays and developing multiplexed readout schemes.

Even though the energy resolution has steadily been improving, TES-based detectors still fail to reach the theoretical limits. All TES devices exhibit excess electrical noise of unknown origin which limits the performance. There are several theories that try to explain this excess noise but no general consensus on a definite noise mechanism has been reached so far.

Before one can talk of excess noise, we first need to be sure that all the conventional noise sources are taken into account. We show that by constructing a suitable thermal block model, the measured noise can be explained in terms of energy fluctuations between the different parts. The problem then is in correctly identifying the blocks and understanding the thermal links between them. Measured data indicates the existence of larger than expected heat capacity in the system. One possible source could be two-level systems. In addition to the noise data, we also need to simultaneously fit the measured complex electrical impedance curves of these devices.

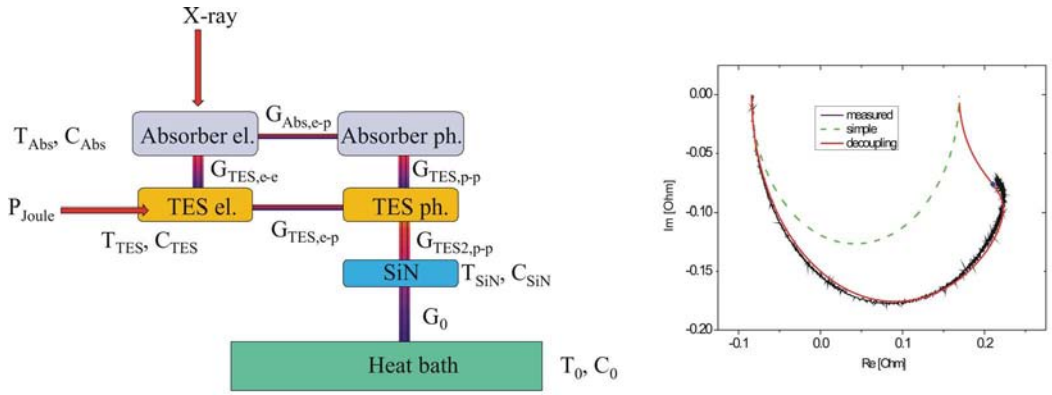

Figure 1: (Left) One possible thermal block model. (Right) Measured complex impedance data and calculated curves using a simple calorimeter model and a more complex model.

FABRICATION AND CHARACTERIZATION OF GRAPHENE-BASED SPIN VALVES

M. Pesonen[a], S. Majumdar[a,b], H. S. Majumdar[a] and R. Österbacka[a]

[a]Center of Excellence for Functional Materials and Department of Physics at Åbo Akademi University, Porthansgatan 3, 20500 Åbo, Finland
[b]Wihuri Physical Laboratory University of Turku , Vesilinnantie 5, 20014 Turku, Finland
email: markus.pesonen@abo.fi

Spintronics, being defined as electronics based on the spin properties of electrons, is a rapidly growing field. The spin valve is a typical spintronic device used in hard-disk drive technology. It is a layered structure consisting of two magnetic layers separeted by a non-magnetic spacer layer. The electric resistance of the device depends on the spin state of the electrons transported through the structure. The spin state can be altered by an external magnetic field which results in a differential electrical resistance. [1]

In recent years graphene has attracted a lot of interest in the field of condensed-matter physics and spintronics due to its unique intrinsic material properties, including zero band gap and exhibiting near ballistic transport at room temperatures. Such electronic properties make graphene an excellent choice of material as spacer layer in a spin valve structure. However, fabrication of devices wih monolayer or few layer of graphene is still a challenge.

The purpose of this work is to fabricate and characterize graphene-based spin valves, both in sandwich and planar configuration. Spin valves will be fabricated using a solution processable technique from an aqueous dispersion of graphene oxide (GO). GO will be spin-coated or drop-cast on desired substrates with ferromagnetic metals. The semiconductive GO film will be reduced to graphene by thermal annealing. A graphene spacer, with a few layers, will be obtained [2]. In case of sandwiched structures an additional layer of ferromagnetic material will be deposited on the reduced graphene layers. Magnetotransport measurements will be done in a temperature range of 300K to 5K. Results obtained from such measurements will be reported.

[1] Žutić et al., Spintronics: Fundamentals and applications, Rev. Mod. Phys. **76**, 323-410 (2004)
[2] Héctor A. Becerril et al., Evaluation of Solution-Processed Reduced Graphene Oxide Films as Transparent Conductors, ACS Nano **2**, 463-470 (2008)

LIGHT, WATER AND ELECTRICAL PROPERTIES OF LISICON BASED Al_2O_3 OFETS

F. S. Pettersson, N. Björklund and R. Österbacka

CoE for Functional Materials and Department of Physics, Åbo Akademi University, Porthansgatan 3, 20500 Åbo, Finland.
E-mail: frpetter@abo.fi

The promise of low-voltage operation and low-cost fabrication methods has fuelled the research into organic field-effect transistors (OFETs). Their performance has now reached a point where they can be compared to that of amorphous silicon transistors. OFETs, as opposed to traditional transistors, can be used to manufacture light-weight, flexible and large-area devices. In addition, OFETs can be manufactured utilizing solution processes, which is important if we want to use roll-to-roll (R2R) fabrication processes. Still, for R2R fabrication, several properties of the OFET need to be improved, such as lowering the operation voltage and improving stability in air.

The transistor model we have chosen is bottom-gate and we selected aluminum oxide as isolator and a commercially available amorphous polymer Lisicon as semiconductor. Using an organic low-*k* self assembled monolayer on the isolator reduces the disorder at the interface and improves the overall performance of the transistor. The advantages with this model is that it operates at low voltages (>5 V) and has fairly good on-off ratio (~400). The main problem is the low threshold voltage (<-2 V) and the fact that the electrical characteristics of the device seem to change with time.

To clarify why the performance changes with time we have examined the influence of oxygen, water and illumination on the transistor characteristics. We show that humidity and light affect the properties of the OFET, whereas the influence of oxygen is minimal. Also the dynamics of the transistor has been studied. The transistor shows a stretched exponential decay of the on-current when subjected to gate bias stress.

Characterization of defects in homoepitaxial non-polar ZnO:N grown by CVD

C. Rauch*,[1], F. Tuomisto[1], S. Eisermann[2], S. Lautenschläger[2], B. K. Meyer[2], M. R. Wagner[3], and A. Hoffmann[3]

[1] Department of Applied Physics, Aalto University, P.O. Box 11100, FI-00076 Aalto, Finland
[2] I. Physics Institute, Justus Liebig University Giessen, Heinrich-Buff-Ring 16, 35392 Giessen, Germany
[3] Department of Solid State Physics, Technical University Berlin, Hardenbergstrasse 38, D-10623 Berlin, Germany
* email: christian.rauch@tkk.fi

ZnO is regarded one of the most promising materials for the fabrication of future optoelectronic devices. Nevertheless, the lack of a reliable p-dopant still limits its full application. Amongst potential group-V acceptors nitrogen has been considered the most feasible candidate [1], although a recent theoretical study claims contradicting evidence [2]. In order to investigate the nature of intrinsic and extrinsic defects introduced by the doping process we used Positron annihilation and Raman spectroscopy to study ZnO:N thin films that have been deposited on nonpolar (a-plane) surfaces of hydrothermally grown ZnO single crystals by chemical vapor deposition (CVD) [3]. The detection of characteristic nitrogen Raman modes [4] confirms the successful incorporation of nitrogen into the lattice. Additionally, temperature dependent Doppler broadening measurements reveal a significant amount of large defect clusters, containing ar least two Zn-vacancies. The visible concentration of these $(V_{Zn})_n$-X clusters increases with the NH3-flow up to a saturation point at 60 sccm, from which it starts to decrease again. The Doppler measurements are strongly affected by the de-trapping of positrons to shallow traps, which extends up to temperatures of 500 K and hints at the presence of negative ions, i.e. active acceptors, in the material. Applying the temperature dependent positron trapping model [5] conclusions about the trapping coefficients and hence concentrations of both vacancy complexes and negative ions can be obtained.

[1] C. H. Park, S. B. Zhang and S. H. Wei, Phys. Rev. B 66 (2002) 073202.
[2] J. L. Lyons, A. Janotti and C. G. Van de Walle, Appl. Phys. Lett. 95 (2009) 252105.
[3] S. Lautenschläger, S. Eisermann, B. K. Meyer, G. Callsen, M. R. Wagner and A. Hoffmann, Phys. Stat. Sol. RRL 3 (2009) 1.
[4] A. Kaschner, U. Haboeck, M. Strassburg, M. Strassburg, G. Kaczmarczyk, A. Hoffmann and C. Thomsen, Appl. Phys. Lett. 80 (2002) 1909.
[5] M. J. Puska, C. Corbel and R. M. Nieminen, Phys. Rev. B 41 (1990) 9980.

Properties of random networks of carbon nanotube bundles

S. Seppälä[1], E. Häkkinen[1], M. J. Alava[1], V. Ermolov[2], E. T. Seppälä[2]

[1] Dept. of Appl. Phys., Aalto University, P.O.Box 11000, FI-00076 Aalto, Finland
[2] Nokia Research Center, Itämerenkatu 11-13, FI-00180 Helsinki, Finland

Carbon nanotubes form bundles due to van der Waals interaction. Carbon nanotube bundles can be broken down using various methods, but they can also be used as an electronic material without any post processing[1]. The properties of networks made from such bundles are dependent on the bundle properties (average number of parallel tubes inside a bundle D and the bundle length compared to the nanotube length l_{CNT}), and not only the usual parameters that define carbon nanotube networks, such as density and length of single nanotubes. Here we propose a novel approach to bundle networks by combining results from a bundle segment simulation with a stick network simulation. We then compare the results with those of ordinary carbon nanotube networks[2]. Using experimentally motivated parameters for the electronic properties of bundles, we find further statitstical investigation of carbon nanotube bundles interesting.

[1] Zavodchikova M. Y. *et al.* Phys. Stat. Sol. B 245 (2008) 2272.
[2] Li J., Zhang Z.-B. and Zhang S.-L. Appl. Phys. Lett. Vol. 91 (2007) 253127

NONEQUILIBRIUM GREEN FUNCTION APPROACH TO ELECTRONIC DYNAMICS IN FINITE INHOMOGENEOUS SYSTEMS

Adrian Stan[1], Anna-Maija Uimonen[1], Petri Myöhänen[1], Robert van Leeuwen[1,2]

1) Department of Physics, Nanoscience Center, University of Jyväskylä, Finland.
2) European Theoretical Spectroscopy Facility (ETSF).

We study charge transport through correlated molecular chains by propagating the Kadanoff-Baym equations [1]. The self-energy of the system is taken to be Hartree-Fock, Second Born, GW and T-matrix. After applying a bias voltage to the system or a weak "kick" (linear response), we determine the nonequilibrium properties of the system [2]. The results obtained within these approximations, for both long and short range interactions, are compared to exact numerical solutions [3].

[1] A. Stan, N. E. Dahlen and R. van Leeuwen *J. Chem. Phys.* **130** (2009) 224101.
[2] N. E. Dahlen and R. van Leeuwen *Phys. Rev. Lett.* **98** (2007) 153004.
[3] M. Puig von Friesen, C. Verdozzi, C.-O. Almbladh *Phys. Rev. Lett.* **103** (2009) 176404.

REAL-TIME SWITCHING BETWEEN MULTIPLE STEADY-STATES IN QUANTUM TRANSPORT

Anna-Maija Uimonen[1], Adrian Stan[1], Petri Myöhänen[1], Robert van Leeuwen[1,2]

1) Department of Physics, Nanoscience Center, University of Jyväskylä, Finland.
2) European Theoretical Spectroscopy Facility (ETSF).

We study transport through an interacting model system consisting of a central correlated site coupled to finite bandwidth tight-binding leads, which are considered as effectively noninteracting. Its nonequilibrium properties are determined by real-time propagation of the Kadanoff-Baym equations after applying a bias voltage to the system. The electronic interactions on the central site are incorporated by means of self-energy approximations at Hartree-Fock, second Born and GW level. We investigate the conditions under which multiple steady-state solutions occur within different self-energy approximations, and analyze in detail the nature of these states from an analysis of their spectral functions. At the Hartree-Fock level at least two stable steady-state solutions with different densities and currents can be found. By applying a gate voltage-pulse at a given time we are able to switch between these solutions. With the same parameters we find only one steady-state solution when the self-consistent second Born and GW approximations are considered. We therefore conclude that treatment of many-body interactions beyond mean-field can destroy bistability and lead to qualitatively different results as compared those at mean-field level.

[1] P. Myöhänen, A. Stan G. Stefanucci, R. van Leeuwen *Phys. Rev. B* **80**, 115107 (2009)

[2] Christian F.A. Negre and Pablo A. Gallay and Cristián G. Sánchez *Chem. Phys. Lett.* **460**, 220 (2008)

[3] N. C. Kluksdahl, A. M. Kriman, and D. K. Ferry, *Phys. Rev. B* **39**, 7720 (1989)

CONDUCTIVITY, SHOT NOISE, AND HOT PHONONS IN BILAYER GRAPHENE

A. Fay,[1] J. K. Viljas,[1] R. Danneau,[1] F. Wu,[1] M. Y. Tomi,[1] J. Wengler,[1] M. Wiesner,[1,2] and P. J. Hakonen[1]

[1]Low Temperature Laboratory, Aalto University School of Science and Technology, P.O. Box 15100, FI-00076 AALTO, Finland
[2]Faculty of Physics, Adam Mickiewicz University, 61-614 Poznan, Poland
email: janne.viljas@tkk.fi

We have measured the conductivity $\sigma = (dI/dV)(L/W)$ and Fano factor $F = S/2eI$ in short and wide ($L = 0.3$ μm, $W = 1.3$ μm) samples of bilayer graphene up to bias voltage $V = 1$ V [1]. At low bias ($V \lesssim 0.2$ V) we find that σ increases with V and at higher bias it begins to decrease. At $V \gtrsim 0.1$ V also F is reduced from the low-V value of ~ 0.3. These basic characteristics of the experimental results can be understood in terms of a simple model based on mean-free path arguments [2]. The high-V behavior is interpreted as a sign of the scattering of electrons from optical phonons and the associated heating of the latter, while the low-V increase in σ is due to the increase in the number of transport channels with V. The Fano factor is a measure of the effective electronic temperature and we find that the electrons can heat up to 1000 K at $V = 1$ V. Similar high-bias experiments have recently been carried out also for monolayer graphene [3].

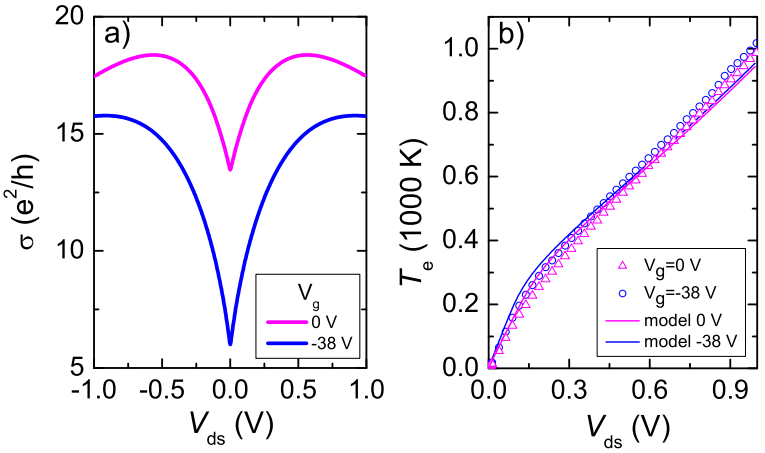

Figure 1: (a) Model result for conductivity σ vs. drain-source voltage $V_{\rm ds}$ at two gate voltages V_g, with $V_g = -38$ V corresponding to the charge neutrality point. (b) Electronic temperature T_e extracted from the experimentally measured Fano factor (symbols) and the model result (lines).

[1] A. Fay *et al.*, arXiv:0904.4446.
[2] See for example E. Pop *et al.*, Phys. Rev. Lett. **95**, 155505 (2005).
[3] A. Barreiro *et al.*, Phys. Rev. Lett. **103**, 076601 (2009).

SHOT NOISE IN SUPERCONDUCTOR-GRAPHENE SUPERCONDUCTOR JUNCTIONS

A. Fay, M. Tomi, P. Lähteenmäki, J. Viljas, and P. Hakonen

Low temperature Laboratory, Aalto University School of Science and Technology
P.O. Box 15100, FI-00076, FINLAND

A superconductor-graphene-superconductor (SGS) junction constitutes a superb system to probe the mesoscopic properties of graphene. When the junction is biased below the super-conducting gap (subgap region), the transport of quasiparticles from one super-conducting lead to the other one is achieved by multiple Andreev reflections (MAR) [1]. The transmitted effective charge q^* in a MAR process can be revealed by shot noise measurements [2]. Theory on SNS junctions [3-5] predicts different behavior for the shot noise and for the conductance depending whether the graphene sample is diffusive or ballistic. Interestingly, for the same SGS junction, we expect to reach both regimes: the quasi-diffusive regime at the charge neutrality point (CNP) and the ballistic regime far away from the CNP, as observed in our shot noise experiments [6].

We have investigated differential conductance and shot noise of Al-graphene-Al junctions at temperatures of 70 mK – 0.7 K. A layer of 10 nm of Ti was used in between the Al layer and graphene in order to achieve contacts with high transmission. The measured conductance shows subharmonic gap singularities at $V=2\Delta/n$ (n=1,2,3,4), which we attribute to coherent multiple Andreev reflections. All our measured junctions exhibit a supercurrent which demonstrates the good quality of our contacts. The shot-noise was measured at microwave frequencies (600-900 MHz), so that contributions from 1/f noise could be neglected. Far away from the Dirac point, the shot noise presents steplike behavior as a function of voltage. This result is in agreement with transport via several channels all having the same transmission coefficient on the order of 0.6. In this regime, each noise step is associated to a specific effective charge, related to the order of the MAR process. At the Dirac point, the steps disappear as expected for a diffusive junction [4]. We have also measured the shot-noise in the supercurrent branch and we find a significant increase of the noise close to the critical current due to phase diffusion.

[1] A. F. Andreev, Sov. Phys. JETP **19**, 1228 (1964).
[2] Ya. M. Blanter and M. Büttiker, Phys. Rep. **336**, 1 (2000).
[3] J. Cuevas, A. Martin-Rodero, and A. Levy Yeyati, Phys. Rev. Lett. **82**, 4086 (1999).
[4] Y. Naveh and D. V. Averin, Phys. Rev Lett. **82**, 4090 (1999).
[5] E. V. Bezuglyi, E. Bratus, V. Shumeiko, and G. Wendin, Phys. Rev. B. **63**, 100501 (2001).
[6] R. Danneau, F. Wu, M.F. Craciun, S. Russo, M.Y. Tomi, J. Salmilehto, A.F. Morpurgo, and P.J. Hakonen, Phys. Rev. Lett. **100**, 196802 (2008).

Corrections for Charged-Defect Supercell Density Functional Calculations

V. Virkkala and V. Havu

Aalto University, Department of Applied Physics, P.O. Box 11100, FI-00076 AALTO Finland
email: vvirkkal@cc.hut.fi

Density functional theory (DFT) is a quantum mechanical theory in which the electronic structure of the many-body system is determined based on the density of electrons in the system. DFT calculations are a common way to model defects in semiconductors. In DFT calculations, charged defects in periodic solids are typically modelled by supercells with periodic boundary conditions. This approach however leads to an unphysical electrostatic interaction between the defect and its periodic images. In this case the calculation of the total energy of the supercell diverges. To handle this divergence, the charge of the defect is typically compensated with a neutralizing background. This approach however leads to a slow convergence of the defect energy with respect to the supercell size.

Numerous attempts to remove finite-size effects in charged systems are presented in literature [1]-[4]. One way to estimate the interaction energy is to use a periodic array of point charges with a neutralizing background [1]. This leads to the Madelung correction $-\frac{1}{2}\frac{\alpha Q^2}{\varepsilon L}$, of the interaction energy, where α is the appropriate Madelung constant, Q is the defect charge, ε is the macroscopic dielectric constant and L is the lattice constant. In the Makov-Payne correction scheme [2] a further L^{-3} term, arising from the quadrupole moment, is added to the Madelung correction. However, in some cases these corrections do not improve the results [3] and for many defects the use of the Makov-Payne correction requires extremely large supercells. In ref. [3] an alternative approach to handle charged defects is introduced. In this method a localized charge q gives rise to the defect potential $V_{q/0}(\mathbf{r})$ with respect to the neutral cell. For practical purposes $V_{q/0}(\mathbf{r})$ is written as a sum of long-range Coulomb potential $V_q^{lr}(\mathbf{r})$ and short-range potential $V_{q/0}^{sr}(\mathbf{r})$. Their periodic versions $\tilde{V}_{q/0}(\mathbf{r})$, $\tilde{V}_q^{lr}(\mathbf{r})$ and $\tilde{V}_{q/0}^{sr}(\mathbf{r})$ are obtained using the Fourier transform. With help of these potentials and an alignement term C the energy correction can be written as a sum of the lattice energy E_q^{lat} of the charge density q_d with the compensating background and an alignement like energy $q\triangle_{q/0}$. In ref. [3] a very fast convergence of the formation energy in the case of Ga vacancy in GaAs is reported, when using this correction scheme.

In this work the method introduced in ref. [3] is implemented and its applicability to GaAs systems is studied. The required DFT calculations are performed using the Vienna *Ab initio* Simulation Package (VASP) with the projector augmented wave method and the local density approximation.

[1] M. Leslie and M. J. Gillan, Journal of physics C 18 (1985) 973.
[2] G. Makov and M. C. Payne, Physical Review B 51 (1994) 4014.
[3] C. Freysoldt and J. Neugebauer, Physical Review Letters 102 (2009) 016402.
[4] P. A. Schultz, Physical Review B 60 (1998)1551.

Modellization of Positronium in soft matter

A. Zubiaga and F. Tuomisto and M. Puska

Department of Applied Physics, Aalto University, P.O. Box 11100, Fin-00076 Aalto, Espoo, Finland
email: asier.zubiaga@tkk.fi

The study of the biomolecules and biolayers (lipid bi-layers) is important in biology and medicine. Biochemistry techniques have been very useful for the study of the the functionality of these techniques. In addition, physical techniques (X-rays difraction, Electron Paramagnetic Resonance, ...) are able to resolve the structure of the biomolecules and their spatial folding. Still some important properties are elusive to the presently available techniques. In case of lipid bi-layers, changes in their packing density are difficult to measure. They can affect the void size and density that is critical for the lateral diffusions of molecules through the cell membranes (lipid rafts) [1].

The positron annihilation spectroscopy is well suited for the study of the size and the density of nanometre scale voids in polymers. Recently, this technique has shown its applicability to measure changes in the voids size of lipid membranes during a thermal phase transformation [2]. Nevertheless, a complete discussion of the experimental data, will require theoretical modelling of the Ps molecule in biostructures, as has been done previously for positrons in condensed matter [3].

The positron wavefunction is the most relevant magnitude to be calculated but modeling the Ps (a light molecule) is challenging because its interaction with the matter is more complicated than for a positron (a particle). In addition, the big size of the discussed systems requires the use of molecular dynamics techniques to solve them. The problem can be treated with different levels of detail depending if the detailed wavefunction of Ps or only the Ps density distribution in the voids are required. While approximate solutions for the center of the mass has been obtained, they might not be accurate enough to describe the overlap of the positron wavefunction with the electrons in the matter. A discussion about the difficulties for a realistic modeling of Ps in soft matter and the possible strategies for its implementation will be presented.

[1] M. Edidin Ann. Rev. Biophys. Biomol. Struct. **32**, 257 (2003).
[2] P. Sane, E. Salonen, E. Falck, J. Repakova, F. Tuomisto, J. M. Holopainen and I. Vattulainen J. Phys. Chem. B **113**, 1810 (2009).
[3] K. Saarinen and P. Hautojarvi and C. Corbel, Semiconductors and Semimetals, *Positron Annihilation Spectroscopy of Defects in Semiconductors*, Academic Press (1998).

6 Particle and nuclear physics

6.1 Oral session I, Thursday 11 March 15:00-16:30
6.2 Oral session II, Friday 12 March 14:30-16:00
6.3 Oral session III, Saturday 13 March 9:00-10:30
6.4 Poster session I, Thursday 11 March 16:30-18:30
6.5 Poster session II, Friday 12 March 16:00-18:00

STATUS OF THE GEM-TPC DETECTORS FOR THE BEAM DIAGNOSTICS OF THE SUPER-FRS

F. Garcia[1], R. Janik[2], M. Kalliokoski[1], R. Lauhakangas[1], A. Numminen[1], M. Pikna[2], B. Sitar[2], P. Strmen[2], I. Szarka[2] and E. Tuominen[1]

[1]Detector Laboratory, Helsinki Institute of Physics and University of Helsinki, P.O.B. 64, FIN-00014 University of Helsinki, Finland
[2]Faculty of Mathematics, Physics and Informatics, Comenius University, Mlynská dolina, 842 48 Bratislava, Slovakia

email: matti.k.kalliokoski@helsinki.fi

Beam diagnostics system of the Superconducting Fragment Recoil Separator (Super-FRS) [1] is used for beam monitoring, ion identification and tracking. In the slow extraction part of the separator, Time Projection Chambers (TPCs) with GEM-amplification, GEM-TPCs, will be used for the diagnostics.

Prototype detector has sensitive volume of 264x120x56 mm with double GEM-amplification stage. The uniform electric in the TPC drift volume was up to 250 V/cm in the performances tests in a laboratory. Results were compared to simulations that were established with Garfield [2] and Geant4 [3] simulation tools.

[1] H. Geissel et al., The Super-FRS project at GSI, Nuclear Instruments and Methods in Physics Research B 204 (2003) 71–85.
[2] Garfield –simulation of gaseous detectors
[3] S. Agostinelli et al., Geant4 – a simulation toolkit, Nuclear Instruments and Methods in Physics Research A 506 (2003) 250–303

Masses for nuclear astrophysics with JYFLTRAP

A. Kankainen, V.-V. Elomaa, T. Eronen, J. Hakala, A. Jokinen, V.S. Kolhinen, I.D. Moore, J. Rissanen, A. Saastamoinen and J. Äystö
Department of Physics, University of Jyväskylä, P.O.Box 35 (YFL), FI-40014 University of Jyväskylä, Finland
email: anu.k.kankainen@jyu.fi

Atomic masses are one of the key input parameters in the modeling of astrophysical processes such as nucleosynthesis in novae or rapid proton capture (rp) and rapid neutron capture (r) processes taking place in hydrogen and neutron-rich environments, respectively. In a given environment (described by *e.g.* initial abundances, density and temperature), the path, time scale, energy release and final abundances of these processes depend on the masses and half-lives of the involved nuclides.

JYFLTRAP[1], a double Penning trap mass spectrometer at IGISOL, is ideal for measuring masses of astrophysically interesting nuclides with high precision. For explosive hydrogen burning in lower mass regions, the Q-values for the reactions ^{22}Mg(p,γ)^{23}Al[2], ^{25}Al(p,γ)^{26}Si[3] and ^{56}Ni(p,γ)^{57}Cu[4] have been measured with sub-keV precision. These results have an effect on calculated reaction rates. For example, the stellar production rate of ^{26}Si in nova ignition temperatures changes by about 10% and the uncertainties in the calculated reaction rate on ^{56}Ni decrease remarkably. Recent mass measurements with JYFLTRAP have shown a quenching of the SnSbTe cycle in the end-point region of the rp process in x-ray bursts [5]. With the new $^{104-108}$Sn, $^{106-110}$Sb, ^{108,109}Te and ^{111}I masses, strong cycling via alpha decays of Te isotopes can be excluded with high confidence. This results in a broader distribution of ^{68}Zn, ^{72}Ge, ^{104}Pd, ^{105}Pd and residual helium in the final composition and a slightly longer, less luminous burst tail. During the last 5 years, masses for about 90 neutron-deficient and 170 neutron-rich nuclides have been measured at JYFLTRAP. In this contribution, an overview of mass measurements for nuclear astrophysics with JYFLTRAP will be given.

[1] V.S. Kolhinen *et al.,* Nucl. Instrum. and Methods in Phys. Res. A 528 (2004) 776.
[2] A. Saastamoinen *et al.,* Phys. Rev. C 80 (2009) 044330.
[3] T. Eronen *et al.,* Phys. Rev. C 79 (2009) 032802(R).
[4] A. Kankainen *et al., to be published.*
[5] V.-V. Elomaa, G.K. Vorobjev, A. Kankainen *et al.,*
Phys. Rev. Lett. 102 (2009) 252501.

LASER SPECTROSCOPY: ACTIVITIES AT ISOLDE AND PROSPECTS AT THE FUTURE FAIR FACILITY

I.D. Moore for the ISOLDE IS457 Collaboration, the LaSpec collaboration and for the Manchester-JYFL-Birmingham collaboration.
Department of Physics, University of Jyväskylä, PB 35 (YFL) FI-40014, Jyväskylä, Finland

email: iain.d.moore@jyu.fi

The competition and balance between nuclear shell and collective effects results in a spectacular range of shapes and sizes within nuclear systems. High-resolution optical measurements provide sensitive, model-independent nuclear structure data. In particular, the size, shape, spin and moments of the nuclear charge distribution can be uniquely and reliably determined. The combination of sensitive atomic tools with on-line isotope separators and novel ion manipulation techniques are a powerful combination to provide fundamental information at the limits of stability.

In 2009 a successful campaign of high resolution optical spectroscopy measurements at ISOLDE using cooled and bunched beams from the newly installed ISCOOL device was performed on the gallium system. During the ISOLDE campaign, measurable yields of isotopes $^{67\text{-}82}$Ga across the N=50 shell closure enabled the extraction of nuclear spins, magnetic and quadrupole moments and isotope shift measurements, largely unknown prior to these measurements. The primary physics motivation, an investigation of the phenomenon of monopole migration, was validated via the ground state nuclear spin determination which showed a spin inversion taking place between ^{79}Ga and ^{81}Ga.

Novel optical manipulation techniques have been developed at JYFL in close collaboration with the Universities of Manchester and Birmingham, UK. Such new methods have dramatically extended the number of accessible ionic transitions, opening up new elemental regions previously thought to be inaccessible [1]. Such techniques will be directly transferrable to planned laser spectroscopy setups including that of LaSpec at the future Facility for Antiproton and Ion Research (FAIR), GSI, Germany. The LaSpec collaboration has been founded to exploit the opportunities at FAIR's Low-Energy Beamline (LEB) of the Super-Fragment Recoil Separator (S-FRS) [2]. Radioactive beams produced with the in-flight facility will be stopped in a gas cell, extracted as an ISOL-type beam and delivered to the low-energy mass spectrometry station (MATS) and to LaSpec.

This contribution will briefly discuss the recent ISOLDE success and present the future LaSpec facility, physics opportunities and present status.

[1] B. Cheal *et al*., Phys. Rev. Lett. **102** (2009) 222501.
[2] W. Nörtershäuser, P. Campbell and the LaSpec Collaboration, Hyp. Int. **171** (2006) 149.

NEW CHALLENGES BEYOND LOW BETA-DECAY Q VALUES

M.T. Mustonen and J. Suhonen

Department of Physics, P. O. Box 35 (YFL), FI-40014 University of Jyväskylä, Finland
email: mika.t.mustonen@jyu.fi

The record for the lowest measured beta-decay Q value was recently broken by two independent experiments for the ^{115}In decay to the first excited state of ^{115}Sn. These measurements were carried out by JYFLTRAP group in the University of Jyväskylä [1] and by Mount et al in the Florida State University [2]. Their results, 0.35(17) keV and 0.155(24) keV respectively, establish that this rare decay first observed by Cattadori et al [3] has roughly an order of magnitude lower Q value than the previous record-holder ^{187}Re.

Our theoretical study [1, 4] complementing the experimental effort of the JYFLTRAP group and HADES underground laboratory revealed that there is a significant gap in our understanding of the contributions from atomic effects for ultra-low Q values. As these corrections have the trend of growing more important the lower the Q value in the traditional domain of low Q values, they may play a dramatic role in the decays where the established approximations break down.

We present the case of ^{115}In ultra-low-Q-value decay and discuss the open question of different atomic corrections. We call for new theoretical efforts to fill this gap in the borderline between nuclear and atomic physics and new experimental efforts to support the theory with a reasonable amount of data on such decays.

[1] J.S.E. Wieslander et al, Phys. Rev. Lett. 103 (2009) 122501.
[2] B.J. Mount, M. Redshaw and E.G. Myers, Phys. Rev. Lett. 103 (2009) 122502.
[3] C.M. Cattadori et al, Nucl. Phys. A 748 (2005) 333.
[4] M.T. Mustonen and J. Suhonen, J. Phys. G: Nucl. Part. Phys. Focus Section: Open Problems in Nuclear Structure, in print.

RECOIL DECAY TAGGING STUDIES OF ^{173,175}PT

P. Peura[1], C. Scholey[1], T. Bäck[3], D. O'Donnell[2], P. T. Greenlees[1], U. Jakobsson[1], P. Jones[1], D. T. Joss[4], D. S. Judson[4], R. Julin[1], S. Juutinen[1], S. Ketelhut[1], M. Labiche[1], M. Leino[1], M. Nyman[1], R. D. Page[4], P. Rahkila[1], P. Ruotsalainen[1], M. Sandzelius[1], P. J. Sapple[4], J. Sarén[1], J. Simpson[2], J. Thomson[4], J. Uusitalo[1], and H. V. Watkins[4]

[1] Department of Physics, University of Jyväskylä, P. O. Box 35, FI-40014, Jyväskylä, Finland
[2] STFC Daresbury Laboratory, Daresbury, Warrington, WA4 4AD, United Kingdom
[3] Department of Physics, Royal Institute of Technology, Stockholm SE-10691, Sweden
[4] Oliver Lodge Laboratory, University of Liverpool, Liverpool, L69 7ZE, United Kingdom
email: pauli.j.peura@jyu.fi

The very neutron deficient region near or below the Z = 82 proton shell closure has been actively studied for many years. Nuclei in this region are well known to exhibit characteristics typically associated with shape coexistence. Studying odd-mass nuclei sheds light on the single-quasiparticle orbitals present near the Fermi surface. Two nuclei, ^{173}Pt and ^{175}Pt, have not been studied extensively before mainly due to the difficulties with clean correlations in recoil decay tagging (RDT) measurements. Problems arise from relatively low production cross-sections and alpha-decay branching ratios accompanied by long alpha-decay half-lives.

Recently, two separate measurements have been performed at JYFL both using a ^{86}Sr beam to bombard thin self-supporting ^{92}Mo targets. The first of these measurement was a RDT measurement, while the latter was a differential plunger life-time measurement. The nuclei ^{173}Pt and ^{175}Pt were produced via αn and 2pn particle evaporation channels, respectively.

In this work the previously observed yrast bands for ^{173}Pt [1] and ^{175}Pt [2] have been confirmed. For ^{175}Pt additional non-yrast structures have been discovered and the 13/2+ band head of ^{173}Pt was found to be isomeric. The ground state of these nuclei have shown evidence of alpha-decay fine structure. The results of these studies will be presented.

[1] D.T. Joss *et al.* Phys. Rev. C 74 014302 (2006)
[2] B.Cederwall *et al.* Z. Phys. A - Atomic Nuclei 337 (1990) 283–292

STUDY OF ^{180}Pb

P. Rahkila, P. Greenlees, U. Jakobsson, P. Jones, R. Julin, S. Juutinen, H. Koivisto, M. Leino, P. Nieminen, M. Nyman, P. Peura, T. Ropponen, P. Ruotsalainen, J. Sarén, C. Scholey, J. Sorri, J. Uusitalo
Department of Physics, University of Jyväskylä, Finland
email: panu.rahkila@phys.jyu.fi

D.G. Jenkins, O.J. Roberts, A.G. Tuff, R. Wadsworth
Department of Physics, University of York, United Kingdom

J. Pakarinen, C. Gray-Jones, P. Papadakis, S. Paschalis, M. Petri
Oliver Lodge Laboratory, University of Liverpool, United Kingdom

M. Bender
CNRS/IN2P3 & Université Bordeaux, Centre d'Etudes Nucléaires de Bordeaux Gradignan, France

P.-H. Heenen
Service de Physique Nucléaire Théorique, Université Libre de Bruxelles, Belgium

K. Heyde
Department of Subatomic and Radiation Physics, Ghent University, Belgium

Both theoretical and experimental evidence for shape coexisting configurations has been achieved in neutron deficient lead isotopes [1–3]. The phenomenon is rather striking particularly close to the neutron mid-shell N=104, where the intruding, deformed structures fall down to energies close to the spherical ground state.

In the late 1990's the first detailed experimental evidence of coexistence *beyond* the mid-shell in the lead isotopes (^{184,182}Pb) was achieved at the Jyväskylä Accelerator Laboratory [4, 5]. The almost vanishing production cross section ($\sim$10nb) delayed the extension of the data to ^{180}Pb for a decade. Combining newly developed Zr beams and the state of the art JUROGAM2/GREAT/RITU/TDR equipment allowed the first observation of excited states in 2009. Data shows slight deviations from the smooth parabolic trend, originating possibly from a perturbation caused by the proton unbound nature of the states or mixing with unobserved configurations at similar excitation energies.

[1] J. L. Wood, et.al, Phys. Rep.215, 101 (1992)
[2] W. Nazarewicz, Phys.Lett. B305, 195 (1993)
[3] R. Julin, K. Helariutta, and M. Muikku. J.Phys.(London) G27, R109 (2001)
[4] J. F. C. Cocks, et.al, Eur.Phys.J. A3, 17 (1998)
[5] D. G. Jenkins, et.al, Phys.Rev. C62, 021302 (2000)

News from ALICE Collaboration at CERN LHC

J. Rak for the **ALICE Collaboration**

University of Jyväskylä, P.O.B. 35 (YFL), FIN-40014 University of Jyväskylä, Finland
email: jan.rak@phys.jyu.fi

The first test with the colliding proton beams at the Large Hadron Collider took place on 23rd November 2009 giving the long-awaited opportunity to check detector performance in real conditions. Already these data, based on the total of 284 events acquired during the LHC test lasting just over 40 minutes, were sufficient for ALICE to produce the first paper [1] with the pseudorapidity dependence of $dN^{\rm ch}/d\eta$ for inelastic and non-single diffractive collisions, and with the charged-particle density in the central rapidity region. The measured values agree with UA5 results at the same centre-of-mass energy [2]. As the luminosity increased ALICE collected 0.5 million proton-proton events, corresponding to integrated luminosity of the order of 10 $\mu{\rm b}^{-1}$, at $\sqrt{s} = 900$ GeV accumulating sufficient statistics for comprehensive analysis. Just one week after the first collision LHC has reached the new world record in beam energy. The first preliminary results for the charged particle pseudo-rapidity density at $\sqrt{s} = 2.36$ TeV are shown in Fig. 1. By the time of the presentation we expect to have a multitude of new results that we intend to share with you.

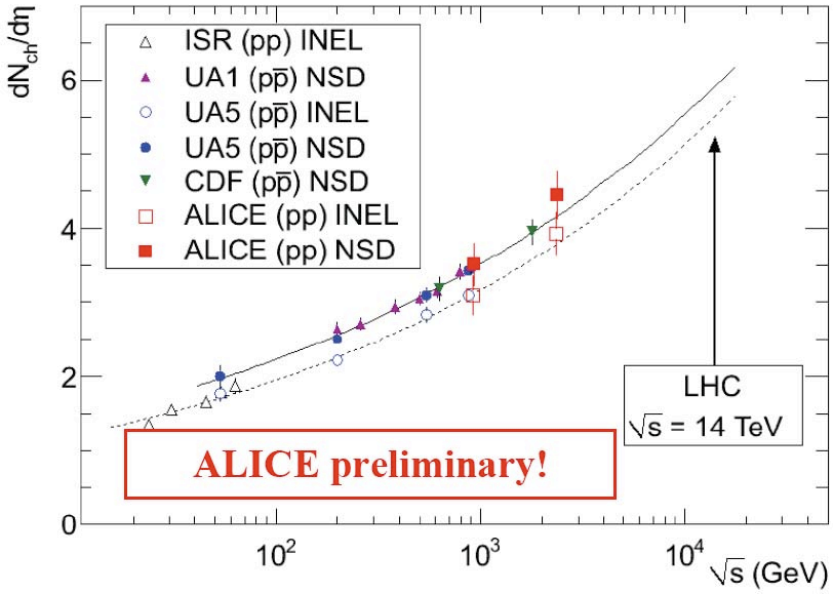

Figure 1: Charged particle rapidity density as a function of collision energy. The ALICE $\sqrt{s} = 2.36$ TeV points present the new (preliminary) results in this world record energy.

[1] ALICE Collaboration, Eur. Phys. J. C **65** (2010) 111
[2] UA5 Collaboration, Z. Phys. C **33** (1986) 1

UNNATURAL ORIGIN OF FERMION MASSES FOR TECHNICOLOR

Matti Antola, Matti Heikinheimo, Francesco Sannino and Kimmo Tuominen

Department of Physics, P.O.Box 35, FI-000140, University of Jyväskylä, Finland
email: matti.p.s.heikinheimo@jyu.fi

I will present our work published in [1]. We explore the scenario in which the breaking of the electroweak symmetry is due to the simultaneous presence and interplay of a dynamical sector and an unnatural elementary Higgs. We introduce a low energy effective Lagrangian and constrain the various couplings via direct search limits and electroweak and flavor precision tests. We find that the model we study is a viable model of dynamical breaking of the electroweak symmetry.

[1] M. Antola, M. Heikinheimo, F. Sannino and K. Tuominen, "Unnatural Origin of Fermion Masses for Technicolor," arXiv:0910.3681 [hep-ph].

PHYSICS TOPICS FOR EMMA

J. Sarkamo[1], T. Enqvist[1], J. Joutsenvaara[1], J. Karjalainen[1], P. Kuusiniemi[1], K. Loo[1,2], L. Olanterä[1], T. Räihä[1], P. Jones[2], T. Kalliokoski[2], M. Slupecki[2], W.H. Trzaska[2], A. Virkajärvi[2], L. Bezrukov[3], L. Inzhechik[3], B. Lubsandorzhiev[3], V. Petkov[3], H. Fynbo[4]

[1]University of Oulu, Finland
[2]University of Jyväskylä, Finland
[3]Russian Academy of Sciences, Moscow, Russia
[4]University of Arhus, Denmark
email: juho.sarkamo@oulu.fi

The main aim of EMMA[1], Experiment with MultiMuon Array, is to study the cosmic-ray composition by measuring the high-energy muon bundles and the lateral distribution of muons. The shower data can also be used to test the interaction models of air showers. Together with the the main aims, EMMA may offer a versatile physics programme of underground and astroparticle physics.

With muon tracking units we measure the high-energy muon intensity, search for muon anisotropies and muon bursts. Challenging topics include, for instance, the measurement of moon shadow or a measurement of the height of primary cosmic-ray interaction. Also, the timestructure of the shower front will be studied. The full array may act as 135 m^2 muon counter. Periodicity searches and seasonal modulation of the high-energy muon flux will be investigated.

A calibration setup on ground has a geometric acceptance of ~ 1 Sr m^2 and is, as a by-product, recording data. The well known dependence[2] of the intensity is shown below.

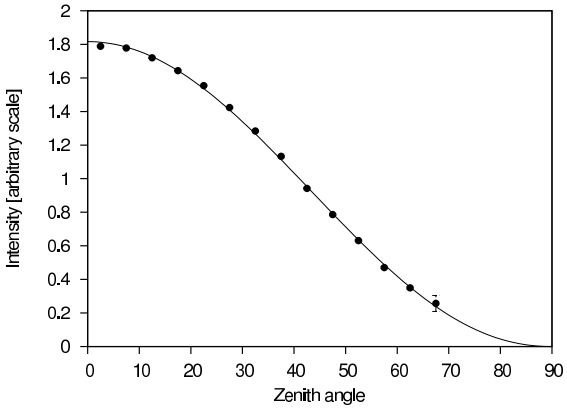

Figure 1: The measured zenith angle dependence of the surface muon intensity (circles), a cosine-law (line).

[1] T. Enqvist et al., Nucl. Phys. B (Proc. Suppl.) 196 (2009) 255-258.
[2] P. Grieder: "Cosmic Rays at Earth", Elsevier 2001, p. 372

SEARCH FOR THE LIGHT CHARGED MSSM HIGGS BOSON WITH HADRONIC FINAL STATE IN THE CMS EXPERIMENT AT THE CERN LHC

L. Wendland with A. Attikis, R. Kinnunen, M.J. Kortelainen, S. Lehti, and A. Nikitenko

Helsinki Institute of Physics, P.O.B. 64, FIN-00014 University of Helsinki, Finland
email: lauri.wendland@cern.ch

The Higgs boson(s) are a manifestation of a mechanism breaking the electroweak symmetry and generating masses to particles. The existence of charged Higgs bosons is predicted in all supersymmetric models such as the minimal supersymmetric standard model (MSSM), which is one of the most popular extensions of the standard model of particle physics.

The search for the light charged MSSM Higgs boson ($\mathrm{m_{H^{\pm}}} < \mathrm{m_{top}}$) produced with the $\mathrm{gg/q\bar{q}} \rightarrow \mathrm{t\bar{t}} \rightarrow \mathrm{tbH^{\pm}}$ process and decaying through the $\mathrm{H^{\pm}} \rightarrow \tau^{\pm}\nu_{\tau}, \tau \rightarrow \mathrm{hadrons} + \nu_{\tau}$ decay mode is discussed in the fully hadronic final state in the CMS experiment. This process is the most important one for the discovery of the light charged Higgs boson. The challenge of this decay channel is the identification of the hadronic τ decays amongst the copious production of hadronic jets in QCD multi-jet events at the LHC.

Simulation studies for separating the signal from the hadronic as well as electroweak backgrounds are reviewed. Preliminary results for the charged Higgs boson transverse mass spectrum and discovery significance are presented. Preliminary simulated results for the QCD multi-jet background measurement from the early LHC data are shown. Furthermore, a plan is presented for measuring the electroweak background from the early LHC data of muonic multi-jet events by replacing the measured and identified muon with a simulated τ jet.

The preliminary results indicate that the exclusion limits for the charged Higgs boson discovery published by the Tevatron experiments could be exceeded already for 200 pb^{-1} of integrated luminosity, which is expected to be collected within the first two years of LHC operation.

QUANTUM BOLTZMANN EQUATIONS FROM cQPA

M. Herranen, K. Kainulainen and P. M. Rahkila

Department of Physics, P.O. Box 35 (YFL), FIN-40014 University of Jyväskylä, Finland
Helsinki Institute of Physics, P.O. Box 64, FIN-00014 University of Helsinki, Finland
email: pmrahkil@phys.jyu.fi

Lately there has been considerable interest finding extended Boltzmann type equations for near equilibrium systems incorporating quantum corrections. We derive such equations for fermionic fields from Kadanoff-Baym equations using coherent quasiparticle approximation (cQPA) introduced in [1, 2, 3, 4, 5]. These equations describe bulk behaviour of quantum fields near thermal equilibrium with correlated internal degrees of freedoms; in particular we treat the effects of flavour coherence and coherent particle production or quantum reflection. Novel resumming methods needed to calculate the collision integrals are introduced. We also discuss the validity of the spectral ansatz inherent to cQPA in context of inhomogeneous backgrounds. Finally we discuss some applications of the formalism to the early universe particle physics processes such as leptogenesis, baryogenesis or neutrino flavor oscillations.

[1] M. Herranen, K. Kainulainen and P. M. Rahkila,
Nucl. Phys. B 810 (2009) 389 [arXiv:0807.1415 [hep-ph]].
[2] M. Herranen, K. Kainulainen and P. M. Rahkila,
JHEP 0809 (2008) 032 [arXiv:0807.1435 [hep-ph]].
[3] M. Herranen, K. Kainulainen and P. M. Rahkila,
JHEP 0905 (2009) 119 [arXiv:0812.4029 [hep-ph]].
[4] M. Herranen, K. Kainulainen and P. M. Rahkila,
Nucl. Phys. A 820 (2009) 203C [arXiv:0811.0936 [hep-ph]]
[5] M. Herranen, K. Kainulainen and P. M. Rahkila,
arXiv:0912.2490 [hep-ph]

BARYOGENESIS FROM STANDARD MODEL CP-VIOLATION

Anders Tranberg[a], Andres Hernandez[b], Thomas Konstandin[c], Michael G. Schmidt[b]

a) Helsinki Institute of Physics, P.O.Box 64, FIN-00014 University of Helsinki, Finland and Department of Physical Sciences, University of Oulu, Finland; b) Institut für theoretische Physik, University of Heidelberg, Germany; c) Institut de Fisica d'Altes Energies, Universitat Autónoma de Barcelona, Spain.
email: anders.tranberg@helsinki.fi

A central puzzle in Cosmology is the observed asymmetry between particles and anti-particles in the Universe. Although the two are equivalent from the point of view of quantum field theory, some process in the very early Universe, *Baryogenesis*, must have been biased in favour of matter, disfavouring anti-matter.

Recent measurements of the Cosmic Microwave Background [1] and fitting observations to calculations of the light element production during Nucleosynthesis [2], reveal that the asymmetry must have been established within the first second after the Big Bang, $T > 1\,\mathrm{MeV}$. The asymmetry is often encoded in the ratio of net baryon number density n_B to photon number density n_γ, and is found to be [1, 2] $\frac{n_B}{n_\gamma} \simeq 6 \times 10^{-10}$.

Models of baryogenesis require a combination of C-, CP- and B(aryon number)-violating processes, taking place out of thermal equilibrium. Surprisingly, these are all present in the Standard Model of particle physics (SM), prompting detailed investigation of what is known as *Electroweak Baryogenesis* [3]. Two caveats emerge from these studies: SM CP-violation is much too small at electroweak temperatures $T \simeq 100\,\mathrm{GeV}$ [3]; and the electroweak phase transition is too weak to account for the out-of-equilibrium conditions necessary for successful baryogenesis [4].

In the present work, we note that SM CP-violation is substantial at zero temperature [5]. This allows for direct numerical computation of the baryon asymmetry generated at a cold electroweak transition, triggered by the end of inflation. In this scenario of *Cold Electroweak Baryogenesis* [6, 7], post-inflationary reheating, electroweak symmetry breaking and baryogenesis happen simultaneously. Remarkably, we find that the observed asymmetry can be reproduced by this mechanism [8].

[1] D. N. Spergel *et al.* [WMAP Collaboration], Astrophys. J. Suppl. **170** (2007) 377.
[2] G. Steigman, arxiv:0912.1114.
[3] V. A. Rubakov and M. E. Shaposhnikov, Usp. Fiz. Nauk **166**, 493 (1996).
[4] K.Kajantie, M.Laine, K.Rummukainen and M.E.Shaposhnikov, Phys. Rev. Lett. **77**, 2887 (1996).
[5] A. Hernandez, T. Konstandin and M. G. Schmidt, Nucl. Phys. B **812** (2009) 290.
[6] E.J.Copeland, D.Lyth, A.Rajantie and M.Trodden, Phys. Rev. D **64**, 043506 (2001).
[7] A. Tranberg and J. Smit, JHEP **0311** (2003) 016.
[8] A. Tranberg, A. Hernandez, T. Konstandin and M. G. Schmidt, arxiv:0909.4199.

AN OVERVIEW OF THE SAGE SPECTROMETER

J. Sorri, P. Greenlees, P. Jones, P. Rahkila, P. Peura, R. Julin, S. Juutinen, P. Nieminen, M. Nyman, S. Ketelhut, M. Leino, J. Uusitalo, C. Scholey, J. Sarén, U. Jakobsson, P. Ruotsalainen, A. Herzan, K. Hauschild, A. Lopez-Martens

Department of physics, University of Jyväskylä, Finland
email:juha.m.t.sorri@jyu.fi

R.-D. Herzberg, P. Papadakis, J. Pakarinen, P.A. Butler, R.D. Page, E. Parr, J.R. Cresswell, D.A. Seddon, J. Thornhill, D. Wells, D. Cox

University of Liverpool, UK

J. Simpson, P.J. Coleman-Smith, I.H. Lazarus, S.C. Letts, V.F.E. Pucknell

STFC Daresbury Laboratory, UK

SAGE - a Silicon And GErmanium spectrometer - is a combined electron- and gamma-ray spectrometer especially designed for heavy element research [1]. The SAGE project was set in motion in 2005 and has made steady progress over the years. A full scale prototype of the required magnetic system was constructed and functionality and electron transport efficiency were tested successfully with the prototype system. The mechanical design required to combine the solenoid magnets and silicon detector with the existing JUROGAM II Ge-array [2], RITU recoil separator [3] and GREAT focal plane detector [4] is ready. Installation of the spectrometer is underway and the first on-line tests will be carried out at the end of February 2010. The results obtained during the first test experiment will be discussed.

The project is a collaboration of University of Liverpool, Daresbury Laboratory and University of Jyväskylä and is funded by the U.K. EPSRC, European Research Council (ERC), Finnish academy and Magnus Ehrnrooth's foundation.

[1] R.-D. Herzberg, P.T. Greenlees, In-beam and decay spectroscopy of transfermium nuclei, Progress in Particle and Nuclear Physics **61** (2008) 674-720
[2] P. J. Nolan, F. A. Beck, D. B. Fossan, Large Arrays of Escape-Suppressed Gamma-Ray Detectors, Annual Review of Nuclear and Particle Science, December 1994, Vol. **44**, Pages 561-607
[3] M. Leino, et al., Gas-filled recoil separator for studies of heavy elements, Nucl. Instrum. Meth. B **99** (1995) 653.
[4] R.D. Page et al. The GREAT spectrometer Nuclear Instruments and Methods in Physics Research B **204** (2003) 634-637
[5] I. H. Lazarus, The GREAT Triggerless Total Data Readout Method , IEEE TRANSACTIONS ON NUCLEAR SCIENCE, VOL. **48**, NO. 3, JUNE 2001 567

ALPHA CLUSTERS IN ^{32}S, ^{34}S AND ^{40}Ca

M. Norrby

Department of Physics, Åbo Akademi University, 20500 Turku, Finland
email: mnorrby@abo.fi

The three nuclei ^{32}S, ^{34}S and ^{40}Ca have been examined with the relatively new method of inverse kinematics and thick gas target. Experiments were carried out using the K-130 cyclotron at Jyväskylä University, accelerating 150 MeV beams of ^{28}Si, ^{30}Si and ^{36}Ar into a scattering chamber filled with helium gas. Detectors at forward angles recorded scattered α-particles and with the help of computer code the events can be traced back to the center-of-mass system and an excitation function constructed. This powerful method gives a continuous energy spectrum for several different angles in one single run, compared to the hundreds of measurements needed to obtain the same data with traditional methods that measure the cross section for many small energy intervals.

The data have been analyzed within the R-matrix formalism along the same lines as in [1]. The nucleus ^{32}S has been thoroughly investigated from an α-cluster point of view also in e.g. [2], [3] and the new data is compared to previous measurements. For both ^{34}S and ^{40}Ca the present data is mostly completely new. More than 100 resonances have been identified in each of the investigated nuclei. Most of these resonances have been assigned a spin value, although, quite tentative in some cases. The resonances in ^{32}S are interpreted as indication of a fragmented rotating α+^{28}Si cluster structure, as illustrated in figure 1.

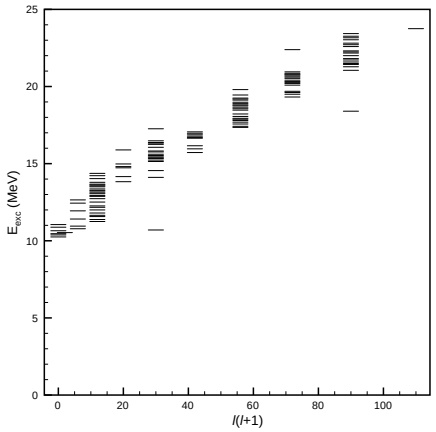

Figure 1: The linear dependency of energy vs. $l(l+1)$ for the resonances in ^{32}S indicates a rotational behavior.

[1] V. Z. Goldberg *et al.*, Physics of Atomic Nuclei **63**, 1518 (2000).
[2] K.-M. Källman *et al.*, Eur. Phys. J. A **16**, 159 (2003).
[3] M. Brenner *et al.*, Acta Phys. Hung. N.S. **11**, 221 (2000).

THEORETICAL DESCRIPTION OF NEUTRINO-NUCLEUS SCATTERING ON THE STABLE MOLYBDENUM ISOTOPES

E. Ydrefors and J. Suhonen

Department of Physics, P. O. Box 35 (YFL), FL-40014 University of Jyväskylä
email: emanuel.ydrefors@jyu.fi

The physics of the neutrino is one of the top questions of modern nuclear/particle physics. Neutrino-nucleus experiments constitute a promising tool for detection of neutrinos. One such example is the MOON (Mo Observatory of Neutrinos) experiment [1]. Theoretical estimates of rates of neutrino-nucleus scattering are therefore of great interest.

The stable molybdenum isotopes are promising targets of neutrino-nucleus scattering exeriments and we have calculated cross sections for them. The basic formalism originally developed by T.W. Donnelly and J.D. Walecka [2] has been combined with modern nuclear models to receive realistic results. We present our latest results and they are used to illustrate the basic features of the formalism.

[1] H. Ejiri, et. al., Eur. Phys. J. Special Topics 162 (2008) 239.
[2] J. S. O'Conell et. al., Phys. Rev. C 3 (1972) 719

DETERMINING ^{7}BE PRODUCTION RATE BY COSMIC RAYS USING WATER TARGET

A.-P. Leppänen

Radiation and Nuclear Safety Authority - STUK, Louhikkotie 28, 96500 Rovaniemi, Finland
email: ari.leppanen@stuk.fi

Galactic cosmic rays bombard the atmosphere continuously. In the nuclear reactions between atmospheric O and N and galactic cosmic rays cosmogenic isotopes ^{7}Be is formed. The use of ^{7}Be as a tracer for vertical atmospheric mixing has been proposed long time ago [1]. Recent theoretical developments in cosmic ray interactions and atmospheric has allowed a better use of ^{7}Be as atmospheric tracer [2], [3]. The full exploitation of ^{7}Be as atmospheric requires accurate models. The production rate ^{7}Be in atmosphere needs experimental data to validate theoretical models.

An experiment was performed in order to determine ^{7}Be production rate. Purified water was sealed into five plastic containers, approximately 7 liters per container. Few millilitres of HNO_3 was added to prevent ^{7}Be from sticking to the container walls. The containers were sealed and exposed to cosmic rays for 120 days at ground level. After exposure water was evaporated in a bowl coated with plastic sheet. The ^{7}Be atoms stuck to the plastic during the evaporation. After evaporation the plastic sheet was ashified in an oven. The ashes were then measured with HPGe detector to determine the amount of ^{7}Be. The measurement times were around 70-90 hours.

During the irradiation 50 000 -100 000 atoms of ^{7}Be were produced per sample thus production rates of 0.4-1.1x 10^{-5} atoms/(g s) were determined. This agrees with previously measured value of 0.90×10^{-5} atoms/(g s) [4].

[1] Lal, D., and Peters B. (1962), in *Progress in Elementary Particle and Cosmic Ray Physics*, v. 6, (eds. J. Wilson and S. Wouthuysen), pp. 77-243, North Holland, Amsterdam.
[2] I.G. Usoskin and G.A. Kovaltsov, Journal of Geophys. Res. 113, D12107, 2008
[3] I.G. Usoskin et al., Journal of Geophys. Res. 114, D011333, 2009
[4] D. Lal, J.R. Arnold and M. Honda, Phys. Rev. vol. 118, No 6, pp. 1626-1632, 1960

ELLIPTIC FLOW IN HYDRODYNAMICS WITH FLUCTUATING INITIAL CONDITIONS

H. Holopainen [a], H. Niemi [b] and K.J. Eskola [a]

[a] Department of Physics, P.O.B. 35, FIN-40014 University of Jyväskylä, Finland
[b] Frankfurt Institute for Advanced Studies, Ruth-Moufang-Str. 1, D-60438 Frankfurt am Main, Germany
email: hannu.l.holopainen@jyu.fi

Strong azimuthal anisotropy measured in Au+Au collisions at BNL-RHIC is one of the strongest signals of quark-gluon plasma formation in ultrarelativistic heavy-ion collisions. Hydrodynamical models have succeeded in predicting and explaining the measured azimuthal anisotropy which is quantified by Fourier coefficients. We are interested in the second coefficient called "elliptic flow". This far, however, almost all hydrodynamic models have underestimated elliptic flow in the most central collisions.

Studies of initial states for hydrodynamics, done via Monte Carlo Glauber modeling, show that eccentricity fluctuations are important in understanding the origins of elliptic flow especially in the most central collisions [1]. The drawback in these studies, however, is that the eccentricity is a calculational quantity which cannot be directly measured.

In the current work we use ideal relativistic hydrodynamics to evolve the fluctuating initial states to actually measurable particles on an event-by-event basis. We see that inclusion of the initial state fluctuations increases the elliptic flow to the level of the data.

[1] B. Alver et al., Phys. Rev. C 77 (2008) 014906.

SU(2) GAUGE THEORY WITH TWO ADJOINT DIRAC FLAVORS ON THE LATTICE

A. Hietanen[1], T. Karavirta[2], A-M. Mykkänen[3], J. Rantaharju[3], K. Rummukainen[3] and K. Tuominen[2]

[1]Department of Physics, Florida International University, Miami, FL 33199, USA
[2]University of Jyväskylä, PL 35 (YFL), 40014 University of Jyväskylä, Finland
[3]Department of Physics and Helsinki Institute of Physics, P.O.Box 64, FI-00014, University of Helsinki, Finland
email: tuomas.karavirta@jyu.fi

Recently there has been lot of interest in quantum field theories whose renormalization group evolution is governed by an infrared stable fixed point. This is due to phenomenological applications in beyond standard model physics: Such theories can underlie unparticles and walking technicolor. As a continuation of an initial lattice study of the two-color gauge theory with two adjoint Dirac flavors [1, 2, 3], we have carried out O(a) improvement with Wilson fermions using perturbative and nonperturbative methods. In this talk I will discuss the phenomenological motivations for this study, some technical issues and some physical results from simulations.

[1] A. Hietanen, J. Rantaharju, K. Rummukainen, K. Tuominen, Nucl.Phys.A820:191C-194C,2009.
[2] A. Hietanen, K. Rummukainen, K. Tuominen, Phys.Rev.D80:094504,2009.
[3] A. Hietanen, J. Rantaharju, K. Rummukainen, K. Tuominen, JHEP 0905:025,2009.

FEASIBILITY STUDIES OF LASER-ENHANCED RADIOACTIVE DECAY OF NUCLIDES

P. Aarnio[1], A.A. Andreev[2] and R. Salomaa[1]

[1]Aalto University, Department of Applied Physics, PO Box 14100, 00076 Aalto, Finland
[2]Laser Physics, St. Petersburg, 12 Birzhevaya Line, 199034, Russia
email: aarnio@tkk.fi

The basic idea is to excite a mother nucleus from its ground or long lived meta-stable state to a higher energy level from where it can decay to other states or to new daughter nuclei. In this process new isotopes will be generated. To achieve energy-selective excitation narrow band high energy photons are used. These photon-assisted nuclear processes have several interesting applications in nuclear technology: transmutation, development of novel type of radiation sources, efficient generation of e.g. Mössbauer and tracer isotopes [1].

Selective excitation in resonances in particle collisions is well known, similarly the giant gamma resonances. The photon interaction rates are, however, quite low because of the small cross sections and the weak spectral density of even the most intense, presently available photon sources. We have explored methods to generate intense narrow-band X-ray flashes arising in plasma interactions with super-intense lasers. Besides the assessment of laser based X-ray generation, the study involves finding suitable isotopes for demonstration and a survey of the possible show-stoppers of the method.

As regards, promising target isotopes for demonstration we have made a comprehensive search of nuclei taking into account production of the mother nucleus, its excitation scheme and detection. Several cases have been found: ^{87}Rb, ^{93}Mo, ^{94}Nb, ^{96}Tc, ^{99}Tc, etc. As photon sources we consider the laser-plasma excitation of selected targets emitting proper X-ray K -lines which have to match sufficiently with the excited nuclear state of the mother nuclide. Several alternatives where found and good X-ray conversion efficiency has been predicted for laser pulses of energy about 20 J, pulse length 200 ps, and a focal spot diameter of about 50 μm. We have also discussed the mass limited laser-targets consisting of nanometer scale spheres, cylinders or tube nets [2]. The Coulombic eplosion of such targets suggest very high X.ray intensities to be achieved.

The funding by the Academy of Finland is acknowledged

[1] R. Salomaa, P. Aarnio et al., Energy Conversion and Management 49 (2008) 1910.
[2] T. Sokollik et al., Phys. Rev. Lett. 103 (2009) 135003.

Resizing the Conformal Window: A beta function Ansatz

O. Antipin and K. Tuominen

Department of Physics, University of Jyväskylä, P.O.Box 35, FIN-40014 Jyväskylä, Finland and Helsinki Institute of Physics, P.O.Box 64, FIN-00014 University of Helsinki, Finland
email: oleg.a.antipin@jyu.fi, kimmo.tuominen@jyu.fi

We proposed an ansatz for the nonperturbative beta function of a generic non-supersymmetric Yang-Mills theory with or without fermions in an arbitrary representation of the gauge group. While our construction is similar to the recently proposed Ryttov-Sannino all order beta function, the essential difference is that it allows for the existence of an unstable ultraviolet fixed point in addition to the predicted Bank-Zaks -like infrared stable fixed point. Our beta function preserves all of the tested features with respect to the non-supersymmetric Yang-Mills theories. We predict the conformal window identifying the lower end of it as a merger of the infrared and ultraviolet fixed points.

MONTE-CARLO SIMULATION FOR ELASTIC ENERGY LOSS OF HIGH-ENERGY PARTONS IN A HYDRODYNAMICAL BACKGROUND

J. Auvinen, K. J. Eskola and T. Renk

Department of Physics, P.O. Box 35 FI-40014 University of Jyväskylä, Finland
email: jussi.a.m.auvinen@jyu.fi

Quark-gluon plasma (QGP) is formed when two ultrarelativistic heavy nuclei collide. This can be deduced e.g. from the azimuthal anisotropy of the produced particle spectra in non-central collisions [1], which implies early pressure formation, and from the substantial suppression of high-energy hadrons [2], hinting at the existence of a strongly interacting medium. We examine the significance of elastic collisions as the suppression mechanism of high-energy partons in the QGP. For this purpose we have developed a Monte Carlo simulation for describing the interactions of perturbatively produced high-energy partons with the quarks and gluons from the expanding QCD medium. The partonic collision rates are computed in leading-order perturbative QCD while the hydrodynamic properties of the QCD medium in the simulation are based on our group's previous work [3]. We compare our results [4] with the suppression observed in central Au+Au collisions at the BNL-RHIC.

[1] J. Adams et al. [STAR Collaboration], Phys. Rev. C72 (2005) 014904.
[2] S.S. Adler et al. [PHENIX Collaboration], Phys. Rev. Lett. 96 (2006) 202301.
[3] K. J. Eskola, H. Honkanen, H. Niemi, P. V. Ruuskanen, S. S. Räsänen, Phys. Rev. C72 (2005) 044904.
[4] J. Auvinen, K. J. Eskola and T. Renk, arXiv:0912.2265.

High-Precision Q_{EC} Values of Superallowed Beta Emitters for Testing the Standard Model

T. Eronen, V.-V. Elomaa, J. Hakala, J. C. Hardy†, A. Jokinen, A. Kankainen, I.D. Moore, M. Reponen, J. Rissanen, A. Saastamoinen, C. Weber and J. Äystö

University of Jyväskylä, Deparment of Physics, P.O. box 35 (YFL), FI-40014 University of Jyväskylä, Finland

†Cyclotron Institute, Texas A & M University, College Station, Texas 77843, USA

email: tommi.o.eronen@jyu.fi

The Standard Model is a theory that describes well three out of the four fundamental interactions and all elemental particles such as different flavour quarks and leptons that take part in these interactions. The Cabibbo-Kobayashi-Maskawa (CKM) matrix is used to explain mixing of different quark flavours. If the Standard Model is valid, the CKM matrix should be unitary.

The most stringent test for the CKM unitarity is the square-sum of the top-row matrix elements

$$V_{\mathrm{ud}}^2 + V_{\mathrm{us}}^2 + V_{\mathrm{ub}}^2 = 1. \quad (1)$$

The three matrix elements can be measured. At present, the precision of the elements V_{ud} and V_{us} have about same absolute precision. Contribution from V_{ub} in the current level of precision is negligible. Using the most recent world data, the unitarity is fully satisfied with a precision of about 0.1%.

Currently, the most precise value of V_{ud} is from superallowed nuclear beta decays [1]. These are decays between nuclear states having spin-parity $J^\pi = 0^+$ and isospin $T = 1$. About a dozen different decays have been measured to such a precision that they contribute to the determination of Vud. Among the three experimental quantities that are needed is the decay energy, also known as the Q_{EC} value. The experimental program to measure these Q values with the JYFLTRAP Penning trap mass spectrometer [2] has proven very successful owing to the IGISOL technique [3] which allows simultaneous production of both the decay parent and daughter ions. Also utilizing state-of-the art cleaning techniques to prepare clean samples of ions [4] and ion motion excitation with time-separated oscillatory fields [5, 6] provide record-breaking Q value precisions. In this contribution, an overview of JYFLTRAP Q_{EC} measurements will be given.

[1] J. C. Hardy and I. S. Towner, Phys. Rev. C **79**, 055502 (2009).
[2] A. Jokinen *et al.*, Int. J. Mass Spectrom. **251**, 204 (2006).
[3] J. Äystö, Nucl. Phys. A **693**, 477 (2001).
[4] T. Eronen *et al.*, Nucl. Instrum. Methods Phys. Res., Sect. B **266**, 4527 (2008).
[5] T. Eronen *et al.*, Phys. Rev. Lett. **100**, 132502 (2008).
[6] T. Eronen *et al.*, Phys. Rev. Lett. **103**, 252501 (2009).

CONSTRAINTS ON THE REHEATING TEMPERATURE FROM GRAVITINO DARK MATTER PRODUCTION AFTER INFLATION

A. Ferrantelli[1] and J. McDonald[2]

[1] University of Helsinki and Helsinki Institute of Physics,
P.O.Box 64, FIN-00014 University of Helsinki, Finland
[2] Cosmology and Astroparticle Physics Group,
University of Lancaster, Lancaster LA1 4YB, UK

We consider the dynamics of the supersymmetry-breaking scalar field and the production of dark matter gravitinos via its decay in a gauge-mediated supersymmetry breaking model with metastable vacuum [1]. We find that the scalar field amplitude and gravitino density are extremely sensitive to the parameters of the hidden sector. For the case of an O'Raifeartaigh sector, we show that the observed dark matter density can be explained by gravitinos even for low reheating temperatures $T_R < 10$ GeV. Such low reheating temperatures may be implied by detection of the NLSP at the LHC if its thermal freeze-out density is in conflict with BBN.

email: andrea.ferrantelli@helsinki.fi

[1] A. Ferrantelli and J. McDonald, "Cosmological evolution of scalar fields and gravitino dark matter in gauge mediation at low reheating temperatures,"
JCAP **1002** (2010) 003 [arXiv:0909.5108 [hep-ph]].

High-Precision Momentum Measurements of Projectile Fragments in ^{112,124}Sn + ^{112,124}Sn Collisions at 1 AGeV

V. Föhr[1,2], A. Bacquias[2], V. Henzl[2], A. Kelic[2], V. Ricciardi[2], K.-H. Schmidt[2], J. Äystö[1]

[1]Department of Physics, P.O. Box 35 (YFL), FI-40014 University of Jyväskylä, Finland
email: ville.t.fohr@jyu.fi

[2]GSI, Planckstraße 1, D-64291 Darmstadt, Germany

In peripheral heavy-ion collisions at relativistic energies, part of the projectile survives as an excited nucleus, named spectator. Nucleons in the overlap zone, the "participants", are subjected to violent collisions which can result in the emission of several fast nucleons or groups of nucleons which further on can modify significantly the characteristics of the spectators, introduce a certain amount of excitation energy, and change their kinematical properties. The influence of the participants on the spectators have been investigated and the results seem to indicate a sensitivity of the spectators mean longitudinal velocity to momentum dependence of the nuclear equation of state [1].

An innovative experimental technique which used the high-resolution magnetic spectrometer, the Fragment Separator (FRS) [2], at GSI Darmstadt [3, 4, 5], showed that it is possible to fully identify all final residues of high-energy nucleus-nucleus reactions and measure their longitudinal velocities with the extremely high precision required by the theory [1]. The experimental results confirmed the expected tendency predicted in ref. [1], in particular the re-acceleration of the lightest fragments. This work is devoted to study the effect of the isospin composition on the longitudinal velocity of the final fragments. At the FRS, GSI, we study the fragmentation of the two systems:^{112}Sn + ^{112}Sn and ^{124}Sn + ^{124}Sn at 1 AGeV.

For less peripheral collisions we observe again the complex phenomena of re-acceleration of spectator fragments which deviates from the empirical prescription of Morrissey [6]. Theoretical calculations with BUU transport code combined with an elaborate statistical evaporation code ABLA [7], have revealed the capability to reproduce the residue velocities when a momentum dependent mean field is introduced. The re-acceleration magnitude is not only ruled by the strength of the momentum dependent effects, but also by the incident velocity of the projectile, the size and composition of the reaction zone and nucleon-nucleon cross section.

[1] L.Shi, P.Danielewicz and R.Lacey, Phys. Rev. C64 (2001) 034601
[2] H. Geissel et al., Nucl. Instrum. Meth. B 70, 286 (1992)
[3] T. Enqvist et al., Nucl. Phys. A 658 (1999) 47-66
[4] M. V. Ricciardi et al., Phys. Rev. Lett. 90 (2003) 212302
[5] V. Henzl, PhD thesis, University of Prague, March 2006]
[6] D.J. Morrissey, Phys. Rev. C 39 (1989) 460.
[7] J.-J. Gaimard and K.-H. Schmidt, Nucl. Phys. A 531 (1991) 709

NUCLEAR STRUCTURE STUDIES OF NEUTRON-RICH NUCLEI PERFORMED BY JYFLTRAP

J. Hakala[1], J. Rissanen[1], V.-V. Elomaa[1], T. Eronen[1], A. Jokinen[1], J. Kurpeta[2], I. D. Moore[1], A. Kankainen[1], P. Karvonen[1], A. Plochocki[2], H. Penttilä[1], S. Rahaman[1], M. Reponen[1], A. Saastamoinen[1], J. Szerypo[3], W. Urban[2], C. Weber[1] and J. Äystö[1]

[1]Department of Physics, P.O.B. 35, FIN-40014, University of Jyväskylä,, Finland
[2]Faculty of Physics, University of Warsaw, ul. Pasteura 7, PL-02-093 Warsaw, Poland
[3]Sektion Physik, University of Munich (LMU), Am Coulombwall 1, D-85748 Garching, Germany
email: jani.hakala@phys.jyu.fi, juho.rissanen@phys.jyu.fi

Nuclear structure studies of neutron-rich nuclei becomes difficult at conventional ISOL facilities when going far from beta-stability due to high background generated by the nuclei within the same isobaric chain. Therefore, when studying the properties of the most exotic nuclei, the background level can be significantly reduced by using the Penning trap as a high-resolution mass filter to separate the nuclei of interest from the isobaric contaminants.

The unique possibilities of the IGISOL mass separator [1] coupled to the JYFLTRAP double Penning trap setup [2] have been used for nuclear spectroscopic studies at the University of Jyväskylä. The fission products have been isobarically purified with the Penning trap and sent forward to subsequent beta and gamma decay spectroscopy studies. By looking the gamma radiation emitted by the studied nuclei, one can build decay schemes to see a structure of the excited states fed by the beta-decaying parent nucleus.

The mass of the nucleus is an important ground state property having close connection for example to the shape of the nucleus. The JYFLTRAP Penning trap setup allows to measure atomic masses very precisely with a typical relative uncertainty of the order of 10^{-8}. By looking systematically the properties extracted from the mass values, the nuclear structure effects, such as shell and sub-shell closures as well as the deformation effects become visible. In this contribution, highlights of the latest nuclear structure studies, including mass measurements near the double-magic ^{132}Sn and spectroscopic studies in A = 110 region, will be presented.

[1] J. Äystö, Nucl. Phys. A **693** (2001) 477.
[2] A. Jokinen et al., Int. J. Mass Spectrometry 251 (2006) 204.

THE JYVÄSKYLÄ MCC30/15 CYCLOTRON PROJECT

P. Heikkinen

Department of Physics, P.O. Box 35 (YFL), FI-40014 University of Jyväskylä, Finland
email: pauli.heikkinen@jyu.fi

An Intergovernmental Agreement between Finland and Russia on the debt compensation by goods and services was signed in August, 2006. An H^- cyclotron from NIIEFA, St. Petersburg, Russia, for the University of Jyväskylä was proposed to be included in the list of goods. It took 10 months until the contract of the cyclotron was finally approved and the project could start. According to the contract the cyclotron should have arrived 19th of June, 2009. The cyclotron required an extension for the old experimental hall. The building of the extension started in late August, 2008, and it was scheduled to be ready by Midsummer, 2009. Both the cyclotron and the building projects took a little more time than planned. However, the delay of both projects was less than two months, and so the building was ready to host the cyclotron by the beginning of August, 2009. The cyclotron arrived at Jyväskylä on 10th of August, and the installation started immediately. The cyclotron was installed by the manufacturer's specialists. According to the plan the cyclotron should be ready and running six months after arrival.

The new MCC30/15 cyclotron accelerates protons (H^-) to energies 18 – 30 MeV and deuterons (d^-) to energies 9 – 15 MeV. Maximum intensity in the tests was 200 μA for protons and 62 μA for deuterons, well above the guaranteed values of 100 and 50 μA, respectively. The beams will be used for the IGISOL facility, which will move into the new premises during 2010 as well as for isotope production, which will start later.

EFFECTIVE MODELS OF TWO-FLAVOR QCD: FROM SMALL TOWARDS LARGE $\mathbf{m_q}$

T. Kähärä and K. Tuominen

Department of Physics
P.O.Box 35, FIN-40014 University of Jyväskylä, Finland

email: topi.kahara@jyu.fi

We study effective models of chiral fields and Polyakov loop expected to describe the dynamics responsible for the phase structure of two-flavor QCD. We consider chiral sector described either using linear sigma model or Nambu-Jona-Lasinio model and study how these models, on the mean-field level when coupled with the Polyakov loop, behave as a function of increasing bare quark (or pion) mass. We find qualitatively similar behaviors for the cases of linear sigma model and Nambu-Jona-Lasinio model and, by comparing with existing lattice data, show that one cannot conclusively decide which of the two approximate symmetries drives the phase transitions at the physical point [1].

[1] T. Kahara and K. Tuominen, Phys. Rev. D **80** (2009) 114022

THE PROSPECTS OF THE IGISOL SHIFT

T. Eronen, J. Hakala, A. Jokinen, A. Kankainen, P. Karvonen, V. S. Kolhinen, I.D. Moore, H. Penttilä, J. Rissanen, M. Reponen, A. Saastamoinen, V. Sonnenschein and J. Äystö

Department of Physics, P.O.Box 35 (YFL), FI-40014 University of Jyväskylä, Finland
email: penttila@jyu.fi

The IGISOL mass separator facility [1] at the Accelerator Laboratory of the University of Jyväskylä, JYFL, has been a stage of vivid research of the nuclear landscape in its extremes. Light- and heavy-ion induced fusion reactions have been used to produce neutron deficient isotopes up to N = Z line, while proton- and deuteron-induced fission of natural uranium has been the source of neutron-rich nuclei in the mass region A = 70 - 170. The ion guide technique utilized at the IGISOL allows the production of mass separated ion beams of any element, enabling the possibility to perform systematic studies.

The JYFLTRAP Penning trap is an intrinsic part of the IGISOL facility. Atomic masses of over 200 neutron-rich nuclei have been measured with JYFLTRAP with an accuracy of a few keV. JYFLTRAP can also be used to produce mass separated sources of atoms of a single isotope or even a single isomer.

The IGISOL facility will have a major upgrade starting in the summer of 2010. The whole facility will be moved to a new experimental area next to a new high current MCC30/15 light-ion cyclotron. The beam from the JYFL heavy ion K-130 cyclotron can be directed to the IGISOL target as well. This will allow the doubling of the run time of the IGISOL facility to about 4000 hours a year. Neutron converter targets are planned to be utilized in order to study neutron-induced fission. An extend beam distribution system and a larger floor space will afford more permanent spectroscopic setups. Extended space allows also a better access for laser beams used in ion production and manipulation. In the presentation, the possibilities of the extended IGISOL laboratory are summarized and discussed.

[1] P. Karvonen, et al., Nucl. Instr. and Meth. B 266, 4454 (2008).

EXPONENTIALLY DECAYING NUMBER ALWAYS OBEYS A BINOMIAL DISTRIBUTION

S. Kasi

Kajavankatu 6 B 45, FIN-04230 Kerava, Finland
email: servo.kasi@kolumbus.fi

Let N be a number decaying as

$$n = N(1-\exp(-\lambda T)) \qquad (1)$$

during the time period T. The number n has been decayed (failed, disintegrated, etc.), and N-n is left. $\lambda = \ln(2)/T_{½}$. $T_{½}$ is the half-life of the decay. (1) is generally valid for the radioactive nuclides. That n has the binomial distribution is in [1] shown thoroughly.

$$p = (1-\exp(-\lambda T)) \qquad (2)$$

has been set for the probability of disintegration of a single nuclide. We have the standard deviation

$$\Delta n = \sigma(r) = \sqrt{n}\exp(-\lambda T/2) \qquad (3)$$

for the stochastic variable r of n. Δn is small when T is very small, and also when T is very large, that is, when $n = N$. If $T << T_{½}$ you can use the Poisson statistics. The binomial distribution can be calculated as fast as that of Poisson statistics (below, also [2]).

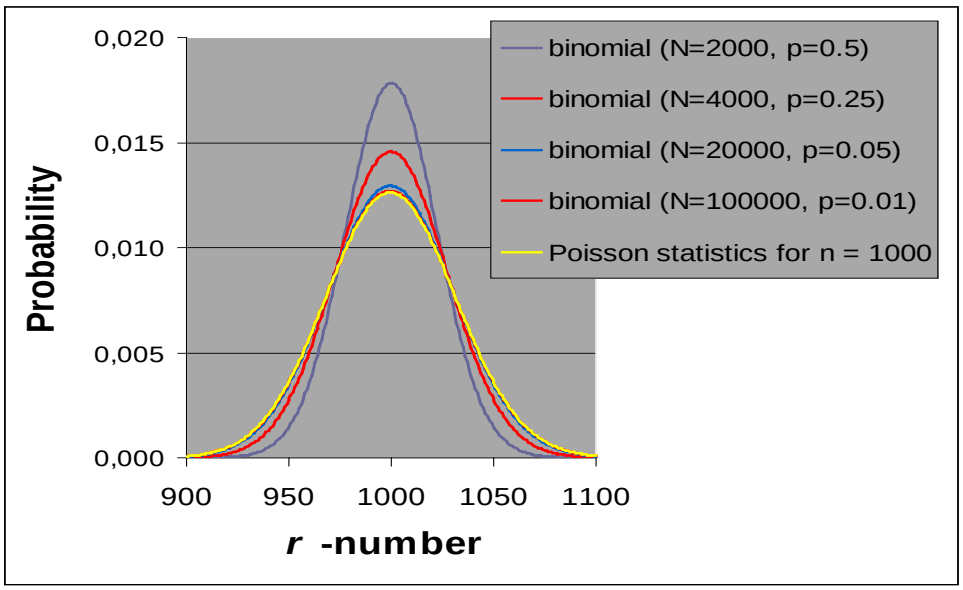

Above the estimate E(r) = n. However, N is seldom known exactly. The problem is Bayesian. n can often be determined (measured). When $T << T_{½}$ then E(r) = n + 1 [3]. The situation must be another (maybe contrary) when n is close to N.

[1] S.S.H. Kasi, Error of number of radioactive disintegrations is to be published.
[2] S.S.H. Kasi, Stochastics of radioactive decay is to be published. It has a poster.
[3] Rainwater, L.J., Wu, C.S., 1947, Application of probability theory to nuclear particle detection. Nucleonics 1, October, 60-69.

Accurate Q value for the $^{74}\mathrm{Se}$ double-electron-capture decay

V.S. Kolhinen, V.-V. Elomaa, T. Eronen, J. Hakala, A. Jokinen, M. Kortelainen*, J. Suhonen J. Äystö.

Department of Physics, Post Office Box 35(YFL), FIN-40014 University of Jyväskylä, Finland
email: veli.kolhinen@jyu.fi
*Department of Physics and Astronomy, University of Tennessee, Knoxville, Tennessee 37996, USA and Physics Division, Oak Ridge National Laboratory, P.O. Box 2008, Oak Ridge, Tennessee 37831, USA

A massive neutrino is an indication of physics beyond Standard Model (SM). Several experiments like SNO, K2K and MINOS are showing proof of nonzero neutrino mass. These experiments, however, can only provide evidence on neutrino mass without revealing nature of it (Dirac or Majorana) nor do they give absolute scale for neutrino masses. Therefore, it is important to investigate other methods to gain information on these issues. Neutrinoless double-β decay, if detected, would provide a possible tool to probe these questions. We have started to look for a possible candidate for $0\nu\beta\beta$ resonant decay where the daughter has excited state which energy is close to the Q value between the mother and daughter atoms. The degeneracy of the initial state and final excited state can enhance the decay rate by factor of 10^6 [1]. Recently we have measured the Q value for $^{74}\mathrm{Se} \rightarrow ^{74}\ \mathrm{Ge}$ with the record accuracy of 50 eV [2] by using the JYFLTRAP double Penning trap spectrometer by applying Ramsey excitation pattern in the Time-of-Flight measurements. The achieved accuracy of 50 eV is more than sufficient for experiments searching neutrinoless 0νECEC decay. The determined value is 1209.169(49) keV, which practically excludes the possibility of a complete energy degeneracy with the second 2^+ state (1204.205(7) keV) of $^{74}\mathrm{Ge}$ in a resonant 0νECEC decay. We have also computed the associated nuclear matrix element by using a microscopic nuclear model with realistic two-nucleon interactions. The computed matrix element is found to be quite small. The failure of the resonant condition, combined with the small nuclear matrix element and needed p-wave capture, suppresses the decay rate strongly and thus excludes $^{74}\mathrm{Se}$ as a possible candidate to search for resonant 0νECEC processes. We intend to continue this search with the Q value measurement for $^{96}\mathrm{Ru} \rightarrow ^{96}\ \mathrm{Mo}$ decay during spring 2010.

[1] S. Rahaman et al., Phys. Rev. Lett. 103 (2009) 042501.
[2] V.S. Kolhinen, V.-V. Elomaa, T. Eronen, J. Hakala, A. Jokinen, M. Kortelainen, J. Suhonen J. Äystö, Phys. Lett. B. Article in press, doi:10.1016/j.physletb.2009.12.052.

THE TRANSVERSE SHAPE OF THE ELECTRON

S. Kurki

Department of Physics and Helsinki Institute of Physics,
P.O.B. 64, FIN-00014 University of Helsinki, Finland
email: samu.kurki@helsinki.fi

We study [1] the transverse charge density, electromagnetic form factors, and spin composition of the electron in impact parameter space. We calculate the charge density of the $|e\gamma>$ Fock state in light-front quantization, which allows us to answer an old question already posed by Feynman. We show that the $|e\gamma>$ Fock state contributing to the electron form factors is compact as the momentum transfer goes to infinity. We calculate the angular momentum contributions of the electron and the photon, which conserve the spin of the electron locally in impact parameter space.

[1] P. Hoyer and S. Kurki, The transverse shape of the electron, arXiv:0911.3011 [hep-ph].

TRACK RECONSTRUCTION AND VISUALISATION IN EMMA

T. Räihä[1], L. Bezrukov[2], T. Enqvist[1], H. Fynbo[3], L. Inzhechik[2], P. Jones[4], J. Joutsenvaara[1], T. Kalliokoski[4], J. Karjalainen[1], P. Kuusiniemi[1], K. Loo[1], B. Lubsandorzhiev[2], L. Olanterä[1], V. Petkov[2], J. Sarkamo[1], M. Slupecki[4], W.H. Trzaska[4], A. Virkajärvi[4]

[1]University of Oulu, Finland, [2]Russian Academy of Science, Moscow, Russia, [3]University of Århus, Denmark, [4]University of Jyväskylä, Finland
email: tomi.raiha@oulu.fi

The cosmic-ray experiment EMMA [1] is being built at a depth of 80 metres in the caverns of Pyhäsalmi mine in Finland. It will consist of nine detector stations of which three are so-called tracking stations that can be used to reconstruct muon tracks and the shower arrival direction. EMMA will measure high-energy muon bundles that are characterised by a relatively high density and by a parallelism of tracks. By detecting hits of muons in up to six positions in three position sensitive double-layer detectors it is possible to reconstruct tracks of muons since they travel along straight lines and are parallel with the shower direction with one-degree accuracy. In addition, tracking stations will be upgraded by high-resolution scintillation units [2] that will improve the reconstruction of high-multiplicity muon bundles.

We have developped the track reconstruction programme ETANA (EMMA Tracking ANAlysis programme) for the reconstruction of hit positions and tracks of muons with the tracking stations. The maximum muon multiplicity that can be reconstructed with the station (~ 15 m^2) is around 200 which is sufficient even for the highest muon densities expected from simulations.

It is important to have a good visualisation programme to present simulated and reconstructed events. The visualisation is especially needed in the development of algorithm of the track reconstruction and when scanning real reconstructed events to ensure that track reconstruction is working properly.

We have designed the visualisation programme for EMMA by using Root TEve classes. They offer a flexible and relatively easy way to create an elegant and versatile environment to display OpenGL graphics. In the programme events can be browsed by arrow buttons and, in case of simulated data, both the reconstructed and simulated tracks can be shown in the same view. Tracks and hits can be classified into different categories and their information can be checked via pop-ups. Tabs were also added to show histograms and information related to a current event. So far the visualisation works only for one tracking station at a time but the programme will be extended to cover all nine stations.

[1] T. Enqvist et al., Nucl. Phys. B (Proc. Suppl.) 196 (2009) 255-258.
[2] E.V. Akhrameev et al., NIMA 610 (2009) 419-422.

HOMOGENISATION OF GROUP CONSTANTS IN REACTOR PHYSICS

Antti Räty
VTT Technical Research Centre of Finland & Department of Physics, University of Helsinki. Mail address: P.O.B. 1000 (Tietotie 3), FI-02044 VTT, Finland
email: antti.raty@vtt.fi

Many analysis on reactor physics model a reactor core as homogeneous regions or nodes each usually covering a fuel bundle in the horizontal direction. Moreover, the present neutrons are classified according to their kinetic energy to discrete energy group assuming similar physical properties for all the neutrons within a group. Consequently, a diffusion equation, eq. (1), can be written to describe the movement of neutrons for a group g in a single node

$$-\nabla\cdot D_g\nabla\Phi_g+\sum_{g'\neq g}\Sigma_{g\to g'}\Phi_g=\sum_{g'\neq g}\Sigma_{g'\to g}\Phi_{g'}+(1-\beta)\chi_g\sum_{g'}\nu\Sigma_{f,g'}\Phi_{g'}$$
$$+\chi_g\sum_k\lambda_k\beta_g\int_{-\infty}^{t}e^{-\lambda_k(t-\tau)}\nu\Sigma_{f,g'}\Phi_{g'}d\tau. \qquad (1)$$

Group constants are parameters of diffusion equation (D, Σs, β, ν, λ).
Homogenisation of group constants means changing the representation of the process parameters to one dimension in the axial direction assuming that the correct node-averaged reaction rates are preserved separately. This results in defining the one-dimensional quantity as flux-volume weighted averages of the three-dimensional values. Nevertheless, it requires introducing a new degree of freedom to conduct the flux-weighting for the parameters defining the equation for the flux. The problem was studied in ref. [1] with two different methods.

1. Parametrising the group constants as functions of thermal hydraulic state parameters (e.g. moderator pressure or density, fuel temperature etc.) of the core such that the response in one-dimensional case equals response in three-dimensional case.
2. Equivalence theory, or introducing a certain continuity condition for the flux between adjacent nodes and thus re-defining the whole equation in one-dimension.

Technical Research Centre of Finland (VTT) has applied for homogenisation a code called CROCO using the former method. Especially in the case of boiling water reactors (BWR) the code was outmoded in the current calculation scheme, so a few new modules were written in Fortran language to update these features. The construction was tested with three points from an even power-up situation in a BWR comparing the results to values produced with the code SIMULATE-3 applying equivalence theory. Results displayed sufficient correspondence in level-wise relative power distributions and group constants from the two first groups.

[1] A. Räty, *Homogenisation of Group Constants in Reactor Physics*, Master's Thesis (Theoretical Physics), University of Helsinki, 2009

FAIR ACTIVITIES AT JYFL; HISPEC/DESPEC, MATS AND LASPEC

S. Rinta-Antila, P.T. Greenlees, A. Jokinen, R. Julin, V.S. Kolhinen, M. Leino, I.D. Moore, H. Penttilä, J. Sarén, C. Scholey and J. Äystö

Department of Physics, P.O.B. 35 (YFL), FIN-40014 University of Jyväskylä, Finland
Helsinki Institute of Physics, P.O.B. 65, FIN-00014 University of Helsinki, Finland
email: sami.rinta-antila@phys.jyu.fi

FAIR is an international accelerator facility at GSI for the research with ion and antiproton beams. At the moment this 1.2 billion EUR project is about to enter into its construction phase. Once completed the FAIR accelerators will deliver 1 GeV/u beams of heavy ions with intensities upto 10^{11} ions/s to the experimental setups of the multi user facility [1].

Nuclear Structure, Astrophysics and Reactions research at FAIR is organised under NuSTAR collaboration. NuSTAR experiments exploit the exceptional range of radioactive beams provided by SuperFRS in its three branches for different energies and characteristics. University of Jyväskylä, Department of Physics (JYFL) is involved in three of the sub projects of NuSTAR, namely HISPEC/DESPEC, MATS and LaSpec.

In the HISPEC (High-resolution In-flight SPECtroscopy) setup radioactive beams in the energy range of 3-150 MeV/u are used to create nuclear reactions to study transition probabilities, single particle spectroscopic factors, high-spin states, nuclear shape etc. The main tool in HISPEC is the novel AGATA gamma ray tracking array that records nuclear de-excitation through gamma emission after nuclear reaction. DEcay SPECtroscopy (DESPEC) with rare radioactive beams implanted in an active stopper provides a tool to probe properties of nuclei at the extreme regions of the nuclide chart. Topics like r-process nucleo-synthesis of heavy elements in supernova explosions and the unitarity of the CKM matrix in the Standard Model of electroweak interactions can be explored.

MATS (Precision Measurements of very short-lived nuclei using an Advanced Trapping System for highly-charged ions) is a novel Penning trap facility. The aim is to measure atomic masses of radioactive species and perform trap assisted spectroscopy with isobarically purified beams. By measuring the masses of atoms accurately enough one can for example get information on nuclear structure, reaction Q values which is among the most critical nuclear parameters in reaction network calculations for nucleosynthesis and find new isomeric states in nuclei.

The LaSpec (Laser Spectroscopy of short-lived nuclei at FAIRs low energy branch) setup consists of a number of complementary experimental devices to provide a complete system with respect to the physics and isotopes that can be studied at FAIR. Laser spectroscopy of radioactive isotopes and isomers is an efficient, selective and model-independent approach for the determination of nuclear ground and isomeric state properties.

[1] http://www.gsi.de/fair/index_e.html.

RECOIL-BETA TAGGING STUDY OF N=Z NUCLEUS ^{66}As

P. Ruotsalainen[a], C. Scholey[a], B.S. Nara Singh[b], R. Wadsworth[b], D.G. Jenkins[b], C.J Barton[b], M.A. Bentley[b], L. Bianco[c], J.E. Brown[b], P.J. Davies[b], P.T. Greenlees[a], U. Jakobsson, P. Jones[a], D.T. Joss[c], R. Julin[a], S. Juutinen[a], S. Ketelhut[a], M. Leino[a], M. Nyman[a], R.D. Page[c], P. Peura[a], P. Rahkila[a], P. Sapple[c], J. Sarén[a], J. Sorri[a], M.J. Taylor[b], J. Uusitalo[a]

[a]Department of Physics, University of Jyväskylvä, P. O. Box 35 (YFL), FI-40014, Finland
[b]Department of Physics, University of York, Heslington, York YO10 5DD, UK
[c]Oliver Lodge Laboratory, University of Liverpool, Liverpool L69 7ZE, UK
email: panu.ruotsalainen@jyu.fi

A Recoil-Beta Tagging (RBT) experiment was recently performed in order to identify T=1 excited states in the medium-heavy N=Z=33 nucleus ^{66}As. The aim of this study was to yield information especially on the Coulomb energy differences (CED) between the T=1 isobaric analogue states of ^{66}As and ^{66}Ge. The CED can reveal various nuclear phenomena such as nucleon-nucleon pairing effects and shape co-existence. In the case of mirror nuclei, where the nuclei have inverse neutron and proton numbers the CED can be used to extract information about the proton-neutron (p-n) pairing interaction. The possible changes in the p-n pairing strength also have an influence on nuclear shapes. This leads to the concept of shape co-existence where the same nucleus can have either spherical, oblate or prolate shapes depending on the configuration of valence nucleons. In addition the information gained for excited states in the neutron deficient $A \sim 70$ mass region, adds to our understanding of the astrophysical rp-process.

The experiment was carried out at the University of Jyväskylä accelerator laboratory utilising the JUROGAM II γ-ray spectrometer in conjunction with the gas-filled recoil separator RITU and the GREAT focal plane spectrometer system. The ^{66}As-nuclei were produced via ^{28}Si(^{40}Ca,pn)^{66}As reaction at a beam energy of 75 MeV. This experiment was successful due to the technical developments in the measurement set-up. New 50 μm thick Mylar windows were installed for the multi-wire proportional counter, which allowed a higher gas pressure to be used in RITU, thereby improving the separation between the recoils of interest and beam like projectiles. The planar germanium detector was used to detect the beta particles as well as γ-rays.
A tentative level scheme for ^{66}As was reported by Grzywacz et al [1], [2]. The data obtained from this experiment reveals some discrepancies with the previous work. This presentation will discuss the most recent results regarding the ^{66}As, lightest nucleus ever studied at RITU.

[1] R. Grzywacz et al., Nucl. Phys. A 682 41 (2001)
[2] R. Grzywacz et al., Phys. Lett. B 429, 247 (1998)

EXOTIC DECAYS FOR ASTROPHYSICS BY IMPLANTATION TECHNIQUE

A. Saastamoinen[a], L. Trache[b], A. Banu[b], M. A. Bentley[d], T. Davinson[c], V. E. Iacob[b], D. Jenkins[d], A. Jokinen[a], M. McCleskey[b], B. Roeder[b], E. Simmons[b], G. Tabacaru[b], R. E. Tribble[b], P. J. Woods[c], J. Äystö[a] and the MARS group

[a] Department of Physics, University of Jyväskylä, Jyväskylä, Finland
[b] Cyclotron Institute, Texas A&M University, College Station, Texas, USA
[c] School of Physics and Astronomy, University of Edinburgh, Edinburgh, UK
[d] Department of Physics, University of York, Heslington, UK
Contact email: antti.j.saastamoinen@jyu.fi

The key parameters in understanding the astrophysical reaction rates are the energies and decay widths of the associated nuclear states along the reaction paths. The relevant states for particle capture reactions are located in the Gamov window, just above the associated particle separation threshold (e.g. proton separation energy, S_p). The properties of these states can be probed by using direct reaction studies or by indirect methods, which include β-decay studies.

The challenge in β-decay studies of the states that are proton unbound and near the separation threshold, is that the energy of the emitted protons is low and the particle detector setups are also sensitive to β-particles emitted. In these exotic decay modes the β-particles are by far more frequent than the interesting decay products of small branchings. In addition to challenges posed by the detection setup, the production of the exotic nuclei for the samples is demanding and usually a trade-off between purity and intensity of the sample has to be done.

In this contribution we introduce our method, where we couple the intense secondary beams of high purity available from the Momentum Achromat Recoil Separator [1] at the Cyclotron Institute of the Texas A&M University to a novel detector setup. With this setup we can measure simultaneously particle and gamma emissions from well defined implantation source. A description of the detector setup and results of the performance in studies of β-decays of ^{23}Al and ^{31}Cl with a comparison to earlier studies (e.g. [2, 3], respectively) are given.

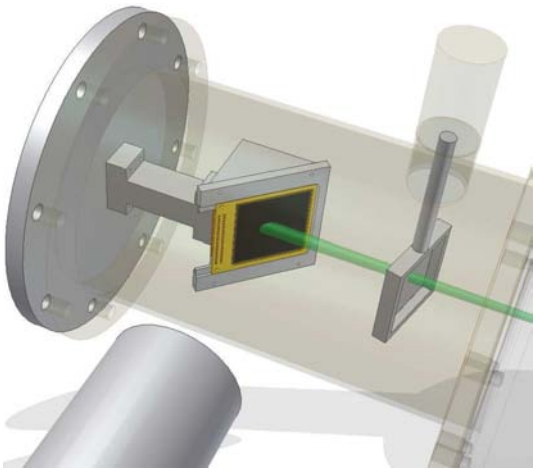

[1] R. E. Tribble et al., Nucl. Phys. A701 (2002) 278c
[2] K. Peräjärvi et al., Phys. Lett. B492 (2000) 1
[3] A. Kankainen et al., Eur. Phys. J. A27 (2006) 67

Measuring absolute transmission values of the RITU gas-filled separator

J. Sarén, J. Uusitalo and M. Leino

Accelerator Laboratory, University of Jyväskylä, P.O. Box 35 (YFL), FI-40014 University of Jyväskylä
email: jan.saren@jyu.fi

Absolute transmission values through the RITU gas-filled recoil separator [1] has been measured in the Accelerator Laboratory of the University of Jyväskylä for several different fusion evaporation residues. For the transmission measurements three different stable isotope beams, ^{20}Ne, ^{40}Ar and ^{84}Kr, were taken from K130 cyclotron and for each beam several different target materials were used. In all reactions well known isotopes in mass region 170-190 were produced mostly in neutron evaporation channels. Also the pressure of the Helium gas was varied in the range between 0.2 and 1.8 mbar to achieve the largest transmission for each reaction.

A reaction channel was identified using the JUROGAM Ge-detector array. At the RITU focal plane multi-wire proportional counter (MWPC) and double sided Silicon-strip detector (DSSD) were used to register the transmitted fusion products. Production yields for reactions channels used were large enough so that gamma-gamma coincidences could be used to achieve clear identification also without recoil tagging which is crucial when measuring the absolute transmission. In the reaction ^{168}Er(^{20}Ne,4n)^{184}Pt the transmission of 8 % through the RITU to MWPC was obtained for ^{184}Pt. In the more symmetric reaction ^{150}SmF(^{40}Ar,4n)^{186}Hg the transmission was 47 % and in the most symmetric reaction ^{90}Zr(^{84}Kr,2n)^{172}Os the transmission was 77 %. However, when symmetric reaction were used more scattered beam reached the focal plane. The optimal gas pressure was observed to be a function of reaction asymmetry. The magnetic rigidity of the products was seen to decrease monotonically in function of increasing gas pressure.

Additionally to the measured experimental transmissions, also the physical processes causing observed behavior will be discussed in more detail. Some principles of gas-filled separator modeling will be presented and results of simple fusion kinematics and ion-optical models applied to the studied reactions will be compared to the measured results.

[1] M. Leino et al., Nucl. Instr. and Meth. B 99, (1995) 653

ASPECTS OF HOLOGRAPHIC QUANTUM HALL TRANSITION

J. Alanen, . Keski-Vakkuri and V. Suur-Uski

Department of Physics, P.O.B. 64, FIN-00014 University of Helsinki, Finland
email: ville.suur-uski@helsinki.fi

A review of recent developments in the holographic methods in condensed matter physics.

[1] J. Alanen, V. Suur-Uski and E. Keski-Vakkuri , JHEP 0911:014,2009.

FINNISH KNOW-HOW BEHIND THE FIRST PUBLISHED LHC EVENT

W. H. Trzaska

HIP and Dep. of Phys., P.O. Box 35 (YFL), FI-40014 University of Jyväskylä, Finland
email: wladyslaw.h.trzaska@jyu.fi

The first proton collisions at LHC took place at 16:47 on Monday, 23 November 2009. Within seconds from the first event, when a handful of tracks have been reconstructed in the Silicon Pixel Detector (SPD) as originating from a unique vertex, the event was visualized on the ALICE display. Apparently, the LHC operators must have managed a direct hit immediately after converging the two beams for the first time! Over the next 40 minutes nearly 300 more collision events were seen before the beam was switched off completing a successful LHC test. Just five days later the first ALICE paper was submitted and, after a small revision, published online on 11 December 2009. This first "real" LHC paper [1, 2] became an instant hit: EPJ has chosen it as a Highlight Paper and the pictured event adorns now the cover of the January 2010 issue of EPJ C (Fig.1).

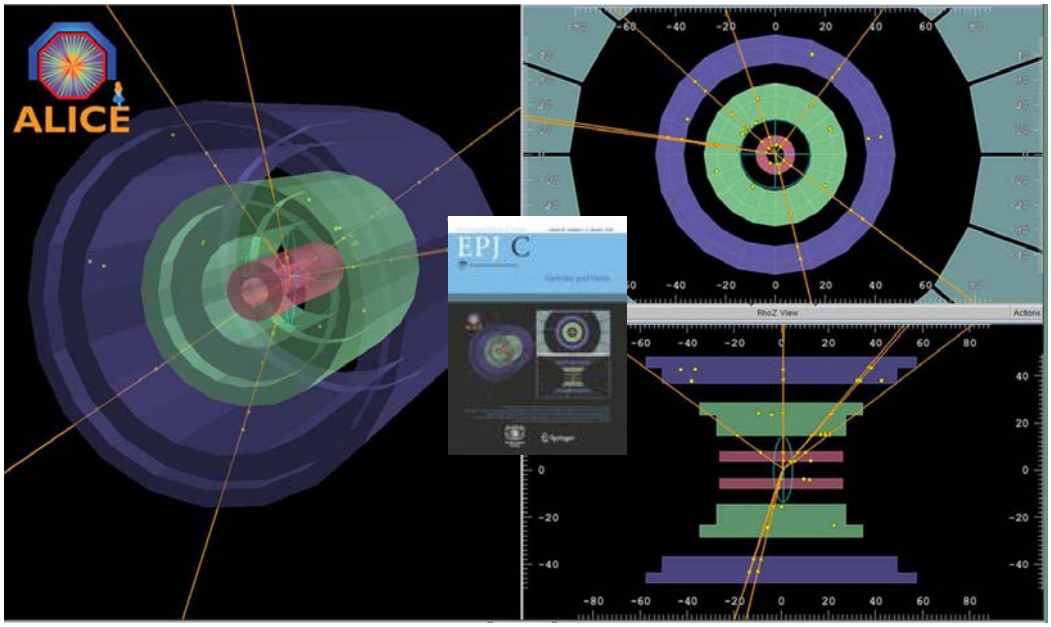

Fig.1. The first LHC event appeared on the front cover of Jan. 2010 issue of EPJ C.

What is much less known is the extent to which the Finnish know-how made the detection of the first LHC collision possible. In my talk, in addition to reminding the work done within HIP, I'll present the amazing contribution from the Finnish High-Tech Industry that remains completely unknown event to the scientific community in the country. One can safely state that without Finnish know-how ALICE would not have won the race for the first LHC event.

[1] The ALICE Coll., Eur. Phys. J. C DOI 10.1140/epjc/s10052-009-1227-4
[2] J. Rak, et al. in these proceedings.

DISTRIBUTED DATA-ANALYSIS WITH ADVANCED RESOURCE CONNECTOR MIDDLEWARE IN THE COMPACT MUON SOLENOID EXPERIMENT

E. Edelmann[2], K. Happonen[1], J. Klem[3], J. Koivumäki[1], T. Lindén[1], A. Pirinen[1], J. Välimaa[1]

[1] Helsinki Institute of Physics, P.O.B. 64, FIN-00014 University of Helsinki, Finland
email: Joni.Valimaa@Helsinki.FI

[2] Nordic Data Grid Facility, Kastruplundgade 22, DK-2770 Kastrup, Denmark

[3] European Organization for Nuclear Research, CERN CH-1211, Genève 23, Switzerland

To solve the Large Hadron Collider (LHC) computational challenge a worldwide computing system called the Worldwide LHC Computing Grid (WLCG) has been constructed. The WLCG is as important for the succesful analysis of the data as the LHC and the detectors. Helsinki Institute of Physics (HIP) has created together with CSC a Tier-2 computing resource, which is part of WLCG, for distributed analysis of Compact Muon Solenoid (CMS) data. HIP has has participated in the last few CMS computing challenges " Computing, Software and Analysis Challenge 08", "Scale Testing for the Experimental Program in 2009" and the October Exercise to demonstrate the readiness of the Tier-2 facility for data-analysis of LHC collision data.

The CMS computing model from a Tier-2 perspective is described as well as the Advanced Resource Connector (ARC) grid infrastructure in Finland. The integration of the CMS computing infrastructure with ARC middleware resources for distributed analysis is presented.

HEAVY QUARK-ANTIQUARK POTENTIALS IN HOT QCD

M. Vepsäläinen

Department of Physics, P.O. Box 64, FI-00014 University of Helsinki, Finland
email: mikko.vepsalainen@helsinki.fi

At high temperatures ordinary hadronic matter goes over to a new phase, where quarks and gluons are liberated from their confinement to color neutral hadrons. Properties of deconfined QCD matter are actively studied both experimentally in heavy-ion collisions and theoretically using analytical and numerical calculations.

One of the classic probes for forming a quark-gluon plasma is the change in the properties of heavy quarkonium [1]. Because of the heavy mass scale, potential models have been very succesful in quarkonium studies. In finite temperature, however, their use is complicated because of the multitude of independent definitions for the $Q\overline{Q}$ potential.

I review the recent perturbative results on the static potential describing the $Q\overline{Q}$ bound states at finite temperature [2], and discuss the possibility of promoting the definition to the non-perturbative level [3]. I will also discuss the problems residing in the usual definitions of the $Q\overline{Q}$ potential via Polyakov loop correlators [4], as they have been traditionally used for non-perturbative determinations of the heavy quark interaction.

[1] T. Matsui and H. Satz, Phys. Lett. B 178 (1986) 416.
[2] M. Laine, O. Philipsen, P. Romatschke and M. Tassler, JHEP 03 (2007) 054.
[3] A. Rothkopf, T. Hatsuda and S. Sasaki, arXiv:0910.2321 [hep-lat].
[4] Y. Burnier, M. Laine and M. Vepsäläinen, arXiv:0911.3480 [hep-ph].

LAGUNA – LARGE UNDERGROUND INFRASTRUCTURES FOR NEUTRINO ASTROPHYSICS AND PROTON DECAY

T. Enqvist[1], J. Joutsenvaara[1], T. Kalliokoski[2], P. Kuusiniemi[1], K. Loo[1], J. Maalampi[2], G. Nuijten[3], J. Roinisto[3], K. Rummukainen[4], T. Räihä[1], J. Sarkamo[1], W.H. Trzaska[2]
on behalf of the LAGUNA Collaboration

[1]University of Oulu, [2]University of Jyväskylä, [3]Kalliosuunnittelu Oy Rockplan LTD, Helsinki, [4]University of Helsinki
email: timo.enqvist@oulu.fi

Future advances in the low-energy neutrino astronomy and the observation of the proton decay require the construction of massive (from several tens to few hundreds kilotons) detectors deep underground. Currently there is no such existing underground infrastructure in the world that would be able to host experiments in the scale of several kilotons.

LAGUNA [1] (Large Apparatus for Grand Unification and Neutrino Astrophysics) is an undergoing two-year (01.07.2008–30.06.2010) study in the Framework Programme 7 of the EU focusing on the design of a new and large underground infrastructure in Europe. There are seven European site options to host the new infrastructure, Pyhäsalmi in Finland being a strong candidate site. The detector options under the study include 50 kton liquid scintillation detector LENA, 100 kton liquid argon detector GLACIER and 700 kton water Cherenkov detector MEMPHYS.

The new European underground infrastructure would provide new and unique scientific opportunities in low-energy neutrino astronomy and Grand Unification physics. The following phenomena, among others, could be studied

- Matter instability: The proton-decay life time could be determined up to approximately 10^{35} years. This is within the predicted range of Grand Unified Theories.
- Galactic and diffuse supernova neutrinos: Several thousands neutrinos of all flavours could be detected from a (standard) galactic supernova. These results could reveal the mechanism of supernova core collapse. Diffuse supernova neutrinos are believed to provide a new source of information on the star formation rate up to redshift of $z \approx 5$.
- Solar neutrinos: The solar neurino rates would be several thousends per day for ^{7}Be and several hundreds per day for CNO-cycle neutrinos.
- Geoneutrinos: Neutrinos emitting from the radioactive isotopes of the Earth may provide information on the heat production and isotopic composition of the mantle.

[1] D. Autiero *et al.*, JCAP 11 (2007) 011 ((arXiv:0705.0116v2 [hep-ph]).

KNEE IN COSMIC RAY PHYSICS

T. Kalliokoski[a], L. Bezrukov[b], T. Enqvist[c], H. Fynbo[d], L. Inzhechik[b], P. Jones[a], J. Joutsenvaara[c], J. Karjalainen[c], P. Kuusiniemi[c], K. Loo[c], B. Lubsandorzhiev[b], L. Olanterä[c], V. Petkov[b], T. Räihä[c], J. Sarkamo[c], M. Slupecki[a], W.H. Trzaska[a] and A. Virkajärvi[a]

Tuomo Kalliokoski, Department of Physics, P.O. Box 35 (Y5), 40014 University of Jyväskylä, Finland email: Tuomo.Kalliokoski@jyu.fi

[a] University of Jyväskylä
[b] Russian Academy of Science, Moscow, Russia
[c] University of Oulu, Finland
[d] University of Århus, Denmark

Earth is constantly showered with cosmic rays coming from various sources. The rays consist of many different particles, from neutrinos and photons to iron nuclei. The cosmic ray spectra is usually measured for nuclei. Many aspects of this spectrum are still under discussion, one among them is the “knee” (shown in the spectrum). The knee is outside of the area of energy spectrum which is easily measurable with direct measurements due sparsity of the high energy rays. This is reason why experiments measure air showers created by the cosmic ray particle hitting an atom in the atmosphere. Large arrays are needed for this kind of measurements.

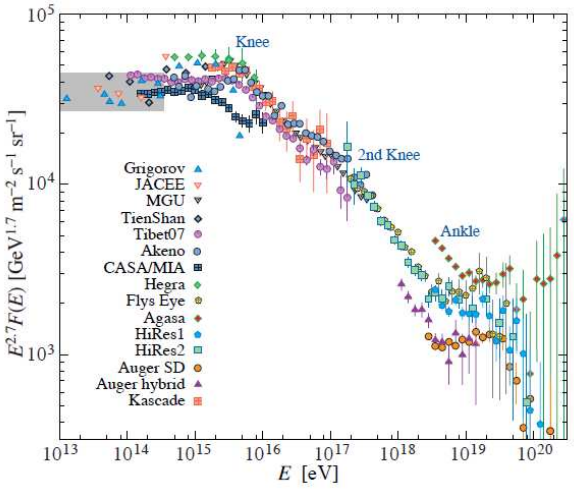

All particle spectrum of cosmic rays (Figure from [1])

There are multiple different explanations for the knee[2]. Among these explanations are change of the acceleration processes in knee energies, leakage of cosmic rays from the Galaxy, interactions with background particles in the Galaxy and change of the air shower development for these high energy particles (new physics).
The shape of the spectrum varies with the particle and this variation gives us possibility to exclude different models. One of the new experiments to do precision measurements on the knee is EMMA[3], situated in the Pyhäsalmi mine.

[1] C. Amsler et al. (Particle Data Group)
Physics Letters B667, 1 (2008)
[2] J. R. Hörandel
Astroparticle Physics 21 (2004) 241-265.
[3] T. Enqvist et al.
Nucl. Phys. B (Proc. Suppl.) 196 (2009) 255-258.

SIMULATIONS OF SCINTILLATOR RESPONSE FOR EMMA-EXPERIMENT

J. Karjalainen[1], T. Enqvist[1], J. Joutsenvaara[1], P. Kuusiniemi[1], K. Loo[1,2], L. Olanterä[1], T. Räihä[1], J. Sarkamo[1] P. Jones[2], T. Kalliokoski[2], M. Slupecki[2], W.H. Trzaska[2], A. Virkajärvi[2], L. Bezrukov[3], L. Inzhechik[3], B. Lubsandorzhiev[3], V. Petkov[3], H. Fynbo[4]

[1]University of Oulu, Finland
[2]Department of Physics, University of Jyväskylä, Finland
[3]Russian Academy of Science, Moscow, Russia
[4]University of Arhus, Denmark
email: joonaska@paju.oulu.fi

The tracking unit of EMMA(Experiment with MultiMuon Array) [1] consist of three layers of drift chamber detectors and a layer of scintillator units(SC16) [2]. The SC16 units consist of 16 scintillators(SC1), that are made of 3cm thick layer of polystyrene. There are altogether 786 SC1's in one tracking unit.

Response of the SC1 scintillators and the scintillator layer in an EMMA tracking unit have been studied by simulations. All simulations are done in Geant4 environment.

Muon induced secondary electrons and γ-rays create a background for muon multiplicity measurement. To study the the background the energy deposition distributions of muons, electrons and γ-rays in SC1 have been simulated. High-energy electrons are practically indistinguishable with muons when comparing the energy deposition. Most of the high-energy γ-rays on the other hand penetrate the detectors without interactions.

The background reduction of lead shielding on top of the scintillator layer was also simulated. For one primary muon, these simulations show that lead shielding reduces the background logarithmically as the thickness of the lead increases. Simulations also show that the best shielding is obtained when lead is placed directly on top of the scintillators. In addition to single muon simulations, the response of the scintillator layer has been studied using air showers generated with CORSIKA simulation program.

[1] T. Enqvist et al., Nucl. Phys. B(Proc. Suppl.) 196 (2009) 255-258.
[2] E.V. Akhrameev et al., NIMA 610 (2009) 419-422.

REACTOR NEUTRINOS AS A BACKGROUND FOR LOW ENERGY NEUTRINO ASTRONOMY IN THE LAGUNA –PROJECT

K. Loo [1,2], T. Enqvist[2] and W. H. Trzaska[1]

[1]University of Oulu, [2]University of Jyväskylä
email: kai.loo@jyu.fi

Reactor neutrinos emerge from decay chains of fission products of the nuclear fuel. Every fission produces on average 6 neutrinos. Typical neutrino production rate for average pressurized water reactor is $\sim 2 \cdot 10^{20}$ per GW of thermal power in a second, which makes it a very powerful neutrino source.

Reactor antineutrinos are laying on same energy region as neutrinos emitted from radioactive isotopes of the Earth – so called geo-neutrinos – and neutrinos from the supernove explosions of the past – so called diffuse supernova neutrinos. Geo-neutrino measurements are one key to understand the physics of the Earth, e.g. isotopic composition, heat production and mantle circulation. The flux of diffuse supernova neutrinos is one way to study supernova rate, star formation rate and evolution of supernovae. To measure accurately these kind of phenomena, the detector must be located far from nuclear reactors.

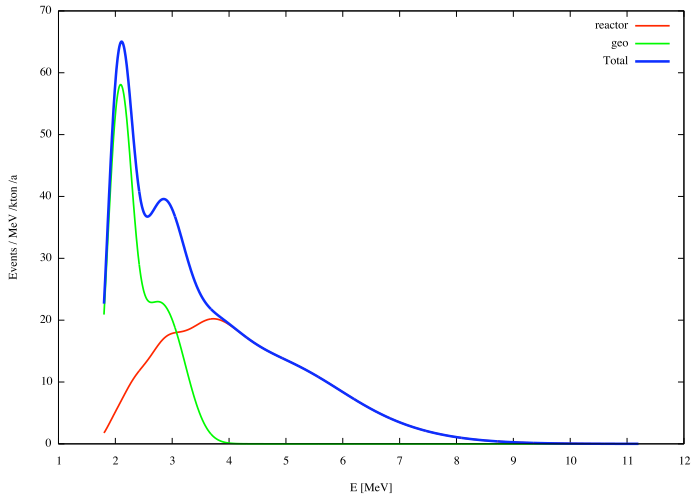

Figure 1: Expected reactor and geo neutrino spectrum in the Pyhäsalmi mine

In the present study the effect of neutrinos produced in all commercial fission reactors of the World on the possible low energy neutrino astronomy –experiment in the LAGUNA [1]-sites is investigated and comparison is made. Especially, focus is on the Pyhäsalmi mine. Comparison of event rates and spectrum of reactor background to the event rates and spectrum of geo and diffuse supernova neutrinos in Pyhäsalmi is made. It is also concluded that such low energy neutrino experiment can be conducted in the Pyhäsalmi in spite of new (and close–by) planned reactors Pyhäjoki (130 km) or Simo (230 km).

[1] D. Autiero *et al.*, JCAP **0711** (2007) 011 [arXiv:0705.0116 [hep-ph]].

EVENT-BY-EVENT BASED COSMIC-RAY PHYSICS IN LHC EXPERIMENTS

T. Räihä[1], T. Enqvist[1], J. Sarkamo[1], W.H. Trzaska[2]

[1]University of Oulu, Finland
[2]University of Jyväskylä, Finland
email: tomi.raiha@oulu.fi

Large LHC experiments ALICE, ATLAS, and CMS are desinged for studying high-energy beam collisions but they can also contribute to cosmic-ray physics by measuring high-energy muon bundles produced in the atmosphere. So far cosmic rays are studied in LHC mainly by assuming some shape and composition of the cosmic-ray energy spectrum and then comparing predictions from simulations to measurements. This method can not say much about the properties of single events but is rather reflecting the average behavior of all events. In order to perform analysis on event-by-event basis it is necessary to be able to locate the core position of the muon bundle for each event.

The advantage of LHC experiments compared to typical cosmic-ray experiments is that they can reconstruct the energies of high-energy cosmic muons precisely up to several hundreds of GeVs or even higher. For instance, the energy resolution of the Time Projection Chamber (TPC) [1] in ALICE is around 10% for 500 GeV muons. We present here an idea how LHC experiments could be utilised for cosmic-ray studies on event-by-event basis in a completely new way by taking the advantage of the energy information.

According to simulations, muons with highest energies ($E_\mu > 500$ GeV) tend to locate close to shower core. Hence, by requiring some minimum number of highest-energy muons measured by the detector and claiming that the core locates in the centre-of-mass of these muons, one could achieve a few metres accuracy for the core position. For instance, using only the TPC of ALICE, one could reach $2-4$ metres accuracy still with reasonable good efficiency around the so-called knee region in the cosmic-ray energy spectrum. The accuracy for locating the shower core might be improved by taking also the benifit of the measurements of Time-Of-Flight (TOF) detector. The TOF is placed around the TPC giving a full coverage and hence expanding the projected surface area for cosmic-ray studies roughly from 25 m^2 to 50 m^2.

The EMMA experiment [2] being built in the Pyhäsalmi mine in Finland has a resemblance to LHC experiments. They are underground experiments and can be used to measure high-multiplicity muon bundles. EMMA cannot measure the energies of muons but their lateral distribution up to 30 metres can be measured which is an advantage in comparison with LHC experiments. These experiments are complementary and thus it is important to compare results to obtain maximum contribution for cosmic-ray physics.

[1] ALICE Physics Performance Report Vol. II.
[2] T. Enqvist et al., Nucl. Phys. B (Proc. Suppl.) 196 (2009) 255-258.

COSMIC-RAY EXPERIMENT EMMA: UNDERGROUND MUON TRACKING UNIT

J. Sarkamo[1], T. Enqvist[1], J. Joutsenvaara[1], J. Karjalainen[1], P. Kuusiniemi[1], K. Loo[1,2], L. Olanterä[1], T. Räihä[1], P. Jones[2], T. Kalliokoski[2], M. Slupecki[2], W.H. Trzaska[2], A. Virkajärvi[2], L. Bezrukov[3], L. Inzhechik[3], B. Lubsandorzhiev[3], V. Petkov[3], H. Fynbo[4]

[1]University of Oulu, Finland
[2]University of Jyväskylä, Finland
[3]Russian Academy of Science, Moscow, Russia
[4]University of Arhus, Denmark
email: juho.sarkamo@oulu.fi

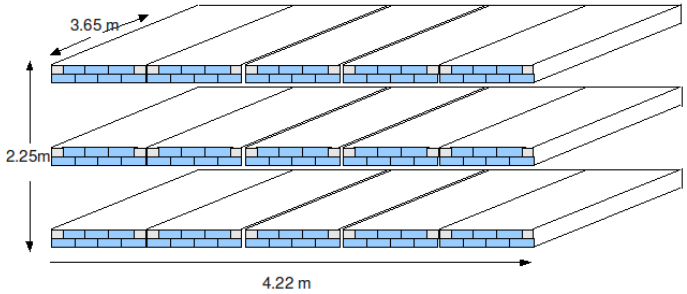

EMMA[1], Experiment with MultiMuon Array, is under construction in the Pyhäsalmi mine. It aims to resolve the cosmic-ray composition in the knee region by measuring the lateral distribution of high-energy muons. The array will consist of nine detector stations at a depth of 75 m.

The testing, calibration and repairements of the drift chambers are progressing on ground and the commissioning of the first underground tracking unit is underway.

The tracking unit consists of 15 detectors (each consisting of 7 drift chambers) arranged in three overlapping layers. It has the dimensions of 3.65x4.22x2.25 m^3 and a geometric acceptance of 18 Sr m^2 for isotropic flux. A fourth layer consisting of fine-resolution scintillators (786 pieces, 12x12x3 cm^3 each) is installed at a later phase.

The tracking accuracy is ~ 0.5 degrees.

[1] T. Enqvist et al., Nucl. Phys. B (Proc. Suppl.) 196 (2009) 255-258.

7 Nanophysics and new materials

7.1 Oral session I, Thursday 11 March 15:00-16:30
7.2 Oral session II, Saturday 13 March 9:00-10:30
7.3 Poster session I, Thursday 11 March 16:30-18:30
7.4 Poster session II, Friday 12 March 16:00-18:00

FORMATION MECHANISMS OF GOLD CLUSTERS PRODUCED BY MAGNETRON SPUTTERING ON THIOL SELF-ASSEMBLED-MONOLAYERS

L. Costelle[1], T.T. Järvi[2], M. Räisänen[3], J. Räisänen[1]

[1]Department of Physics, Division of Materials Physics, P.O.B. 43, FIN-00014 University of Helsinki, Finland - [2]Fraunhofer-Institut für Werk-stoffmechanik IWM, Freiburg, Germany - [3]University of St Andrews, St Andrews, UK
email: leila.costelle@helsinki.fi

Recently, cluster deposited on self-assembled monolayers have attracted a great interest. Metal clusters interact in many different ways with organic surfaces. The possibility to control the size and morphology of deposited clusters and tune their properties, makes self-assembled monolayers (SAMs) well-suited for studies and applications in nanoscience and nanotechnology. Thus a better understanding of the interaction between clusters, the organic layer and the substrate should be assessed as a starting point towards further possible applications. We report on investigations of low deposition energy (0.3 eV/atom) of gas-phase gold clusters on dodecanethiol self-assembled monolayers (SAMs) on a Au(111) substrate. The deposition of pre-formed clusters in the gas phase offers the possibility to control the size and morphology of deposited clusters and tune their properties, unlike single-atom deposition by molecular beam epitaxy (MBE) methods, where the nanostructures properties are strongly dependent on the cluster-substrate interaction.
Combining the experimental measurements to molecular dynamics simulations, we obtain a description of the clusters penetration mechanism and a better understanding of the cluster-SAMs interactions.

QUICK AND EASY PREPARATION OF CONDUCTIVE AND TRANSPARENT SWCNT-FILMS

Antti Kaskela[a], Albert G. Nasibulin[a], Marina Y. Zavodchikova[a], Brad Aitchison[b], Ying Tian[a], Zhen Zhu[a], David P. Brown[b] and Esko I. Kauppinen[a,c]

[a] NanoMaterials Group, Department of Applied Physics, Aalto University, P.O.Box 15100, FI-00076 Aalto, Finland
email: antti.kaskela@tkk.fi
[b] Canatu Ltd., Tekniikantie 21, FI-02150 Espoo, Finland
[c] VTT Biotechnology, Biologinkuja 7, FIN-02044, Espoo, Finland

Single-walled carbon nanotube (SWCNT) networks are a promising material for future electronics applications due to their optical transparency and electrical properties1,2. Study of SWCNT-networks is well motivated as transparent metal oxides like indium-tin oxide (ITO) have several drawbacks such as limited flexibility and raw material supply3,4. Traditionally, the preparation of SWCNT-networks has been a time and resource consuming process, involving several liquid phase purification steps5, which can introduce defects and decrease the average length of SWCNTs6. We have developed a continuous aerosol-CVD process to synthesize and deposit large area SWCNT-networks on several substrate materials without purification. The prepared SWCNT-networks can be chemically functionalized on a substrate to produce performance which approaches low temperature processed ITO.

[1] Wu Z., et.al., Science , Vol. 305, 27 August 2004.
[2] Cao Q., et.al., Nature, Vol. 454, 24 July 2008.
[3] L. Ke et. al., Appl. Phys. A: Mater. Sci. Process, Vol. 81, 2005.
[4] Segal M., Nature Nanotechnology, Vol. 4, October 2009.
[5] J-H Shin, et.al., J. Phys. D: Appl. Phys. vol. 42, 2009.
[6] Schrage C., et.al., ACS Appl. Mater. Interfaces, July 17, 2009.

SELF-ASSEMBLY AND HIERARCHIES IN PYRIDINE-CONTAINING HOMOPOLYMERS AND BLOCK COPOLYMERS WITH HYDROGEN-BONDED CHOLESTERIC SIDE-CHAINS

J. T. Korhonen,[1] T. Verho,[1] P. Rannou,[2] and O. Ikkala[1,2]

[1] Aalto University, Applied Physics, P.O.Box 15100, FIN-00076 Aalto, Finland
[2] Laboratoire d'Electronique Moléculaire, Organique et Hybride, Grenoble, France
email: juuso.t.korhonen@tkk.fi

Physical interactions, such as hydrogen bonding, can be used to construct liquid crystalline side-chain polymers, where there is a flexible backbone with mesogenic side-groups. We have investigated supramolecular complexes where a mesogenic molecule, cholesteryl hemisuccinate (CholHS), is hydrogen bonded to a homopolymer, poly(4-vinylpyridine) (P4VP), to allow liquid crystallinity, and to a block copolymer polystyrene-*block*-poly(4-vinylpyridine) (PS-*b*-P4VP), to allow hierarchical self-assembly.[1]

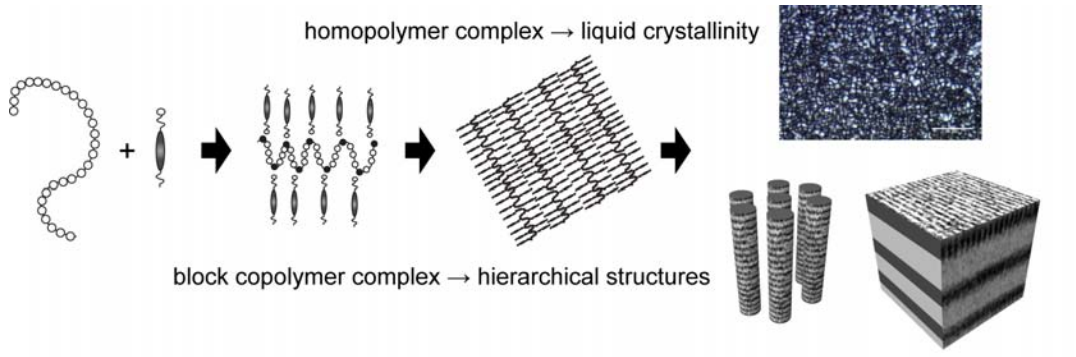

Figure 1. Schematic representation of the self-assembly process where homopolymer complexes lead to liquid crystallinity (smectic A) and block copolymer complexes lead to hierarchical structures (e.g. smectic-*within*-lamellar). Actual TEM images are imposed on the surfaces of the structure models.

P4VP and CholHS form microphase-separated smectic A liquid crystals, which correspond to a periodic morphology of the polymer chains and end-to-end arrangement of the mesogens. Heating the complex leads to an isotropic melt as the thermal energy of the system increases. Liquid crystallinity is most stable at low degrees of CholHS complexation, whereas at high degrees of complexation competing effects due to crystallization of CholHS can take place, especially under prolonged stay at elevated temperatures. When CholHS is complexed with PS-*b*-P4VP block copolymer, hierarchical structure-*within*-structure morphologies are observed, where the inner structure is smectic and the larger structure depends on the volume fractions of the corresponding blocks. The observed hierarchies can turn out to be useful to construct functional self-assemblies.

[1] J. T. Korhonen, T. Verho, P. Rannou, O. Ikkala, accepted to Macromolecules (2010).

Aalto University
School of Science
and Technology

MODELING CELLULOSE NANOFIBRILS WITH NON-CRYSTALLINE PARTS

S. Paavilainen, Tomasz Róg, J. Järvinen and I. Vattulainen

Department of Physics, Tampere University of Technology,
P.O.Box 692, FIN-33101 Tampere, Finland
Email: sami.paavilainen@tut.fi

Nanofibrillar cellulose (NFC) is a potential raw material for various products. Due to the small size of the fibrils it is possible to construct fibrillar networks having extremely high strength [1], to make paper with high porosity, or even transparent films [2]. NFC consists mainly of pure cellulose but even more than 50 % of the material may be in non-crystalline form.

We have performed molecular dynamics simulations of cellulose nanofibrils having an amorphous coverage consisting of disordered cellulose chains. The core of the fibrils is crystalline in $I\beta$ [3] structure and has a cross-diameter of 5 nm. Previously, we have shown that the crystalline cores are twisted due to opposite reorientation of individual cellulose chains at opposite sides of the fibril [4].

The presented studies show that the disordered chains do not crystallize at room temperature but due to mutual interaction form amorphous, porous, metastable structures on top of the twisted crystallines. In addition, we have studied the role of these amorphous structures in interaction between two fibrils. Their ability to reshape during the binding process is found to be very important and clearly increases the interaction between the fibrils.

We have also studied fibrils in which the crystalline parts are disconnected by non-crystalline regions along the long axis of the fibril. Our studies show that the structure of the non-crystalline region is critical for the elastic properties of the fibril. On the figure on the right is shown a snapshot from a simulation of a nanofibril which has ten chains (highlighted) continuing from one crystalline part to another through a non-crystalline region.

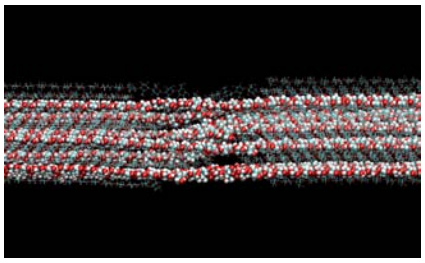

The simulations have been carried using OPLS (Optimized Potential for Liquid Simulations) force field and Gromacs simulation package.

[1] M. Henriksson, L. A. Berglund, P. Isaksson, T. Lindström and T. Nishino, Biomacromolecules **9**, 1579(2008).
[2] M. Nogi, S. Iwamoto, A. N. Nakagaito and H. Yano, Advanced Materials **20**, 1(2009).
[3] Y. Nishiyama, G. P. Johnson, A. D. French, V. T. Forsyth and P. Langan, Biomacromolecules **9**, 3133(2008).
[4] S. Paavilainen, T. Róg, and I. Vattulainen, in preparation.

NANOSCALE PATTERNING OF SILICON WITH FOCUSED ION BEAM AND ANISOTROPIC WET ETCHING

P. Sievilä, N. Chekurov and I. Tittonen

Department of Micro and Nanosciences, School of Science and Technology,
Aalto University P.O.B. 13500, FI-00076 Aalto, Finland
email: paivi.sievila@tkk.fi

The development of nanotechnology based devices requires rapid prototyping methods that can be applied in combination with well-known microsystems processing techniques. Focused ion beam (FIB) writing enables straightforward fabrication of various types of arbitrary shaped nanostructures by means of milling, deposition and ion implantation [1].

We have developed a fast silicon nanostructure fabrication method combining local FIB Ga^+ ion implantation and IC compatible, anisotropic tetramethylammonium hydroxide (TMAH) wet etching. The masking properties of gallium-doped, single crystalline silicon have been studied and a threshold dose of 2×10^{13} ions/cm^2 for observable etching resistance has been found. A very thin, approx. 50 nm surface layer is durable enough to serve as a mask with a high selectivity of at least 2000:1 between implanted and non-implanted areas.

The method has been used to fabricate various types of nanostructures including gratings with the resolution of 20 lines/µm, freestanding beams and bridges with the narrowest features being only 25 nm wide, and high aspect ratio (1:30) nanochannels separated by very thin, nearly vertical sidewalls (Fig. 1). The potential applications of the fabrication method include e.g. nanoscale cantilever sensors and integrated optical components with subwavelength features.

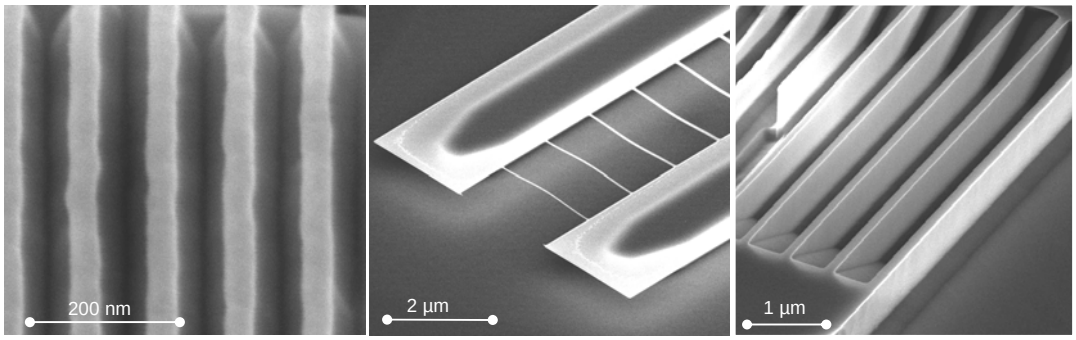

Fig. 1. Grating structure, freestanding bridges and nanochannels with vertical walls fabricated on Si by FIB Ga^+ ion implantation and TMAH wet etching.

[1] A. A. Tseng, Small 1, No.10 (2005) 924.
[2] P. Sievilä, N. Chekurov and I. Tittonen, article submitted to Nanotechnology (2009).

LIGHT-INDUCED SURFACE PATTERNING OF DYE–POLYMER THIN FILMS

J. Vapaavuori, A. Priimagi and M. Kaivola

Department of Applied Physics, Aalto University, POB 13500, 00076 Aalto, Finland
email: jaana.vapaavuori@tkk.fi

Macroscopic mass transport can be induced to polymeric materials by light through nanoscale photoisomerization of azobenzene derivatives. When an azobenzene-containing polymer sample is irradiated with an interference pattern of light, the initially flat sample surface can reproduce the intensity and/or polarization modulation of the incident light field as a surface-relief grating (SRG) (Fig. 1a). Such gratings are temporally stable, and their surface-modulation depth can be hundreds of nanometers, showing potential for applications ranging from holographic storage to fabrication of diffractive optical elements and photonic components.

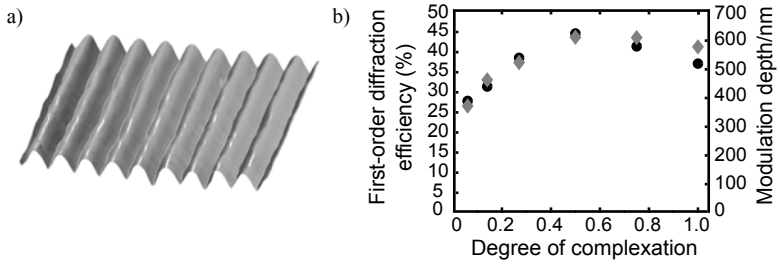

Figure 1: a) Typical AFM image of an SRG; b) First-order diffraction efficiencies (gray diamonds) and modulation depth (black spheres) of the gratings.

In the present study we show that hydrogen-bonded azobenzene–polymer complexes will give rise to efficient SRG formation, characterized by *in-situ* light diffraction measurements and *ex-situ* atomic-force microscopy (AFM) scans [1]. The main results are summarized in Fig. 1b, which shows that the SRG formation takes place for all complexes with the degree of complexation ranging from 0.06 to 1.0 chromophores per one repeat unit of the polymer. When every second polymer repeat unit is occupied, the grating formation is the most efficient, yielding a surface-modulation depth of 625 nm, and first-order diffraction efficiency of 44 %.

All the inscribed gratings are thermally erasable and no photodegradation of the chromophores is observed. Together with our previous study on phenol–pyridine hydrogen-bonded complexes[2], we have demonstrated a facile supramolecular route towards efficient light-induced surface patterning.

[1] J. Vapaavuori, A. Priimagi and M. Kaivola, Photoinduced Surface-Relief Gratings in Supramolecular Bisazobenzene–Polymer Complexes (2010), submitted

[2] A. Priimagi, K. Lindfors, M. Kaivola and P. Rochon, ACS Appl. Mater. Interfaces 1 (2009) 1183

FEMTOSECOND FOUR-WAVE-MIXING SPECTROSCOPY OF FREELY SUSPENDED AND FULLY CHARACTERIZED SINGLE-WALL CARBON NANOTUBES

P. Myllyperkiö[†], O. Herranen[††], J. Rintala[†], H. Jiang[†††], A. Johansson[††], P. R. Mudimela[†††], Z. Zhu[†††], A. G. Nasibulin[†††], E. I. Kauppinen[†††], M. Ahlskog[††] and M. Pettersson[†]

[†]Department of Chemistry, P.O.B. 35, FIN-40014 University of Jyväskylä, Finland
[††]Department of Physics, P.O.B. 35, FIN-40014 University of Jyväskylä, Finland
[†††]Department of Applied Physics, P.O.B. 1000, FIN-02044 Aalto University, Finland
email: andreas.johansson@jyu.fi

We have characterized the individual properties of freely suspended single-wall carbon nanotubes, using both Raman spectroscopy and electron diffraction measurements in a transmission electron microscope. The two techniques give mutually independent routes to determine the chirality of the nanotube [1,2], which allows us to find the corresponding detailed band structure.
With help of that knowledge we set up time-resolved (femtosecond) four-wave-mixing (FWM) measurements and show that it is possible to obtain fs-FWM signals from individual suspended semiconducting single-wall carbon nanotubes. These measurements are the first in the femtosecond regime and they open interesting perspectives for measurements of ultrafast dynamics and nonlinear optical response from individual nanotubes. Within this study we next intend to measure the coherence time of excited vibrational states in nanotubes of known chirality.

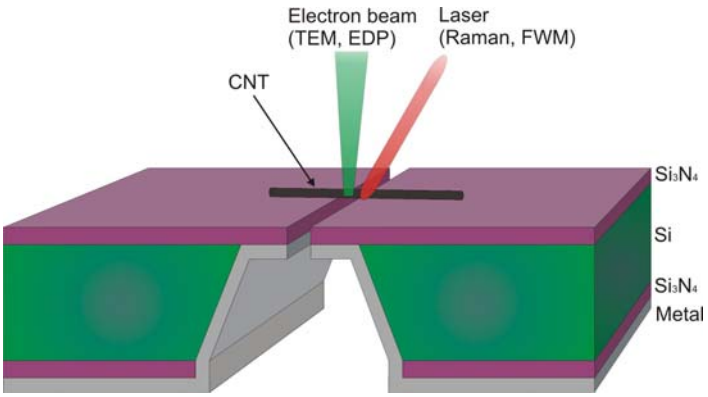

Figure 1: Schematic of the measurement setup. A single-wall carbon nanotube stretches across an open slit in a Si_3N_4 membrane, allowing both transmission electron microscopy and optical measurements to be carried out on the same nanotube.

[1] J. Rintala *et al.*, J. Phys. Chem. C 113 (2009) 15398.
[2] H. Jiang et al., Carbon 45 (2007) 662.

UNIVERSITY OF JYVÄSKYLÄ

FIELD INDUCED NANOLITHOGRAPHY (FINAL)

T.K. Hakala[2], V. Linko[2], A.-P. Eskelinen[1], J.J. Toppari[2], A. Kuzyk[1], and P. Törmä[1]

[1]Aalto University, Department of Applied Physics, P.O. Box 11000, FI-00076 AALTO Finland
email: anteske@cc.hut.fi

[2]Nanoscience Center, Department of Physics University of Jyväskylä P.O. Box 35, FI-40014 Finland

While self-assembly has proven its usefulness for the generation of various nano- and mesoscopic structures, there remains a fundamental obstacle in creating integrated, highly ordered multicomponent nanodevices: the precise spatial control over each of the device components has proven to be exceedingly difficult. Here, a high-precision, high-throughput method for pattern transfer of nano-objects is demonstrated by producing arrays of quantum dots [1]. The method, field-induced nanolithography (FINAL), utilizes dielectrophoresis for trapping and it can be extended to arranging carbon nanotubes, biomolecules, and other objects into desired configurations. The trapping as well as the subsequent deposition from the master stamp to the target plate are made in parallel fashion, enabling large area printing and mass production. Furthermore, the master stamp is i) reusable, and ii) more importantly and in contrast to conventional methods such as microcontact printing and nanoimprint lithography, universal: one master stamp having a 2D matrix of electrodes could be used to transfer any desired pattern to the target plate. Due to its robustness, versatility, and universality, the method has remarkable application potential in nanotechnology.

[1] T. K. Hakala, V. Linko, A.-P. Eskelinen, J. J. Toppari, A. Kuzyk, and P. Törmä, Small 5 (2009) 2683-2686.

CHARACTERIZATION OF THE CONDUCTANCE MECHANISMS OF DNA ORIGAMI BY AC IMPEDANCE SPECTROSCOPY

V. Linko[1], A. Kuzyk[1,3], B. Yurke[2], S.-T. Paasonen[1], P. Törmä[3], and J.J. Toppari[1]

[1] Nanoscience Center, Department of Physics, P.O.B. 35, FI-40014 University of Jyväskylä, Finland
[2] Materials Science and Engineering Department, Boise State University, Boise ID 83725, USA
[3] Department of Applied Physics, P.O.B. 5100, FI-02015 Helsinki University of Technology, Finland
email: veikko.linko@jyu.fi

Due to its exceptional self-assembly properties, DNA could become a key player in bottom-up fabrication of nanoscale systems. Controlled positioning and immobilization of DNA molecules and structures on the chip is a crucial open challenge for the realization of the full potential of DNA as a template. A striking example of a DNA self-assembly technique is 'DNA origami', which involves folding a long single-stranded DNA with the help of short oligonucleotides.

We have shown that dielectrophoresis (DEP) can be used to trap various kinds of DNA molecules and structures (also DNA origami [1]) efficiently. The method gives a high yield of single structure trapping between nanoelectrodes and controlled positioning on a chip, and provides means of bridging bottom-up and top-down fabrication approaches. DEP trapping of DNA origami structures is the first demonstration of the DEP manipulation of complex self-assembled structures.

After the immobilization of an individual DNA structure between the nanoelectrodes the electrical conductivity of the structure was characterized. We have fully analyzed both DC and AC characteristics (AC impedance spectroscopy) of a single trapped DNA origami structure with different humidity levels and also defined the detailed equivalent circuit model describing the conductivity mechanism of the structure [2]. The results showed that the nature of the conductivity is not purely Ohmic but that it is a combination of an ionic diffusion and electronic conductivity. Also other kinds of self-assembled DNA structures are being measured and analyzed with the same method, showing some variations compared to the conductivity of DNA origami.

[1] A. Kuzyk, B. Yurke, J.J. Toppari, V. Linko, and P. Törmä, Small 4(4) (2008) 447.
[2] V. Linko, S.-T. Paasonen, A. Kuzyk, P. Törmä, and J.J. Toppari, Small 5(21) (2009) 2382.

UNIVERSITY OF JYVÄSKYLÄ

DC CHARACTERISTICS OF NBN/TAN/NBN SNS JOSEPHSON JUNCTIONS GROWN BY PULSED LASER ABLATION

M. Nevala[1], I. Maasilta[1], K. Senapati[2,3] and R. Budhani[3]

[1]Nanoscience Center, Department of Physics, P.O.Box 35, University of Jyväskylä, FIN-40014, Finland
email: minna.nevala@phys.jyu.fi
[2]Department of Materials Science and Metallurgy, University of Cambridge, Pembroke Street, Cambridge, U.K.
[3]Department of Physics, Indian Institute of Technology Kanpur, Kanpur 208016, India

Rapid single flux quantum (RSFQ) logic is a promising technology for high speed digital electronic devices, based on non-hysteretic Josephson junctions [1]. Superconductor/normal metal/superconductor (SNS) based Josephson junctions have intrinsically non-hysteretic current I vs. voltage V response [2].

In RSFQ circuitry the appropriate figure of merit of a Josephson junction is the product of the critical current I_C and the normal resistance of junction R_n, since it is inversely proportional to SFQ pulse width [3], and for operation at ~50 GHz frequency the product I_CR_n should be greater than 0.3 mV [3].

We have fabricated SNS Josephson junctions from NbN, where the normal metal material is tantalum nitride (TaN). The trilayer films were prepared on single crystal MgO substrate by pulsed laser deposition [4,5], patterned into junctions using e-beam lithography, chemical vapor deposition and e-beam evaporation. The quality of junctions was tested by measuring the differential resistance as a function of current bias and temperature from 1.5 K to ~14 K, yielding information of the junctions' I_CR_n values (from 5 μV to 220 μV). We also observed that the I_CR_n value could be increased 2.5 times by cooling the sample further from 4.2 K to 1.5 K, while still retaining non-hysteretic behavior. In addition we discuss the details of the finite voltage state, which shows complex steps and peaks in the differential resistance, possibly due to multiple Andreev reflection processes.

[1] K. Likharev and V. Semenov, IEEE Trans. Appl. Supercond., vol. 1, no. 1 (1991) 3
[2] T. Van Duzer and C. Turner, Principles of Superconductive Devices and Circuits. Prentice Hall, Upper Saddle River, New Jersey, USA, 1999.
[3] A. Kaul, S. Whiteley, T. Van Duzer, L. Yu, N. Newman and J. Rowell, Appl. Phys. Lett. 78 (2001) 99
[4] K. Senapati, N. Pandey, R. Nagar, and R. Budhani, Phys. Rev. B 74 (2006) 104514
[5] M. Nevala, I. Maasilta, K. Senapati, and R. Budhani, IEEE Trans. Appl. Supercond., vol. 19, No. 3 (2009) 253

FEW-ATOM SILVER CLUSTERS AS FLUOROPHORES: COLOUR TUNABILITY AND ELECTROCHEMILUMINESCENCE

Robin H. A. Ras and Isabel Díez

Molecular Materials, Department of Applied Physics, Aalto University
P.O. Box 5100, FI-02015 TKK, Espoo
email: robin.ras@tkk.fi

Silver clusters, composed of only two or three silver atoms, have remarkable optical properties based on electronic transitions between quantized energy levels. They have large extinction coefficients and fluorescence quantum yields, in common with conventional fluorescent markers. But importantly silver clusters have an attractive set of features, including sub-nanometer size, non-toxicity and photostability, which makes them competitive as fluorescent markers compared with organic dye molecules and semiconductor quantum dots.
We have demonstrated recently that the absorption and emission properties of few-atom metal clusters respond dramatically to changes in the chemical environment, such as solvent and relative amount of silver (see Fig. 1) [1]. In other words they are solvatochromic. Moreover, the Ag nanoclusters exhibit also electrochemiluminescence [1]. Fluorescent silver clusters have attractive properties for molecular sensing applications.

.

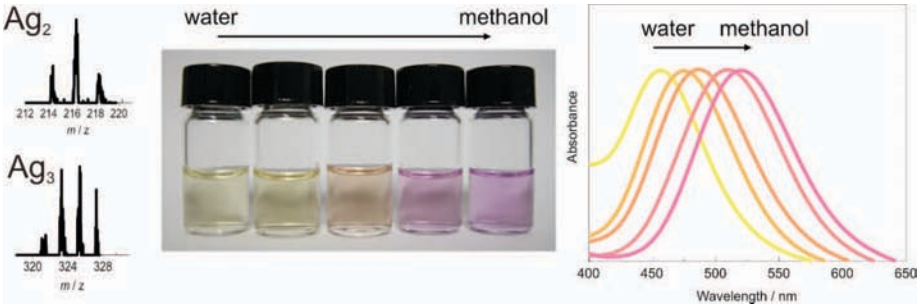

Figure 1. (left) Silver clusters of two and three atoms are made in stable aqueous solution using acrylate polymer as stabilizer. (center) Photograph and (right) absorption spectra of the silver clusters in water-methanol mixtures, showing the wavelength-shifting properties.

[1] Díez I., Pusa M., Kulmala S., Jiang H., Walther A., Goldmann A. S., Müller A. H. E., Ikkala O., Ras R. H. A. Angewandte Chemie International Edition 48 (2009) 2122.

ENHANCED BULK-TYPE MULTIPOLAR SECOND-HARMONIC GENERATION FROM THIN METAL FILMS

F. X. Wang[1], F. J. Rodriguez[1], W. M. Albers[2], and M. Kauranen[1]

[1]Department of Physics, Tampere University of Technology, P. O. Box 692, FI-33101 Tampere, Finland
[2]VTT Microtechnology and Sensors, P. O. Box 1300, FI-33101 Tampere, Finland
email:fuxiang.wang@tut.fi

Within the electric-dipole approximation of the light-matter interaction, optical second-harmonic generation (SHG) is forbidden in materials with inversion symmetry. The symmetry is broken at surfaces, thus giving rise to an electric-dipole-allowed surface nonlinearity. When higher multipole (magnetic-dipole and electric-quadrupole) effects are taken into account, SHG can occur even in the centrosymmetric bulk [1]. Rough metal surfaces can enhance SHG due to the dipolar surface response through local-field effects [2]. In this paper, we show that the nanoscale surface morphology has a much stronger influence on the bulk-type multipolar second-order response than on the surface response.

The surface and bulk effects in SHG of isotropoic and centrosymmetric materials can be separated only by two-beam SHG and by relying on their different dependence on the polarization properties of light. The differences are particularly evident for *s*-polarized SHG signals. Our experimental technique is therefore based on detailed measurements of the s-polarized SHG signals as a function of the polarization of incident fundamental beams.

Our samples were 20-nm and 150-nm thick gold films sputtered on microscope glass slides. All the SHG measurements were performed with a Nd:YAG laser. The recorded *s*-polarized SHG data in reflection were fitted with different theoretical models. The results indicate that both the surface and bulk effects contribute to the measured SHG signals. Compared to the 150-nm thick sample, the surface response of the 20-nm thick sample was enhanced by 20% through enhanced local fields due to increased surface roughness of the thin film [2]. Surprisingly, the bulk-type response was enhanced even more (80%) and can be explained by field retardation across the nanoscale features of the rough surface [3].

In conclusion, we have shown that, compared to the dipolar surface SHG, the bulk-type multipolar SHG has a superior sensitivity to the nanoscale morphology of metal surfaces. This result can lead to new sensing applications and suggests that nanostructured materials could give rise to efficient multipolar second-order materials, not limited by the noncentrosymmetry requirement of traditional materials.

[1] N. Bloembergen *et al.*, Phys. Rev. **174**, (1968) 813.
[2] C. K. Chen *et al.*, Phys. Rev. Lett. **46**, (1981) 145; C. S, Chang, and J. T. Lue, Surf. Sci. **393**, (1993) 231.
[3] I. Russier-Antoine *et al.*, J. Phys. Chem. C **111**, (2007) 9044.

MOLECULAR BEAM EPITAXY AND ANNEALING OF 1 eV GaInNAs FOR HIGH-EFFICIENCY MULTI-JUNCTION SOLAR CELLS

A. Aho, V.-M. Korpijärvi, A. Tukiainen, V. Polojärvi, M. Guina and M. Pessa

Optoelectronics Research Centre, Tampere University of Technology
P.O.B. 692, FIN-33101 Tampere, Finland
email: arto.j.aho@tut.fi

We report on molecular beam epitaxy (MBE) and rapid thermal annealing of dilute nitride GaInNAs. This material is potentially useful in increasing the efficiency of multi-junction III-V solar cells but requires thorough growth optimization for reaching the high optical quality necessary for the application [1].

Lattice-matched bulk layers of GaInNAs were grown on GaAs(100) substrates by MBE reactor using a radio-frequency (RF) nitrogen plasma source. The band gap of GaInNAs was tuned to 1 eV, which is the theoretical optimum for the bottom junction of a three-junction solar cell [2]. The samples were analyzed using double crystal x-ray diffractometry (XRD) and room temperature photoluminescence (PL).

XRD and PL results show that nitrogen incorporation into lattice-matched GaInNAs depends on the growth temperature and arsenic pressure. The optimum growth temperature, with respect to PL peak signal, was observed to depend on the used plasma source RF power. The post-growth annealing improved significantly the optical quality of the samples but simultaneously caused a large PL wavelength blue shift.

[1] D. B. Jackrel, S. R. Bank, H. B. Yuen, M. A. Wistey, J. S. Harris, Jr., A. J. Ptak, S. W. Johnston, D. J. Friedman, and S. R. Kurtz, *J. Appl. Phys. 101, 114916 (2007)*
[2] S. Kurtz, D. Myers and J. Olson, *Proc. 26th IEEE Photovoltaic Specialist Conference, 875-878 (1997)*

High performance material for SINIS tunnel junction thermometry and cooling

S. Chaudhuri, M. R. Nevala and I. J. Maasilta

Nanoscience Center, P.O.Box 35 FI-40014, University of Jyväskylä, FINLAND
email: saumyadip.s.chaudhuri@jyu.fi

Superconductor-insulator-metal-insulator-superconductor (SINIS) based tunnel junctions exhibit electronic cooling, whereby upon the quasiparticle tunneling induced by the application of a suitable bias voltage lowers the temperature of the normal metal below the bath temperature [1]. Furthermore electrical characteristics of the NIS junction are extremely sensitive to the temperature of the normal metal which makes these junctions ideal for accurate thermometry. Traditionally most SINIS junctions employ aluminum (Al) as the superconductor which has some disadvantages. Firstly, the use of Al limits the application of such thermometry and refrigeration to sub-kelvin temperatures owing to its low superconduction transition temperature (T_C = 2 K). Secondly, the cooling power, which depends directly on the superconducting gap (Δ), is low for Al due to its low $\Delta \sim 0.22$mV. An ideal candidate for more practical and higher temperature use of such junction based devices is niobium nitride (NbN) having $T_C \sim 16$ K and $\Delta \sim 3$ mV.

We have fabricated thin films of NbN on (100) oriented MgO single crystal using pulsed laser deposition technique which involves ablation of a niobium target in ultra high purity nitrogen environment. The fundamental frequency (hν = 1.17 eV) of a Nd:YAG laser was used for ablation. The films reveal a low particulate density and surface roughness of about 5 nm. The nitrogen base pressure and deposition temperature were varied to obtain NbN thin films with $T_C \sim 15.4$ K. The T_C of our films depends strongly on the nitrogen base pressure with slope as high as 1.6 K/mTorr. Different junction barrier materials (AlO_x, AlN) will be investigated to optimize performance.

The inadvertent Joule heating of the normal metal electrode is also an important factor that can affect the performance of these junctions. Manganese doped aluminum (Al:Mn) is an alloy whose resistivity can be tuned by varying the concentration of Mn [2]. Another ongoing effort of ours is the investigation of the effect of the metal electrode resistivity on cooling characteristics of Al-AlO_x-Al:Mn based NIS junctions.

[1] L. J. Taskinen and I. J. Maasilta, Appl. Phys. Lett. 89 (2006) 143511.
[2] F. Giazotto, T. T. Heikkilä, A. Luukanen, A. M. Savin, and J. P. Pekola, Rev. Mod. Phys. 78 (2006) 217 .

Hole-induced electron tunneling in core-shell quantum dots

Z. Sun[a], I. Swart[a,b], W. Evers[a], D. Vanmaekelbergh[a] and P. Liljeroth[a,c]

[a] Condensed Matter and Interfaces, Debye Institute for Nanomaterials Science, University of Utrecht, PO Box 80000, 3508 TA Utrecht, the Netherlands
[b] Institute for Experimental and Applied Physics, Faculty of Physics, University of Regensburg, Universitätsstrasse 31, D-93053, Regensburg, Germany
[c] Low-Temperature Laboratory, Aalto University, PO BOX 15100, 00076 AALTO, Finland
email: P.Liljeroth@uu.nl

Recent advances in wet-chemical synthesis of colloidal nanocrystals have made it possible to create hetero-nanostructures, where two different materials are integrated into the same colloidal particle. These systems have attracted increasing attention due to the possibility of generating indirect excitons through type-II band alignment that leads to the spatial separation of electrons and holes in the heterostructure. As the band off-sets can be tuned through the choice of the materials and by quantum confinement, the optoelectronic properties of these materials can be engineered with high level of control.

In this talk, we will present the results of our low-temperature scanning tunneling microscopy (STM) and spectroscopy (STS) experiments on PbSe-CdSe core-shell nanocrystals. We observe splitting of the tunneling resonances on both sides of the zero-conductivity gap into pairs of sharp peaks with a spacing of ca. 100meV. The spectra are clearly different from those measured on pure PbSe or CdSe nanocrystals[1, 2] suggesting of a novel electron transport mechanism through these heteronanostructures. We will show that this phenomenon can be explained by a hole-induced Coulomb "anti-blockade" mechanism, where the peak splitting is caused by two parallel tunneling processes: normal electron tunneling and coulomb enhanced electron tunneling due to the presence of a trapped hole in the PbSe core of the QDs. Based on this picture, the spacing between the pairs of peaks is determined by the electron-hole interaction energy. The interpretation is supported by a theoretical analysis based on master-equation simulations of the electron and hole transport through the QD. Our results provide fundamental information relevant for understanding the electronic structure and transport phenomena in colloidal heteronanostructures.

[1] P. Liljeroth, P.A. Zeijlmans van Emmichoven, S.G. Hickey, H. Weller, B. Grandidier, G. Allan and D. Vanmaekelbergh, Phys. Rev. Lett. 95 (2005) 086801.
[2] Z. Sun, I. Swart, C. Delerue, D. Vanmaekelbergh and P. Liljeroth, Phys. Rev. Lett. 102 (2009) 196401.

STRUCTURE OF SI/GE NANOCLUSTERS AS STUDIED BY MOLECULAR DYNAMICS AND SEMI-GRAND-CANONICAL MONTE CARLO METHODS

A. Harjunmaa and K. Nordlund

Department of Physics, University of Helsinki, P.O. Box 43, FIN-00014 Helsinki, Finland
email: ari.harjunmaa@helsinki.fi

A. Stukowski and K. Albe

Institut für Materialwissenschaft, Technische Universität Darmstadt, Darmstadt, Germany

Ionized cluster beam deposition can be used to create anything from individual nanostructures to nanocrystalline films, depending on the amount of clusters deposited and the deposition energy. Experimentally, there is a number of ways to make these atomic clusters — for example, the newly constructed facility at the University of Helsinki Department of Physics employs a magnetron sputtering device and a condensation chamber filled with argon to condense the clusters. The clusters thus formed can then be accelerated and deposited onto the desired surface.

We have previously used molecular dynamics (MD) simulations to simulate the formation of silicon, germanium, and Si/Ge nanoclusters in an argon atmosphere at room temperature [1]. The results indicated that in the time frame of MD simulations, not all clusters were able to form radially symmetrical shapes. Whether this was an effect of short simulation time (of the order of nanoseconds), or if the resulting shapes were indeed stable, was left an open issue. In addition, it was noted that germanium atoms had the tendency to segregate to the outer layers of the clusters, which confirmed earlier findings done in our group [2].

This work continues the investigation into the energetically favorable shape and element distribution of Si and Ge nanoclusters. In addition to annealing the least spherical of the clusters to prompt radial symmetry, we use a new method that combines molecular dynamics with a semi-grand-canonical Monte Carlo algorithm to investigate the element distribution that is most favorable in terms of free energy. The results show that when annealed for at least 100 ns at 1800 K, the clusters become more spherical, and that the preferred location of the Ge atoms is indeed closer to the surface.

[1] A. Harjunmaa and K. Nordlund, Comp. Mat. Sci. 47 (2009) 456.
[2] J. Tarus, M. Tantarimäki and K. Nordlund, Nucl. Instr. and Meth. B 228 (2005) 51.

THE EFFECT OF CLUSTERING AND PERIODICITY OF ADSORBATE ATOMS ON ELECTRONIC PROPERTIES OF CARBON NANOTUBES

M.J. Hashemi and M.J. Puska

Department of Applied Physics, Aalto University, Espoo, Finland
email: jha@fyslab.hut.fi

Electronic properties of carbon nanotubes (CNTs) depend strongly on their geometrical structure. Especially, the chirality and diameter determine if a CNT is metallic or semiconducting. CNT applications are remarkably limited by the difficulty in controlling these structural details in fabrication processes. Moreover, point defects and adsorbed atoms considerably change their electronic properties. We have studied the effects of periodicity and clustering of adsorbate atoms on the band structures and the transport properties of CNTs using electronic structure calculation methods. The results can be rationalized on the basis of simple analytic rules. Understanding the functioning of adsorbate clusters and their periodicity may eventually enbe the tuning of CNTs into various nanoelectronics applications.

FABRICATION OF FREELY SUSPENDED CARBON NANOTUBE AND GRAPHENE DEVICES FOR ADVANCED APPLICATIONS

O. Herranen, K. Hannula, A. Johansson, T. Lahtinen, M. Ahlskog

Nanoscience Center, P.O.Box 35 FI-40014 University of Jyväskylä, FINLAND
email: olli.herranen@jyu.fi

Carbon nanotubes (CNTs) and graphene are strong candidates (in one and two dimensions, respectively) for making nanoscale electronic devices that both supplements and partly replaces conventional silicon technology. Nanotubes and graphene samples that are suspended have minimal interactions with the substrate and give therefore better possibilities to explore their intrinsic properties [1]. We realize our samples on thin Si_3N_4 membranes with a µm wide slit opening. On these samples it is easy to combine electrical transport measurements, optical spectroscopy and electron microscopy (TEM, electron diffraction) to a same individual CNT or graphene ribbon. These kinds of suspended devices can be used for varied advanced applications, e.g. resonators or nano-sensors.

One challenge in the making of nanoscale devices is to get a desired individual nanotube or a graphene ribbon in the right location, which for us means across the slit. Single walled carbon nanotubes (SWCNTs) can be grown individually from nanometer scale catalyst particles but in other synthetic conditions they tend to bundle together into SCWNT “ropes”. Separation of individual SWCNTs from such ropes, or debundling them, is an important and challenging task. Current methods involve to some degree harmful procedures that, for example, cut the tubes into submicron lengths. A connected issue is the question of solubility of individual SWCNTs, which are rigid macromolecular rods and therefore not generally dissolved. Dissolution of SWCNTs can be performed by transforming it into a polyelectrolyte salt [2], which is spontaneously dissolving in polar organic solvents without any sonication, use of surfactants or covalent functionalization that may be harmful to the carbon lattice. The method has been later extended to graphene [3].

We present here a method to fabricate highly advanced suspended carbon nanotube and grapheme devices using the polyelectrolyte salt to dissolve and debundle different SWCNT raw materials and graphene.

[1] J. Cao, Q. Wang, H. Dai, *Nature Mat.* **4** (2005) 745.
[2] A. Penicaud, *et al.*, *J. Am. Chem. Soc.* **127** (2005) 8.
[3] C. Vallés, *et al.*, *J. Am. Chem. Soc.* **130** (2008) 15802.

UNIVERSITY OF JYVÄSKYLÄ

FABRICATION OF ALL-OXIDE TUNNEL JUNCTIONS WITH SPIN-FILTERING FERRITE TUNNEL BARRIERS

L. Korhonen, Qi Hang Qin, and S. van Dijken

Aalto university, Department of Applied Physics, P.O.B 15100, FI-00076 Aalto, Finland
email: laura.korhonen@tkk.fi

Ferrite oxides such as $CoFe_2O_4$ and $NiFe_2O_4$ are insulating and ferrimagnetic. Their application as a tunnel barrier in magnetic tunnel junctions is anticipated to provide efficient spin-filtering of tunneling electrons due to spin-splitting in the conduction band and this could form the basis for large tunneling magnetoresistance (TMR). To study the physics behind quantum mechanical tunneling through complex magnetic oxide materials and explore their potential as active tunnel barrier materials, we are now working towards the fabrication of all-oxide tunnel junctions with ferrite tunnel barriers.

In our experiments we use $CoFe_2O_4$ as ferrimagnetic barrier, perovskite $La_{2/3}Sr_{1/3}MnO_3$ as magnetic electrode, and $SrRuO_3$ as counter-electrode. Thin films of these materials are grown onto single-crystalline $SrTiO_3$(001) substrates using a multi-target pulsed laser deposition (PLD) system. X-ray diffraction (XRD), atomic/magnetic force microscopy (AFM/MFM), SQUID magnetometry, and magnetotransport measurements are used to characterize the structural, magnetic, and electronic properties of the oxide films and tunnel junctions.

An important step towards epitaxial films with low defect densities is a proper preparation of the $SrTiO_3$(001) substrate. The crystal structure of $SrTiO_3$ consists of alternating SrO and TiO_2 layers. As a result, the surface of commercial $SrTiO_3$ substrates contains both terminations and rough step edges. Growth of oxide films on top of this substrate will lead to inhomogeneities and defects. To avoid this we have optimized a cleaning procedure which involves etching in buffered HF and subsequent high temperature annealing in O_2 atmosphere. After this treatment the $SrTiO_3$ surface is fully terminated by TiO_2 and the step edges are straight as confirmed by AFM. Another crucial requirement for tunnel junctions with a ferrimagnetic barrier is independent magnetic switching in the magnetic electrode and tunnel barrier. Through growth optimization of $CoFe_2O_4$/$La_{2/3}Sr_{1/3}MnO_3$ bilayers we were able to limit magnetic coupling between the layers and this resulted in gradual magnetization reversal in $CoFe_2O_4$ at large magnetic field and abrupt switching in $La_{2/3}Sr_{1/3}MnO_3$ at much smaller field. Finally, we have set up a reliable photolithography process for the fabrication of all-oxide magnetic tunnel junctions. This process involves two ion beam milling steps to define the bottom electrode and tunnel junction area, respectively, and one lift-off step to pattern the top electrode. To increase the uniformity of the junctions and limit the number of pinholes, the junction area can also be defined by e-beam lithography which limits the lateral size to about 100 nm.

3D UV-STAMPS BY COMBINED THERMAL AND UV-IMPRINTING

T. Haatainen, T. Mäkelä, J. Ahopelto

[a]VTT Micro and Nanoelectronics, P.O. Box 1000, FIN-02044 VTT Espoo, Finland
email: tomi.haatainen@vtt.fi

In comparison to conventional materials, plastic offers a flexiple and cost-effective substrate material for integrating printed electronics and optics. It can be utilized for fabrication of various devices e.g. optical gratings, printed transistors, flexible displays and solar cells. Nanoimprinting [1] is promising candidate for a low-cost and high-throughput method for pattern transfer of submicron scale features on various substrates. Thermal Step and Stamp Imprint Lithography SSIL [2,3] is a sequential imprinting method in which a features of a small silicon master is replicated into thermoplastic material using pressure and elevated temperature. The method can be combined with UV-Imprinting [4] to fabricate 3D structures into substrate.

In this work, we report a simple method to fabricate 3D polymer stamps by combining thermal SSIL and UV-SSIL [5]. The thermal imprinting was done using a small silicon stamp different microstructures. The stamp patterns were replicated into 100 x 100 mm2 PET substrate by thermal imprinting. The schematic presentation of the method is presented in Figure (left). In the second lithographic step submicron features of a quartz stamp were transferred into this pre-patterned PET substrate by UV-NIL as shown schematically in Figure (right). As a result, we have a PET substrate with 3D structures; micron scale recessed structures and elevated features with submicron dimensions.

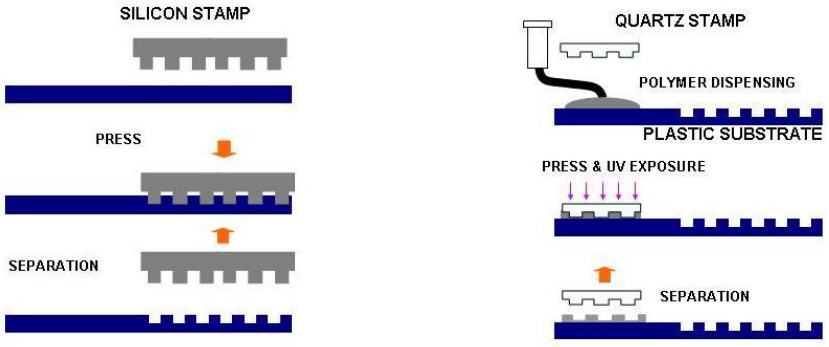

[1] T. Haatainen, J. Ahopelto, G. Gruetzner, M. Fink and K. Pfeiffer, Proc. SPIE 3997 (2000) 874
[2] S.Y. Chou, P.R. Krauss, P.J. Renstrom, Appl. Phys. Lett. 67 (1995) 3114.
[3] T. Haatainen and J. Ahopelto, Phys. Scri. 67(4) (2003) 357
[4] J. Haisma, M. Verheijein, K. van den Heuvel and J. van den Berg, J. Vac. Sci. Technol. B14 (1996) 4124
[5] T. Haatainen, P. Majander, T. Mäkelä, J. Ahopelto, Y. Kawaguchi, Jpn. J. Appl. Phys. 47(6) (2008) 5164

ROLL-TO-ROLL UV NANOIMPRINTING

T. Mäkelä[a], T. Haatainen[a] J. Ahopelto[a] and Y. Kawaguchi[b]

[a]VTT Micro and Nanoelectronics, P.O. Box 1000, FIN-02044 VTT Espoo, Finland
[b]Asahi Glass Co., Ltd. Yokohama, 221-8755 Japan
email: tapio.makela@vtt.fi

A method of making organic electronics, optoelectronics or functional surfaces with a low cost and high speed in large areas will be one of the critical issues in the future. Embossing a large area requires a relative high force, but also it may cause a high adhesion force making the mold–sample separation difficult as emphases in Ref. [1]. Roll-to-roll UV imprinting for UV curable resists will be an excellent alternative when low pressure and adhesion force is needed. In this work we demonstrate roll-to-roll UV stamp manufacturing principle and continuous roll-to-roll UV imprinting process. We have used a custom made nanoimprinter device [2] to demonstrate stamp preparation and manufacturing of polymer structures.

The flexible UV stamps were manufactured by using roll-to-roll imprinting on the fluorinated mold material (F-template) [9] on polycarbonate substrate from Asahi Glass or cellulose acetate film from Clarifoil. Mold material was patterned with conventional thermal roll-to-roll nanoimprinting process using a flexible Ni-master as a stamp. This allows us to prepare tens of UV molds very easily for further processing. Patterned templates were cut off from the web and wrapped on two printing rolls thereby making a “printing belt”. This belt works as a mold for roll-to-roll UV imprint experiments.

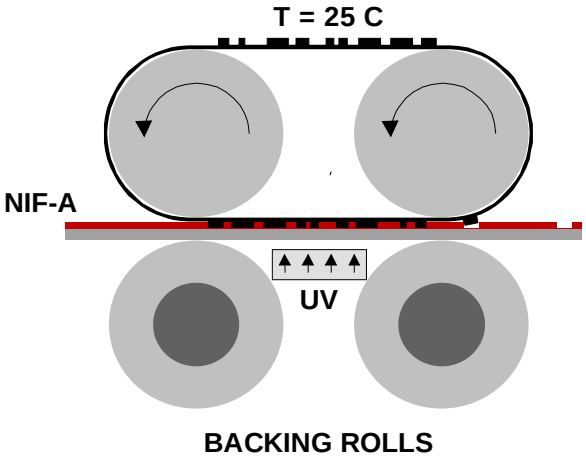

Figure shows a schematic principle of the roll-to-roll UV process. Patterned F-template is wrapped between two metallic cylinder and therefore ca. 10 cm long contact area can be achieved. Fluorinated phosensitive polymer NIF-A from Asahi Glass Co on the polymer web were used as a UV printing material. NIF-A were coated using a reverse gravure coating method. In the UV process polymers were cured when the mold is kept in constant. Resist curing is done by using UV-exposure unit (EFOS Ultracure 100ss) when printing speed 0.1 - 0.2 m/min (ca. 30 s curing time) and pressure less than 0.1 MPa were used. The feature sizes from 100 nm up to the 100 microns have been demonstrated.

[1] S. H. Ahn and L. Jay Guo, Adv. Mater. 20 (2008) 2044–2049.
[2] T. Mäkelä, T. Haatainen, P. Majander, J. Ahopelto and V. Lambertini, Jpn. J. Appl. Phys. 47 (2008) 5142-5144.

INVESTIGATIONS OF NON-IDEAL GRAIN BOUNDARIES OF GRAPHENE

S. Malola, H. Häkkinen and P. Koskinen

NanoScience Center, Department of Physics, P.O.B. 35, FIN-40014 University of Jyväskylä, Finland
email: sami.a.malola@jyu.fi

We investigate structural details and energetics of several different non-ideal grain boundaries of graphene. Based on statistics of polygons at the grain boundary area we explain differences in their height and vibrational spectra with respect to the chiral angle. The intensity and energy of the high-energy vibrational modes will decrease for the grain boundaries at the mid-chiral angles with relatively the lowest number of hexagons, reffering to less uniform structures. We represent also hydrogen adsorption energies as a benchmark for the reactivity of the grain boundary area together with densities of dangling bonds. Results show that the grain boundaries at the armchair side have the highest dangling bond densities while the mid-chiral angles the lowest. Over the half of the calculated structures have dangling bond densities between $1/7.5$ Å and $1/20$ Å. We discuss the relation of our calculations to experimental observations made by recent STM and AFM measurements.

[1] S. Malola, H. Häkkinen and P. Koskinen, in preparation

A PHENOMENOLOGICAL STUDY OF CARBON NANOTUBE GROWTH IN HOT WIRE GENERATOR UNDER CO / CO_2 ATMOSPHERE

K. Mustonen, A. Nasibulin and E. Kauppinen

Nanomaterials Group, Laboratory of Physics and Center for New Materials, Aalto University, P.O.B. 1000, FIN-02044, Finland
email: kimmoa.mustonen@hut.fi

The growth of carbon nanotubes in a chemical vapor deposition (CVD) based aerosol reactor for single walled carbon nanotube synthesis was observed. Nanosized iron catalyst particles were formed in pure CO / CO_2 atmosphere using a Hot Wire Generator (HWG) through evaporation-nucleation-condensation cycle [1]. The carbon nanotube growth took place in the gas suspension inside the vertical laminar flow reactor at temperatures between 650 and 870 °C. A capillary probe for super isokinetic aerosol sampling was utilized to quickly remove aerosols from the reactor. The conditions for carbon nanotube growth as well as active phase of iron catalyst particles were inspected by quick sample removal and consequent deposition on copper grids by electric field. The samples were observed in transmission electron microscope (TEM), and the composition was probed by the means of x-ray diffraction (XRD) and electron diffraction.

The carbon nanotube growth was shown to begin already at temperature conditions of 650 ± 50 °C. Also, indications that iron carbide (Fe_3C) is not a main constituent in the particle supporting the carbon nanotube growth was shown. Instead, the x-ray diffraction data suggested that the active phase of catalyst iron is either α-Fe, or both α and γ-Fe.

[1] Nasibulin, A.G., et al., Chemical Physics Letters 402(1-3): p. 227-232 (2005)

NANOCLUSTER MODIFICATION BY SWIFT HEAVY ION TRACKS, STUDIED WITH MOLECULAR DYNAMICS

O. H. Pakarinen, M. Backholm, F. Djurabekova and K. Nordlund

Department of Physics and Helsinki Institute of Physics, P.O. Box 43, FIN-00014 University of Helsinki, Finland
email: olli.pakarinen@helsinki.fi

Swift heavy ion irradiation leaves a latent ion track around the ion path in many materials, a few nanometers in diameter. Ion tracks are used in many applications, ranging from material modification to generation of nanostructures and to geological dating, but the microscopic structure of tracks has remained unknown. In recent experiments, a previously unresolved fine structure in latent ion tracks in amorphous silica was found comprising a low-density core and a high-density shell, and was confirmed by molecular dynamics (MD) simulations [1].

To further study the effect of swift heavy ion tracks on material properties, we model track generation in several different materials by MD simulations to see if the density fine structure is visible in other materials than silica. We also model a high dose of irradiation by successive track generation by large-scale molecular dynamics simulations, and show how overlapping tracks explain a recently found inhomogeneous steady state in irradiated amorphous silica.

Elongation or flattening of metal and semiconductor nanoclusters inside an insulating substrate has recently been demonstrated on several materials under swift heavy ion irradiation. The effect has been shown to be related to track formation properties of the substrate. We present large-scale MD simulations on Ge nanocluster modification under swift heavy ion irradiation, showing how nanocluster and ion track dimensions affect the shape transformation.

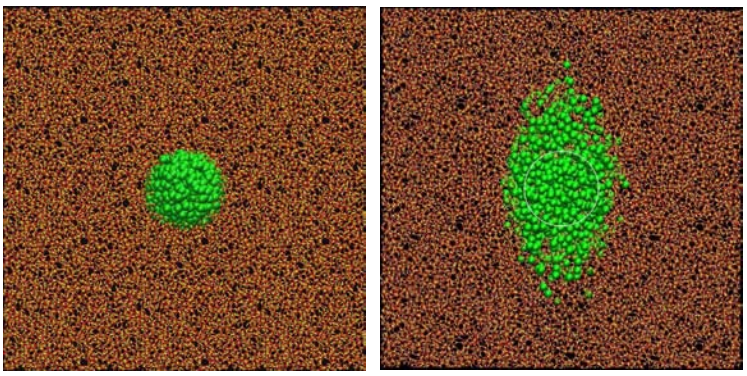

Swift heavy ion irradiation leads to elongation of the originally spherical 4 nm Ge nanocluster. MD simulations show how part of the cluster atoms dissolve into the surrounding silica matrix.

[1] P. Kluth, C. S. Schnohr, O. H. Pakarinen, F. Djurabekova, D. J. Sprouster, R. Giulian, M. C. Ridgway, A. P. Byrne, C. Trautmann, D. J. Cookson, K. Nordlund, and M. Toulemonde, Phys. Rev. Lett. 101 (2008) 175503.

GROWTH STUDIES OF SELF-ASSEMBLED INAS QUANTUM DOTS ON PATTERNED SUBSTRATES

A. Schramm, A. Tukiainen, J. Tommila, V. Polojärvi, T.V. Hakkarainen, A. Aho, M. Guina, and M. Dumitrescu

Optoelectronics Research Centre, Tampere University of Technology, P.O. Box 692, FIN-33101 Tampere
email: andreas.schramm@tut.fi

Deterministic addressing of single quantum dots (QDs) is a key requirement in order to employ QDs for future quantum and cryptographic devices [1]. One suitable QD system for aforementioned applications is self-assembled InAs QDs on GaAs deposited via molecular beam epitaxy. The self-organization of QDs can be controlled by patterning the GaAs substrate. Here we use nanoimprint lithography (NIL) in order to create large-scale pattern [2] on substrates. Results are present concerning to the growth of InAs quantum dots on NIL-prepared GaAs substrates.

[1] A. Zrenner, E. Beham, S. Stufler, F. Findeis, M. Bichler, G. Abstreiter, Nature **418**, 612 (2002)
[2] Jukka Viheriälä, Tuomo Rytkönen, Tapio Niemi and Markus Pessa, Nanotechnology **19**,015302 (2008)

LATERAL FORCE IMAGING OF CARBON NANOTUBES

M. Ahlskog and J. Lievonen

Department of Physics, Nanoscience Center, University of Jyväskylä, P.O.B. 35, FIN-40014 Jyväskylä, Finland
email: ahlskog@jyu.fi

Carbon nanotubes are usually imaged with the atomic force microscope (AFM) in non-contact mode. However, in many applications, such as mechanical manipulation or elasticity measurements, contact mode is used. The forces affecting the nanotube are then considerable and not fully understood. In this work lateral forces were measured during contact mode imaging with an AFM across a carbon nanotube. The effect of different variables, like scan angle, setpoint and tip radius, on lateral force during contact mode imaging, was studied. The imaged object was the multiwall carbon nanotube (MWNT) with well known cylindrical shape. From these measurements it can be concluded that shape of the lateral force signal is due to the slipping of the AFM tip on the round edges of the nanotube [1].

[1] J. Lievonen and M. Ahlskog, Ultramicroscopy, 109 (2009) 825.

UNIVERSITY OF JYVÄSKYLÄ

RESONANCES IN L-SHAPED GOLD NANOPARTICLES

H. Husu[1], J. Mäkitalo[1], J. Laukkanen[2], M. Kuittinen[2], J. Turunen[2], and M. Kauranen[1]

[1]Department of Physics, Optics Laboratory, Tampere University of Technology, P.O. Box 692, FI-33101 Tampere, Finland
[2]Department of Physics and Mathematics, University of Joensuu, P. O. Box 111, FI-80101 Joensuu, Finland
email: hannu.husu@tut.fi

The continuous interest in metal nanostructures is driven by their ability to manipulate light on the nanoscale. The possible applications, such as nanoantennas [1], nanoscale waveguides [2] or metamaterials [3], are based on the nanostructures' ability to exhibit very strong local electromagnetic fields. Two factors affect the local field enhancement; sharp features and plasmon resonances. The resonances have not been well understood so far. We give an extensive analysis of different kinds of resonances that can occur in L-shaped gold nanoparticles. We present both experimental and theoretical results.

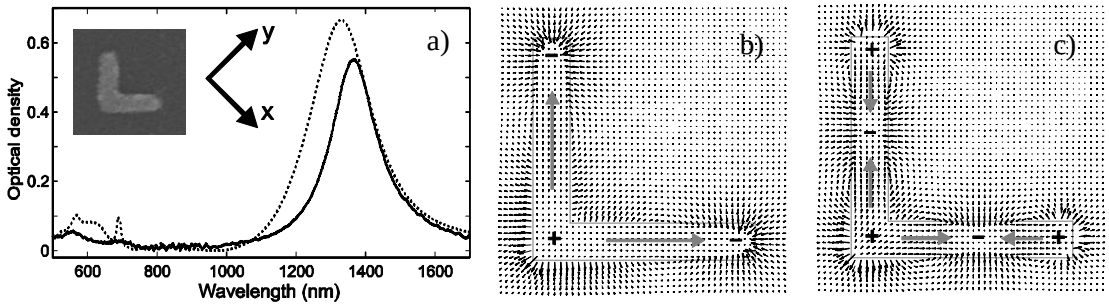

Figure 1 a) Experimental (solid) and calculated (dashed) extinction spectrum for y-polarization. b) Vector electric field distribution at the fundamental resonance and c) at the higher order resonance.

The L-shape has a mirror plane along y-direction and it is highly dichroic. For y-polarization the extinction spectrum shows several resonance peaks (Fig. 1a). The corresponding peaks can be found both from the measured and calculated spectra. To analyze the resonances, the common approach is to look at the distribution of the local electric field amplitude at the resonance. However, we consider the total vector field, calculated using FDTD, which shows not only the amplitude but also the direction of the electric field. From the vector field distribution it is easy to recognize the poles of the structure, which show the type of the resonance and to which part of the structure it is connected.

The fundamental resonance is found at 1350 nm, which corresponds to the oscillation along the arms of the L-particle (Fig. 1b). A small peak at 700 nm can be observed both in the measured and calculated spectrum. It is a higher order resonance, which can be confirmed by looking at the vector field distribution (Fig. 1c). Furthermore, we show that the resonance at 600 nm is related to the width of the arms, which has not been well explained in the past.

[1] J.-J. Greffet, Science 308 (2005) 1561.
[2] L. A. Sweatlock et al., Physics Review B 71 (2005) 235408.
[3] V. M. Shalaev, Nature Photonics 1 (2006) 41.

LEVITATION OF COLLOIDAL PARTICLES ON AN EVANESCENT OPTICAL WAVE

R. Khakimov, A. Shevchenko, A. Havukainen, M. Kaivola

Aalto University, Department of Applied Physics, P.O.B. 3500,
FI-00076 AALTO, Finland
email: roman.khakimov@tkk.fi

Often there is a requirement to control the position of an optically trapped micro- or nanoparticle above a flat substrate at a distance of less than 100 nm from the surface. This task is difficult to accomplish by using traditional optical tweezers. Hence, we have examined, experimentally and theoretically, the possibility to trap and manipulate spherical micro- and nanoparticles at these short distances from the substrate by using two evanescent optical waves. The waves are created by total internal reflection of two counter-propagating focused laser beams from the surface of the substrate. The particles are suspended in water. The distance between a trapped particle and the substrate is on the order of the evanescent-wave decay length, but it can be tuned by tuning the laser beam power. With our setup it is easy to control the position of the particle above the surface simply by translating the substrate with respect to the focal spot. On the other hand the particle can be moved along the Poynting vector of the evanescent field by tuning the powers of the two beams creating this field.

This technique can be used to verify the existing different expressions for electromagnetic force density in a dielectric medium. It can also be further developed to allow creating optical surface traps for particles in vacuum, which can be used, e.g., to investigate van der Waals and Casimir forces between a particle and a substrate.

For calculations of the force acting on a particle in the evanescent wave, we have used the electromagnetic energy-momentum tensor approach. Numerical simulations of optical fields interacting with the particle were performed by using finite difference and finite element methods provided by COMSOL Multiphysics software.

STRONG COUPLING BETWEEN FERROELECTRIC AND FERROMAGNETIC DOMAINS IN THIN Fe FILMS ON $BaTiO_3$

Tuomas Lahtinen and Sebastiaan van Dijken

Aalto University, Department of Applied Physics, P.O. Box 15100, FI-00076 Aalto, Finland
email: tuomas.lahtinen@tkk.fi

Magnetoelectric coupling in hybrid magnetic/ferroelectric structures has gained intense scientific interest in recent years. The effect allows for an active control over magnetic properties such as moment, anisotropy, and permeability by the application of an electric field and tuning of polarization and dielectric permittivity by an external magnetic field. Applications include dc and ac magnetic field sensors, magnetic memory, energy harvesting devices, and tunable microwave components.

In this paper, we report on direct interactions between ferroelectric and ferromagnetic domains. The system under study consists of a thin (10 - 20 nm) Fe film grown onto a $BaTiO_3$ (BTO) substrate with in-plane polarization. At room temperature the BTO lattice is tetragonal and this leads to the formation of alternating a1-a2 stripe domains whereby the elongated c-axis and polarization direction rotate by 90°. This is illustrated by the polarization microscopy image of Fig. 1(a). Using magneto-optical Kerr contrast and background subtraction it is possible to separately image the magnetic domain structure in the overlaying Fe film. An example of the remanent magnetization state is shown in Fig. 1(b). Obviously, the domain structure of the BTO substrate is imprinted into the Fe film. The correlation between the ferroelectric and ferromagnetic domains reflects a strong coupling mechanism, which for this system is explained by lattice strain. The alternating elongation of the BTO lattice in the film plane induces uniaxial magnetoelastic anisotropy in the magnetostrictive Fe film with a 90° rotation of the easy magnetization axis at domain boundaries. From the positive sign of the magnetostriction constant for Fe along <100> directions we infer that the polarization and easy magnetization axis are collinear. As the ferroelectric domains are electrically active this is a promising step towards electric-field controlled ferromagnetism.

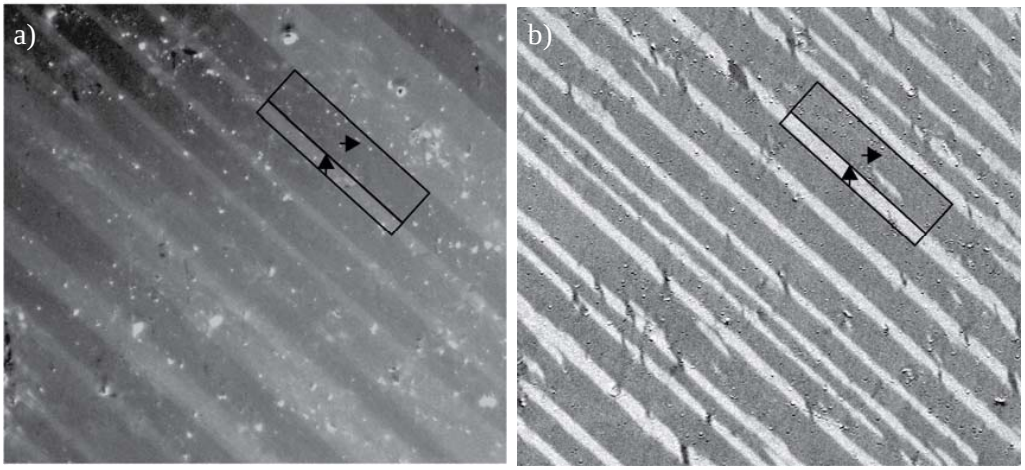

Fig. 1 Polarization microscopy images of (a) the ferroelectric and (b) the remanent ferromagnetic domain structure. The arrows indicate the polarization and magnetization directions, respectively.

MECHANICAL PROPERTIES OF PZT THIN FILMS STUDIED USING NANO-INTENDATION TECHNIQUE

J. Puustinen and J. Lappalainen

Microelectronics and Materials Physics Laboratories, P.O.B. 4500, FIN-90014 University of Oulu, Finland
email: jpuust@ee.oulu.fi

Nanomechanical properties of pulsed laser deposited $Pb(Zr_xTi_{1-x})O_3$ thin films with various thicknesses were measured using scanning probe microscopy (SPM Veeco Dimension 3100). Thin films were deposited at room temperature and post-annealed at temperatures of 700 ºC and 800 ºC. Microstructure of the films was characterized using x-ray diffraction (XRD), Raman spectroscopy, and scanning probe microscopy.

Films were crystallized to perovskite structure with either trigonal or tetragonal orientation preferred. Splitting of (001/100), (011/110), and (002/200) crystal plane reflections and asymmetric peak around ~570 cm^{-1} were clearly observed in XRD and Raman measurements, indicating preferred tetragonal orientation, in films with thickness below 400 nm. Strong (110) crystal plane reflection with symmetric peak around ~570 cm^{-1} was present in films with thickness above 400 nm, indicating preferred trigonal orientation. Average grain size of the films was around ~12 nm according to Warren-Averbach analysis.

Hardness *H* and elastic stiffness *S* values of the films were calculated from indentation load-displacement curves obtained during one cycle of loading and unloading. Indentation load-displacement curves were narrow for films with either tetragonal or trigonal orientation and broader for films with tetragonal-trigonal phase co-existence, indicating higher elasticity of films with tetragonal-trigonal phase co-existence. Hardness and elastic stiffness values around ~6 GPa and ~3×10^{-7} N/nm, respectively, were calculated for well oriented films, while corresponding values were ~2 GPa, ~4×10^{-7} N/nm, respectively, for films with tetragonal-trigonal phase co-existence. Relaxation of the stress state due to phase co-existence in the films was found to decrease hardness *H*, as well as the behavior of dielectric reponse in phase transition.

NANOSCHOOL DEVELOPS INQUIRIES FOR SCIENCE EDUCATION

Anssi Lindell[1)], Anna-Leena Latvala[1)], Tom Nevanpää[2)] Lasse Taskinen[3)] and Jouni Viiri[1)]

1) Department of Teacher Education
2) Teacher Training School
3) Department of Physics
P.O. Box 35, FIN-40014 University of Jyväskylä, Finland.
email: anssi.lindell@jyu.fi

We introduce the "Nanoschool"–program that links scientists, science educators and science education researchers of University of Jyväskylä together. The program was started in 2005, based on the notion that though the social and economical impact of nanotechnology on society and environment were clear, the educational resources were lacking.

"Nanoschool" helps teachers in integrating nanoscience into the traditional science curriculum for grade 7-12 students (ages 13-18) and into introductory university courses. To this aim, "Nanoschool" designs educational inquiries in nanoscience based on everyday products and common school chemicals, devices and facilities. The instructions are shared for free at http://nanokoulu.net. This way the inquiries can be carried out by any interested teacher.

The themes of the inquiries are selected from four big ideas of nanoscience: (1) surface area to volume ratio; (2) quantum effects; (3) microscopy and modelling; and (4) tools and devices.

In the poster we showcase the following sample inquiries:

1) an elastic optical grating ("teledynamometer") based on polydimethylsiloxane (PDMS) polymer [1];
2) an oscillating beam balance [2];
3) a toy model of a scanning probe microscope (SPM) [1];
4) a simulation of the function and properties of Coulomb blockade thermometer (CBT).

[1] G. Planinsic, A. Lindell and M. Remskar, European Journal of Physics 30 (2009).
[2] A. Lindell and J. Viiri, Journal of Science Education and Technology 30 (2009) 6.

UNIVERSITY OF JYVÄSKYLÄ

NONLINEAR TRANSPORT IN POLYPYRROLE NANOLAYERS ON DISCONTINUOUS ULTRATHIN GOLD FILMS

D. Mtsuko and M. Ahlskog

University of Jyväskylä, Nanoscience Center, P.O.B. 35(YFL), FIN-40014 Jyvaskyla, Finland.
email: davie.j.mtsuko@jyu.fi

We have studied the charge transport in nanolayers of polypyrrole (PPy) that were grown electrochemically onto discontinuous ultrathin films of gold. The gold film consisted of 100 nm size islands, separated from each other by nanometer-size gaps. The thickness of PPy nanolayers can be varied from 30 to 200 nm. The I-V characteristics of these hybrid Au-PPy nanostructures show strong non-linearity, especially at low temperatures, and in particular for the more insulating samples. Variable range hopping transport is reconfirmed from the fit to log I vs. $V^{1/4}$ plots. Furthermore, the I-V data follow an empirical relation $dlogI/dV^{1/4} \sim T^{-1/2}$.

[1] D. Mtsuko, A. Avnon, J. Lievonen, R. Menon, and M. Ahlskog, *Nanotechnology*, 17, 125304 (2008).

UNIVERSITY OF JYVÄSKYLÄ

EFFECTIVE MEDIUM MULTIPOLAR TENSOR ANALYSIS OF SECOND-HARMONIC GENERATION FROM METAL NANOPARTICLES

M. Zdanowicz , S. Kujala, H. Husu, and M. Kauranen

Tampere University of Technology, Institute of Physics, Optics Laboratory,
P.O. Box 692, FI-33101 Tampere, Finland;
email: mariusz.zdanowicz@tut.fi

Second-order nonlinear optical effects are electric-dipole-forbidden in centrosymmetric materials, but become allowed through magnetic-dipole and electric-quadrupole effects. Furthermore, such higher multipole effects can play a role also in the response of non-centrosymmetric materials, as demonstrated for second-harmonic generation (SHG) from chiral thin films of organic molecules and from metal nanostructures [1,2].
For nanostructured materials, higher multipole effects can occur due to elementary light-matter interactions or due to field retardation across nanoparticles. For SHG from metal nanostructures, the latter mechanism was operative and associated with nanoscale defects, which attract strong local fields. The evidence of multipolar SHG emission was obtained from the different radiative properties of the various multipolar sources [3].
In this paper, we present a more complementary multipolar tensor analysis of SHG from arrays of L-shaped metal nanoparticles. Evidence of multipole effects at both the fundamental and SHG frequency is obtained from a detailed analysis of the polarization-dependent SHG response. The analysis is based on the different transformation of the various multipolar interactions for SHG emitted in the transmitted and reflected directions and for the fundamental beam incident on the metal or substrate side of the sample.
Our sample consisted of arrays of L-shaped gold nanoparticles (linewidth ~100 nm, arm length ~200 nm) ordered in a square lattice (400 nm period) deposited on a fused quartz substrate. The SHG experiments were performed using a femtosecond laser (200 fs pulse length, 82 MHz repetition rate, 320 mW average power). To account for dipolar and higher multipolar interactions, we define three effective tensors, where the first accounts only for dipole interactions and the other two for lowest-order magnetic interactions at the fundamental and SHG frequencies, respectively. The results suggest that the dipole interactions dominate the response, and that the magnetic interactions at the fundamental frequency are more important than at the SH frequency.

[1] B. K. Canfield, S. Kujala, K. Jefimovs, Y.Svirko, J. Turunen, M. Kauranen, J. Opt. A: Pure Appl. Opt 8, S278 (2006),
[2] S. Kujala, B. K. Canfield, M. Kauranen, Y. Svirko, J. Turunen, Phys. Rev. Lett. 98, 167403 (2007),
[3] S. Kujala, B. K. Canfield, M. Kauranen, Y. Svirko, J. Turunen, Opt. Express, 16, 17196 (2008).

8 Nanophysics and quantum matter

8.1 Oral session, Friday 12 March 14:30-16:00

8.2 Poster session, Friday 12 March 16:00-18:00

Decoherence in adiabatic quantum evolution – application to Cooper pair pumping

J. P. Pekola, V. Brosco, M. Möttönen, P. Solinas and A. Shnirman

Department of Applied Physics/COMP and Low Temperature Laboratory, Aalto University, School of Science and Technology
P.O.B, 15100, FI-00076 Aalto, Finland
email: paolo.solinas@tkk.fi

One of the challenges of adiabatic quantum control theory is the proper inclusion of the effects of dissipation. Here, we study the dynamics of a two-level quantum system, a superconducting Cooper pair pump, subject to adiabatic drive and dissipation, taking consistently into account terms up to second order in the coupling strength to the environment. In the zero temperature regime and in the full adiabatic limit, we are able to obtain analytical results for the evolution of the system in the quasi-stationary regime. It turns out that, if the system is initially in the ground state, the presence of environment does not affect the evolution and the expected geometric pumped charge. This result can be explained as a join effect of the adiabatic evolution and the relaxation due to the environment. At zero temperature, the only effect of the noise is to induce relaxation to the ground state. If the evolution is adiabatic, the system starts and remains in the instantaneous ground state of the driving Hamiltonian during the evolution; then, there cannot be relaxation and the environment has no effect on the dynamics. For finite frequencies the instantaneous excited state is populated. In this case, the presence of the environmental noise induces relaxation from the excited to the ground state helping to restore the ideal evolution (Figure 1).

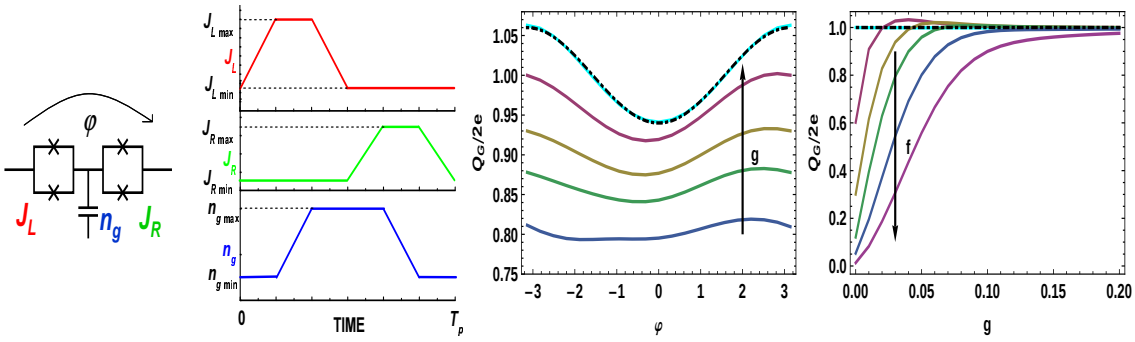

Figure 1: (Left) Schematics of the electric circuit and the pumping cycle. (Center) Pumped charge for zero-temperature environment as function of the phase difference across the superconducting pump φ with finite frequency pumping. The arrow indicates the increasing coupling g. (Right) Pumped charge as a function of the coupling strength g with $\varphi = \pi/2$ and the pumping frequency $f = 10, 25, 50, 75, 100$ MHz. The arrow indicates the increasing frequency. In both cases, the dashed line is the ideal pumped charge in the absence of noise and in the adiabatic limit.

[1] J. P. Pekola, V. Brosco, M. Möttönen, P. Solinas and A. Shnirman: arXiv:0911.3750v1. .

EXTREME DRIVING OF A JOSEPHSON QUBIT IN CIRCUIT CAVITY QUANTUM ELECTRODYNAMICS

Jani Tuorila[1], Matti Silveri[1], Mika Sillanpää[2], Erkki Thuneberg[1], Yuriy Makhlin[2,3] and Pertti Hakonen[2]

[1]Department of Physics, University of Oulu, FI-90014 Finland
[2]Aalto University, School of Science and Technology, Low Temperature Laboratory, FI-00076 Aalto Finland
[3]Landau Institute for Theoretical Physics, 119334 Moscow, Russia
email: matti.silveri@oulu.fi

A superconducting charge-phase qubit was brought to the limit of a large drive amplitude, while simultaneously maintaining a coupling to a resonant cavity used for the measurement via the qubit-cavity interaction. Microwave driving of the qubit was implemented classically by nonlinear coupling to the flux. We use the Floquet approach to explain the measured absorption spectrum.

The extreme driving of the qubit reveals, for example, multiphoton resonances [1, 2] and Landau-Zener-Stückelberg population oscillations [3]. Our measured, simulated and theoretically analyzed results show that Mollow transitions, breaking of rotating wave approximation and forbidden probe transitions between the dressed states [4] can be added to the gallery of strong driving phenomena in macroscopic solid state two-level systems.

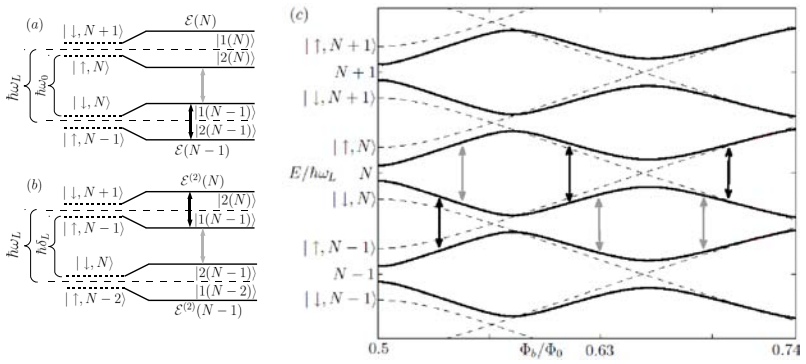

Figure 1: Dressed states of the superconducting qubit. Possible probe transitions between dressed states are denoted with gray and black arrows indicating lower Mollow and Rabi transition respectively. The schematic figures (a) and (b) show the first and second avoided crossing. Dressed state Floquet quasienergies (solid lines) are drawn in Fig. (c) together with uncoupled qubit-cavity energies (dashed lines) as an function of qubit bias flux $\Phi_{\rm b}$ in units of $\Phi_0 = h/2e$.

[1] W. D. Oliver *et al.*, Science **310**, 1653 (2005).
[2] M. Sillanpää *et al.*, Phys. Rev. Lett. **96**, 187002 (2006).
[3] S. N. Shevchenko, S. Ashhab and F. Nori, arXiv:0911.1917v1 (2009).
[4] C. Cohen-Tannoudji, J. Dupont-Roc and G. Grynberg, *Atom-Photon Interactions: Basic Processes and Applications*, (Wiley-VCH, Weinheim 2004).

PROPOSAL FOR A GROUND STATE GEOMETRIC QUBIT IN SUPERCONDUCTING CIRCUITS

J.-M. Pirkkalainen[1], P. Solinas[1], J. P. Pekola[2], and M. Möttönen[1,2]

[1]Department of Applied Physics/COMP, Helsinki University of Technology, P.O.B. 5100, FIN-02015 TKK, Finland.
[2]Low Temperature Laboratory, Helsinki University of Technology, P.O.B. 3500, FIN-02015 TKK, Finland.
email: juha.pirkkalainen@hut.fi

The modern advances in nanotechnology promise accurate means to control quantum systems and states. The concept of quantum computer provides a novel subject into which this knowledge has been increasingly applied in the recent years. In addition to being just an ultimate challenge for control of quantum systems, quantum computers open a realization to a completely new type of computing.

The advantage of quantum computers over classical ones relies on the possibility to perform operations on superpositions. This enables interference between the probability amplitudes of the superposition states when operations are performed on them. This interference can be used to solve problems in a completely different way than in classical computers. Therefore, quantum computer should not be viewed as the ultimately efficient classical computer but rather as a mean to a completely new class of computation.

Quantum bit (qubit) in a traditional quantum computer consists of a two-level quantum system with energy separation between the two states and dynamical means to control the evolution and transitions within these two states. In a geometric quantum computer, however, the two states are kept degenerate and time-independent transformations are induced by adiabatic cycles of the control parameter of the Hamiltonian.

Geometric quantum computer proposals [1, 2, 3, 4] to date have been based on a Hamiltonian involving four quantum states and the computational degenerate eigenspace is not the ground state manifold. Here, we will present a simple superconducting circuit with which a universal qubit working in the ground state can be realized. In addition, the Hamiltonian introduced here can be applied to other physical realizations and has only three quantum states involved.

[1] L.-M. Duan, J. I. Cirac, and P. Zoller, Science 292, 1695 (2001).
[2] L. Faoro, J. Siewert, and R. Fazio, Phys. Rev. Lett. 90, 028301 (2003).
[3] M.-S. Choi, J. Phys.: Condens. Matter 15, 7823 (2003).
[4] V. Brosco, R. Fazio, F. W. J. Hekking, and A. Joye, Phys. Rev. Lett. 100, 027002 (2008).

SUPERCONDUCTING QUANTUM INTERFERENCE PROXIMITY TRANSISTOR

F. Giazotto,[1] J.T. Peltonen,[2] M. Meschke,[2] and J.P. Pekola[2]

[1] NEST CNR-INFM and Scuola Normale Superiore, Piazza dei Cavalieri 7, I-56126 Pisa, Italy
[2] Low Temperature Laboratory, Aalto University School of Science and Technology, P.O. Box 13500, FI-00076 Aalto, Finland
email: joonasp@ltl.tkk.fi

We present the realization and characterization of a new type of a superconducting interferometer, the superconducting quantum interference proximity transistor (SQUIPT) [1]. Its operation relies on the modulation with the magnetic field of the DOS of a proximized metallic wire embedded in a superconducting ring. The modulation of the DOS is detected as a change in the current–voltage characteristic of a normal metal – insulator – superconductor tunnel junction. Flux sensitivities down to $\sim 10^{-5}\Phi_0\mathrm{Hz}^{-1/2}$ ($\Phi_0 = 2 \times 10^{-15}$ Wb is the flux quantum) were achieved already in our non-optimized design, with an intrinsic dissipation ($\simeq 100$ fW) which is several orders of magnitude smaller than in conventional superconducting interferometers. Our measurements are in agreement with the theoretical prediction of the SQUIPT behavior, and suggest that optimization of the device parameters would lead to a large enhancement of sensitivity for the detection of small magnetic fields. We further discuss the features of this setup and their potential relevance for applications.

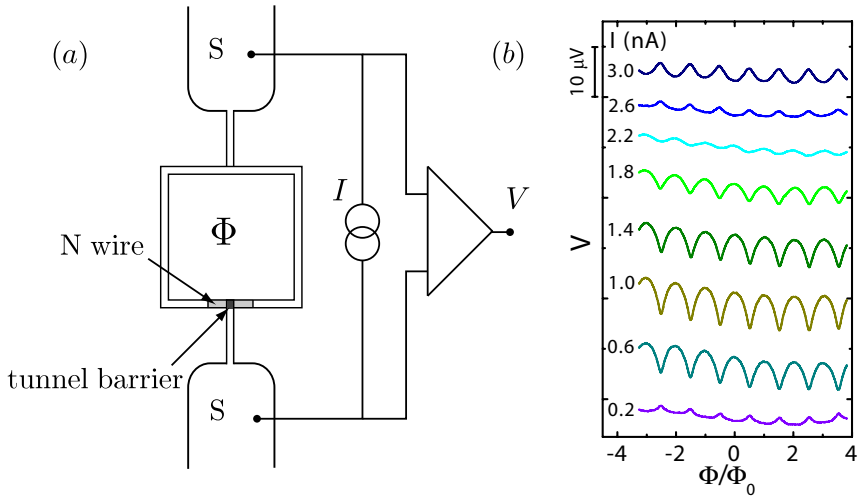

Figure 1: (a) Schematic model of the device structure together with the measurement configuration. The structure is biased by a constant current I, and the voltage drop V is recorded as a function of the applied magnetic flux Φ through the loop. (b) Typical measured voltage modulations $V(\Phi)$ at 50 mK for various values of the bias current I. The curves are vertically offset for clarity.

[1] F. Giazotto *et al.*, arXiv:0909.3806, submitted for publication (2009).

Reducing 1/f noise in Al-AlO$_x$-Al tunnel junctions by thermal annealing

J.K. Julin, P.J. Koppinen and I.J. Maasilta

Nanoscience Center, Department of Physics, University of Jyväskylä,
P. O. Box 35, FIN–40014 University of Jyväskylä, Finland.
email: juhani.julin@phys.jyu.fi

Al–AlO$_x$–Al tunnel junctions can be stabilized by annealing them in a vacuum chamber at temperature of 400°C [1]. Here we report for the first time that the annealing procedure also reduces the characteristic 1/f noise in the samples. Both ultra high vacuum and high vacuum fabricated samples demonstrated a significant reduction in the 1/f noise level, but no effect was found between substrates of nitridized and oxidized silicon wafers. Temperature dependence of noise levels was studied at temperatures between 4.2 and 340 Kelvin where neither linear nor quadratic dependence was detected. The low frequency noise was measured using an AC bridge amplitude modulation technique, which effectively eliminates the otherwise dominating preamplifier 1/f noise [2].

Tunnel junction is a versatile nanoelectrical component, which has many applications such as radiation detectors, Coulomb blockade thermometers, single electron transistors, SINIS coolers and thermometers and an usage in quantum computation as a solid-state realization of a qubit. The instability of the junctions is a common problem for applications. The oxide barrier has imperfect crystal structure after fabrication, thus the barrier atoms may try to spontaneously reorganize to equilibrium positions. This is seen as an increase of tunneling resistance with time. At room temperature, this spontaneous relaxation takes a long time. One other possible explanation might be that the barrier absorbs other unwanted molecules inside to fill vacancies, since vacuum conditions prevent aging significantly.

1/f noise is still without commonly accepted theory, but experimental results indicate it originates from defects like a two-level system which spontaneously oscillates, like an impurity atom in a lattice [3]. One motivation to study 1/f noise in Al–AlO$_x$–Al tunnel junctions is the possible use of tunnel junctions in quantum computation. Our results may have some relevance in reducing the critical current fluctuations in superconducting quantum bits based on tunnel junctions, where the 1/f noise causes decoherence [4].

[1] P. J. Koppinen, L. M. Väisto, and I. J. Maasilta. Complete stabilization and improvement of the characteristics of tunnel junctions by thermal annealing. *Applied Physics Letters*, **90**:053503, 2007.

[2] John H. Scofield. ac method for measuring low-frequency resistance fluctuation spectra. *Rev. Sci. Instrum.*, **58**:985, 1987.

[3] M. B. Weissman. $1/f$ noise and other slow, nonexponential kinetics in condensed matter. *Rev. Mod. Phys.*, **60**:537, 1988.

[4] J. Bergli, Y. M. Galperin, and B. L. Altshuler. Decoherence in qubits due to low-frequency noise. *New Journal of Physics*, **11**:025002, 2009.

VACUUM RABI SPLITTING AND STRONG-COUPLING DYNAMICS FOR SURFACE-PLASMON POLARITONS AND RHODAMINE 6G MOLECULES

T.K. Hakala[1], J.J. Toppari[1], M. Pettersson[2], H. Kunttu[2], A. Kuzyk[3], and P. Törmä[3]

[1]Department of Physics, [2]Department of Chemistry, Nanoscience Center,
P.O. Box 35, 40014 University of Jyväskylä, Finland
[3]Department of Applied Physics, P.O. Box 5100, 02015 Helsinki University of Technology, Finland
email: j.jussi.toppari@jyu.fi

Surface plasmon polaritons (SPPs) are coupled excitations of electromagnetic field and free electrons in metal, which can propagate in a wavelike fashion along a metal-dielectric interface. SPPs can be confined below the diffraction limit of free space light, and thus may provide the way to integrated optical circuits in nanoscale. Also, a high field strength due to the confinement leads to increased interactions. We have studied interactions between organic dye molecules, quantum dots (semiconductor nanocrystals) and waveguided SPPs. Plasmonic energy transfer from donor molecules to acceptor molecules as well as surface plasmon coupled emission from the donor molecules is observed over ten micrometer distances [1]. Also frequency conversion of SPPs by organic dye molecules has been demonstrated [2].

In this work we report on strong coupling between SPPs and Rhodamine 6G (R6G) molecules, with double vacuum Rabi splitting energies up to 230 and 110 meV [3]. In addition, we demonstrate the emission of all three energy branches of the strongly coupled SPP-exciton hybrid system, revealing features of system dynamics that are not visible in conventional reflectometry. Finally, in analogy to tunable-Q microcavities, we show that the Rabi splitting can be controlled by adjusting the interaction time between the waveguided SPPs and R6G deposited on top of the waveguide (see Fig. below).

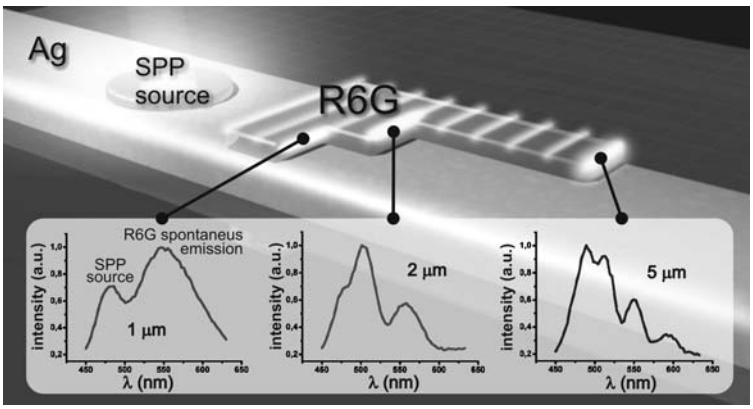

Figure: Measured spectra of scattered SPPs after propagating through 1, 2 and 5 µm long R6G interaction areas. As observed in the spectra, the strong coupling characteristics can be controlled by controlling the interaction time via R6G area length. The method allows adjusting of the interaction time between SPP and R6G with sub-fs precision by standard lithography methods, and gives access to extremely non-adiabatic phenomena of strongly coupled systems.

[1] A. Kuzyk, *et al.*, Opt. Exp. 15 (2007) 9908.
[2] T.K. Hakala, *et al.*, Appl. Phys. Lett. 93 (2008) 123307.
[3] T.K. Hakala, *et al.*, Phys. Rev. Lett. 103 (2009) 053602.

UNIVERSITY OF JYVÄSKYLÄ

LOCALIZED SUPERFLUID PHASES WITHIN SOLID HELIUM

V. Apaja[1], H. Lauter[2] and E. Krotscheck[3]

[1]Nanoscience Center , Department of Physics, University of Jyväskylä, Finland
email: vesa.apaja@gmail.com
[2] Institut Laue-Langevin, 6, rue Jules Horowitz, 38042 Grenoble, France
[3] Institut für Theoretische Physik, Johannes Kepler Universität, 4040 Linz, Austria

Superfluidity appears in bulk liquid helium due to the quantum nature and the interaction between helium atoms. Recent elastic and inelastic neutron scattering experiments[1] show that superfluid phases exist at high pressures in solid helium in Aerogel. Superfluidity is present beyond the limits where superfluidity exists in the bulk helium liquid. The new mechanisms that cause phase coherence and superfluidity are confinement and localization due to the interaction of the helium atoms with an external body. Microscopic many-body calculations [2] model the localization effect and provide, by investigating the roton-gap parameters, evidence for two quasi 2-dimensional liquid phases inside the solid helium.

The figure below shows the helium phase diagram, supplemented with the new superfluid phases. The three triangles indicate where the low temperature measurements were taken. The rectanglular area indicates the phase that contains a superfluid double layer sandwitched between solid helium. The striped area is a second superfluid phase, localized in the interface between the Aerogel and the solid helium.

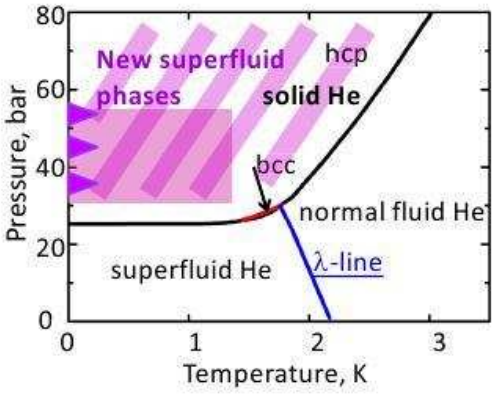

[1] H. Lauter, V. Apaja, I. Kalinin, E. Katz, M. Koza, E.Krotscheck, V. V. Lauter and A. V. Puchkov, submitted (2009)
[2] V. Apaja and E. Krotscheck, Phys.Rev. B 64, 134503-21 (2001).

SIZE-DEPENDENCE OF THE KONDO EFFECT IN NANOCONTACTS OF THE PURE METALS

K. Gloos and E. Tuuli

Wihuri Physical Lab, Dept. of Physics and Astronomy, FIN-20014 University of Turku
email: kgloos@utu.fi

We have investigated *Al*, *Cd*, *Cu*, *Fe*, and *Ni* break junctions at around 1 K. At this temperature also *Al* and *Cd* are in the normal state. All devices showed zero-bias anomalies that depend strongly on the contact radius ($0.1-20$ nm). Large contacts usually had a single zero-bias maximum which can be described by Kondo scattering with effective spin $S \approx 0.2$ and Kondo temperatures in the 10 - 1000 K range like for spear-anvil type point contacts [1]. Small contacts showed additional structure which disappeared at the onset of electron-phonon scattering. Those anomalies could be described by multiple Fano resonances. For *Fe* and *Ni* contacts the size of the anomalies varied like $\delta R \propto R^2$, but *Al*, *Cd*, and *Cu* had a slightly weaker $\delta R \propto R^{3/2}$ dependence. Since such size dependencies exclude material impurities, we attribute these zero-bias anomalies to Kondo scattering at a single 'impurity' caused by a spontaneous spin polarisation at the contact interface. Our break-junction data agree with recent results of atomic size contacts of *Co*, *Fe*, and *Ni* [2].

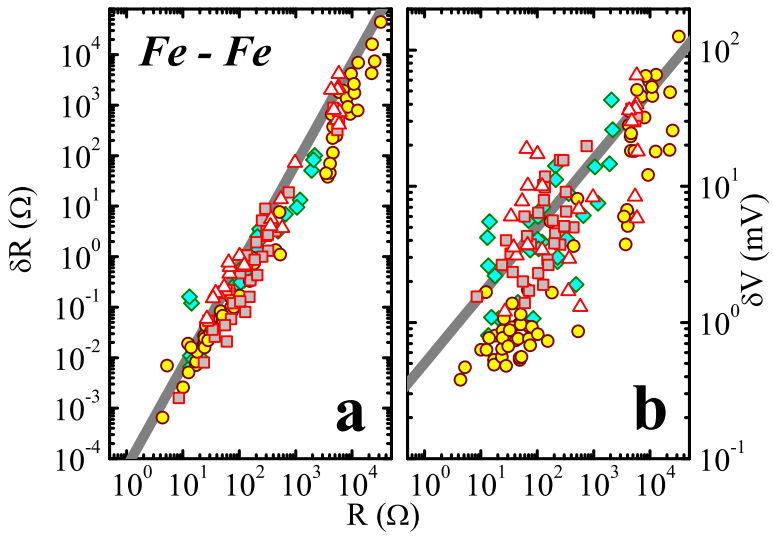

Figure 1: (a) Magnitude δR and (b) width δV of the zero bias anomaly of *Fe* break junctions versus contact resistance R at around 1 K. Solid lines: expected magnitude for scattering at a single Kondo impurity in the unitary limit as well as the expected width when the Kondo length ξ_K equals 100 times the contact radius a.

[1] K. Gloos, *Fiz. Nizk. Temp.* **35** (2009) 1204.
[2] M. R. Calvo, J. Fernández-Rossier, J. J. Palacios, D. Jacob, D. Natelson, and C. Untiedt, *Nature* **458** (2009) 1150.

LATERAL ORDERING OF SELF-ASSEMBLED INAS QUANTUM DOTS ON STRAINED GAINP

T.V. Hakkarainen, A. Schramm, A. Tukiainen, R. Ahorinta, and M. Guina

Optoelectronics Research Centre, Tampere University of Technology, P.O. Box 692, FIN-33101 Tampere
email: teemu.hakkarainen@tut.fi

Being able to fabricate laterally ordered InAs quantum dots (QDs) is essential for numerous electronic and photonic applications including single-photon emitters and single-electron transistors. The lateral ordering of InAs QDs can be achieved with several methods including the use of pre-patterned substrates [1] and exploitation of the strain field of misfit dislocations (MDs) in the underlying GaInAs layer [2-4].The purpose of the experiment reported here is to investigate the effect of strain in an underlying GaAs-capped GaInP layer on the growth of InAs QDs.

A set of three QD samples were grown on GaAs(100) substrates with molecular beam epitaxy. All the QD samples comprised a 60 nm thick partially relaxed strained layer capped with a 30 nm GaAs layer and covered with 2.2 monolayers of InAs to form QDs. The strained layers under investigation were tensile and compressively-strained GaInP, and compressively-strained GaInAs, which served as a reference. For post growth characterization, we used atomic force microscopy and high-resolution X-ray diffractometry.

Alignment of QDs on MDs was observed in all samples. In the compressively-strained samples the QDs were localized on the ridges formed on the MDs. However, in the tensile-strained sample, arrays of QDs were formed in grooves resulting in significantly stronger QD ordering. Another form of ordering was observed in the tensile-strained sample: The QDs in between the MDs formed couple-dot long lines along [0-11] crystal direction. As a cause for this we propose lateral composition modulations along with surface corrugation, which was caused by the accumulation of segregated indium above the In-rich domains of the GaInP layer.

[1] P. Atkinson, S.P. Bremner, D. Anderson, G.A.C. Jones and D.A. Ritchie, Microelectronics Journal **37**, 1436 (2006).
[2] C.L. Zhang, Z.G. Wang, F.A. Zhao, B. Xu, P. Jin, J. Crystal Growth **265**, 60 (2004).
[3] C.L. Zhang, B. Xu, Z.G. Wang, P. Jin, and F.A. Zhao, Physica E **25**, 592 (2005).
[4] Chunling Zhanga, Lei Tang, Yuanli Wang, Zhanguo Wang, and Bo Xu, Physica E **33**, 130 (2006).

FLUCTUATIONS OF TEMPERATURE IN A SMALL METALLIC PARTICLE

S. Kafanov, S.J. MacLeod, and J.P. Pekola

Low Temperature Laboratory, Aalto University School of Science and Technology, P.O. Box 13500, FI-00076 AALTO, Finland
email: jukka.pekola@tkk.fi

We discuss a small body exchanging energy with the bath via thermal conductance $G_{\rm th}$. According to basic thermodynamics, the instantaneous temperature of the body with heat capacity C fluctuates around its mean T_0 such that, classically, $\langle \delta T^2 \rangle = k_B T_0^2/C$. These fluctuations have Lorentzian spectrum with the cut-off frequency $G_{\rm th}/C$. We discuss this picture and its extensions in the context of a mesoscopic metal grain coupled to the bath by electron-phonon (ep) relaxation and by tunneling. Experiments to detect the effect seem feasible, with $\sqrt{\langle \delta T^2 \rangle}/T_0 > 10$ % being a realistic magnitude of it, for a metal particle that can be realized by standard electron beam lithography and measured at the temperature of $T_0 = 100$ mK, also easily achievable in the experiment. The expected cut-off frequency determined by the ep coupling is well below 1 MHz. We aim to detect the temporal variation of temperature by an rf-reflection measurement on a tunnel junction connected to the metal grain.

SUPERCONDUCTIVITY IN THE FERROMAGNETIC METALS CO, NI AND FE

E. Tuuli and K. Gloos

Wihuri Physical Lab., Dept. of Physics and Astronomy, FIN-20014 University of Turku
email: estuul@utu.fi

Most elemental metals have either a superconducting or a ferromagnetic ground state. The mechanisms compete with each other and magnetism usually excludes superconductivity. Therefore a small amount of residual magnetic impurities is enough to prevent superconductivity in Cu and the noble metals [1]. However, bulk Cu can be driven into a superconducting state via the proximity effect [2].

Point-contact spectroscopy with a superconducting tip offers a straightforward method to induce local superconductivity in an otherwise normal metal and to investigate its properties. We have studied contacts between superconducting Nb (T_c = 9.2 K) and ferromagnets Co, Ni and Fe. Depending on the area of the interface we have observed various type of spectra. In very small contacts the superconducting signal is usually absent. In intermediate contacts we normally see either the typical Andreev reflection double-minimum structure or a single minimum with side peaks (Figure 1 a) indicating a proximity-induced superconducting layer [3]. In very large contacts we sometimes see a Josephson-like spectra (Figure 1 b).These observations indicate that at large contacts the proximity of Nb can suppress the ferromagnetic ordering locally, and induce superconductivity in this then non-magnetic metal.

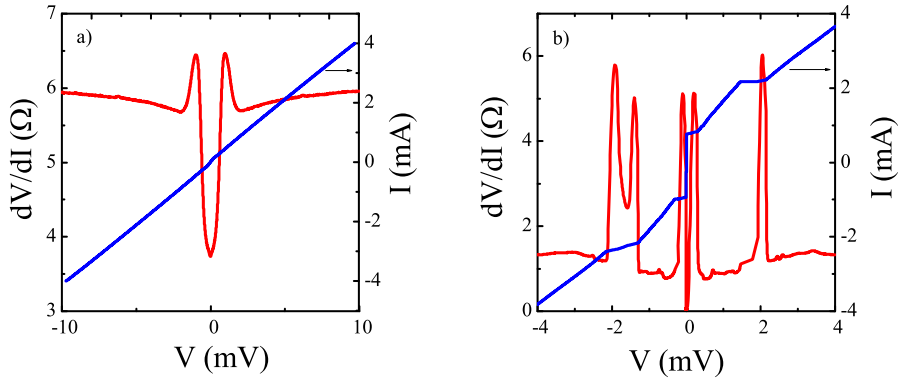

Figure 1: The dV/dI-spectra and $I(V)$-characteristics of two Fe-Nb point contacts at 4.2 K. The side peaks and the missing zero-bias anomaly in Figure 1a indicate the presence of a superconducting layer in the Fe electrode opposite to Nb tip. In Figure 1b the superconductivity in Fe is stronger, resulting in a Josephson-like spectra with a supercurrent.

[1] Ch. Buchal, R.M. Mueller, F. Pobell, M. Kubota and H.R. Folle, Solid State Communications 42 (1982) 43.
[2] B. Schröder, K. Gloos, F. Pobell and P. Smeibidl, Z. Phys. B 75 (1989) 197.
[3] G.J. Strijkers, Y. Ji, F.Y. Yang, C.L. Chien and J.M. Byers, Phys. Rev. B 63 (2001) 104510.

FABRICATION OF PHONONIC CRYSTALS WITH NORMAL METAL-INSULATOR-SUPERCONDUCTOR (NIS) TUNNEL JUNCTION THERMOMETERS

N. Zen, T. Isotalo and I. Maasilta

Nanoscience Center, Department of Physics, P.O.B. 35, FIN-40014 University of Jyväskylä, Finland
email: nobuyuki.zen@jyu.fi

Interests in the phononic crystals have been rapidly increasing year by year because of their unique physical properties. The periodical structure of the phononic crystal forbids the transmission of the elastic waves in certain ranges of frequencies, in other words, creating phononic bandgaps within the crystal [1]. The position and the width of the bandgap determine the reflection or localization of the elastic waves and they are controllable by changing structures of phononic crystals. Because recent progress on nanotechnologies makes it possible to fabricate fine-structured phononic crystals, the controllable frequencies get over hundreds of MHz [2]. Thus, phononic crystals are promising devices for the ultrasonic sensors, acoustic filters or waveguides, in addition to high efficient thermoelectric transducers or the next-generation ultra high sensitive superconducting detectors of which performances strongly depend on behaviors of phonons.

Here we discuss progress towards studying the effect of a phononic crystal on thermal transport using Normal metal – Insulator – Superconductor (NIS) tunnel junction thermometric technique at sub-Kelvin temperatures [3]. The first advantage of using the NIS thermometer is that it can measure the local phonon temperature because of the small size of the junction (~100 x 100 nm). The second merit is the ultra high sensitivity of the NIS thermometer.

As a material of the phononic crystal, we have chosen the Si_3N_4 membrane because of its importance in industries or MEMS technologies, unique thermal properties and the ease of controlling its dimensions [4]. Using ultra-high-vacuum film evaporation and electron-beam lithography, we have succeeded in fabricating the 2-D Si_3N_4 phononic crystals with cyclic through holes. Moreover, in terms of fabrication of 3-D phononic crystals, we have been investigating self-assembled arrays of nano spheres.

[1] W. Cheng et al., Nature Materials 5 (2006) 830.
[2] T. Gorishnyy et al., Phys. Rev. Lett. 94 (2005) 115501.
[3] J. Karvonen , J. Low Temp. Phys. 149 (2007) 121.
[4] J. Karvonen, Dissertation of Ph.D (2009).

9 Atomic and molecular physics

9.1 Oral session, Friday 12 March 14:30-16:00

9.2 Poster session, Friday 12 March 16:00-18:00

SPIN-ASYMMETRIC JOSEPHSON EFFECT

M.O.J. Heikkinen, F. Massel, J. Kajala, M.J. Leskinen, G.-S.Paraoanu and P. Törmä

Department of Applied Physics, Aalto University School of Science and Technology
P.O.Box 15100, FI-00076 Aalto, Espoo, Finland
email: miikka.heikkinen@tkk.fi

We study a system of two weakly linked BCS superfluids in which the two components of a Cooper pair are subjected to different potentials. In such a system the Josephson effect is generalised into a phenomenon in which the tunneling currents of the two spin channels have a different magnitude. We explain this seemingly paradoxical breakdown of the Cooper pair tunneling picture by describing the Josephson effect as interfering Rabi processes. We examine the implications of this result for devices based on the Josephson effect. Moreover, we discuss the various possible experimental realisations of the spin-asymmetric Josephson effect. [1]

[1] M.O.J. Heikkinen, F. Massel, J. Kajala, M.J. Leskinen, G.-S.Paraoanu and P. Törmä, http://lanl.arxiv.org/abs/0911.4678

PHOTOFRAGMENTATION OF CORE IONIZED MOLECULES

E. Itälä[a, b], D. T. Ha[a], K. Kooser[a], S. Granroth[a] and E. Kukk[a, c]

[a] *Dept. of Physics and Astronomy, University of Turku, FIN-20014 Turku, Finland*
[b] *Graduate School of Materials Research, Turku, Finland*
[c] *Turku University Centre of Materials and Surfaces (MatSurf), Turku, Finland*

Investigations of some organic molecules of astrophysical and biological relevance has been carried out. Soft X-ray induced photofragmentation in vacuum conditions was studied. The experimental method used, was photoelecton-photoion-photoion coincidence (PEPIPICO) technique, which utilizes a Wiley-McLaren type time-of-flight ion mass spectrometer combined with a modified Scienta SES-100 hemispherical electron energy analyzer [1]. Measurements were carried out at MAX-II synchrotron radiation lab (Lund, Sweden) at soft X-ray undulator beamline I-411 [2].

PEPIPICO method allows one to extract detailed information about the fragmentation processes caused by photoionization. Questions such as whether the fragmentation is site dependent or can the fragmentation processes be explained by simple bond cleavages can be answered with our method of research.

Among the studied samples are acrylonitrile and thymine, which are presented in Figure 1.

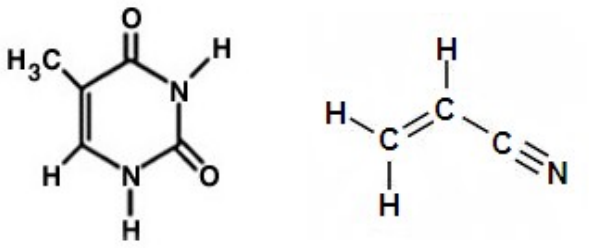

Figure 1. Measured samples; thymine (left) and acrylonitrile (right).

In addition to the fragmentation products followed the C 1s core ionization some of the results are particularly worth mentioning. Firstly, acrylonitrile has a great variety of fragmentation channels, some of which require molecular rearrangement to take place before the actual fragmentation process. Thymine on the other hand seems to fragmentate via fairly straightforward bond cleavages presented in Figure 2.

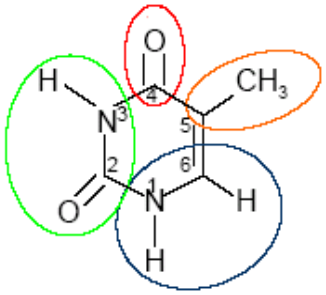

Figure 2. Bond cleavage sites of thymine

[1] E. Kukk, R. Sankari, M. Huttula, A. Sankari, H. Aksela and S. Aksela, J. Electron Spectroscopy Relat. Phenomena **155**, 141-147 (2007).
[2] M. Bässler, A. Ausmees, M. Jurvansuu, R. Feifel, J.-O. Forsell, P. de Tarso Fonseca, A. Kivimäki, S. Sundin, S.L. Sorensen, R. Nyholm, O. Björneholm, S.Aksela, S. Svensson, Nucl. Instrum. Methods in Phys. A, 469 382 (2001)

DYNAMICS OF GIANT VORTICES IN DILUTE BOSE-EINSTEIN CONDENSATES

P. Kuopanportti,[1] E. Lundh,[2] J. A. M. Huhtamäki,[1,3] V. Pietilä,[1] and M. Möttönen[1,4]

[1]Department of Applied Physics/COMP, Aalto University School of Science and Technology, PO Box 15100, FI-00076 AALTO, Finland
[2]Department of Physics, Umeå University, SE-90187 Umeå, Sweden
[3]Department of Physics, Okayama University, Okayama 700-8530, Japan
[4]Low Temperature Laboratory, Aalto University School of Science and Technology, PO Box 13500, FI-00076 AALTO, Finland
email: pekko.kuopanportti@tkk.fi

The experimental realization of quantized vortices in dilute Bose-Einstein condensates (BECs) of alkali atoms in 1999 was an important demonstration of the superfluid properties of these systems. Since then, the study of vortices in BECs has flourished both theoretically and experimentally.

Recently, it has been suggested that multiply quantized vortices with very large quantum numbers could be created in BECs with the so-called topological vortex pump, i.e., by cyclically pumping vorticity into the condensate [1, 2]. In principle, giant vortices with an arbitrarily large quantum number κ can be produced. In practice, however, κ is limited by the stability properties of the vortex. Motivated by these aspects, we have theoretically studied the core sizes, dynamical instabilities, and splitting mechanisms of giant vortices in the zero-temperature limit [3, 4].

The giant vortices were found to be dynamically unstable against splitting into singly quantized vortices at all values of the atom-atom interaction strength. However, as a function of κ, the strength of the dynamical instability either saturated to a fairly low value or increased extremely slowly for large values of κ. The splitting of a giant vortex was observed to result in vortex-free condensate fragments which were separated by vortex sheets.

On the other hand, the core size of a vortex was found to increase roughly as a square-root function of κ. Consequently, it is possible to gradually increase the operation frequency of the vortex pump without challenging adiabaticity. Our studies suggest that giant vortices of very high angular momenta may be achieved with the pump.

[1] M. Möttönen, V. Pietilä, and S. M. M. Virtanen, Phys. Rev. Lett. 99 (2007) 250406.
[2] Z. F. Xu, P. Zhang, C. Raman, and L. You, Phys. Rev. A 78 (2008) 043606.
[3] P. Kuopanportti, E. Lundh, J. A. M. Huhtamäki, V. Pietilä, and M. Möttönen, Phys. Rev. A (in press), e-print arXiv:0907.3077.
[4] P. Kuopanportti and M. Möttönen, e-print arXiv:0911.4042 (unpublished).

OFF-RESONANT QUANTUM ZENO AND ANTI-ZENO EFFECTS ON THE ENTANGLEMENT

S. Maniscalco[1], F. Francica[2], and F. Plastina[2]

[1] Turku Centre for Quantum Physics, Department of Physics and Astronomy, University of Turku, FIN-20014 Turku, Finland
email: smanis@utu.fi
[2] Dip. Fisica, Università della Calabria, & INFN - Gruppo collegato di Cosenza, 87036 Arcavacata di Rende (CS) Italy

We study the occurrence of Zeno and anti-Zeno effects [1, 2] in the entanglement dynamics of two qubits off-resonantly coupled to the same lossy cavity when the unitary evolution of the system is interrupted by repeated projective measurements. We describe in detail these quantum effects by comparing the measurement-induced coarse-grained dynamics to the entanglement evolution in absence of measurements in several scenarios [3]. In particular, we focus on the strong and weak coupling regimes, we single out the role of the relative coupling strengths between the two qubits and the reservoir, and we investigate the effect of the detuning from the main cavity frequency.
We show that the anti-Zeno effect can occur in the entanglement dynamics when the qubits frequencies are detuned from the main reservoir frequency. Furthermore, we find that Zeno and anti-Zeno effects can even appear sequentially as a function of the interval between the measurements. Finally we show that, in the off-resonant regime, we can preserve the entanglement using the quantum Zeno effect more efficiently than in the resonant limit [4], even if, in this case, no sub-radiant state exists.

[1] B. Misra and E.C.G. Sudarshan, J. Math. Phys. 18 (1977) 756.
[2] A. G. Kofman and Kurizki, Nature 405 (2000) 546.
[3] F. Francica, S.Maniscalco, Y. Piilo, F. Plastina, and K-A Suominen, Phys. Rev. A 79 (2009) 032310.
[4] S.Maniscalco, F. Francica, R.L. Zaffino, N. Lo Gullo, and F. Plastina, Phys. Rev. Lett. 100 (2008) 090503.

PROSPECTS OF EMERGING PROCESSOR TECHNOLOGIES IN COMPUTATIONAL MOLECULAR SCIENCE

Pekka Manninen

CSC – IT Center for Science Ltd., P.O.Box 405, FI-02101 Espoo, Finland
email: pekka.manninen@csc.fi

As performance gains using interconnected traditional processors are becoming increasingly difficult to obtain, alternative processing architectures are emerging. These new architectures - the Cell CPU, hardware-based application accelerators and graphics processors capable of general purpose computing (GPGPUs) - have become the most hyped about topic in the high-performance computing community. Promising to provide teraflop/s of computing power for a fraction of the power consumption and cost of a conventional system, they seem very appealing. Applications that employ these processors show already speedups of 150x as compared to using traditional x86 CPUs in e.g. classical molecular dynamics. Their support is being implemented currently in many of the widely used molecular science softwares.

Today the use of these architectures, however, faces a number of challenges and only a handful of supercomputer centers have taken the plunge and adopted them. Yet they are evolving at a rapid pace and becoming increasingly feasible for use in production-class supercomputing systems.

The purpose of this talk is describe these architectures, their usage, benefits and shortcomings, and the great promise to computational molecular science – among other disciplines of computational science – they present. In addition, I will describe the efforts and plans at CSC, the Finnish IT Center for Science, to study the different issues in using these technologies in scientific computing and catalyze these technologies into Finnish research community.

QMC SIMULATION OF THERMAL DISSOCIATION OF DIPOSITRONIUM

Ikka Kylänpää and Tapio T. Rantala

Department of Physics, Tampere University of Technology
P.O.Box 692, FI-33101 Tampere, Finland
email: Tapio.Rantala@tut.fi

Positronium is a hydrogen atom like pair of a positron and an electron, and correspondingly, dipositronium is a four-particle molecule formed by two bound positronium atoms. Theoretically, stability of the dipositronium molecule was established by Hylleraas in 1947 [1], already, but not experimentally observed until recently [2]. This system of four light particles sets challenges for both theoretical and experimental consideration and in finite temperature, in particular.

The experimental observations are based on the observation of positronium decay rate and its changes related to dipositronium formation or dissociation. It turns out that the finite-temperature modeling of such light quantum particles has to done fully nonadiabatically. This is what we have accomplished by using the Path-Integral Monte Carlo (PIMC) approach for simulation of the relevant temperature dependent thermal equilibrium.

As the dissociation energy of dipositronium is about 0.4 eV, the recent observation of the thermal activation energy of about 0.07 eV was interpreted to follow from the experiment related desorption process [2]. Based on our quantum statistical simulation we suggest, however, that the observed low activation energy relates to the dissociation of the molecules, rather than desorption of those [3]. We also analyze the nature of the interatomic interaction at varying distances and find the dispersion forces to dominate at large separations.

[1] Hylleraas, E.A. and Ore A., Phys. Rev.**71**, 493 (1947).
[2] Cassidy D.B. and Mills A.P. Jr., Nature **449**, 195 (2007); Phys. Rev. Lett. **100**, 013401 (2008).
[3] Kylänpää I. and Rantala T.T., *Thermal dissociation of dipositronium: Path-integral Monte Carlo approach*, Phys. Rev. A **80**, 024504 (2009).

DRIVEN QUBIT IN A STRUCTURED RESERVOIR

P. Haikka and S. Maniscalco

Turku Center for Quantum Physics, Department of Physics and Astronomy, 20014 Turku, Finland
email: pmehai@utu.fi

All quantum systems are open, i.e., they interact with an environment. The interaction with the environment leads to dissipation and decoherence due to a flow of energy and/or information from the system to the environment. The coupling of the quantum system to the environment is described by the spectral density function. If the spectral density function strongly varies with the frequency of the environmental oscillators, the environment is said to be structured. In these systems the reservoir memory effects induce a feedback of information from the environment into the system. We call these systems non-Markovian.

We study a driven two-state system interacting with a structured environment. We introduce the non-Markovian master equation ruling the system dynamics, and we derive its analytic solution for general reservoir spectra [1]. We compare the non-Markovian dynamics of the Bloch vector for two classes of reservoir spectra: the Ohmic and the Lorentzian reservoir.

We study the system dynamics with and without the widely used secular approximation, singling out its limits of validity. The investigation of the effects of nonsecular terms on the dynamics of the Bloch vector brings to light the existence of nonsecular oscillations in the population of the two-state systems. Contrarily to oscillations due to non-Markovianity, such oscillations persist for times much longer than the reservoir correlation time. Moreover, our analysis shows that the nonsecular terms affect also the asymptotic long time values of the Bloch vector components.

Finally, a very important result we present is the analysis of conditions for complete positivity (CP) of the system with and without the secular approximation. Interestingly, the CP conditions have a transparent physical interpretation in terms of the characteristic timescales of phase diffusion and relaxation processes.

[1] P. Haikka, arXiv:0911.4600v1, to be published in Physica Scripta.

Continuous variable entanglement dynamics in structured reservoirs

R. Vasile[1], S. Olivares[2], M.G.A. Paris[2] and S. Maniscalco[1]

[1]Turku Center for Quantum Physics, Department of Physics Astronomy University of Turku, FI-20014 Turun Yliopisto, Finland
[2]Dipartimento di Fisica, Università degli Studi di Milano, I-20133 Milano, Italy
email: ruggero.vasile@utu.fi

Entanglement is an essential resource for quantum computation and communication protocols. However, this fundamental quantum property is also fragile: the unavoidable interaction of quantum systems with their external environment leads to the irreversible loss of both quantum coherence (decoherence) and quantum correlations in multi-partite systems. A crucial requirement for a physical system to be of interest for quantum technologies is that the survival time of entanglement is longer than the time needed for information processing. Therefore it is important to develop a deep and precise understanding not only of the mechanisms leading to decoherence and entanglement losses but also of the dynamical features of these phenomena.

We consider the entanglement dynamics in noisy continuous variable (CV) quantum systems [1]. More specifically we focus our attention on a system of two non-interacting quantum harmonic oscillators bilinearly coupled to two independent structured reservoirs at temperature T. Using an exact approach [2, 3] under the only assumption of weak coupling we study the time evolution of the entanglement between the two oscillators for different temperature regimes, different system-reservoir parameters and different reservoir spectra. Rather than limiting ourself to present a plethora of dynamical behaviors, we try to identify general features in order to single out universal properties of the disentanglement process, namely those properties that do not depend either on the specific model of reservoir chosen or on the specific initial value of the entanglement. Moreover, we also compare the differences in the dynamics arising from different spectral distributions of the reservoir in order to identify those physical contexts leading to stronger or weaker entanglement losses.

[1] R. Vasile, S. Olivares, M. G. A. Paris, and S. Maniscalco Phys. Rev. A **80**, 062324 (2009)
[2] F. Intravaia, S. Maniscalco, and A. Messina, Phys. Rev. A **67**, 042108 (2003).
[3] S. Maniscalco, S. Olivares, and M. G. A. Paris, Phys. Rev. A **75**, 062119 (2007)

DYNAMICS OF ONE DIMENSIONAL FERMI GASES

Jussi Kajala and Päivi Törmä

Helsinki University of Technology, P.O.B. 1100, FI-02015 TKK, Finland
email: jussi.kajala@hut.fi

We have studied numerically the time evolution of two interesting settings of one dimensional Fermi gases. Firstly, we have simulated the collision of a spin up gas with a spin down gas. In this setting, we observed that there is a crictical attractive interaction which sticks the gases together, preventing penetration.

Secondly, in a homogenous system of spin up and down fermions, we have simulated turning on a harmonic trap which affects only the up component. We observe that the up component picks up the down component with it as the up component moves into the trap. However, after a characteristic time the up component drops the down component and the distribution of the down component becomes again homogenous.

We modelled the systems using single band Hubbard Hamiltonian. The time evolution has been determined using mean field time-dependent Hartree-Fock Bogoliubov-de-Gennes [1] algorithm. To verify the validity of the approach, we will compare the results to those obtained using exact time-evolved block decimation [2] algorithm. In the future, we aim to extend the mean-field algorithm into two dimensions.

[1] Aurel Bulgac, Phys. Rev. C 41 (1988) 2333-2339.
[2] Guifrè Vidal, Phys. Rev. Lett. 91 (2003) 147902.

PHASE TRANSITION BETWEEN CLASSICAL AND QUANTUM DECOHERENCE

L. Mazzola, J. Piilo and S. Maniscalco

Turku Centre for Quantum Physics, Department of Physics and Astronomy, University of Turku, FI-20014 Turun Yliopisto, Finland
email:laumaz@utu.fi

We study the dynamics of quantum and classical correlations in the presence of decoherence. We discover a class of initial states for which the quantum correlations, quantified by the quantum discord, are not destroyed by decoherence for times $t < \bar{t}$. In this initial time interval only classical correlations decay. For $t > \bar{t}$, on the other hand, classical correlations do not change in time and only quantum correlations are lost due to the interaction with the environment. Therefore, at the transition time $\bar{t}$ the open system dynamics exhibits a sudden change from classical to quantum decoherence regime.

DECOHERENCE CONTROL IN DIFFERENT ENVIRONMENTS

J. Paavola and S. Maniscalco

Turku Centre for Quantum Physics, Department of Physics and Astronomy, University of Turku, FI-20014, Turun yliopisto, Finland
email: jshpaa@utu.fi

The use of qubits (quantum analog of a classical bit) promises huge advances to certain information processing fields, such as quantum simulation and cryptography. Qubits can be implemented in various ways, a trapped ion in a cavity being one of the most prominent candidates. Currently the key limiting factor in developing large scale quantum computing devices is quantum decoherence, which tends to destroy the relevant physical properties, namely entanglement and superposition between, e.g., two qubits needed in quantum computing. Decoherence stems from the unavoidable interaction with the environment and as such, is strongly dependent on the form of the environmental spectrum [1].

Reservoir engineering, which is currently achievable in the trapped ion context [2], offers one way to reduce harmful decoherence effects in a qubit. Another possibility is to make non-selective measurements on the system checking to see if it is still in its initial state or not. If such measurements are conducted at sufficiently short time intervals, the decay dynamics of the system is slowed down. This phenomena is called the quantum Zeno effect (QZE) [3]. An opposite reaction, namely the acceleration of the decay process is also possible. It is known as the anti-Zeno effect. The occurrence of either QZE or AZE depends on the type of the environment and on the frequency of the measurements.

We have compared the decoherence dynamics of a superposition of two coherent states coupled to a bosonic environment with different spectral structures. We have also examined what are the conditions a reservoir and measurements have to satisfy in order to obtain either Zeno- or anti-Zeno type dynamics. The ultimate goal behind our study is to both shed light on the possibilities of realizing a large scale quantum computing device and to investigate the quantum-classical transition.

[1] J. Paavola, J. Piilo, K.-A. Suominen, and S. Maniscalco, Phys. Rev. A **79**, 052120 (2009).
[2] C.J. Myatt et al., Nature **403**, 269 (2000).
[3] S. Maniscalco, J. Piilo, K.-A. Suominen, Phys. Rev. Lett. **97**, 130402 (2006).

QUANTUM PROPERTIES OF A THREE-LEVEL SUBRADIANT SYSTEM

M. Borrelli, N. Piovella, M.G.A. Paris
Turku Centre for Quantum Physics, Department of Physics and Astronomy, University of Turku, 20014 Turku, Finland

Subradiance is a many-boby cooperative effect which inhibites light emission, both in strong and weak QED coupling. It was first predicted by R.H. Dicke [1] in the same article predicting superradiance. Whereas superradiance has been largely investigated, both theoretically and experimentally, subradiance has received less attention. The only experimental evidence has been given by Pavolini [2] in 1985. Crubellier *et al.*, in a series of theoretical papers [3, 4, 5], proposed a three-level degenerate cascade configuration in which cooperative spontaneous emission is expected to exhibit new and striking subradiance effects.
We focus here on such a three-level degenerate cascade (momentum levels) and we study the quatum properties of subradiant states. It has been demostrated [6] that an ensemble of N bosonic cold atoms, placed in an optical cavity with photon losses and interacting with a two-frequency strong beam and a cavity resonant weak probe beam, asympotically reaches a collective subradiant configuration. This result has been obtained within the semiclassical approximation. Rather we treat atoms as indistinguishable particles and quantize probe radiation too. We numerically solve the $T = 0$ master equation governing the time-evolution of $N = 2$ and $N = 3$ systems, demonstrating that they achieve subradiance. We study statistics and gaussianity of subradiant states, showing and quantifying their non-gaussianity. Finally we adress the entanglement among atomic modes: the atomic steady-state turns out to be genuinelly tripartite entangled and, in the case $N = 2$, we find an analytical link between entanglement and statistics.

References

[1] R.H. Dicke Phys. Rev. **93**, 99 (1954) Phys. Rev. **93**, 99 (1954)

[2] D. Pavolini, A. Crubellier, P. Pillet L. Cabaret, and S. Liberman Phys. Rev. Lett. **54**, 1917 (1985)

[3] A. Crubellier, S. Liberman, D. Pavolini, and P. Pillet J. Phys. B: At. Mol. Phys. **18**, 3811 (1985)

[4] A. Crubellier, and D. Pavolini J. Phys. B: At. Mol. Phys. **19**, 2109 (1986)

SELF-ASSEMBLY OF THERMALLY SWITCHABLE POLYMER p(NIPAM)

I. Juurinen[1], M. Hakala[1], S. Galambosi[1], A. G. Anghelescu-Hakala[2] and K. Hämäläinen[1]

[1]Department of Physics, P.O.B. 64, FIN-00014 University of Helsinki, Finland
email: iina.juurinen@helsinki.fi
[2]Laboratory of Polymer Chemistry, Department of Chemistry, University of Helsinki

Smart polymers are materials that respond to slight changes in their environment, such as temperature, pH or magnetic field. These polymers are potentially useful for a variety of applications, for example in biotechnology. Poly(N-isopropylacrylamide), p(NIPAM), is a well-known thermoresponsive polymer. Aqueous p(NIPAM) undergoes a reversible volume phase transition at about $32°$C, changing from a swollen hydrophilic state (low temperatures) to a collapsed hydrophobic one. This very sharp transition is attributed to the alteration of the hydrogen bonding of water molecules around the amide group of the side chain [1]. Recently, it was shown that inelastic x-ray scattering in the Compton regime can give detailed information on the local molecular and electronic structures [2]. We use this method to study the hydrogen bonding of aqueous p(NIPAM) solution.

In this work we extend our recently developed computational scheme [3] to study the polymer solvation and self-organization at the atomic level. First, classical molecular dynamics is used to obtain local molecular geometries of the solution. These geometries are used as an input for an electronic structure calculation. The resulting Compton profile, which is a ground state electronic property of the system, is a sensitive probe of changes in the hydrogen bonding strength around the amide groups of the polymer. Experimentally, we have prepared the polymer at different concentrations. By studying differences of the Compton profiles below and above the transition temperature one obtains a unique signature reflecting the polymer's self-assembly. We present details of the experimental procedure and preliminary computational results for the geometrical properties of p(NIPAM) (e.g. h-bonds around the amide group) and for the Compton profiles related to the amide-water-interaction.

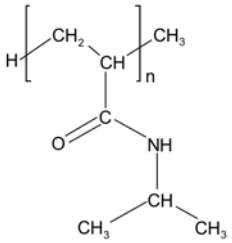

Figure 1: Chemical structure of poly(N-isopropylacrylamide), p(NIPAM).

[1] Y. Tamai, H. Tanaka and K. Nakanishi, *Macromolecules*, **29**, 6750 (1996).
[2] M. Hakala, K. Nygård, J. Vaara, M. Itou, Y. Sakurai and K. Hämäläinen, *J. Chem. Phys.*, **130**, 034506 (2009).
[3] I. Juurinen, M. Hakala, K. Nordlund, E. Salonen, M. Itou, Y. Sakurai and K. Hämäläinen, manuscript in preparation.

SOLITONS IN A HOLOGRAPHIC MODEL OF A SUPERFLUID

V. Keränen, E. Keski-Vakkuri, S. Nowling and K. P. Yogendran

Helsinki Institute of Physics, P.O.B. 64, FIN-00014 University of Helsinki, Finland
email: ville.keranen@helsinki.fi

A useful way to address questions in strongly interacting quantum field theories is provided by the AdS/CFT duality, which provides a new way of addressing difficult quantum field theory questions in terms of semiclassical general relativity. An important question is what class of physical phenomena can be addressed in terms of such dual theories. A recent advance in the field has been the realization that the duality can give a model of superfluidity.

We construct two kinds of solitons [1, 2] in a bottom up model of superfluidity in the context of AdS/CFT duality. The solitons in the superfluid are mapped into solitons in the gravity model by the duality and thus, the difficult problem of studying solitons in a strongly coupled superfluid, in finite temperature and chemical potential, is mapped into a relatively easier problem of solving partial differential equations. The two classes of solitons are vortices, and domain walls of reduced charge density, called dark solitons. Such solitons can be realized experimentally in bosonic and fermionic superfluids. The solitons provide interesting information about the system under study since they probe both the large and the short length scale properties of the system. From the solitons we find partial evidence that the duality can describe both BCS and BEC type superfluids.

[1] V. Keranen, E. Keski-Vakkuri, S. Nowling and K. P. Yogendran, Phys. Rev. D **80** (2009) 121901 [arXiv:0906.5217 [hep-th]].
[2] V. Keranen, E. Keski-Vakkuri, S. Nowling and K. P. Yogendran, arXiv:0912.4280 [hep-th].

APPROXIMATIVE APPROACHES TO THE PARABOLIC MODEL

J. Lehto and K.-A. Suominen

Turku Centre for Quantum Physics, Department of Physics and Astronomy, FI-20014 University of Turku, Finland
email: jmsleh@utu.fi

Quantum mechanical level crossing problems are widely applied in many different fields in physics. The well-known and analytically solvable Landau-Zener model [1] is a prominent example of this. When the adiabatic energy levels of the system are swept through an avoided crossing there exists a probability for a non-adiabatic transition.

We consider the two-state parabolic level crossing model [2, 3] where the time-dependence of the diabatic energy levels is quadratic and the coupling between the levels is constant (Figure 1.). The double crossing character of the model leads to oscillations in the final populations. This interference effect emphasizes the importance of the correct calculation of the phases acquired by the different states during the evolution.

We study different approximative methods for obtaining the final state populations. By comparing these with the numerical results we show that one is able to get good approximative expressions for the asymptotic transition probability that work in a large part of the parameter region. By applying the Dykhne-Davis-Pechukas method [4] and modifying it, we can include also cases where the normal perturbation approach or the assumption of independent crossings fail.

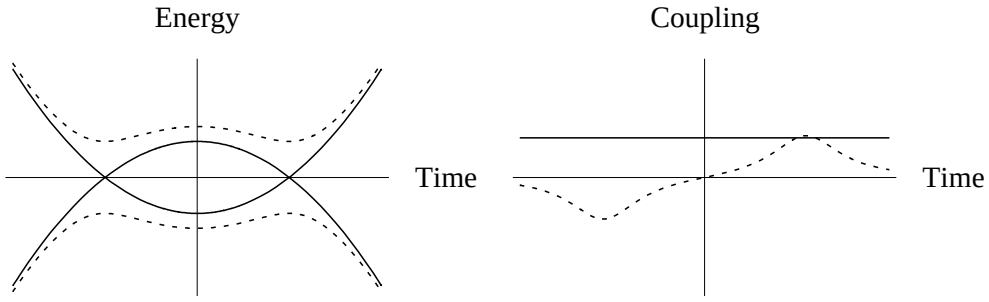

Figure 1: The level energies and the coupling between the levels for the parabolic model. The solid lines refer to the diabatic quantities whereas the corresponding adiabatic quantities are dashed.

[1] C. Zener, Proc. R. Soc. London, A **137**, 696 (1932).
[2] K.-A. Suominen, Optics Comm. **93**, 126 (1992).
[3] E. Shimshoni and Y. Gefen, Ann. Phys. **210**, 16 (1991).
[4] J. P. Davis and P. Pechukas, J. Chem. Phys. **64**, 3129 (1976).

SURFACE AND SUBSURFACE C ON PD(111) AND PD(211) SURFACES: A COMPUTATIONAL STUDY

L. Nykänen[†], J. Andersin[†] and K. Honkala[†‡]

[†] Department of Chemistry, Nanosciece Center, University of Jyväskylä, Finland
[‡] Department of Physics, Nanoscience Center, University of Jyväskylä, Finland
email: lauri.j.a.nykanen@jyu.fi

It has been discovered in recent experimental studies that pure palladium surfaces are not responsible for selective hydrogenation of ethyne [1]. Instead the selectivity is provided by a metastable phase composed of palladium surface atoms and carbon impurities. The exact structure of the carbide is unclear, but the amount of carbon close to the surface has been defined to be 35 atomic %.

We have simulated the formation and composition of the subsurface C layer by applying DACAPO software [2] which is based on density functional theory. First we looked at C diffusion from the surface to the Pd lattice. The results showed that the migration from surface to subsurface is more favourable from step sites than from terrace sites. We also studied the diffusion within the lattice and our results agree well with earlier theoretical and experimental works [3, 4, 5].

In order to understand better the behaviour of C at the Pd(111) surface we investigated different adsorption structures with C on and below the surface. With C concentrations higher than 25 at.% (or 1/3 ML) the best adsorption energies are no longer obtained with all C atoms below the surface. Instead the energy minimum is reached with 25 at.% C below the surface and rest of the C atoms on the surface.

[1] D. Teschner, J.Borsodi, A. Wootsch, Z. Révay, M. Hävecker, A. Knop-Gericke, S.D. Jackson and R. Schlögl, Science 320 (2008) 86.
[2] https://wiki.fysik.dtu.dk/dacapo
[3] H. Yokoyama, H. Numakura and M. Koiwa, Acta Mater. 46 (1998) 2823.
[4] M.K. Rose, A. Borg, D.F. Ogletree and M. Salmeron, J. Chem. Phys. 115 (2001) 10927.
[5] L. Gracia, M. Calatayud, J. Andrés, C. Minot and M. Salmeron, Phys. Rev. B 71 (2005) 033407.

Implementation of electronic processes into molecular dynamics simulations of nanoscale metal tips under electric fields

S. Parviainen, F. Djurabekova, K. Nordlund

Department of Physics, P.O.B. 43, FIN-00014 University of Helsinki, Finland
email: stefan.parviainen@helsinki.fi

Strong electric fields appear in connection with many modern applications operated at high vacuums, such as particle accelerators and fusion reactors. The fields can lead to electric arcs (local plasma discharges) on metal surfaces, which damage equipment and lower their performance. It is necessary to understand the underlying mechanisms of the high vacuum arcs to increase the performance of these equipments.

It has been suggested that electron emission, especially field emission, from a surface plays a significant role in the arcing phenomenon. Due to the electric currents produced by field electron emission, the surface is heated, and sufficiently large currents can cause melting of the metal surface, providing evaporated atoms to build up plasma over the surface. If a microscopic protrusion is present on the surface, the threshold of the applied electric field for plasma formation is lower because of the local enhancement of the electric field above the tip. The geometry of the protrusion also affects its melting rate: a tall tip is heated to its melting point much more easily than a small tip.

To investigate the effects of high electric fields on metal surfaces mentioned above, a new model of handling heat conduction was implemented into the molecular dynamics code PARCAS. In classical molecular dynamics lattice heat conduction is implicitly handled, while the electronic component of the heat conduction is ignored. In a metal, however, electronic heat conduction dominates and thus special care has to be taken when simulating heat flow. In the implemented model, electron emission has been considered using the classical Fowler-Nordheim law and electronic heat conduction is included by explicitly solving the heat equation of the simulated protrusion.

To verify the new model, simulation results were compared with theoretical predictions based on the analytical solution of the heat equation. Both the protrusion temperature as a function of time, and the protrusion equilibrium temperature as a function of size and current density were investigated. Comparisons with the theoretical predictions show that the implemented model works well.

MEASURE FOR THE NON-MARKOVIANITY OF QUANTUM PROCESSES

H.-P. Breuer[1], E.-M. Laine[2], and J. Piilo[2]

[1] Physikalisches Institut, Universität Freiburg, Hermann-Herder-Strasse 3, D-79104 Freiburg, Germany
[2]Turku Center for Quantum Physics, Department of Physics and Astronomy, University of Turku, FI-20014 Turun yliopisto, Finland

We construct a general measure for the degree of non-Markovian behavior in open quantum systems [1]. This measure is based on the trace distance which quantifies the distinguishability of quantum states. It represents a functional of the dynamical map describing the time evolution of physical states, and can be interpreted in terms of the information flow between the open system and its environment. The measure takes on nonzero values whenever there is a flow of information from the environment back to the open system, which is the key feature of non-Markovian dynamics.

[1] H.-P. Breuer, E.-M. Laine, and J. Piilo, Phys. Rev. Lett. 103, 210401 (2009). Accompanying Physics Synopsis: http://physics.aps.org/synopsis-for/10.1103/PhysRevLett.103.210401

DENSITY MATRIX RECONSTRUCTION FROM DISPLACED PHOTON NUMBER DISTRIBUTIONS

J. Schultz

Turku Centre for Quantum Physics, Department of Physics and Astronomy, University of Turku, Turku, Finland
email: jussi.schultz@utu.fi

We consider state reconstruction from the measurement statistics of phase space observables generated by photon number states. We focus on the mathematically rigorous derivations of reconstruction formulas for the associated phase space probability distributions. The results are obtained by inverting certain infinite matrices. In particular, we obtain reconstruction formulas, each of which involves only a single phase space observable.

[1] J. Kiukas, J.-P. Pellonpää, J. Schultz, arXiv:0910.3571..

Index

A

Aaltonen, 25, 50, 84
Aarnio, 192
Agueda, 69
Ahlskog, 228, 239, 247, 253
Aho, 52, 234, 246
Aho-Mantila, 20
Ahopelto, 241, 242
Ahorinta, 264
Aitchison, 223
Akola, 138
Ala-Nissilä, 107
Ala-Nissila, 122
Alanen, 211
Alarinta, 34
Alatalo, 115, 121, 132
Alava, 166
Albe, 237
Albers, 233
Ali-Löytty, 103
Alves, 17
Andersin, 100, 285
Andersson, 116
Andreev, 192
Anekallu, 63, 75
Anghelescu-Hakala, 282
Annila, 87
Antipin, 193
Antola, 181
Apaja, 262
Arcot, 39
Arridge, 81
Arstila, 47
Attikis, 183
Aula, 80
Auterinen, 86
Auvinen, 132, 194

B

Backholm, 245
Bacquias, 197
Banu, 209
Baranovskii, 161
Barchenko, 45
Barton, 208
Bastek, 118
Battarbee, 69
Belova, 158
Bender, 179
Bentley, 208, 209
Bertram, 118
Bezrukov, 182, 205, 216, 217, 220
Bianco, 208
Björkas, 128
Björklund, 164
Blomqvist, 124, 144
Blum, 146
Blunt, 22
Bonn, 83
Borrelli, 281
Breuer, 287
Brosco, 256
Brown, 208, 223
Budhani, 231
Bunkov, 106
Butler, 8, 186
Bårdsen, 133
Bäck, 178

C

Chan, 17
Chaudhuri, 235
Chekurov, 16, 226
Chen, 28
Christen, 118
Clark, 17
Clilverd, 74
Coleman-Smith, 186
Corfe, 110
Costelle, 222
Cox, 186
Cresswell, 186
Czellar, 50

D

Dadgar, 118
Dandouras, 63, 75
Danneau, 169
Davies, 208
Davinson, 209
Dazuz, 105

Dietlein, 13
Díez, 232
Dijken, 240, 250
Djurabekova, 123, 245, 286
Donkelaar, 17
Donovan, 70
Dudley, 24
Dumitrescu, 246
Dyadechkin, 68
Dzurak, 17

E

Edelmann, 213
Efimov, 32
Elomaa, 57, 175, 195, 198, 203
Eltsov, 102, 106
Enell, 74
Engelhardt, 95
Enkovaara, 147
Enqvist, 37, 182, 205, 215–220
Erkintalo, 24, 32
Ermolov, 166
Eronen, 21, 57, 175, 195, 198, 201, 203
Eskelinen, 30, 229
Eskola, 190, 194
Evers, 236

F

Fabritius, 30
Fagerstedt, 110
Fay, 159, 169, 170
Fei, 116
Ferrantelli, 196
Finley, 7
Fitzgerald, 123
Foster, 107, 129, 145
Francica, 273
Freund, 135
Friberg, 31, 59
Friedrich, 6
Fuchs, 105
Fynbo, 182, 205, 216, 217, 220
Föhr, 197

G

Galambosi, 143, 282
Ganchenkova, 104, 152
Garcia, 174
Gebhard, 161
Genty, 24
Giazotto, 259
Giordano, 98
Gloos, 263, 266
Gopakumar, 67
Graaf, 102, 106
Granroth, 271
Gray-Jones, 179
Grebing, 48
Greenlees, 178, 179, 186, 207, 208
Gross, 5
Grossman, 13
Groth, 20
Grönberg, 13, 15, 29
Grönholm, 13
Guina, 52, 234, 246, 264
Gulans, 145

H

Hæggström, 25, 30, 38, 51
Ha, 271
Haario, 132
Haatainen, 241, 242
Haikka, 276
Hakala J., 21, 57, 175, 195, 198, 201, 203
Hakala M., 98, 139, 143, 282
Hakala T.K., 229, 261
Hakkarainen, 31, 246, 264
Hakola, 20
Hakonen, 159, 169, 170, 257
Hamilton, 28
Hannula, 239
Hantschel, 47
Happonen, 213
Hardy, 195
Harju, 133, 148, 157
Harjunmaa A., 237
Harjunmaa E., 110
Hashemi, 134, 238
Hassel, 15, 29
Hauschild, 186
Havu P., 134
Havu V., 146, 149, 171
Havukainen, 249
Heenen, 179
Hegedus, 129
Heikinheimo, 181
Heikkinen L.M., 54, 84

Heikkinen M.O.J., 270
Heikkinen P., 199
Heikkinen P.J., 106
Heikkinen S., 93
Heikkinen V., 25
Heikkonen, 95
Heinonen, 107
Helistö, 13, 29
Hempel, 118
Henzl, 197
Hernandez, 185
Herranen M., 184
Herranen O., 228, 239
Herzan, 186
Herzberg, 186
Heyde, 179
Hietanen, 191
Hippeläinen, 79, 86
Hirsimäki, 103, 111
Hirvijoki, 18
Hoenders, 31
Hoffmann, 165
Holm, 160
Holmström, 139
Holopainen H., 190
Holopainen J., 91
Honkala, 100, 285
Honkonen, 62, 63
Hosio, 102
Huhtamäki, 272
Hujala, 108
Huotari, 98, 143
Husu, 43, 248, 254
Huttunen, 27, 32
Hynönen, 95
Hynninen, 107
Hyväluoma, 82
Häkkinen E., 166
Häkkinen H., 135, 150, 243
Häkkinen P., 159
Hämäläinen, 98, 110, 143
Härkönen, 50

I

Iacob, 209
Ihalainen, 82
Ikkala, 224
Immerzeel, 117
Inkinen, 143
Inzhechik, 182, 205, 216, 217, 220
Isaksson, 88
Isotalo, 12, 267
Itälä, 271

J

Jakobsson, 178, 179, 186, 208
Jalava, 132
Jamieson, 17
Janhunen, 62, 64, 68, 73
Janik, 174
Jansson, 161
Javanainen, 85
Jenkins, 179, 208, 209
Jernvall, 110
Jiang, 228
Johansson, 228, 239
Jokinen A., 21, 57, 175, 195, 198, 201, 203, 207, 209
Jokinen N., 111
Jones P., 178, 179, 182, 186, 205, 208, 216, 217, 220
Jones R.O., 138
Joss, 178, 208
Jouppila, 125
Joutsenvaara, 182, 205, 215–217, 220
Judson, 178
Julin, 260
Julin J., 39
Julin R., 178, 179, 186, 207, 208
Junell, 34
Juntunen, 109
Jurvelin, 80, 88
Jussila P., 103, 111
Jussila S., 35
Juurinen, 282
Juutinen, 178, 179, 186, 208
Jämsä, 18, 33
Järvi, 222
Järvinen J., 225
Järvinen K., 84
Järvinen R., 68
Jääskeläinen, 95, 101

K

Kafanov, 16, 265
Kainulainen, 66, 71, 184
Kaipio, 22, 42, 81

Kaivola, 227, 249
Kajala, 270, 278
Kallio, 68
Kalliokoski M., 174
Kalliokoski T., 182, 205, 215–217, 220
Kallonen, 101, 110, 120
Kamanenko, 44
Kankaanranta, 93
Kankainen, 21, 175, 195, 198, 201
Kanninen, 111
Kantorovich, 145
Karavirta, 191
Karhunen, 22
Karjalainen J., 182, 205, 216, 217, 220
Karjalainen J.P., 88
Karppinen, 38
Karvonen, 21, 198, 201
Kasi, 202
Kaskela, 223
Kassamakov, 25, 50
Kataja, 126
Kaukonen, 134
Kauppinen E.I., 223, 228, 244
Kauppinen J., 26
Kauranen, 32, 43, 58, 233, 248, 254
Kauttonen, 112
Kawaguchi, 242
Keihänen, 65
Kelic, 197
Kemppinen, 16
Kero, 74
Keränen, 283
Keski-Vakkuri, 211, 283
Ketelhut, 178, 186, 208
Ketolainen, 54, 84
Kettunen, 57
Khakimov, 249
Kilpeläinen, 113
Kilpua, 72
Kimmelma, 14
Kinnunen J., 114
Kinnunen K., 162
Kinnunen R., 183
Kira, 137
Kirjoranta, 125
Kissmann, 72
Kit, 140
Kiviranta, 15
Klem, 213
Koivisto, 179
Koivu, 126
Koivumäki, 213
Koivunoro, 86
Kokko, 121
Kokkola, 49
Kokkonen, 80
Kolehmainen, 81
Kolhinen, 21, 57, 175, 201, 203, 207
Konstandin, 185
Kooser, 271
Koppinen, 260
Korhonen E., 36
Korhonen H., 49
Korhonen J.T., 224
Korhonen L., 240
Korniyenko, 37
Korolyuk, 114
Korpijärvi, 234
Kortelainen, 183, 203
Koskinen H.E.J., 63
Koskinen P., 135, 140, 150, 243
Kotiluoto, 86
Kotimäki, 136
Krieger, 20
Krost, 118
Krotscheck, 262
Krusius, 102, 106
Kühn, 82
Kuisma, 147
Kuittinen, 248
Kuitunen, 113
Kujala, 254
Kukk, 271
Kunttu, 261
Kuopanportti, 272
Kupiainen, 148
Kurki, 204
Kurki-Suonio H., 65
Kurki-Suonio T., 18, 20, 55
Kurnatowski, 118
Kuronen, 94
Kurpeta, 198
Kuusela, 26
Kuusiniemi, 182, 205, 215–217, 220
Kuzmin, 111
Kuzyk, 229, 230, 261

Kylänpää, 275
Kyrölä, 74
Kähärä, 200
Kärkkäinen, 34

L

Labiche, 178
Lahti, 115
Lahtinen, 239, 250
Lahtonen, 103, 111
Laiho, 108
Laine, 287
Laitinen M., 19, 39, 46, 57
Laitinen T., 69
Lamminäki, 132
Lappalainen, 13, 251
Lashkul, 108
Lassila, 51
Latvala, 40, 41, 252
Lauhakangas, 174
Laukkanen, 248
Lauros, 41
Lautenschläger, 165
Lauter, 262
Lazarus, 186
Leeuwen, 151, 167, 168
Lehesjoki, 110
Lehikoinen, 22
Lehti, 183
Lehtikangas, 81
Lehto, 67, 84, 284
Lehtovaara, 149
Leino, 178, 179, 186, 207, 208, 210
Leivo, 13
Lemmetyinen, 32
Leppänen A.-P., 189
Leppänen K., 101, 116, 117
Leskinen, 270
Letts, 186
Lievonen, 247
Liljeroth, 236
Lin, 135
Lindén, 213
Lindell, 40, 41, 252
Linko, 229, 230
Lipponen, 42
Lipsanen, 14
Loo, 37, 182, 205, 215–218, 220
Lopez-Martens, 186
Lubsandorzhiev, 182, 205, 216, 217, 220
Lucek, 63, 75
Lucenius, 101, 117, 120
Lundbom, 93
Lundh, 272
Luomahaara, 15
Luostari, 27
Luukanen, 13
Lähderanta, 44, 45, 108, 158
Lähivaara, 23
Lähteenmäki, 159, 169, 170
Lääkkö, 38

M

Maalampi, 215
Maasilta, 12, 162, 231, 235, 260, 267
MacLeod, 265
Maijala, 29
Maisi, 16
Majaniemi, 122
Majumdar, 160, 163
Makhlin, 257
Makkonen I., 141
Makkonen T., 20
Malerba, 128
Malmi, 26
Malo, 88
Malola, 243
Maniscalco, 273, 276, 277, 279, 280
Mannila, 89
Manninen A., 16
Manninen O., 110
Manninen P., 274
Martin, 28
Massel, 270
Mazzola, 279
McCleskey, 209
Mellerwicz, 117
Meltaus, 153
Merikoski, 109, 112
Meriläinen, 120
Meschke, 259
Meyer, 165
Micolich, 28
Mikkola, 67
Monaco, 98
Monk, 27

Monteiro, 22
Monticelli, 85
Moore, 21, 53, 57, 175, 176, 195, 198, 201, 207
Morello, 17
Mtsuko, 253
Mudimela, 228
Mura, 145
Mustonen K., 244
Mustonen M.T., 177
Mykkänen, 191
Myllyperkiö, 228
Myöhänen, 151, 167, 168
Mäkelä, 87
Mäkelä, 241, 242
Mäki, 118, 141
Mäkinen, 150
Mäkitalo, 43, 248
Mättö, 39
Möttönen, 16, 17, 142, 256, 258, 272

N

Napari, 39
Nara Singh, 208
Nasibulin, 223, 228, 244
Nenashev, 161
Nevala, 231, 235
Nevanpää, 41, 252
Niemi, 190
Nieminen P., 179, 186
Nieminen R.M., 119, 124, 129, 134, 152
Nieminen V., 39
Nikitenko, 183
Nikitin, 44
Nikitina, 45
Nilius, 135
Nippolainen, 84
Niskanen, 29
Norarat, 46
Nordlund, 123, 128, 139, 237, 245, 286
Norrby, 187
Nowling, 283
Nuijten, 215
Numminen, 174
Nykänen, 101, 285
Nyman, 178, 179, 186, 208
Nyrhinen, 90

O

O'Donnell, 178
Oikkonen, 152
Oja, 119
Ojanen, 147
Olanterä, 47, 182, 205, 216, 217, 220
Olivares, 277
Orsila, 48

P

Paasonen, 230
Paavilainen, 225
Paavola, 280
Page, 178, 186, 208
Pakarinen J., 179, 186
Pakarinen O.H., 145, 245
Palanne, 47
Palmoroth, 62
Palmroth, 63, 75
Palosaari, 162
Palva, 95
Papadakis, 179, 186
Paraoanu, 270
Paris, 277, 281
Parr, 186
Partamies, 70
Partanen, 49
Parviainen, 286
Pasanen, 71
Paschalis, 179
Pashkin, 16
Pekola, 16, 142, 256, 258, 259, 265
Pellinen, 84
Peltola, 50
Peltonen, 259
Pentikäinen, 51
Penttilä, 15, 21, 57, 101, 117, 125, 198, 201, 207
Pepper, 28
Peräjärvi, 57
Pesonen, 163
Pessa, 234
Petkov, 182, 205, 216, 217, 220
Petri, 179
Pettersson, 164, 228, 261
Peura M., 101, 110, 117, 120, 125
Peura P., 178, 179, 186, 208
Pietilä, 272
Piilo, 279, 287
Pikna, 174
Piovella, 281

Pirinen, 213
Pirkkalainen, 17, 120, 258
Pitkänen, 121, 122
Pittalis, 155
Plastina, 273
Plochocki, 198
Pohjalainen, 53
Pohonen, 123
Polojärvi, 52, 234, 246
Pomoell, 72
Poutanen, 65
Priimägi, 58, 227
Proetto, 155
Prunnila, 153
Pucknell, 186
Puertas, 105
Puisto, 121
Pulkkinen A., 108
Pulkkinen T.I., 62, 63, 75
Puska, 141, 145, 149, 172, 238
Pussi, 115
Putaja, 154
Puustinen, 251
Pylkkänen, 98, 143

Q

Qin, 240

R

Rahaman, 198
Rahkila P., 19, 178, 179, 186, 208
Rahkila P.M., 71, 184
Raittila, 26
Rak, 180
Rannou, 224
Rantaharju, 191
Rantala, 147, 275
Ras, 232
Rauch, 165
Rautiainen, 13
Ren, 116
Renk, 194
Reponen, 21, 53, 195, 198, 201
Reurings, 36
Ricciardi, 197
Riekkinen, 88
Rimpiläinen, 54
Rinta-Antila, 207
Rintala, 228
Rissanen, 21, 57, 175, 195, 198, 201
Ritchie, 28
Roberts, 179
Rodger, 74
Rodriguez, 233
Roederb, 209
Róg, 225
Roinisto, 215
Ropo, 121
Ropponen, 179
Rossi, 19
Rummukainen, 191, 215
Ruotsalainen, 178, 179, 186, 208
Räihä, 182, 205, 215–217, 219, 220
Räisänen J., 222
Räisänen M., 222
Räsänen, 136, 154–156
Räty, 206
Röntynen, 143

S

Saastamoinen, 21, 57, 175, 195, 198, 201, 209
Safonchik, 158
Saira, 16, 142
Sajavaara, 19, 39, 46, 47
Sakiroglu, 156
Sakko, 98, 143
Salmi, 38, 74, 120
Salo, 144
Salomaa, 192
Sandzelius, 178
Sane, 91
Sannino, 181
Sapple, 178, 208
Saranpää, 110
Sarén, 178, 179, 186, 207, 208, 210
Sarkamo, 182, 205, 215–217, 219, 220
Savelainen, 65
Savolainen, 86, 92–94
Savonen, 53
Scheffler, 146
Schmidt, 185, 197
Scholey, 178, 179, 186, 207, 208
Schramm, 52, 246, 264
Schultz, 288
Seddon, 186
Seitsonen, 152
Semenov, 44

Senapati, 231
Senda, 124
Seppänen, 22, 42
Seppä, 13
Seppälä A., 74
Seppälä E.T., 134, 166
Seppälä S., 166
Serimaa, 95, 101, 110, 117, 120, 125
Setälä, 31, 59
Shevchenko, 59, 249
Shnirman, 256
Sievilä, 226
Siika-Aho, 101
Siiskonen, 86
Sillanpää, 68, 257
Silpilä, 90
Silvast, 80
Silveri, 257
Simmons, 28, 209
Simonaho, 23, 84
Simpson, 178, 186
Sipilä, 55, 89
Sipola, 13
Sirviö, 65
Sitar, 174
Slotte, 113
Slupecki, 182, 205, 216, 217, 220
Snicker, 55, 141
Soininen, 98
Solehmainen, 35
Solinas, 256, 258
Sonnenschein, 21, 53, 201
Sopanen, 14
Sorri, 179, 186, 208
Sovago, 83
Stan, 151, 167, 168
Starrett, 28
Stefanucci, 151
Steinmeyer, 4, 48
Sterrer, 135
Strmen, 174
Stukowski, 237
Suhonen, 177, 188, 203
Suihkonen, 14
Sun, 236
Suominen, 284
Suur-Uski, 211
Suuronen, 110, 125
Swart, 236
Syrjäsuo, 70
Szarka, 174
Szerypo, 198
Särkkä, 157

T

Tabacaru, 209
Takalo, 56
Tallinen, 99
Tamminen, 74
Tan, 17
Tarvainen, 81, 111
Taskinen, 28, 252
Taylor, 208
Tenkanen, 125
Teretyev, 128
Thomson, 178
Thonhauser, 145
Thornhill, 186
Thuneberg, 127, 257
Tian, 223
Tikander, 29
Timonen, 56, 82, 93, 99, 126
Tittonen, 14, 137, 226
Toivanen, 64, 73
Toivonen, 57
Tomi, 169, 170
Tommila, 52, 246
Toppari, 229, 230, 261
Torkkeli, 95
Toroi, 78
Trache, 209
Traito, 158
Tranberg, 185
Tribble, 209
Trzaska, 37, 182, 205, 212, 215–220
Tsai, 16
Tuff, 179
Tukiainen, 52, 234, 246, 264
Tuominen E., 50, 174
Tuominen K., 66, 181, 191, 193, 200
Tuominiemi, 3
Tuomisto, 36, 91, 113, 118, 141, 165, 172
Tuorila, 257
Turpeinen, 126
Turunen, 57, 74, 248
Tuuli, 263, 266

Tölö, 133
Törmä, 114, 229, 230, 261, 270, 278
Töyräs, 80, 88

U

Uimonen, 151, 167, 168
Ulich, 74
Urban, 198
Uusitalo, 178, 179, 186, 208, 210

V

Vainio, 69, 72
Vaittinen, 39
Valden, 103, 111
Valkiainen, 35
Valtonen, 67
Vanmaekelbergh, 236
Vapaavuori, 227
Várnai, 101
Vartiainen, 83
Vasile, 277
Vattulainen, 85, 91, 225
Vauhkonen, 54, 84
Vepsäläinen, 214
Verho, 224
Verronen, 74
Vesterinen, 29
Viheriälä, 52
Vihinen-Ranta, 82
Viikari, 101
Viiri, 9, 40, 41, 252
Vilen, 95
Viljas, 169, 170
Virkajärvi, 66, 182, 205, 216, 217, 220
Virkkala, 171
Virkki, 32, 58
Virtanen, 127
Vitos, 121
Voipio, 59
Volovik, 106
Vuorimaa, 32
Välimaa, 213
Välimäki, 94
Vänskä, 137
Vörtler, 128

W

Wadsworth, 179, 208
Wagner, 165
Wang, 116, 233
Watkins, 178
Weber, 195, 198
Weckström, 10
Wells, 186
Wendland, 183
Wengler, 169
Whitlow, 19, 39, 46
Wieneke, 118
Wiesner, 169
Withers, 2
Woods, 209
Wu, 169

Y

Yang, 17
Ydrefors, 188
Yogendran, 283
Yurke, 230

Z

Zavodchikova, 223
Zdanowicz, 254
Zelený, 129
Zen, 267
Zhu, 223, 228
Zubiaga, 172

Å

Åström, 99

Ä

Äystö, 21, 53, 57, 175, 195, 197, 198, 201, 203, 207, 209

Ö

Österbacka, 160, 161, 163, 164

Industrial exhibition

Industrial Exhibition is accessible in the 3rd floor throughout the meeting.

Micronova Nanofab – www.micronova.fi

Nanocluster – www.nanocluster.fi

Canberra Solutions AB – www.canberra.com/se/

CSC – Tieteen tietotekniikan keskus Oy – www.csc.fi

Doseco Oy – www.doseco.fi

Sintrol Oy – www.sintrol.com

VTT – www.vtt.fi

Gammadata Finland Oy - www.gammadatafinland.fi

Terra Cognita – www.terracognita.fi

MICRONOVA
Centre for Micro and Nanotechnology

Micronova Nanofabrication Centre

Micronova is a joint centre for micro- and nanotechnology research of VTT Technical Research Centre of Finland and Aalto University's School of Science and Technology.

Micronova Nanofabrication Centre - Nanofab - is one of Finland's National Research Infrastructures. Nanofab operates Micronova's 2600m^2 of cleanrooms with an extensive and versatile base of process equipment.

Micronova has a complete set of processes for the fabrication of microdevices, for instance sensors, MEMS, micro- and nanoelectronics, and photonic devices. Micronova's researchers also have the expertise to solve the most complex processing problems.

We offer open access to researchers from other universities, research institutes and companies.

We can help you with

- Lithography
- Nanostructiring
- Dry etching
- Wet processes
- Furnace processes
- Physical vapour deposition
- PECVD & ALD
- Ion Implantation
- Annealing
- Electrochemichal deposition
- Epitaxial growth
- Wafer bonding
- Back-end processes
- Characterisation

Contact

Tommy Holmqvist
Coordinator
Micronova Nanofab
tommy.holmqvist@tkk.fi
Tel: +358 5056 63497
www.micronova.fi

Aalto University
School of Science and Technology

VTT

OSKE
NANOTECHNOLOGY
CLUSTER PROGRAMME

- GreenNano
- CleanNano
- LeanNano
- HumanNano
- SafeNano

Responsible nanotechnology from Finland

Finland is committed to European and global efforts to carry out sustainable development policy. Nanotechnology is one strategic tool in striving for sustainability and competitiveness. The Finnish Nanotechnology Cluster Programme (2007-2013 has been committed to responsible development and use of nanotechnology from the beginning and will emphasize this approach in the future.

We invite all those who share this position and aim at finding solutions into national or global challenges to join us.
Our ambition is to launch new projects and ventures in collaboration with partners from industry and research institutes.

OSKE
CENTRE OF EXPERTISE
PROGRAMME

Committed to sustainable development

CANBERRA

Worldwide leader in nuclear measurement solutions

The key to our success lies in our ability to identify and understand the needs of our customers, in order to provide the most innovative and value-adding nuclear measurement solutions.

AREVA's commitment to the nuclear community complements CANBERRA's long tradition of unwavering dedication to our customers – to quality, to providing real solutions to complex problems, to meeting or exceeding your expectations. We do this by partnering with you, our customer, and seeking your input in all stages of our process- from product development to final installation to ongoing service.

Our integrated global team is there for you, providing the experience and know-how you need to address the complex measurement challenges we face in our rapidly expanding industry.

Nuclear Measurement Solutions include:

- Radiochemistry Laboratory Solutions
  - Gamma Spectroscopy
  - Alpha Spectroscopy
  - Alpha/Beta Counting
- Health Physics and Radiological Control
- Environmental Monitoring
- Criticality Monitoring
- Applied Systems for Whole Body Counting, *In Situ* Measurements and Waste Measurement
- World-Class Training and Global Service and Support

Contact CANBERRA to learn more.

www.canberra.com

CANBERRA Solutions AB
Kungsgatan 107
SE-75318 UPPSALA, Sweden
Tel +46 18 14 83 00 , fax +46 18 14 83 01

Sales Finland:
Tommy Tallqvist
e-mail: tommy.tallqvist@canberra.com

CANBERRA

Canberra Industries, Inc. is an AREVA company. The AREVA Group, worldwide leader in nuclear power.

CSC SUMMER SCHOOL IN SCIENTIFIC AND HIGH-PERFORMANCE COMPUTING

Nine days of learning and good company in nice surroundings, under the midnight sun. In the first CSC Summer School you will learn all the necessary ingredients of programming and using supercomputers to solve your scientific challenges - and have some good time, too.

What?

CSC Summer School brings together undergraduate and graduate students and postdoctoral researchers in different disciplines of scientific computing. The contents consist of lectures and hands-on training on parallel programming, code optimization and advanced usage of popular scientific programs.

Where?

The school takes place at Nuuksio/ Noux National Park in Espoo, Finland. It is conveniently located in the Helsinki metropolitan area. The near vicinity of the capital city is not visible, however - the venue, Solvalla Sports Institute, is in a nature preservation area that resembles Finland's nature in its best.

When?

School starts on the evening of Saturday June 12 and finishes on Sunday June 20, 2010. The days are filled with high-quality lectures, sports & leisure activities and nice time together. Be warned that at this time of the year, sun will not set almost at all!

To Whom?

The school is aimed for graduate students working with computational sciences, e.g. computational chemistry, physics, biosciences, or engineering; but also undergraduates as well as post-docs will find the school very useful.

Contents

The following topics will be covered

- Basics of parallel programming with the message-passing interface (MPI) paradigm
- More advanced topics in MPI and hybrid MPI+OpenMP parallel programming
- Fortran 95 and Python languages in scientific programming
- Improving application scalability and serial performance
- Parallel tools, compilers and libraries

In addition, tutorials in popular scientific software will be given. They are either introduction to the program and its capabilities, or tips&tricks for advanced users of the code. Tutorial sessions also include introductions to CUDA GPU programming, visualization and to computing cluster system administration.

The lectures are given by experts of CSC. The tutorial sessions feature also visiting specialists. The language of the school is English.

CSC

CSC, the Finnish IT center for science provides and develops versatile information technology and training services for the needs of academia, research institutes, state administration and companies. CSC is administered by the Ministry of Education.

For more information, visit

http://www.csc.fi/hpc/summerschool

DOSECO

Doseco Oy on henkilöannosten mittauspalvelu. Määritämme työssään säteilylle altistuvien henkilöiden säteilyannokset.

Asiakkaanamme on noin 800 työpaikkaa ja yli 10 000 henkilöä terveydenhuollossa, teollisuudessa, tutkimuksessa ja ydinvoimateollisuudessa.

Tarjoamme mittaus- ja asiantuntijapalveluita myös potilasannosmittauksiin ja laadunvarmistukseen sekä koulutukseen.

www.doseco.fi doseco@doseco.fi

Säteilyn käyttäjän palveleva kumppani

A PASSION FOR PERFECTION

PFEIFFER VACUUM

SINTROL

Tops!

Top quality – and top quality only – is what we deliver to our customers. It begins with the exacting demands we place upon our raw materials. We subject them to intensive scrutiny. Like measuring the hardness of the aluminum stock shown here. We enthusiastically inspect. Until everything is just right and works perfectly. As we see it: Only a product that's 100 % defect free is a good product for our customers.

Pfeiffer Vacuum stands for innovative and custom vacuum solutions worldwide. For German engineering art, competent advice and reliable service. Ever since the invention of the turbopump, we've been setting standards in our industry. And this claim to leadership will continue to drive us in the future.

Looking for the perfect vacuum solution?
Ask us:

www.pfeiffer-vacuum.net

Business from technology

VTT's service points in Finland: Espoo, Oulu, Tampere, Jyväskylä, Rajamäki, Turku, Kuopio, Lappeenranta, Kajaani and Raahe. VTT also has regional representatives promoting VTT's contacts with businesses in their areas.

VTT's contact points abroad are located at the FinNode innovation centre in Silicon Valley, California, in St. Petersburg and in Tokyo, at the FinChi innovation centre in Shanghai, on the Konkuk University campus in Seoul and in EARTO premises in Brussels.

VTT Technical Research Centre of Finland is a leading European multitechnological applied research organisation. VTT creates new technology and science-based innovations in co-operation with domestic and foreign partners. VTT's turnover is EUR 280 million and personnel 2,900.

VTT creates **business** from **technology**

Results of goal-oriented research show up as new products, lower production costs, simplified chain of production or even new market opportunities. Simply put innovations to capitalise on.

VTT is a leading European research organisation with an excellent record in cooperating with global market leaders in various businesses. Our expertise in high-end technology combined with an understanding of global business makes us an ideal partner for all your research and development needs.

Ask us how: **www.vtt.fi**

VTT TECHNICAL RESEARCH CENTRE OF FINLAND
P.O. Box 1000
FI-02044 VTT, Finland
Tel. +358 20 722 111

Technology and market foresight • Strategic research • Product and service development • IPR and licensing
• Assessments, testing, inspection, certification • Technology and innovation management • Technology partnership